A Study of Life-type Processes in Liquid Ammonia

Joseph Griffin

April 2015

A thesis submitted to The University of Huddersfield in partial fulfilment of the requirements for the degree of Doctor of Philosophy

IPOS
The Department of Chemical and Biological Sciences
The University of Huddersfield
Queensgate, Huddersfield
HD1 3DH
United Kingdom

Abstract

Liquid ammonia (LNH_3) has a number of properties similar to water, such as the ability to dissolve a diverse range of chemical compounds and, based on the variety of chemical reactions in this non-aqueous solvent, speculation has arisen about the possibility of life processes in liquid ammonia.

'Life' is difficult to define, but the general consensus is that it is comprised of a variety of individual process that could be regarded as 'processes of life', some of which can be modelled within the laboratory. This project is primarily concerned with looking at some of these life processes and attempting to model them in liquid ammonia. This may give rise to the notion that life in liquid ammonia is plausible which could be of great interest to those searching for extra-terrestrial life as ammonia is found in our solar system and very likely in many other parts of the vast universe.

One of life's fundamental processes is compartmentalisation, which is the aggregation of molecules into a protective cellular microenvironment, allowing life to survive and develop. Simple cell models in water and some other solvents have been studied widely allowing for a greater understanding of how the cell membrane works and they also have many commercial applications such as acting as drug delivery systems and as detergents. In this project, the aggregation of a variety of surfactants in liquid ammonia has been studied using a range of detection techniques. The common ionic surfactants, such as sodium dodecyl sulfate (SDS) and perfluorooctanoic acid (PFOA) were found not to aggregate in liquid ammonia, as evidenced by their conductance profiles. The reduced dielectric constant of liquid ammonia ($\varepsilon_r = 16$) compared with that of water ($\varepsilon_r = 80$) does not sufficiently decrease the repulsion between adjacent ionic head groups that naturally repel one another, and so micelle formation is not favoured. However, non-ionic, fully fluorinated fatty acid amides have been shown to aggregate into micelles in liquid ammonia using ^{19}F NMR as a detection method. The aggregation of fluorinated amides in liquid ammonia was found to follow trends observed for hydrocarbon surfactants in water, such as the relationship between critical micelle concentration (cmc) and hydrophobic tail length. Additionally, the magnitude of ^{19}F NMR shifts seem to suggest that the monomeric surfactant is surrounded by a relatively polar ammonia environment whereas those molecules in

the aggregated micelle are surrounded by the neighbouring fluorine atoms from the adjacent hydrophobic chains, as would be expected deep in a micelle core. There is also some evidence of micelle catalysis in liquid ammonia.

Another major contributor to life's processes are enzymes, which are nature's catalysts made up of proteins which fold up into a unique structure because of their interactions with water. Although their natural habitat is generally an aqueous environment, within an organism for example, enzyme catalysis in non-aqueous environments, such as organic media, has been widely studied and they have many applications in industrial processes. Enzyme catalysis has never been reported in pure, anhydrous, ammonia. This part of the project explores the extent at which lipases can catalyse the ammonolysis of triglycerides in liquid ammonia. Immobilized forms of Lipase B from Candida antarctica (CALB) were found to catalyse the ammonolysis of a variety of triglycerides in liquid ammonia and appear to be more selective towards larger molecules. The rates of triester conversion to diester for short-medium chain triglycerides were increased moderately with added lipase, whereas the subsequent ammonolysis of diester and monoester from triacetin showed no significant enhancement by the lipase. Conversely, for the longer chain triglyceride, triolein, a significant increase in conversion to oleamide was observed with the addition of the lipase. In addition to the positive implications for the 'life in ammonia' proposal, the lipase catalysed ammonolysis of triglycerides in liquid ammonia may have potential industrial applications. Triglycerides are abundant in nature, as fats and oils, and so are very cheap to acquire and the products of their ammonolysis, fatty acid amides, have many applications such as lubricating agents in the plastic industry and even medical uses. Oleamide, which is structurally related to the endogenous cannabinoid anandamide, is currently being examined for its sleep inducing effects.

In addition to the preliminary studies of life-type processes in liquid ammonia, some general reactions have been explored, in particular the ammonolysis of esters and its catalysis by the ammonium cation.

Small scale glassware can be used for the safe study of liquid ammonia at room temperature under approximately 10 bar pressure. Reactions in liquid ammonia have been previously studied generally by using a simple sampling method and analysing by GC or HPLC. Additionally, in this project, a variety of analytical techniques in

liquid ammonia have also been developed such as the use of conductance, UV-vis and liquid ammonia NMR.

Acknowledgements

Firstly, I would like to sincerely thank Professor Michael Page and Professor John Atherton for their supervision during the past three years of my PhD studies. In particular, their knowledge of the subject and enthusiasm towards the project has been of enormous value to me.

I would also like to thank members of the IPOS group, especially Dr Nicholas Powles and Dr Matthew Stirling for their professional, academic and personal support throughout the project. To the entire group, it has been a pleasure to work in such a welcoming and friendly environment which has made my day to day work extremely enjoyable.

Special thanks to my fellow researchers, in particular Dr Dharmit Mistry and Dr Haifeng Sun for their useful insight and helpful conversations.

Additionally, financial and technical support from IPOS and the University of Huddersfield is appreciated and I would like to also thank Dr Neil McLay for his assistance with the NMR.

Many thanks also to my family who have supported me throughout the past years, it is greatly appreciated.

Table of Contents

Abbreviations

A list of commonly used symbols and abbreviations in this thesis

LNH_3	liquid ammonia
K	Kelvin
°C	degree Celsius
atm	atmospheres
Å	angstrom
m.p	melting point
DCM	dichloromethane
DMSO	dimethyl sulfoxide
DMF	dimethyl formamide
ε_r	dielectric constant
D	dipole moment
DN	donor number
CALB	Lipase B from Candida antarctica
Novozyme 435	CALB immobilised onto acrylic resin beads
CR	Lipase from Candida rugosa
GC	gas chromatography
FID	flame ionization detector
MS	mass spectrometry
m/z	mass to charge ratio
NIST	National Institute of Standards and Technology database
NMR	nuclear magnetic resonance
UV-vis	ultraviolet-visible spectrophotometry
λ_{max}	wavelength at maximum absorbance (nm)
IS	internal standard

pK_a	negative logarithm ($-1og_{10}$) of the acid dissociation constant
T	tetrahedral intermediate
k_{obs}	observed pseudo-first-order rate constant
β_{lg}	Brønsted constant for leaving group
cmc	critical micelle concentration
SDS	sodium dodecyl sulfate
CTAB	cetyl trimethylammonium bromide
DTAI	decyl trimethylammonium iodide
S	siemens
K_{diss}	equilibrium constant for dissociation of ion-pair
K_{ip}	equilibrium constant for formation of ion-pair
pfh	perfluorohexane
ω	terminal $-CF_3$ or $-CH_3$ group of a surfactant tail
δ_{obs}	observed chemical shift (ppm)
δ_m	chemical shift of surfactant monomer (ppm)
δ_a	chemical shift of aggregate (ppm)
FAA	fatty acid amide

Chapter 1 - Introduction to the project

1.1 The search for ‘life’

1.2 Properties of ammonia and liquid ammonia as a solvent

1.3 General reactions in liquid ammonia

1.1 The search for 'life'

1.1.1 Water - the matrix of life

It is a commonly held assumption that if life exists beyond Earth it is carbon-based with water as the preferred solvent and utilises fuels and light as sources of energy to sustain itself.[1] This outlook is expected and rational as it is, after all, how life as we know it exists on earth. Other suppositions are that the fundamentals of life originate quickly if given the opportunity to do so, but the evolution of multi-cellularity and intelligence takes a long time and, maybe, is an improbable event and so any extra-terrestrial life may be uni-cellular and microbial.[2]

There is speculation that extra-terrestrial life could be based on the silicon atom because it is in the same group as carbon in the periodic table and has many similar chemical properties.[3] Furthermore, silicon can form analogues of common carbon-based molecules (Scheme 1.1.1).

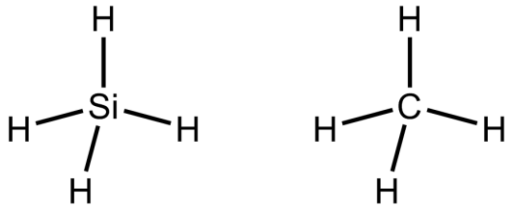

Scheme 1.1.1 Silane (left), the silicon based analogue of methane (right).

Approximately 28% of the earth's crust is composed of silicon compared with very little carbon (0.18%), and yet life on earth is carbon-based.[4] Thus, the fact that silicon-based life did not develop on the earth when given the chance, or was outcompeted by carbon-based life, could infer that life based on the silicon atom is unfavoured. One possible reason is that some silanes react with water and long chained silanes, alkane analogues, spontaneously decompose in water, the earth's most abundant solvent.[5] Thus, it may be the properties of the solvent that determine the chemistry of life.

Generally speaking, for life as we know it, water is the essential component as the universal solvent and is described by Nobel Laureate A. Szent-Györgyi as "the matrix of life".[6] Indeed, one of NASA's official principle exploration strategies in the search for life in the universe is to "follow the water".[7] Thus, from the human perspective, it makes perfect sense to approach the search for extra-terrestrial life by looking for

conditions that best mimic those of the earth. Nevertheless, this doesn't necessarily mean that all life in the vast universe is indeed limited to this particular solvent.

A recent committee on the subject of life in planetary systems emphasized that many of the current views about how water is uniquely suited for life can be slightly geocentric and misleading and they use the many types of water ice to highlight this complacency:[8] Ice I, the most stable form of ice at 273 K and atmospheric pressure, floats on water and so can insulate a body of liquid water below and keep it from freezing whereas all other types of ice (ice II to ice X) are much denser than liquid water and sink, not providing any insulation.[9] A geocentric view would infer that water ice I appears ideal for earth, as the insulation it provides allows life in these conditions to survive, and so this is generally the only type of ice worthy of discussion. It is conveniently omitted that ice I has a much higher albedo (ability to reflect sunlight) than liquid water leading to drastic cooling. This can result in the formation of more surface ice, an even higher albedo and further cooling, leading to a cycle that can amplify glacial events in an ice-age. One could argue that a model solvent for life would continually support a stable environment and yet the fact that ice water on earth floats, cooling down the planet, could certainly be viewed as a disadvantage, and so maybe water is not as 'ideal' as first assumed. Thus, the committee concluded that they had found no compelling reason to limit life to a solely aqueous environment but they do suppose that any terrain life would likely be constrained to carbon based biomolecules. Several candidates for solvents which may have the ability to support life have been suggested (Scheme 1.1.2)

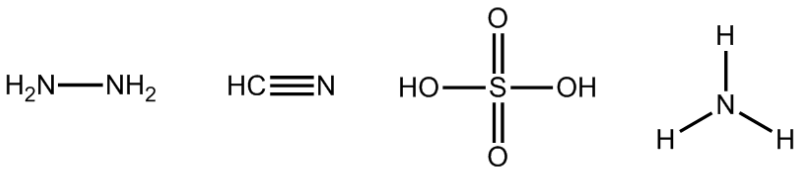

Scheme 1.1.2 Potential 'solvents for life' (left to right); hydrazine, hydrocyanic acid, sulfuric acid and ammonia.

Theoretically, any of these solvents and many more may support life, each with their own rules that govern the fundamentals of life processes such as compartmentalisation, replication, metabolism and catalysis. One could imagine some

extra-terrestrial, non-aqueous based intelligent life-form, exclaiming that their solvent is the "matrix of life", and that the prospect of life in water unthinkable (Figure 1.1.1).

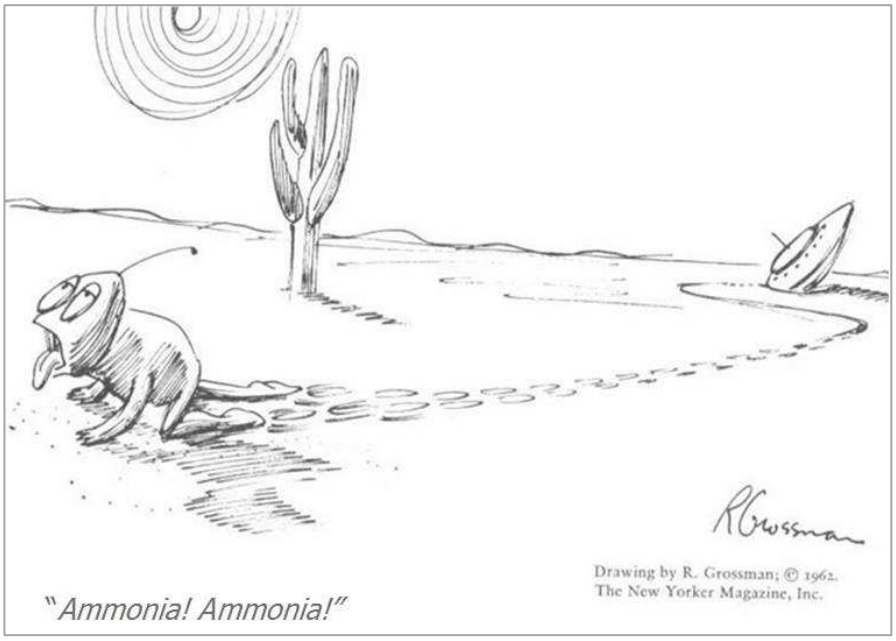

Figure 1.1.1 "Ammonia! Ammonia!" What really happened at the 1947 Roswell UFO incident? [10]

1.1.2 The potential for liquid ammonia to support life

The possibility of life based in liquid ammonia has a long history and it has been suggested that metabolism in liquid ammonia is conceivable. Haldane highlighted ammonia analogues of water could form the building blocks of biomolecules whereby NH groups might replace oxygen atoms (Table 1.1.1) and Firsoff detailed the similarities between synthesis reactions in water and ammonia dominated systems.[11, 12]

Table 1.1.1 Some ammonia analogues of water-based life biochemical functional groups.

Typical biochemical functionality	water-based life form	possible ammonia-based life analogue
alcohol	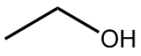	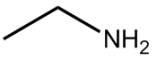
fatty acid	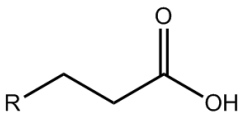	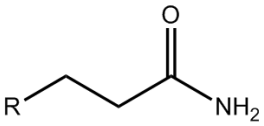
carbohydrate	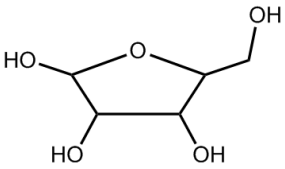	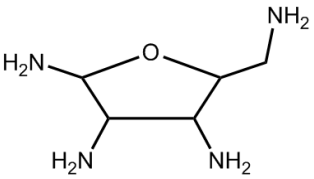

One particular metabolic example highlights the possible synthesis of proteins in an ammonical environment, compared to the orthodox aqueous, and ammonia-water solutions.

In water, two glycine molecules are combined to form a peptide bond, with the release of water (Scheme 1.1.3).

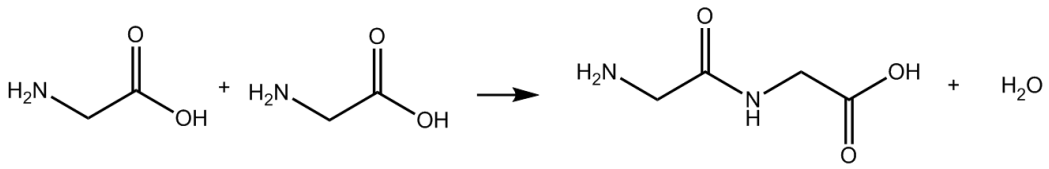

Scheme 1.1.3

Similarly, in an ammonia-water mixture, an amide $CONH_2$ group may substitute for the carboxylic acid COOH and again, with formation of a peptide bond, but this time liberation of ammonia (Scheme 1.1.4).

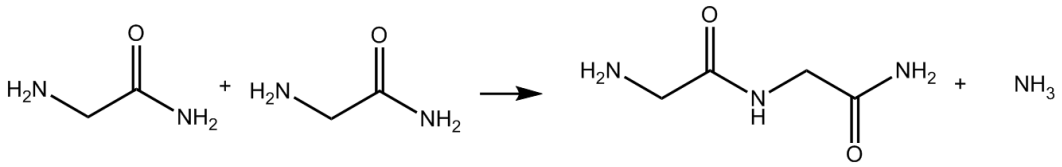

Scheme 1.1.4

Furthermore, in a purely anhydrous, liquid ammonia medium, with the absence of the oxygen atom, one can envisage the replacement of the carboxyl group with -$CH(NH)NH_2$ with a novel 'peptide-like' bond with -CH(NH)NH- structure (Scheme 1.1.5). There is in fact some speculation that the peptide bond may be a relic from the early stages of earth evolution in an ammonia-organic based environment.[12]

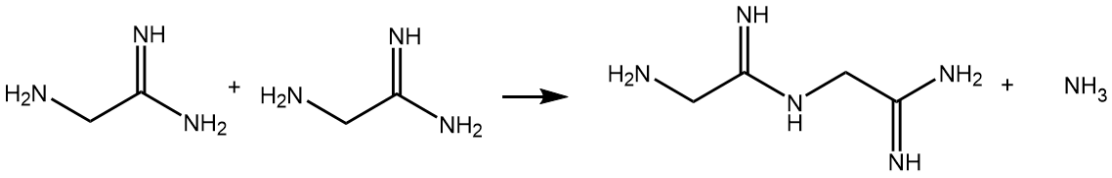

Scheme 1.1.5

Equally, comparable reactions can be shown for phosphate bond formation in nucleic acids, part of the building blocks of DNA.

As a solvent for life, ammonia is comparable to water in many ways such as its ability to solubilise a diverse range of compounds including organic and electrolytic species. On earth, ammonia is liquid at lower temperatures than water and has a smaller range in which it stays liquid; -78 to -33 °C for liquid ammonia compared to 0 to 100 °C for water.[8] This would suggest that in order to survive, life would have to adapt to a much smaller temperature window, although this assumes life is limited to earth like atmospheric pressures. At higher pressures, the range of temperatures for liquefied ammonia increases so, for example, at 60 atm, ammonia is liquid from -77 to 98 °C, so the common notion that 'ammonia-life' equates to 'cold-life' is only applicable to earth like atmospheres. Greater pressures would be experienced on other planets and so liquid ammonia may be abundant throughout space. Indeed, liquid ammonia is found in the clouds in the Jovian atmosphere although many view life in transient clouds as unlikely. This view could be revised if considering continuous (un-broken) cloud systems similar to those found in the atmosphere of Venus.[8]

Liquid ammonia would outperform water with its capacity to dissolve alkali metals without reaction, as is observed in water, which could be advantageous to metabolic pathways in ammonia as they can act as catalysts. The reduced viscosity of ammonia in comparison to water could also benefit ammonia based life. At ambient temperature, the viscosity of ammonia is 120 μPa.s compared with water 1002 μPa.s and so ions and dissolved particles in liquid ammonia would collide more frequently and possibly react more readily with each other.[13, 14]

Additionally, there are some suppositions that ammonia based life may not just be restricted to a purely anhydrous medium. Recent studies of data recovered from the Saturnian moon Titan propose surface oceans comprising a liquid of comparable viscosity to an ammonia-water mixture.[8] Additionally, Fortes speculates that the subsurface oceans of Titan, Triton (of Neptune) and the Galilean satellites may support life, with ammonia acting as an antifreeze for water, lowering the temperature at which water can remain liquid, and several enzymes can remain stable at these low temperatures.[15,16] This does then raise the issue that any ammonia-water medium would be highly basic, and life as we know it, is not capable of withstanding highly basic environments as well as it can survive some acidic conditions. However, this may not be a major obstacle to life because the majority of organisms on earth may not have needed to adapt to basic conditions at all. On earth, there are only a few natural environments of high pH, mainly soda lakes, whereas if the earth was dominated by these environments, the adaptation of most organisms to basic conditions may have become the norm.

1.1.3 Project aim - a study of life processes in liquid ammonia

Surprisingly, defining life is not as simple as one may first assume and there is still a long-standing debate with no real scientifically accepted consensus.[17] The fundamental problem is that living organisms use compounds that are abundant in their surrounding environment and, additionally, many processes that occur in living systems are not intrinsically different to processes that occur abiologically. For example, a simple metabolic process within the cell that would be considered a ‘living reaction’ could be replicated in the laboratory, possibly under different conditions, but would by no means be described as a process of life (Scheme 1.1.6).

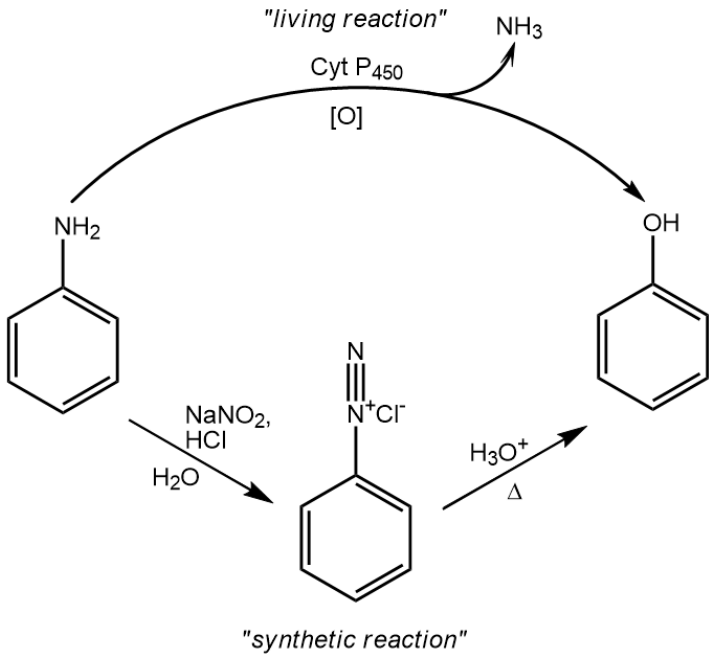

Scheme1.1.6 In living systems, during phase I metabolism, aniline may be converted to phenol by Cytochrome P450 and in the laboratory via formation of a diazonium salt.[18,19]

Although the complexity of the enzyme is well appreciated, its intrinsic mechanisms and functions of the amino acid residues can be well interpreted from a chemistry perspective. Indeed, the synthesis and application of artificial enzymes is a current research area, so enzymes on their own are not necessarily 'living things'.[20, 21] Given this, the notion that enzymatic processes are commonly credited as a 'living process' is probably due to a combination of factors, such as their synthesis in the cell, secretion into extracellular compartments, removal of waste products, requiring an energy source for maintaining concentration gradients etc.

Thus, there is not a single way of defining what life is, but rather, life can be defined through a collection of properties and processes. Some of these processes can be individually modelled in the laboratory but together encompass what would be generally regarded as a living system. For example, one of the fundamental processes of life is the compartmentalisation of molecules into cell structures and, simple, cellular type analogues can be modelled in water.[22] Likewise, the formation of ammonophilic and ammonophobic phases in liquid ammonia, comparable to hydrophilic and hydrophobic phases in water, is conceivable and hence the formation of cellular-type structures may indicate that ammonia can support

compartmentalisation. In fact, the SETI institute (Search for extra-terrestrial life institute, USA) acknowledge the role that amphiphilic vesicle formation may have played in the origin and evolution of life.[23] SETI currently has a number of projects dedicated to understanding how lipids relate to the origin of life.

This project will focus on some of these fundamental processes of life and their potential applications in an ammoniacal environment. In doing so, the notion of liquid ammonia as suitable candidate for a 'solvent for life' may be realised. Admittedly, the search for extra-terrestrial life is not exclusively focused on a suitable solvent medium and Schulze-Makuch et al highlights four major facets that are essential to life: habitat, energy, chemistry and solvent.[24]

1.2 Properties of ammonia and liquid ammonia as a solvent

1.2.1 Structure of ammonia

Ammonia is a tetra atomic molecule with three hydrogen atoms covalently bound to a central nitrogen atom. The nitrogen atom has five outer electrons with an additional electron from each hydrogen, giving a total of 3 bonded electron pairs leaving one lone pair of electrons. It adopts a trigonal pyramidal shape as predicted by the valence shell electron repulsion theory (Scheme 1.2.1).[25]

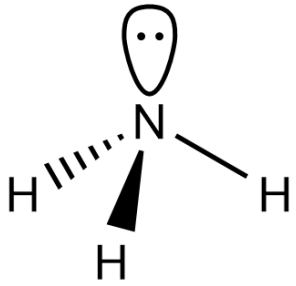

Scheme 1.2.1 Structure of an ammonia molecule.

The N-H bond length is 1.01 Å, which is greater than that of water (0.96 Å) but smaller than that of methane (1.10 Å), and the H-N-H bond angle is 107.8 degrees, again in between that for water (105 degrees) and methane (109.5 degrees). At atmospheric pressure, it has a boiling point of -33.5 °C compared with 100 °C for water and approximately -160 °C for methane. The ammonia molecule pyramidal structure has a low height of 0.360 Å which gives rise to the possibility of the nitrogen atom passing through the plane to an equally stable position on the opposite side

(nitrogen inversion).[26] The energy barrier for this inversion of the nitrogen at room temperature is a relatively low 24.7 kJ mol^{-1} compared to energy required to invert the similarly structured phosphine (PH_3) which is 132 kJ mol^{-1}. [27, 28]

1.2.2 Liquid ammonia as a dipolar aprotic solvent

There are numerous ways of classifying solvents in terms of their physical properties, chemical composition and acid-base behaviour.[29] One of simplest and most widely used methods of characterising solvents is by their polarity. Solvents are generally classed as either polar or non-polar and the solvent dielectric constant (ε_r) can provide a rough estimation as to which of the two groups they best fit. A general rule is that solvents with a dielectric constant of greater than 15 are considered to be polar.[30] Polar solvents can be further classified by their ability to protonate/deprotonate and their hydrogen bonding ability. Solvents which can readily donate hydrogen are called protic whereas solvents which have non-acidic hydrogens and cannot H-bond are aprotic. For example, DMSO (dimethyl sulfoxide) is a polar-aprotic solvent. Hexane, however, is a non-polar solvent showing negligible acid/base behaviour towards the solute. Liquid ammonia has a reasonably low dielectric constant (16.0 at 25 °C), and is thus on the borderline of polarity.[31] It is quite unique therefore in that it can solubilise a wide range of both salts and organic compounds.[32,33]A list of some solvent properties can be found in Table 1.2.1.

Table 1.2.1 Physical properties of some common solvents at 25 °C. [34]

Solvent	Dielectric constant (ε_r)	Dipole moment (D)	Classification
water	80	1.85	polar amphiprotic
DMSO	46.7	3.96	dipolar aprotic
DMF	38	3.82	dipolar aprotic
acetone	21	2.88	polar aprotic
ammonia†	16.7	1.42	dipolar aprotic
benzene	2.3	0	non-polar
n-hexane	1.88	0	non-polar

†Reference [35]

The solubility of ionic species is chiefly dependent on the dielectric constant of the solvent but can also depend on specific solvation effects and in most cases liquid ammonia solvates metal ions better than water. An abundance of synthetically useful salts are highly soluble in liquid ammonia, particularly ammonium salts, e.g., NH_4N_3, 67.3 g/100g at -36 °C and NH_4NO_3 ca. 30 M at 25 °C.[25, 32] Some salts such as fluorides and those with multiple negatively charged ions often show very low solubility in liquid ammonia at ambient temperature. The solubility of different salts in liquid ammonia can be seen in Table 1.2.2.

Table 1.2.2 Solubilities of some inorganic compounds in liquid ammonia at 20-25 °C.[25]

Very soluble	**Moderately soluble**	**Slightly soluble**	**Insoluble**
>100 g/100 g NH_3	**>10 g/100 g NH_3**	**>1 g/100 g NH_3**	**<1 g/100 g NH_3**
AgI	$AgNO_3$	AgBr	AgCl
KI	$Ba(NO_3)_2$	$B(OH)_3$	$CaBr_2$
$LiNO_3$	$Ca(NO_3)_2$	KBr	$CdCl_2$
NH_4Br	KNO_3	$KClO_3$	$KBrO_3$
NH_4Cl	$NaNO_3$	KNCO	KCl
NH_4ClO_3	$Sr(NO_3)_2$	KNH_2	LiBr
NH_4I	NH_4N_3	LiCl	NaF
NH_4HS		NaCl	$NaNH_2$
NH_4SCN			Na_2SO_3
$(NH_4)_2S$			$Na_2S_2O_3$
NaI			RbCl
NaBr			$ZN(NO_3)_2$
NaSCN			

Generally, the solubility of organic compounds is much greater in liquid ammonia than in the highly polar water and some solubilities of aliphatics and aromatics can be seen in Tables 1.2.3 and 1.2.4. Solubility is important for the potential applications of liquid ammonia as a reaction medium and the fact that alcohols, amides, amines and aromatics all have good solubility in liquid ammonia makes liquid ammonia a good solvent for organic reactions.

Table 1.2.3 Solubilities of some aliphatic compounds in liquid ammonia.[33]

Organic class	Example	Solubility in liquid ammonia
Alcohols	ethanol	miscible
Alkanes	hexane	insoluble (medium/long chain)
Amides	urea	soluble
Amines	diethylamine	miscible
Carbohydrates	glucose	soluble
Carboxylic acids	pentanoic acid	soluble (short/medium chain)
Cyano compounds	acetonitrile	miscible
Esters	ethyl acetate	soluble
Ethers	diethyl ether	soluble
Halides	chloroform	soluble
Ketones	pinacolone	soluble

Table 1.2.4 Solubilities of some aromatic compounds in liquid ammonia.[33]

Organic class	Example	Solubility in liquid ammonia
Alcohols (phenols)	catechol	very soluble
Amides	benzamide	very soluble
Amines	aniline	miscible
Carboxylic acids	nitrobenzoic acid	soluble
Cyano compounds	benzonitrile	miscible
Esters	ethyl benzoate	very soluble
Ethers	anisole	miscible
Halides	chlorobenzene	soluble
Hydrocarbons	toluene	slightly soluble
Ketones	acetophenone	soluble
Nitro compounds	1,3,5-trinitrobenzne	very soluble

The nitrogen lone pair makes ammonia a very good hydrogen bond acceptor and this confirms its classification as a dipolar-aprotic solvent which strongly solvates cations, evident by ^{23}Na NMR chemical shifts.[36] Liquid ammonia has a very high donor number (DN_{LNH3} = 59 kcal mol^{-1}) which is much greater than that of water (DN_{water} = 18 kcal mol^{-1}), pyridine ($DN_{pyridine}$ = 33.1 kcal mol^{-1}) and even the highly basic hexamethylphosphorous triamide (DN_{HMPT} = 38.8 kcal mol^{-1}).[37, 38] Unlike amphiprotic

water, it is not a good hydrogen bond donor and does not significantly solvate anions. [39, 40]

1.2.3 Liquid ammonia as a 'green solvent'

It is well known that the nature of the solvent can influence both the kinetics and mechanisms of organic reactions. [29] Dipolar aprotic solvents such as DMF and DMSO are currently used in around 10 % of chemical manufacturing process but have toxicity concerns and are expensive. In addition, they are very difficult to recover due to their water miscibility and high boiling points. Chemical processes using these solvents would often require liquid-liquid extraction and distillation most likely producing even more solvent waste and so they are frequently disposed of by incineration, releasing harmful gases such as CO_2 and SO_3. Liquid ammonia is a promising candidate to replace dipolar aprotic solvents in a number of applications. Ammonia has only one lone pair for three potential N-H hydrogen bonds which leads to a relatively weak association in the liquid state and a boiling point of -33 °C and vapour pressure of around 10 bar at 25 °C. [25] Although it is similar in many ways to the conventional dipolar aprotic solvents it is the low boiling point that makes liquid ammonia much easier to recover and reuse. As a consequence, liquid ammonia as a solvent can be regarded as a front-runner in the need for more environmentally friendly, 'green chemistry'. In crude terms, liquid ammonia is essentially 'green' because it is easily recyclable.

1.3 General reactions in liquid ammonia

Organic research in this unique solvent became popular in the late 19th century when liquid ammonia became commercially available and the early research mainly covered chemical and physical properties of liquid ammonia.[41] In particular, extensive studies of liquid ammonia solutions by Kraus provided fundamental data such as the solubility of inorganic and organic chemicals, conductivities of ammonia solutions and ionisation of metals, and, later, some basic organic reactions in liquid ammonia were studied. [42,43,44] The most recent major review of organic reactions in liquid ammonia was in 1963 by Smith.[33] Generally speaking, liquid ammonia is used as a solvent for organic reactions in the following areas:

i. As a solvent that dissolves alkali metals for reduction of organic compounds.

ii. As a solvent that dissolves alkali metals to produce strong bases for organic reactions.

iii. As a general solvent for organic reactions.

iv. As a reagent for reactions (solvolysis/ammonolysis).

1.3.1 Metal reductions in ammonia

Liquid ammonia solutions of sodium or potassium have been widely used as reducing reagents in organic synthesis, and were investigated in detail by Cady, Franklin and Kraus.[45, 41] Dissolving an alkali metal in liquid ammonia forms a deep blue coloured solution which is characteristic of the solvated electron given up by the metal. The electrons can be donated to substrates to form radical anions/dianions and, following protonation, generate a reduced product.

1.3.1.1 Cycloalkanes and conjugated alkenes and alkynes

Dauben and Wolf demonstrated that α-keto-cyclopropanes can be reduced with lithium in liquid ammonia to the analogous straight chain ketone (Scheme 1.3.1). [46]

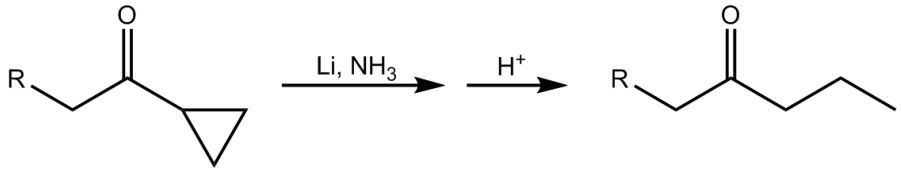

Scheme 1.3.1

Conjugated alkenes are readily reduced to mono-alkenes. For example, butadiene is reduced to a mixture of cis and trans-2-butene with lithium in liquid ammonia the ratio of the two isomers is temperature dependent (Scheme 1.3.2). [47]

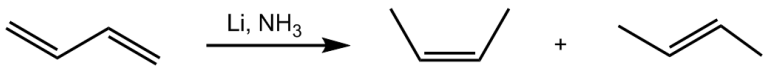

Scheme 1.3.2

Generally, non-conjugated alkynes are predominantly reduced to trans-alkenes. This is because the radical anion or dianion intermediate prefers a trans configuration in order to minimise interaction between the two negatively charged sp^2 centres. For

example, 2-heptyne is reduced via the dianion to form exclusively trans-2-heptene (Scheme 1.3.3). [48]

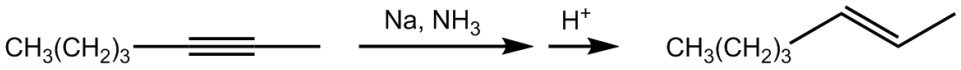

Scheme 1.3.3

1.3.1.2 Aromatic compounds

Probably the most prominent application of the ammonia/metal system as a reducing agent for organic reactions is the Birch reduction.[49,50,51] Regio-selectivity of the reduction depends on whether the substituent is electron-donating or electron-withdrawing. To minimise interactions, the intermediate radical anion tends to locate itself on the carbon meta to an electron-donating group and on the carbon ortho to an electron-withdrawing group.[52,53] Scheme 1.3.4 demonstrates two examples of the Birch reduction of aromatic compounds using sodium in liquid ammonia and the effect of substituent position.[54,55]

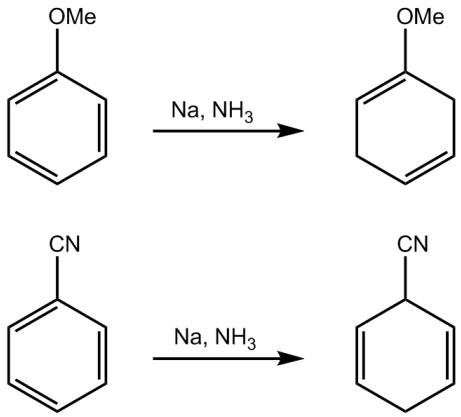

Scheme 1.3.4

1.3.1.3 Carbonyl groups

With the exception of carboxylate salts, all carbonyl groups are reduced in liquid ammonia with alkali metals.[56]

1.3.1.4 Epoxides, nitro and nitrile groups

In alkali metal ammonia solutions, epoxides ring open and form the alcohol. The stability of the anion/dianion will affect the stereochemistry of the process. Interestingly, Kaiser et al observed that when styrene oxide is reduced in sodium/liquid ammonia, 2-phenylethanol is the only product (Scheme 1.3.5).[57]

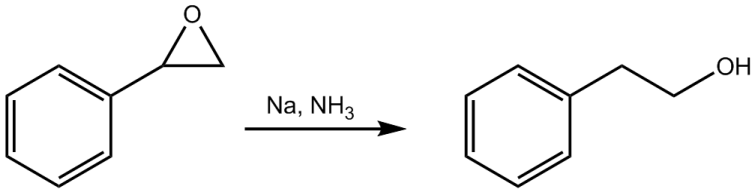

Scheme 1.3.5

1.3.2 Ammonolysis, aminolysis and amidation reactions

Probably the simplest reactions in liquid ammonia are solvolysis reactions. Solvolysis is the term used for a special type of nucleophilic substitution or elimination reaction whereby the attacking nucleophile is the solvent molecule itself. The most common type of solvolysis reactions is hydrolysis, with water solvent nucleophile but there are many others such as alcoholysis, with alcoholic solvent attack, or aminolysis, with an amine solvent nucleophile. For any reaction in liquid ammonia, with nucleophilic attack from ammonia solvent, the general term for the solvolysis reaction is ammonolysis. Ammonolysis or aminolysis to form an amide group can also be described as amidation.

1.3.2.1 Ammonolysis/aminolysis of halides

The importance of the amino group is well acknowledged by chemists due to the presence of this functional group in many areas of applied chemistry including the pharmaceutical, medicinal, agricultural and biochemical industries.[58] Accordingly, the synthesis of amines from organohalides has been examined in detail in both industry and academia. There are currently numerous methods for the synthesis of amines in solvents other than liquid ammonia but most require catalysts and some operate at elevated temperatures. For example, Buchwald et al used hydrazones as the amine

nucleophile and obtained high yield using para-chlorobenzotrifluoride as substrate (Scheme 1.3.6).[59]

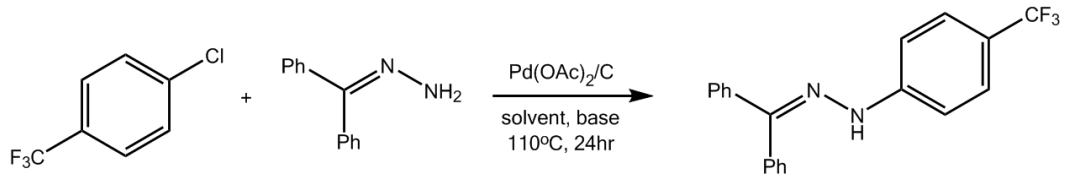

Scheme 1.3.6

Equally, under catalytic conditions, primary amines can be synthesised using an ammonia nucleophile yielding secondary amine side product (Scheme 1.3.7).[60]

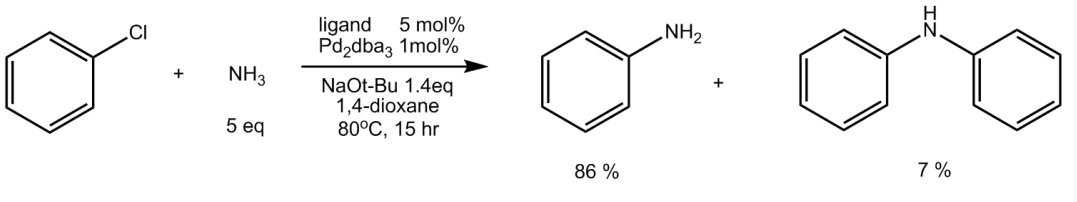

Scheme 1.3.7

In pure ammonia, alkyl halides react with ammonia solvent to initially give the corresponding primary amine and ammonium halide salt as products (Scheme 1.3.8).

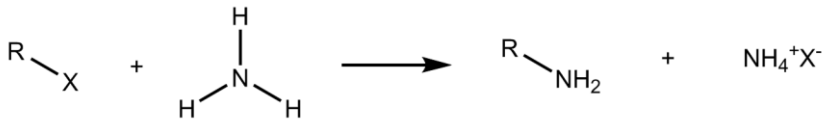

Scheme 1.3.8 General ammonolysis of alkyl halide

However, such reactions are often difficult to control because the amine product formed can react further to form the secondary and even tertiary amines. In some cases the primary amine formed can be more nucleophilic than the ammonia solvent and thus as a means of primary amine synthesis, the ammonolysis of alkyl halides has its limitations. For example, 1-bromooctane undergoes ammonolysis in ammonia yielding roughly equal amounts of primary amine and secondary amine with trace amounts of the trioctylamine and tetraoctylammonium bromide (Scheme 1.3.9).[61]

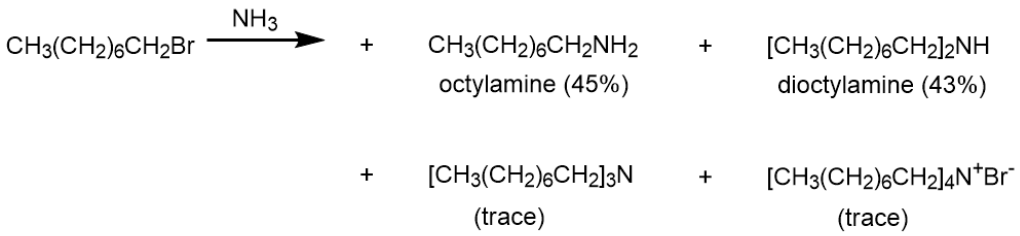

Scheme 1.3.9 1-bromooctane in liquid ammonia

The B. F. Goodrich company patented the synthesis of high yields of morpholine by reaction of dichlorodiethyl ether in liquid ammonia at moderate temperature (Scheme 1.3.10).[62]

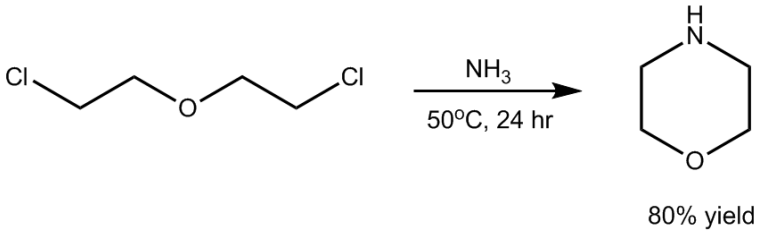

Scheme 1.3.10

For a given aliphatic group, the ease of ammonolysis generally lies in the order iodide > bromide > chloride >> fluoride, which is no different to the order observed for similar nucleophilic substitutions in aqueous environments. [63] Methyl halides readily undergo ammonolysis to the tetramethylammonium salts but the alkyl halide reactivity falls off with increasing size of the alkyl group.

The kinetics of these reactions was further investigated by P. Ji in our laboratory to try understand the mechanisms involved.[64] The rates of ammonolysis of a number of substituted benzyl chlorides can be seen in Table 1.3.1.

Table 1.3.1 Ammonolysis rates of substituted benzyl chlorides in liquid ammonia at 25 °C.

Alkyl halide substrate	**k_{obs} (s^{-1})**	**$t_{1/2}$ (min)**
4-methylbenzyl chloride	$7.87x10^{-4}$	14.7
benzyl chloride	$9.18x10^{-4}$	12.6
4-chlorobenzyl chloride	$9.78x10^{-4}$	11.8
4-carbomethoxybenzyl chloride	$1.10x10^{-3}$	10.5
4-cyanobenzyl chloride	$1.33x10^{-3}$	8.7
4-nitrobenzyl chloride	$1.53x10^{-3}$	7.6
3-methoxybenzyl chloride	$7.80x10^{-4}$	14.8
4-methoxybenzyl chloride	$1.92x10^{-3}$	6
α-methyl benzyl chloride	$6.72x10^{-6}$	1719
α-methyl 4-methoxybenzyl chloride	$9.70x10^{-4}$	11.9

A Hammett plot for the ammonolysis reaction data in Table 1.3.1 for the para-substituted benzyl chlorides gives a slope (ρ value) of zero. This is in contrast to the same compounds in water which give a slope of around – 4.6. This data suggests that for the solvolysis of benzyl chlorides in liquid ammonia, there is little or zero charge developed on the central carbon atom in the transition state. This is indicative of a bimolecular, S_N2 type mechanism whereby any charge developed due to partial fission of the bond to the leaving group is counterbalanced by an equal transfer of charge from the incoming nucleophile.

Similarly, liquid ammonia can be used as a solvent for the reaction of alkyl halides with nitrogen nucleophiles (Scheme 1.3.11).

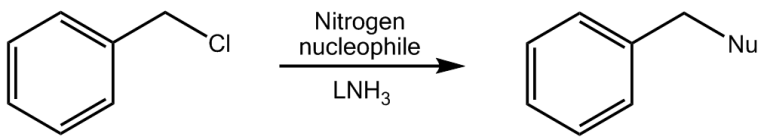

Scheme 1.3.11

P. Ji investigated the effect of varying the nitrogen nucleophile on the rate of reaction and, interestingly, found that the second order rate constants were not greatly sensitive to the nature of the nucleophile (Table 1.3.2).

Table 1.3.2 Second order rate constants for the reaction of benzyl chloride with various nitrogen nucleophiles in liquid ammonia at 25 °C.

nucleophile	k_2 ($M^{-1}s^{-1}$)
pyrrolidine	$2.67x10^{-2}$
piperidine	$1.70x10^{-2}$
morpholine	$3.24x10^{-3}$
sodium azide	$7.73x10^{-3}$
sodium triazolate	$9.42x10^{-3}$
sodium benzotriazolate	$2.61x10^{-3}$
sodium imidazolate	$5.56x10^{-2}$
hydrazine	$5.14x10^{-3}$

Aryl halides tend to be more difficult to convert to primary amines in ammonia and require elevated temperatures and catalysts. US patent 2,001,284 uses gaseous ammonia with ammonium tungstate and cupric chloride as catalyst to prepare aniline from chlorobenzene (Scheme 1.3.12).[65]

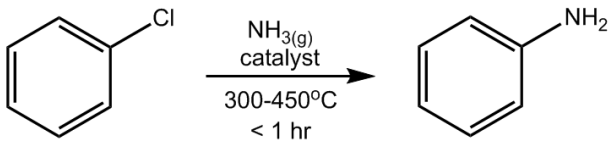

Scheme 1.3.12

For molecules with sensitive functional groups, common in agrochemical and pharmaceutical intermediates, these high temperature conditions are often unsuitable.

In liquid ammonia, P. Ji used copper (I) iodide and ascorbic acid as catalysts for the ammonolysis of halobenzenes at a comparatively moderate temperature (100 °C, 18 hr). [66]

1.3.2.2 Ammonolysis of ketones

Pinck et al found that benzophenone shows no reaction in liquid ammonia after several weeks at ambient temperature. [67] Sterically hindered aliphatic ketones and aryl alkyl ketones react very slowly in liquid ammonia, especially in the absence of any

catalyst. For example, acetophenone gives a low conversion to acetophenone-imine after heating at 180 °C for 4 hr (Scheme 1.3.13). [68]

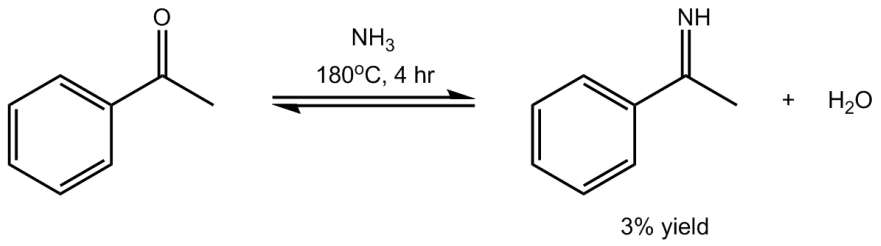

Scheme 1.3.13

With the addition of excess aluminium chloride, a higher yield of 30 % was observed and the method can be applied to a number of other ketones such as fenchone, camphor and methyl-p-tolyl ketone (Scheme 1.3.14)

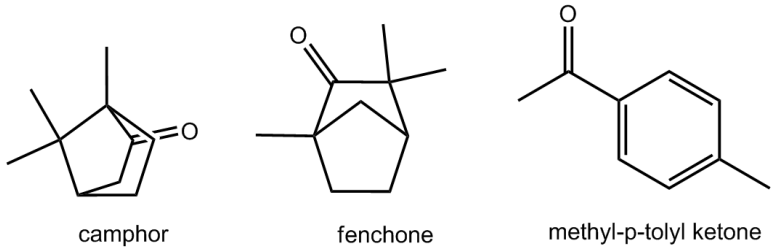

Scheme 1.3.14

P. Ji showed that ammonium salts can increase the yields with a reduced temperature and reaction time. [69] With added ammonium chloride, benzophenone was converted to the imine with a yield > 80 % after 12 hr in liquid ammonia at room temperature. The yield is dependent on NH_4Cl concentration and P. Ji proposed that this could be for two reasons; firstly, the ammonium ion may act as a Lewis acid to activate the carbonyl group, facilitating attack from the ammonia nucleophile; secondly, it may significantly shift the equilibrium to the formation of the imine by removing water from the system (Scheme 1.3.15).

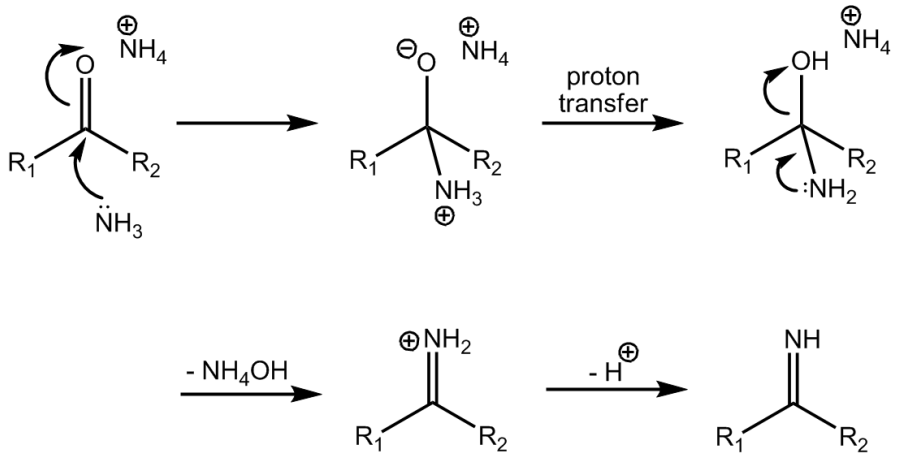

Scheme 1.3.15

Other catalytic processes have been explored to convert ketones to imines and give high yields with much reduced reaction times. Titanium dioxide (anatase) has been used as the catalyst in a process patented by BASF for the conversion of benzophenone to the imine with yields > 95 % (Scheme 1.3.16). [70] Imine products are very useful commodities as intermediates for primary amine synthesis via reduction in liquid ammonia.

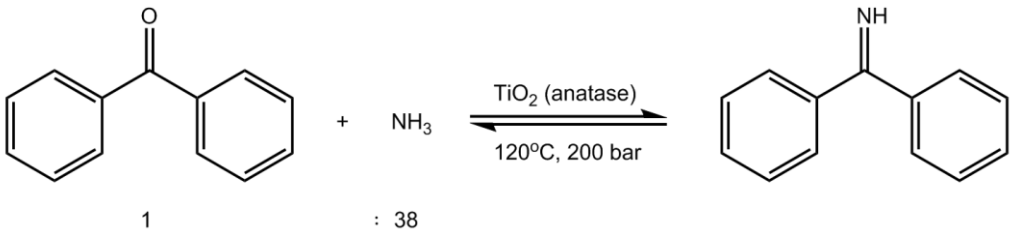

Scheme 1.3.16

1.3.2.3 Amide synthesis

Like amines, the carboxylic amide group is an important functional group found widely in raw materials for industrial production, pharmaceuticals and many consumer products. In the field of medical research, a recent patent describes the high anti-tumor effects of N-vanillyl fatty acid amides, which are themselves similar in structure to Capsaicin, the active component of chilli peppers (Scheme 1.3.17).[71, 72]

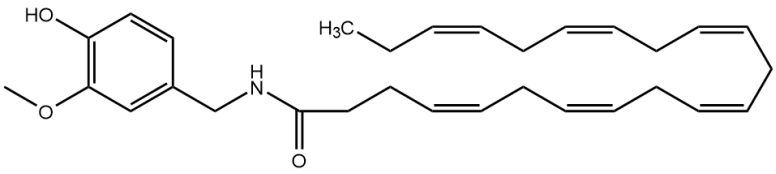

Anti-tumor agent

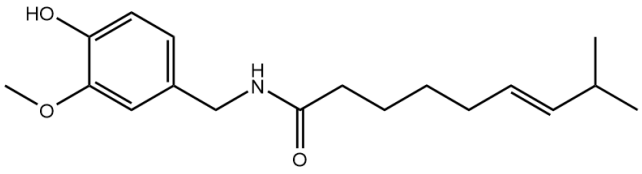

Capsaicin

Scheme 1.3.17

Additionally, capsaicinoids, with highly effective irritant properties, have found widespread use in chemical warfare, deployed primarily for personal protection and riot control. [73] The amide group is also a key functional group of many herbicides used in the agrochemical industry such as Isoxaben and Propyzamide. [74] Thus the synthesis methods for amides are of high importance to the chemical industry,

Amides can be prepared in a number of ways, from both ester and non-ester starting materials.

One of the most common synthesis methods for amides using a non-ester starting material is the Schotten-Baumann reaction. First described by C. Schotten and E. Baumann in 1883, this reaction uses an acyl chloride and amine to prepare amides (Scheme 1.3.18). [75, 76]

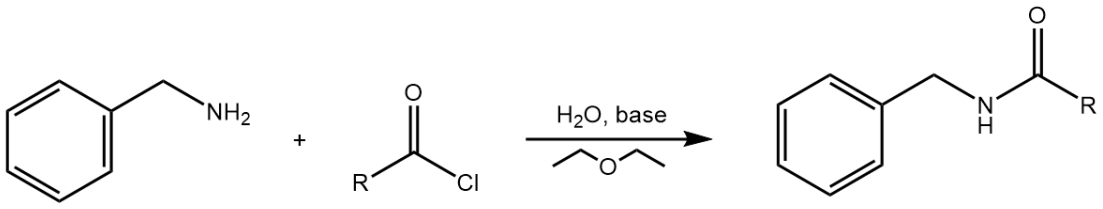

Scheme 1.3.18

Amides can be prepared by the direct amidation of carboxylic acids with an amine, but generally require elevated temperatures to remove water (Scheme 1.3.19). [77]

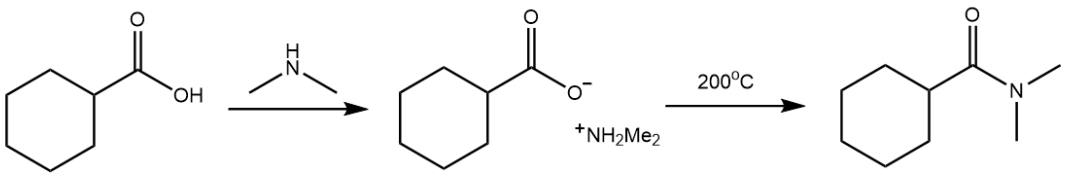

Scheme 1.3.19

Veitch et al showed that a number of primary amides can be prepared from esters using magnesium nitride as a source of ammonia with good yields obtained (Scheme 1.3.20). [78]

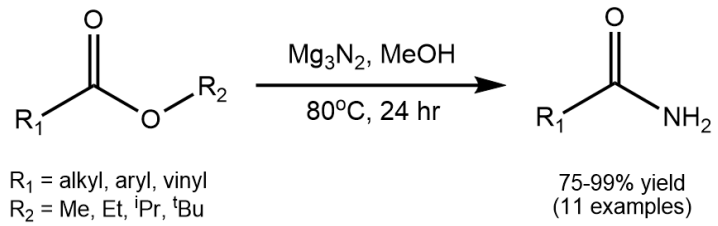

Scheme 1.3.20

Primary amides can be prepared by reacting esters in liquid ammonia with the liberation of amide and alcohol (Scheme 1.3.21)

Scheme 1.3.21

The ammonolysis of esters is discussed in further detail in Chapter 3.

Chapter 2 - Experimental

2.1 Materials and synthesis

2.2 High pressure equipment for liquid ammonia

2.3 Instruments and other equipment

2.4 General procedures

2.1 Materials and synthesis

2.1.1 General

The majority of organic and inorganic chemicals were purchased from commercial providers Sigma-Aldrich and Acros and were used directly without any further purification. Solvents were of Reagent or HPLC grade and likewise were purchased from general commercial providers and were used without any further purification.

Candida antarctica Lipase B (CALB) was obtained from Sigma-Aldrich as immobilised lipase on acrylic resin beads (also known as Novozyme 435). The macroporous beads have a diameter of 0.3-0.9 mm and their activity was reported as 11075 units per gram of bead. Lipases from Candida rugosa and Candida antarctica in powdered form were also obtained from Sigma.

Lewatit VP OC 1600 support beads (enzyme free) were supplied by Lanxess, Germany and were oven dried (≈ 90 °C) prior to use.

Liquid ammonia was purchased from BOC Ltd. and has 99.98 % purity with small levels of moisture (<200 ppm) and also some oil impurities (<5 ppm). [79] Once distilled from the ammonia cylinder to the condensing vessel, no further purification was required prior to use.

2.1.2 Preparation of esters for ammonolysis reactions

2.1.2.1 Preparation of aryl benzoates (Scheme 2.1.1)

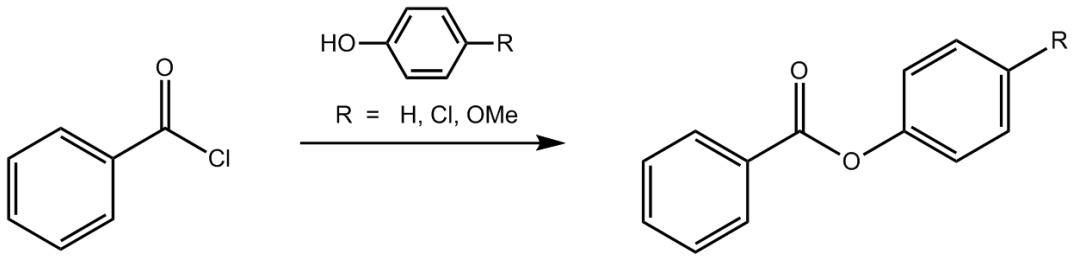

Scheme 2.1.1

The general method for the preparation and purification of phenyl benzoate, 4-methoxyphenyl benzoate and 4-chlorophenyl benzoate was as follows: benzoyl chloride (5 ml, 43 mmol) was added in portions to the phenol (~50 mmol) in a 50 ml

conical flask. The mixture was shaken vigorously and left for 24 hr. The white precipitate was isolated by Büchner filtration and washed through with water. The ester was then dissolved in DCM with a further water wash (liquid-liquid extraction). The DCM was removed under rotary evaporation and fine ester crystals oven dried (50 °C) to constant mass. Purity was measured using GC-MS (>99 %). An example of GC-MS chromatogram and spectrum with NIST library match for phenyl benzoate can be seen in Figure 2.1.1 and Figure 2.1.2.

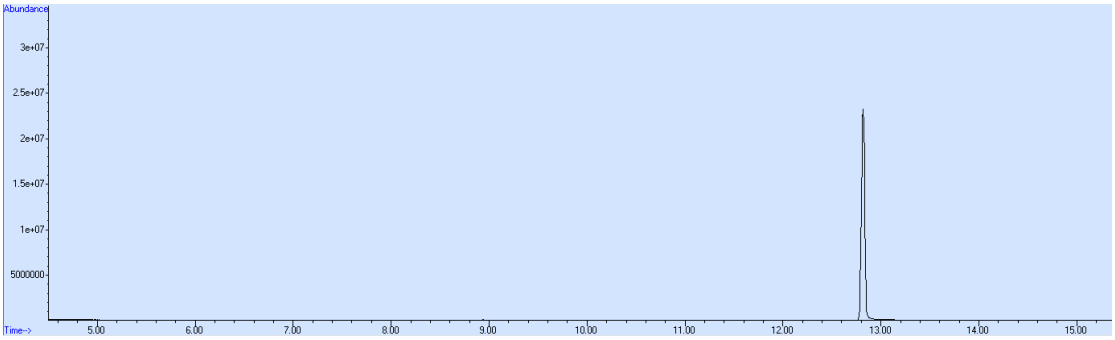

Figure 2.1.1 GC-MS chromatogram for phenyl benzoate giving peak purity of > 99 %.

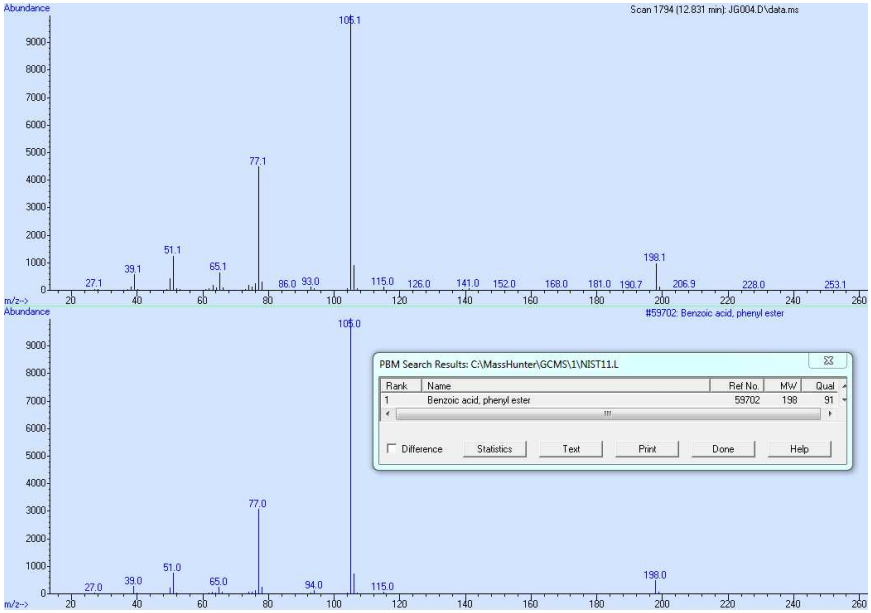

Figure 2.1.2 Mass spectrum of phenyl benzoate with positive match to the NIST database m/z = 198.0.

Aryl benzoates were characterised by MS, NMR, IR and melting point analysis. Phenyl benzoate and 4-chlorophenyl benzoate are not novel compounds and so, where

possible, analytical data and physical properties are compared to those in literature. The bulk of available data is from online commercial suppliers and chemical databases. 4-methoxyphenyl benzoate appears to be a novel compound.

Phenyl benzoate: observed m/z =198.1; ^{1}H NMR (400 MHz, $CDCl_3$, relative to TMS δ = 0): δ = aromatic hydrogens 7.25 (m, 3H), 7.44 (m, 2H), 7.52 (m, 2H), 7.65 (m, 1H), 8.21 (m, 2H)[80]; ^{13}C NMR (100 MHz, $CDCl_3$, relative to TMS δ = 0): δ = aromatic carbons 121.8, 125.9, 128.5, 129.5, 130.1, 133.6, 150.9, carbonyl carbon: 165.2 [80]; IR C=O stretch 1725 cm^{-1} [80, 81]; m.p 69 °C [82]; white needle-like crystals.

4-cholorophenyl benzoate: observed m/z = 232.0; ^{1}H NMR (400 MHz, $CDCl_3$, relative to TMS δ = 0): δ = aromatic hydrogens 7.17 (m, 2H), 7.39 (m, 2H), 7.52 (m, 2H), 7.65 (m, 1H), 8.19 (m, 2H); ^{13}C NMR (100 MHz, $CDCl_3$, relative to TMS δ = 0): δ = aromatic carbons 123.1, 128.6, 129.5, 130.2, 131.3 133.8, 149.4, carbonyl carbon: 164.9; IR C=O stretch 1727 cm^{-1} [83]; m.p 88 °C [84]; white flake-like crystals.

4-methoxyphenyl benzoate: observed m/z = 228.1; ^{1}H NMR (400 MHz, $CDCl_3$, relative to TMS δ = 0): δ = 3.83 (s, 3H, methyl R-O-CH_3), aromatic hydrogens 6.94 (m, 2H), 7.13 (m, 2H), 7.51 (m, 2H), 7.63 (m, 1H), 8.20 (m, 2H); ^{13}C NMR (100 MHz, $CDCl_3$, relative to TMS δ = 0): δ = 55.6 (methyl R-O-CH_3), aromatic carbons 114.5, 122.5, 128.6, 130.2, 133.5, 144.2 157.3, carbonyl carbon 165.6; IR C=O stretch 1729 cm^{-1}; m.p = 90 °C; white powder.

2.1.2.2 Preparation of alkyl phenylacetates (Scheme 2.1.2)

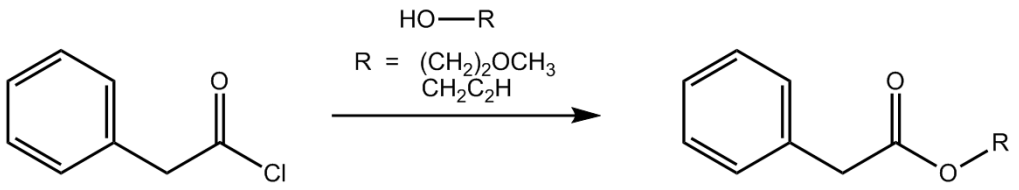

Scheme 2.1.2

The general method for the preparation and purification of 2-methoxyethyl phenylacetate and propargyl (2-propyn-1-ol) phenylacetate was as follows: Phenyl acetyl chloride (3 ml, 22 mmol) was added in portions to the alcohol (~30 mmol). The set-up in Figure 2.1.3 was used to form a white smoke of ammonium chloride by blowing in ammonia gas and compressed air.

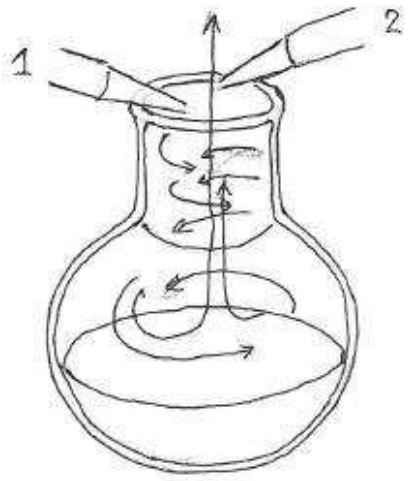

Figure 2.1.3 Set up for the preparation of phenylacetate esters. Compressed air (1) and ammonia gas (2). Courtesy of Dr. H. Sun.

Ammonium chloride and the amide from the acid chloride and ammonia are both insoluble in the liquid ester product. The slurry is filtered by syringe filter and was solubilised in DCM and further washed with water. DCM was removed by rotary evaporation to leave an oily ester product. GC-MS was used to confirm purity of compounds (>98 %). Figure 2.1.4 shows and example of a GC-MS chromatogram for propargyl phenylacetate and Figure 2.1.5 shows the mass spectrum obtained for propargyl phenylacetate.

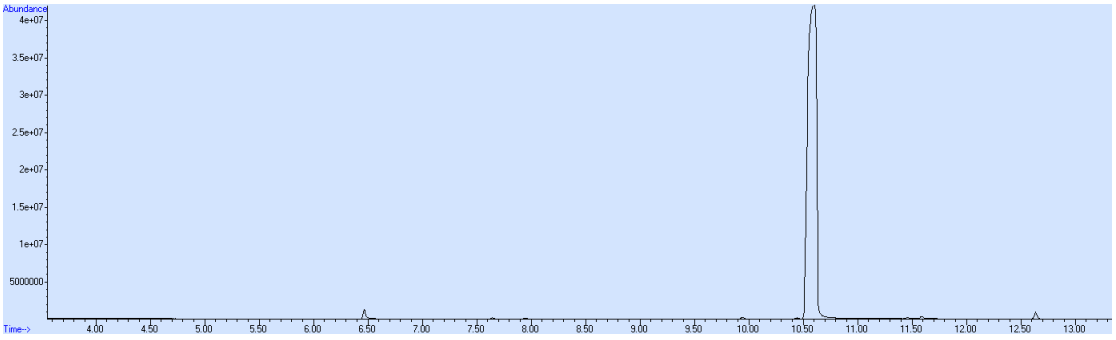

Figure 2.1.4 GC-MS chromatogram for propargyl phenylacetate giving peak purity of > 98 %.

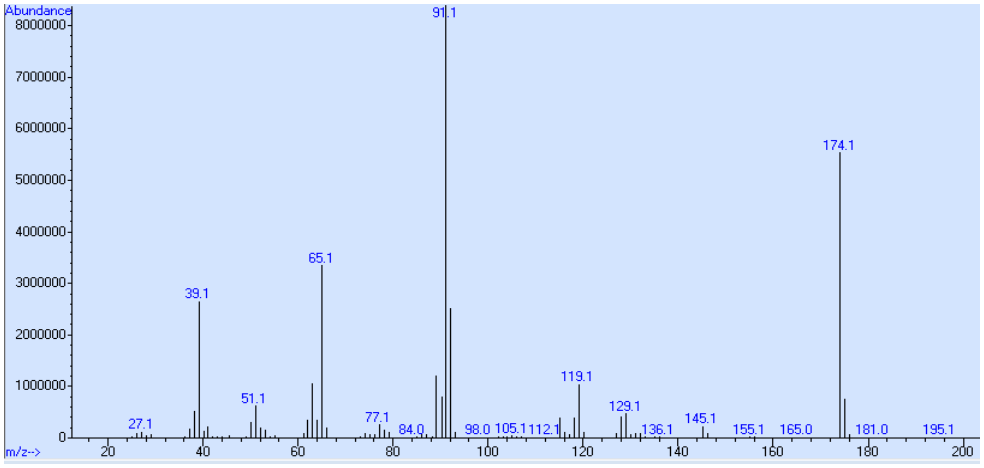

Figure 2.1.5. Mass spectrum for propargyl phenylacetate m/z = 174.1.

The alkyl phenylacetates appear to be novel compounds and so where characterised by MS, NMR and IR.

Methoxyethyl phenylacetate: observed m/z = 194.1; ^{1}H NMR (400 MHz, DMSO-d_6, relative to TMS δ = 0): δ = 3.25 (s, 3H, methyl R-O-CH_3), 3.52 (t, 2H), 3.69 (s, 2H), 4.16 (t, 2H), aromatic hydrogens 7.2-7.4 (m, 5H); ^{13}C NMR (100 MHz, DMSO-d_6, relative to TMS δ = 0): δ = 40.6, 58.5, 63.9, 70.1, aromatic carbons 127.2 128.7, 129.7, 133.7, carbonyl carbon 171.6; IR C=O stretch 1737 cm^{-1}; colourless oil.

Propargyl phenylacetate: observed m/z = 174.1; ^{1}H NMR (400 MHz, DMSO-d_6, relative to TMS δ = 0): δ = 3.51 (t, 1H), 3.70 (s, 2H), 4.7 (d, 2H), aromatic hydrogens 7.2-7.4 (m, 5H); ^{13}C NMR (100 MHz, DMSO-d_6, relative to TMS δ = 0): δ = 40.3, 52.4, alkyne carbons 78.2 and 78.8, aromatic carbons 127.3, 128.8, 129.8, 134.4, carbonyl carbon 170.9; IR C=O stretch 1736 cm^{-1}, C≡C stretch 2125 cm^{-1}, H-C≡ stretch 3287 cm^{-1}; pale orange oil.

2.1.3 Preparation and characterisation of surfactants for aggregation studies

2.1.3.1 Decyltrimethylammonium iodide (DTAI) (Scheme 2.1.3)

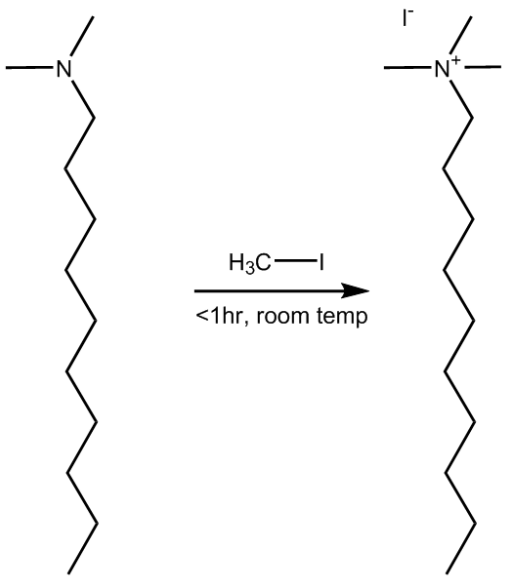

Scheme 2.1.3

In a 25 ml round bottom flask, DTAI was prepared by the reaction of N,N-dimethyldecylamine (2 ml, 0.00841 mol) with excess methyl iodide (5 ml, 0.0807 mol) at room temperature for approximately 1 hr. The white solid product was washed repeatedly with DCM and filtered under vacuum. Excess solvent was removed by oven drying to constant mass (90 °C, 72 hr). Mass (yield %) = 2.41 g (87 %).GC-MS was used to confirm the sample contained none of the methyl iodide and N,N-dimethyldecylamine reactants - a blank chromatogram was observed.

DTAI appears to be a novel compound and so was characterised as follows:

ESI-MS was used to confirm the accurate mass of the compound (Figure 2.1.6).

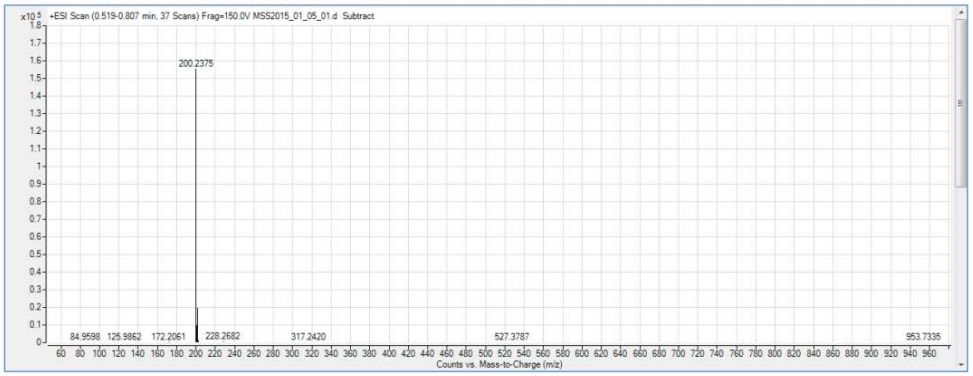

Figure 2.1.6 Mass spectrum of compound. Observed major ion m/z = 200.2375 and observed neutral mass = 200.2380, consistent with decyltrimethylammonium cation (200.2378 g/mol). Mass difference = -1.04 ppm.

NMR was also used to confirm the structure of DTAI with ^{1}H NMR peaks integrating to the correct number of hydrogens and ^{13}C NMR DEPT-135 for analysis of -CH_2/-CH_3 groups:

^{1}H NMR (400 MHz, D_2O, relative to TSP $\delta = 0$): $\delta = 0.9$ (t, 3H), 1.3 (m, 14H), 1.8 (m, 2H), 3.1 (s, 9H), 3.3 (t, 2H); ^{13}C NMR (100 MHz, D_2O, relative to TSP $\delta = 0$): $\delta =$ 16.2 (CH_3), 24.9 (CH_2), 25.0 (CH_2), 28.2 (CH_2), 30.9 (CH_2), 31.2 (CH_2), 31.3 (CH_2), 31.4 (CH_2), 34.0 (CH_2), 55.5 (3 x CH_3), 69.6 (CH_2); IR: C-H stretch 2900 cm^{-1}, C-H bend 1474 cm^{-1}; m.p 196 °C; white powder.

2.1.3.2 Perfluorinated fatty acid amides (Scheme 2.1.4)

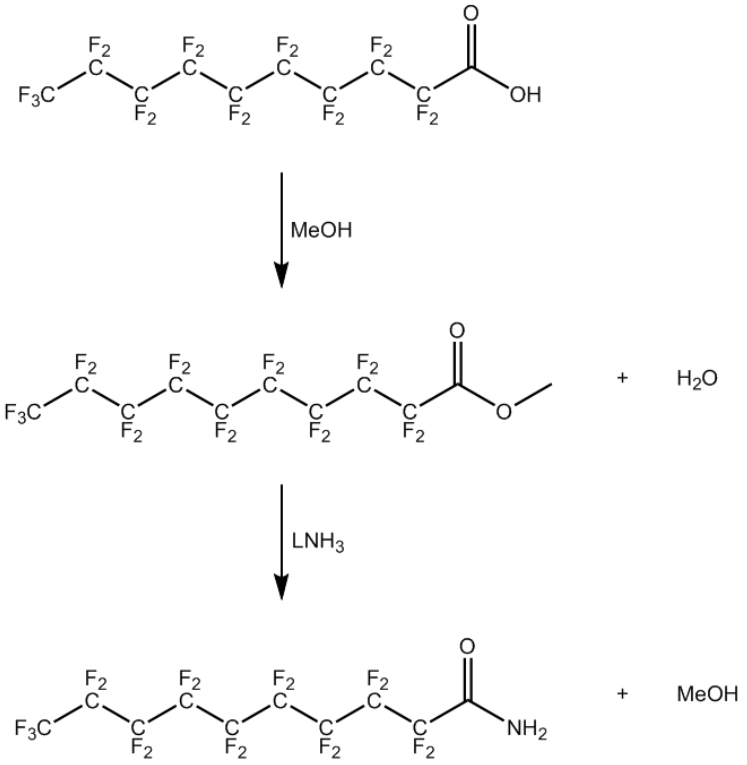

Scheme 2.1.4

Fluorinated amides used for micelle studies in liquid ammonia were either difficult to obtain from the usual commercial sources or were generally too expensive for the quantity required so that their synthesis, purification and characterisation was favoured. Perfluorinated amides were prepared directly from the reaction of the methyl ester in liquid ammonia, or in some cases where the methyl ester was not available, it was itself synthesised from the carboxylic acid.

For example, methyl perfluorodecanoate (C_{10}) was prepared by the following procedure:

Perfluorodecanoic acid (5 g, 0.0097 moles), obtained from Apollo Scientific, was heated in neat methanol (20 ml) at 50 $^{\circ}$C and the reaction monitored by GC-MS until no more acid was observed. When undisturbed, a phase separation was visible between the liquid ester and methanol, highlighting the relatively poor miscibility of fluorinated compounds even in organic solvents. The methyl ester layer was carefully removed by pipette and isolated by liquid-liquid extraction into DCM with a further water wash to remove any traces of the water by-product and methanol. The DCM

was removed under vacuum by rotary evaporation which would also remove any remaining methanol and the ester structure was confirmed by GC-MS with positive match to the NIST database. The purity was measured by GC-MS (>99 %). Mass obtained = 4.243 g (yield 83 %).

Procedure for fluoroamide synthesis was as follows:

Perfluorinated fatty acid methyl ester (approx. 2 g, 0.005 moles) was reacted in liquid ammonia (20 ml) at room temperature for 24 hr. GC-MS was used to monitor the reaction to confirm disappearance of the ester. Ammonia was allowed to evaporate and the white powdered product was solubilised in DCM and washed with water. After rotary evaporation to remove excess DCM and methanol, the powder was oven dried to constant mass (90 °C, 48 hr).

Yields (%), appearance

Perfluoroheptanamide (C_7): 1.540 g (88 %), white powder.

Perfluorooctanamide (C_8): 1.821 g (89 %), white powder.

Perfluorononanamide (C_9): 2.280 g (93 %), white powder.

Perfluorodecanamide (C_{10}): 1.816 g (86 %), white powder.

Characterisation of fluoroamides:

Some of the fluorinated amides are available from online suppliers but, apart from some melting points provided in the MSDS (material safety data sheets), their characterisation data and other properties does not appear to be readily available. Therefore, the newly synthesised fluoroamides were characterised as follows:

ESI-MS was used for accurate mass analysis. An example of an ESI-MS trace for the C_7 fluoroamide can be seen in Figure 2.1.7 and full ESI-MS data for all fluoroamides is in Table 2.1.1.

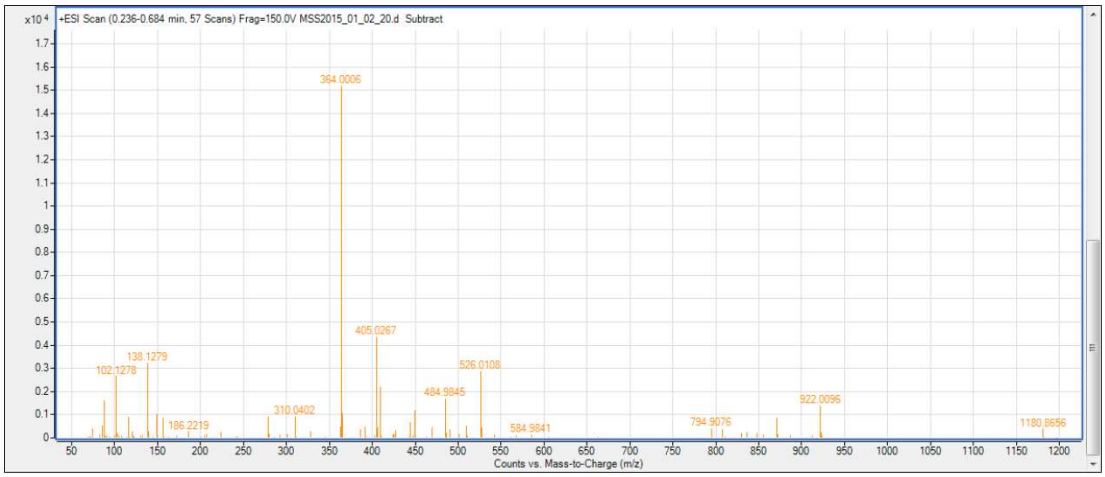

Figure 2.1.7 ESI-MS of perfluoroheptanamide. Major m/z = 364.0006 $[M+H]^+$.

Table 2.1.1 ESI-MS data for fluoroamides.

Fluoroamide carbons	Major peak observed m/z [as ion]	Observed neutral mass	Theoretical neutral mass	Mass difference (ppm)
7	364.0006 $[M+H]^+$	362.9933	362.9929	-1.16
8	413.9974 $[M+H]^+$	412.9902	412.9897	-1.16
9	481.0214 $[M+NH_4]^+$	462.9874	462.9865	-1.86
10	513.9908 $[M+H]^+$	512.9839	512.9833	-1.21

The fluoroamides were also characterised by NMR and Table 2.1.2 shows ^{19}F NMR chemical shifts, multiplicity and integration data for the fluoroamides.

Table 2.1.2 ^{19}F NMR data for fluorinated amides (400 MHz, DMF, relative to trifluoroacetic acid δ = -75.51).

Fluoroamide carbons	^{19}F shift ppm (multiplicity, number of fluorines from integration)†			
	terminal -CF_3	α -CF_2	'middle' -CF_2-	-CF_2 adjacent to terminal
7	-80.4 (t, 3F)	-118.4 (t, 2F)	-121.8 (m, 6F)	-125.7 (m, 2F)
8	-80.6 (t, 3F)	-118.3 (t, 2F)	-121.8 (m, 8F)	-125.7 (m, 2F)
9	-80.8 (t, 3F)	-118.6 (t, 2F)	-121.9 (m, 10F)	-125.8 (m, 2F)
10	-80.8 (t, 3F)	-118.6 (t, 2F)	-122.0 (m, 12F)	-125.9 (m, 2F)

†^{19}F NMR chemical shifts, multiplicity and integration patterns were consistent with those of aqueous solutions of fluorinated carboxylates in the literature.[85]

Table 2.1.3 Melting points and IR analysis of fluoroamides.

Fluoroamide carbons	m.p (°C)	IR shifts (cm^{-1})		
		C=O	N-H stretch	N-H bend
7	121[a]	1703	3194 +3373	1633
8	138[b]	1702	3195 + 3373	1633
9	151	1702	3192 + 3374	1632
10	160[c]	1703	3194 + 3373	1633

[a][b][c] melting points consistent with MSDS data from online suppliers.[86, 87, 88]

GC-MS was used to check purity (Figure 2.1.8) and confirm removal of MeOH. All fluorinated amides gave a peak purity of > 98 %.

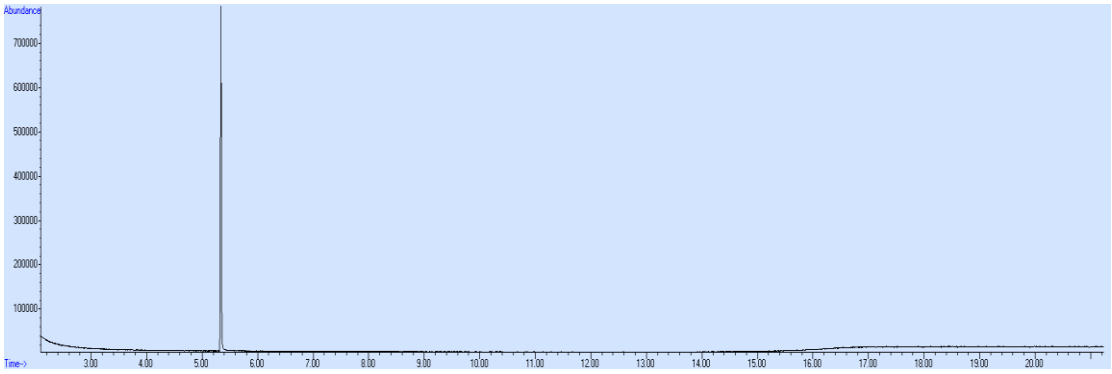

Figure 2.1.8 GC-MS chromatogram of perfluoroheptanamide in DCM.

2.2 High pressure equipment for liquid ammonia

2.2.1 Reaction vessels, glassware and cells

2.2.1.1 Burettes and condenser vessels

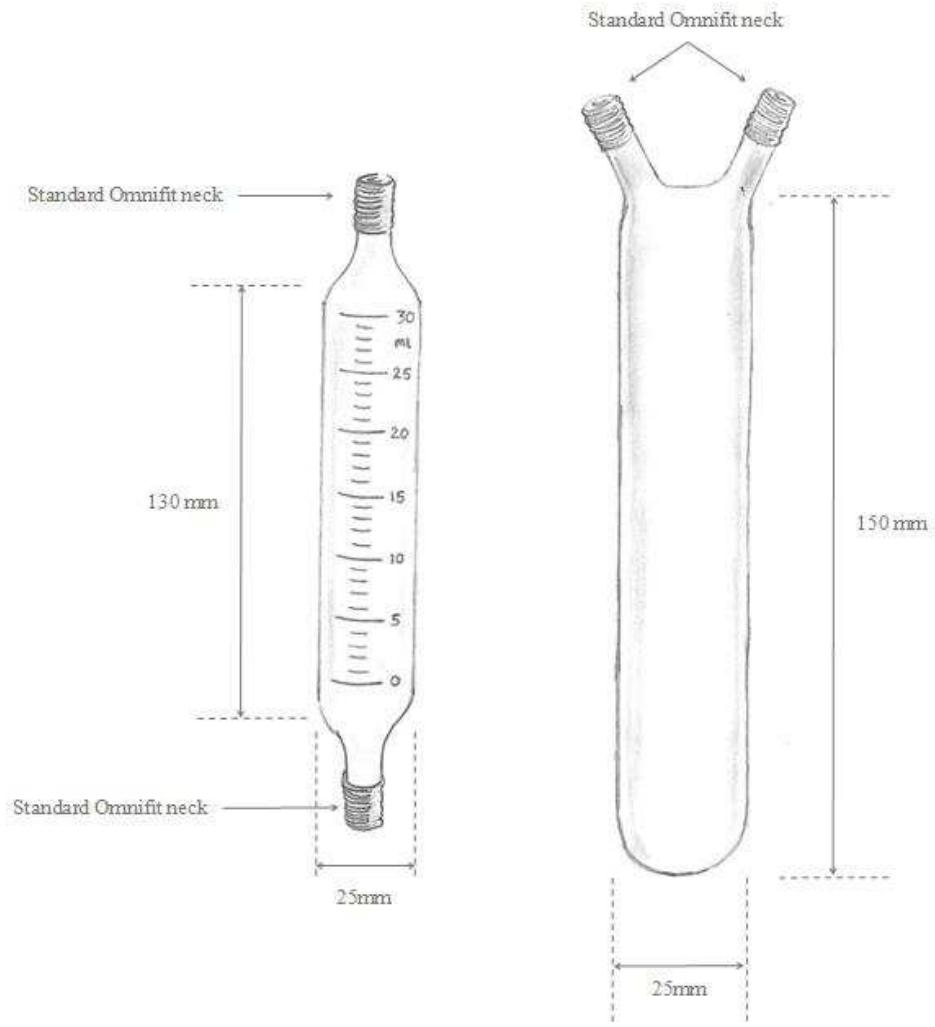

Figure 2.2.1 Burette (left) and ammonia condensing vessel (right).

Glassware was supplied by either Hampshire Glassware (R&D) Ltd. (Southampton, UK) or Cambridge Glassblowing Ltd. (Cambridge, UK). All glassware used for reactions in liquid ammonia at around room temperature was pressure tested up to 35 bar using a HPLC pump (see safety section in Appendix 7.1 for full details). The ammonia condensing vessel was not calibrated and had a total volume capacity of approximately 40 ml, whereas the burette was calibrated, with a total volume of around 30 ml (Figure 2.2.1). The calibration of the burette permitted a minimum volume of 0.5 ml and allowed reasonable accuracy when dispensing liquid ammonia for reactions, as usually 5-10 ml was required. The condensing vessel and burette were fitted with standard Omnifit thread adaptors (1/4") which allowed for gas tight connections between glassware via PTFE tubing and valves.

2.2.1.2 Reaction Vessels

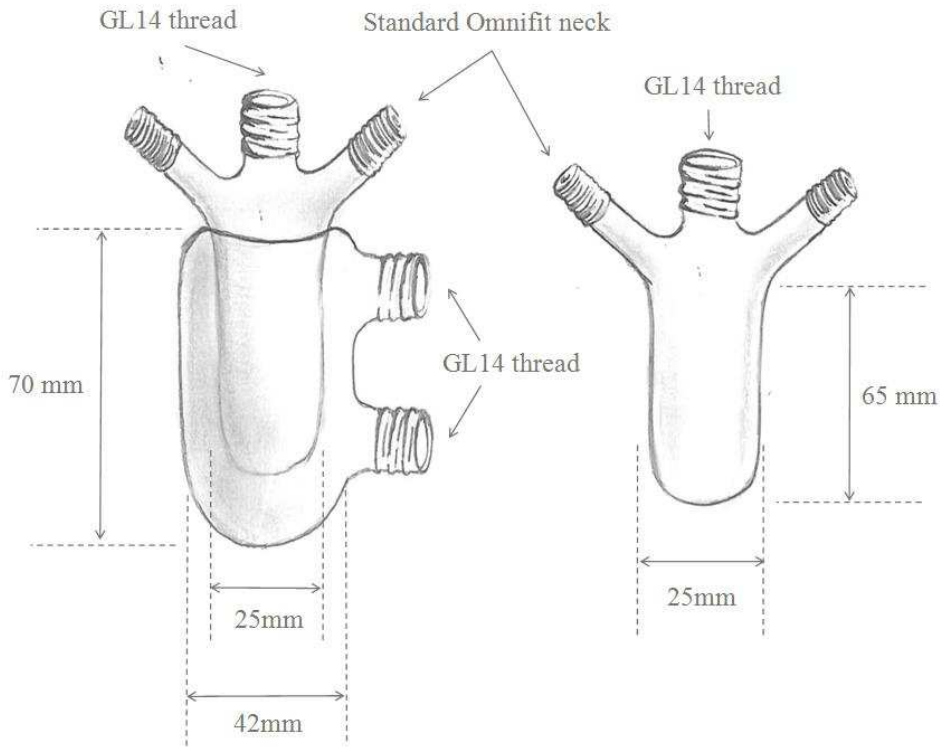

Figure 2.2.2 High pressure rated jacketed (left) and non-jacketed (right) vessels for reactions in liquid ammonia.

Reaction vessels were acquired from the same glass suppliers as above and likewise were pressure tested to the same capacity. For general liquid ammonia reactions, two types of vessels were used (Figure 2.2.2). A jacketed vessel was used for reaction kinetics, whereby the temperature in the vessel could be regulated, and a non-jacketed

vessel was available for other reactions where temperature control was not vital, such as in the preparation of the fluorinated amides. Both vessels had a total volume capacity of approximately 15 ml and usually the maximum volume used was roughly 10 ml. The vessels were equipped with a standard GL14 screw fitting, which can be fitted with a GL14 screw-on lid. The lid comprised of a silicone rubber seal coated in PTFE which was inert to the ammonia and other chemicals used in the vessel. Likewise, the reaction vessels were equipped with the standard Omnifit thread adaptor necks for easy connection between reaction vessels, burette and condensing vessel. This allowed for easy sampling of reactions under pressure via tubing, venting solutions and injecting through a septa to initiate reactions.

The glassware/reaction-vessel used for the conductivity measurements was similar to that used for the general room temperature reactions (ester solvolysis etc.). It was, likewise, supplied by HGL, fitted with 2 standard Omnifit necks and equipped with a thermo jacket for the necessary temperature regulation. The neck of the reaction vessel however was a larger standard GL18 thread to allow the conductivity probe to fit tightly into the vessel through a GL18 hollowed screw cap.

2.2.1.3 NMR tubes

High pressure, quick valve NMR tubes (Figure 2.2.3) were purchased through Sigma-Aldrich (supplier Wilmad-Lab Glass) and were pressure rated to 14 bar (200 psi). They are designed specifically for 500 MHz NMR instruments with a tube length of 7 inches, outside diameter (O.D.) of 5 mm and wall thickness of 0.38 mm. The top inlet valve of the pressure tube has a standard Swagelok connection allowing for easy connection to the Omnifit apparatus and thus practical and safe charging of the NMR tube from the reaction vessel.

Figure 2.2.3 Diagram of high pressure NMR tube.

2.2.1.4 UV cell

Figure 2.2.4 High pressure UV cell for liquid ammonia studies

The high pressure UV cell was designed by J. Griffin and Dr. H. Sun and constructed by the University of Huddersfield Engineering department using a CNC (Computer Numerical Control) cutting machine. It is cut out of a solid aluminium block and has Swagelok threads allowing for easy connection to the Omnifit apparatus and reaction vessels. The windows were made from Quartz glass (diameter 10 mm, width 3 mm) supplied by UQG Optics. The window frame was sealed tightly with PTFE O-rings (I.D 6 mm, C.S 1 mm) supplied by Polymax.

2.2.2 Other

2.2.2.1 High pressure syringe

To maximise accuracy with kinetic measurements, reactions were initiated by injection of the substrate into the liquid ammonia vessel. The high pressure syringe was obtained from SGE, has a total volume capacity of 1 ml, with the minimum volume unit of 0.01 ml. It is pressure rated to 33 bar (500 psi) and is equipped with a special side-hole needle with a length of 71 mm and an outside diameter of 1.07 mm. The syringe has a standard Swagelok fitting and a gas tight PTFE on/off valve.

Figure 2.2.5 High pressure syringe obtained from SGE analytical science

2.3 Instruments and other equipment

2.3.1 General

2.3.1.1 Thermo regulator

For the majority of liquid ammonia reactions, where temperature regulation was required (kinetics), the temperature was controlled at 25 °C. Conductometric studies were performed at -15 °C. The vessel with the jacket allows connection to a thermo regulator. The thermo regulator used was a Huber-Unistat Tango Nuevo (Figure 2.3.1) which allows temperature control of the reaction vessel ranging from -40 °C to

200 °C with good accuracy (± 0.01 °C). Silicone based thermo oil is used in the vessel jacket.

Figure 2.3.1 Thermo regulator Huber-Unistat Tango Nuevo for accurate temperature regulation

2.3.2 Analytical

2.3.2.1 GC-FID/GC-MS

Gas chromatography was used in this project to monitor reactions, identify products and assist characterisation of newly synthesised compounds. For quantitative analysis (purity and monitoring reactions), an Agilent Series 7980 GC with flame ionization detection (FID) was used. When identification of products/reactants was required (qualitative analysis), Agilent Series 7890A GC with MS or QQQ was available. This could also be used to monitor reactions but is generally not as accurate for quantitative analysis as the GC-FID. The choice of column and oven parameters used for a particular GC analysis was dependant on the analyte of interest such as its polarity or boiling point. For the typical analysis of an ester ammonolysis reaction, the parameters would be as follows:

Column:	Agilent J+W 19091J-433 HP-5
Dimensions:	30 m x 0.25 mm x 0.25 µm
Inlet:	250 °C
Split ratio:	50:1

Injection volume:	10 µl
Carrier:	Helium (16.1 psi, 1.5 mL/min)
Oven initial (hold):	45 °C (2 minutes)
Ramp rate:	20 °C/min up to 320 °C
Oven end (hold):	320 °C (2 minutes)

The software used for GC-FID and GC-MS data acquisition and analysis was Agilent Chemstation and Enhanced Mass Hunter, respectively. Figure 2.3.2 shows a TIC (total ion content) gas chromatogram from a typical reaction sample, from which the peaks can then be identified using a NIST MS Search 2.0 mass spectral library (Figure 2.3.3).

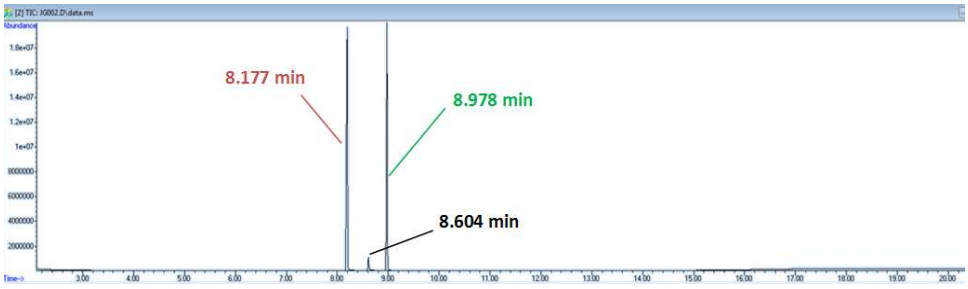

Figure 2.3.2 TIC gas chromatogram obtained from GC-MS analysis of a sample from the ammonolysis of propargyl benzoate in liquid ammonia at 25 °C.

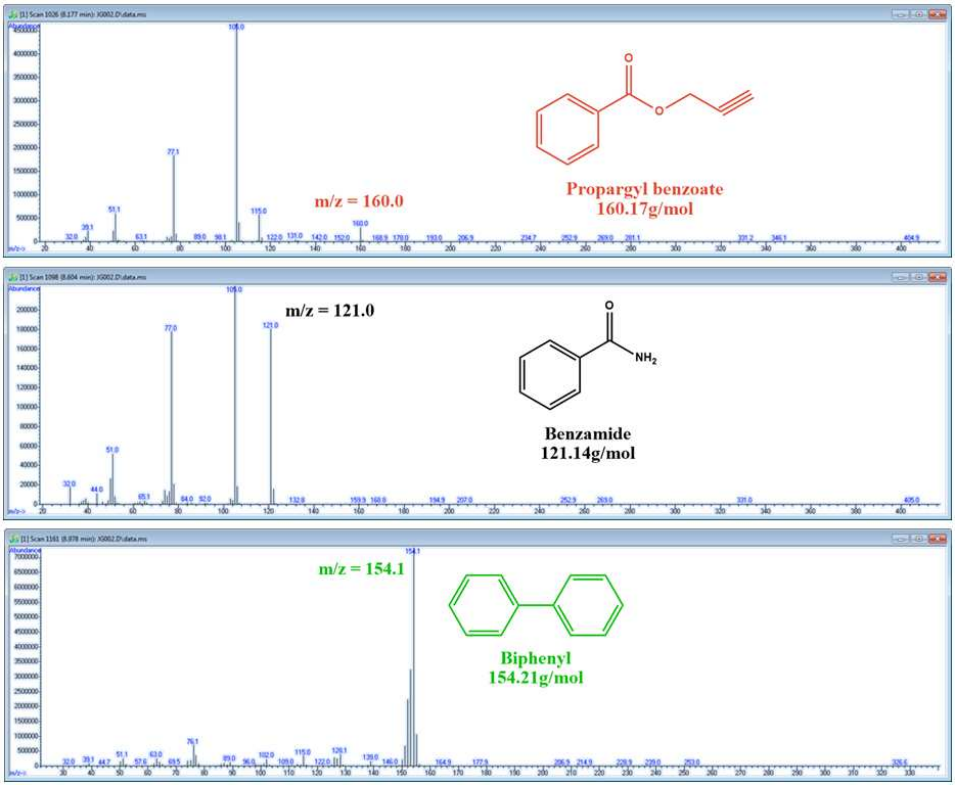

Figure 2.3.3 NIST MS Search 2.0 library identification of ester, amide and internal standard from the TIC in Figure 2.3.2.

GC oven parameters for oleamide analysis:

Oven initial (hold):	40 °C (2 minutes)
Ramp rate:	5 °C/min up to 80 °C
	7 °C/min up to 160 °C
	9 °C/min up to 200 °C
	20 °C/min up to 280 °C
Oven end (hold):	280 °C (10 minutes)

2.3.2.2 Conductivity cells

For conductivity measurements, 2 types of cell were used (Figure 2.3.4). A 5-ring conductivity cell with a PEEK (polyether ether ketone) shaft was supplied by Metrohm. A glass bodied conductivity cell (K=1) with platinum electrodes was obtained from Jenway. Before experiments, the cell was calibrated using a 0.01 M

potassium chloride solution in water which gives a conductance of 1413 µS/cm at 25 °C.

Figure 2.3.4 Both the Metrohm 5-ring conductivity cell (left) and Jenway platinum electrode conductivity cell (right) were used for conductivity measurements in liquid ammonia.

2.3.2.3 Conductivity meter/module

The Jenway platinum electrodes conductivity cell was used with a standard Jenway 4510 conductivity meter which gave a simple conductivity reading and allowed for storage of up to 32 readings. The 5-ring cell was used with the more advanced Metrohm 856 Conductivity Module which allowed connection to a computer. As well as taking readings manually, the module's Tiamo software has an automated function for periodically taking measurements and tabulating/plotting the data against time. This is particularly useful for measuring the kinetics of reactions by conductivity, which, for our work in liquid ammonia, is a relatively novel concept, although this method was not used to any major extent in this project.

2.3.2.4 NMR

Fluorine-19 NMR measurements in liquid ammonia were performed on Bruker 500 spectrometer operating at 470.5 MHz and other ^{1}H NMR spectra (for product identification/characterisation) were recorded using a Bruker 400 spectrometer operating at 400.1 MHz. All raw NMR data was processed using Bruker Top Spin 3.1 software.

2.3.2.5 UV-vis

UV-Vis spectra were acquired using a Cary 4000 UV-Vis spectrophotometer supplied by Agilent Technologies. For liquid ammonia work, the 12 cell compartment block was removed and a steel frame was modified to allow for the new high-pressure ammonia cell to sit correctly in position. The correct positioning of the cell was calibrated using a standard dye solution of methyl yellow in water and was tested in both the standard UV cell and high pressure cell to give consistent readings of absorbance and λ_{max}. Due to the modified cell compartment, temperature regulation was not possible when using the high pressure UV cell for liquid ammonia work.

2.4 General procedures

2.4.1 Ammonolysis reactions

2.4.1.1 Pressure glassware set-up and handling of liquid ammonia

There is always a desire to continually improve our handling procedure of liquid ammonia to create a safe and practical method for working with this solvent of such high pressure at room temperature. The transfer of liquid ammonia between glass condensers, burettes and vessels requires a pressure difference and some of our early methods relied on excessive heating and/or cooling of the glassware to achieve the desired outcome. Condensing of the ammonia from the ammonia tank into the condensing vessel was initially done by cooling the condensing vessel with liquid nitrogen. Likewise, transfer from the condensing vessel to the burette was achieved by intensely heating the nitrogen chilled condensing vessel with a hot air blower. The repeated process of heating and cooling the glassware can stress the glass unnecessarily and could potentially be extremely dangerous.

An improved method was developed for the handling and transfer of liquid ammonia, reducing the extreme heating and cooling of vessels and thus reducing the overall hazards of the procedure (Figure 2.4.1).

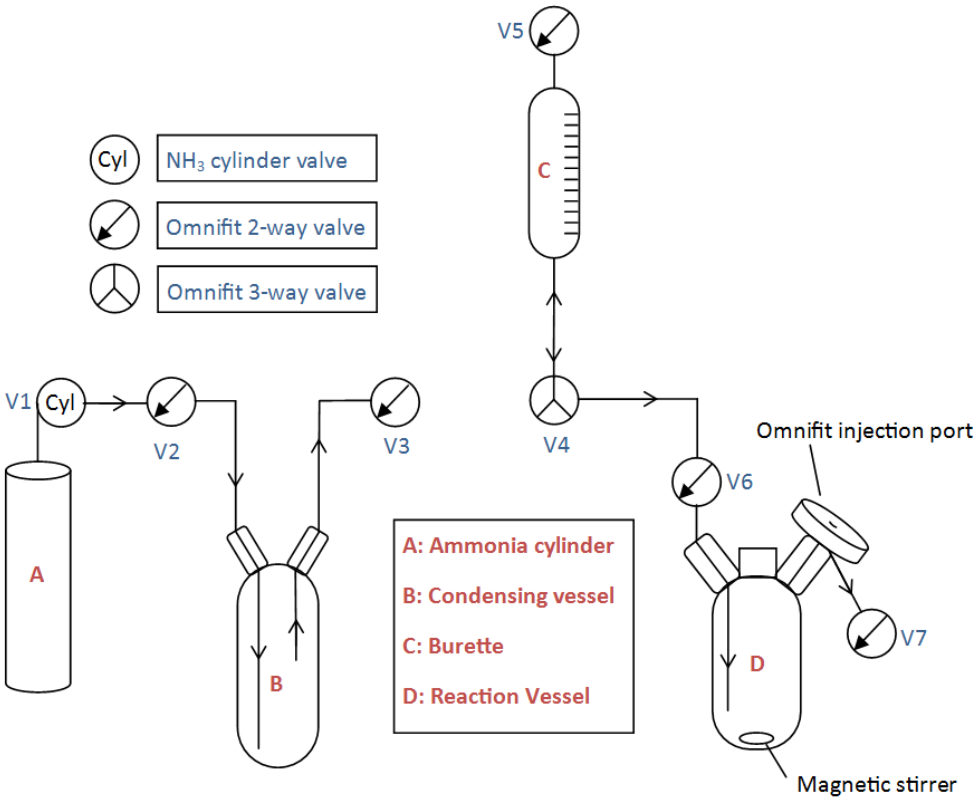

Figure 2.4.1 Set-up for the handling of liquid ammonia using high pressure glassware

The general procedure for setting up a liquid ammonia reaction/solution in the glass vessel reactor **(D)** is as follows: The condensing vessel (**B)** is cooled gently in an ice slurry bath and ammonia is condensed into the vessel from the ammonia cylinder **(A)** by opening valves (**V1)** and (**V2)**. Valve **(V3)** is opened to vent ammonia gas from vessel **(B)**, displacing air and allowing for easy transfer. When condensing vessel **(B)** is approximately 80 % full, it is removed from the ice bath and ammonia continues to condense until the vapour pressure in vessel **(B)** reaches the same as the ammonia cylinder **(A)**. At this point, valves **(V1)**, **(V2)** and **(V3)** are closed. Valve **(V2)** is then connected to the three-way valve **(V4)** and both are opened to allow transfer of ammonia from vessel **(B)** to the burette **(C)**. Vent valve **(V5)** is opened briefly to displace air and aid transfer of liquid ammonia into the burette **(C)**. When a sufficient volume of ammonia has been transferred, valves **(V2)** and **(V4)** are closed. The reaction vessel **(D)** is purged with excess ammonia from the condensing vessel **(B)** by opening 2-way valves **(V2)**, **(V6)** and **(V7)** and then 3-way valve **(V4)** in order to connect these vessels. After adequate purging of ammonia gas, the burette **(C)** is then connected to the reaction vessel **(D)** by switching the 3-way valve **(V4)** allowing for

an accurate delivery of liquid ammonia. Vent valve **(V7)** can be used to aid transfer by displacing air in the reaction vessel **(D).** If using a jacketed reaction vessel **(D)** there was an option to cool it to around 5 °C using the Huber-Unistat, allowing for easier transfer from the burette. This can then be ramped slowly back up to the desired temperature (usually 25 °C). During reactions, the 2-way valve **(V6)** was disconnected from the 3-way valve **(V4)** allowing for sampling from the reaction vessel when required.

During the project, the liquid ammonia handling method was further improved by using an ammonia tank recycled from a GC hydrocarbon trap. This cylinder was made form pure aluminium and so completely inert to ammonia and has a working pressure rating of 250 psi (17 bar). Thus ammonia did not need to be re-condensed for further purification every time into the condensing vessel **(B)** and could be transferred directly to the burette **(C)** by tipping the cylinder upside down. This reduces the time taken for setting up liquid ammonia experiments and also improves safety as less glassware (with risk of explosion) is required.

2.4.1.2 General solvolysis reaction procedure

The following procedure is for a typical ester ammonolysis reaction but also applies to other reactions such as the ammonium catalysed ammonolysis of esters and enzyme catalysed ammonolysis of triglycerides. Other reactants/catalysts (i.e. CALB enzyme, ammonium chloride) were added to the vessel along with the internal standard when required.

An internal standard was used due to the inconsistency of the sampling volume. For most reactions biphenyl was used as an internal standard. Biphenyl (~ 15 mM) was added to the reaction vessel which was then sealed tightly with the GL14 screw cap. An accurate amount of liquid ammonia was charged from the burette as described above. The solution was left to equilibrate at 25 °C for about 1 hour with the magnetic stirrer switched on. Diethyl ether solutions of the substrate (e.g. ester) were prepared with a concentration of around 0.5 to 1 M. An accurate amount (0.1 to 0.3 ml) of these solutions was injected into the vessel using the high pressure syringe through the Omnifit injection port to initiate the reaction. The concentration of substrate in the vessel was therefore usually between 5 and 30 mM. At timed intervals, the 2-way valve **(V6)** was quickly opened and closed allowing for sample collection (~ 0.05 ml)

into a glass vial. The ammonia was allowed to boil off and then the sample was prepared for GC (FID or MS) analysis by diluting in DCM or chloroform.

2.4.1.3 Data analysis and kinetic modelling procedure

Exemplified below is the ammonolysis of propargyl phenylacetate in liquid ammonia at 25 °C:

Samples were analysed by GC-MS in order to identify the propargyl phenylacetate ester peak, amide product (phenyl acetamide) and biphenyl internal standard. If peak retention times were known then GC-FID was used instead. All peaks were integrated to the baseline and the ester and amide peaks were normalised against the internal standard (Table 2.4.1).

Where:

$$\text{Normalised area} = \frac{\text{Integrated peak area of reactants or products}}{\text{Integrated peak area of internal standard}}$$

Table 2.4.1 GC-MS raw data and normalised peak areas for the ammonolysis reaction of propargyl phenylacetate in liquid ammonia at 25 °C.

time (min)	area ester	area IS	area amide	NA ester	NA amide
1	44443126	15434028	572978	2.880	0.037
10	66016882	25275522	5190534	2.612	0.205
30	59581296	25488932	15359122	2.338	0.603
120	14537098	9495286	13823949	1.531	1.456
180	19630529	18554522	41877268	1.058	2.257
240	5994615	9104869	22751273	0.658	2.499
360	5662754	23527478	68168165	0.241	2.897
600	1408724	15384845	49475286	0.092	3.216
720	1150428	16494623	53220816	0.070	3.227

IS = internal standard; NA = normalised area

A reaction profile was obtained by plotting normalised area of the ester and amide as a function of time using Microsoft Excel (Figure 2.4.2).

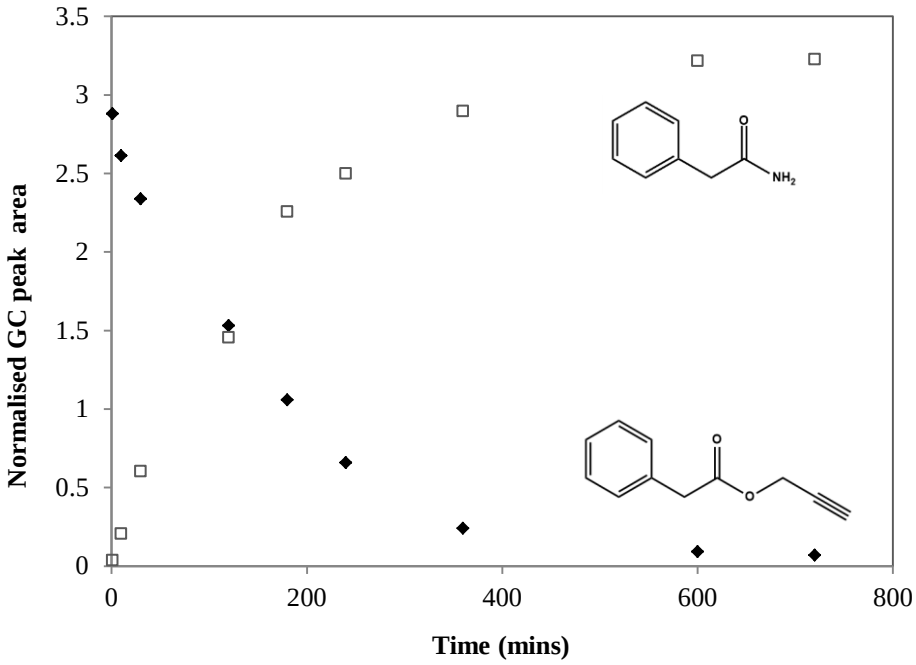

Figure 2.4.2 Reaction profile for the ammonolysis reaction of propargyl phenylacetate in liquid ammonia at 25 °C.

Due to the vast excess of liquid ammonia (~ 35 M) in comparison to the ester substrate (5 – 30 mM) these reactions are pseudo-first-order:

Rate of reaction $= k_2.[\text{ester}].[\text{NH}_3]$ where: $[\text{NH}_3] \gg [\text{ester}]$

Reaction follows pseudo first order kinetics where: $k_2 = k_{\text{obs}}/[\text{NH}_3]$

The data can then be transferred to commercial data fitting software such as Berkeley Madonna where a pseudo-first-order rate constant (k_{obs}) can be obtained (Figure 2.4.3). This is achieved by following both the concentration of the ester starting material and amide product using the individual rate laws for both species:

$$\frac{d[ester]}{dt} = -k_{obs}[ester]$$

$$\frac{d[amide]}{dt} = k_{obs}[ester]$$

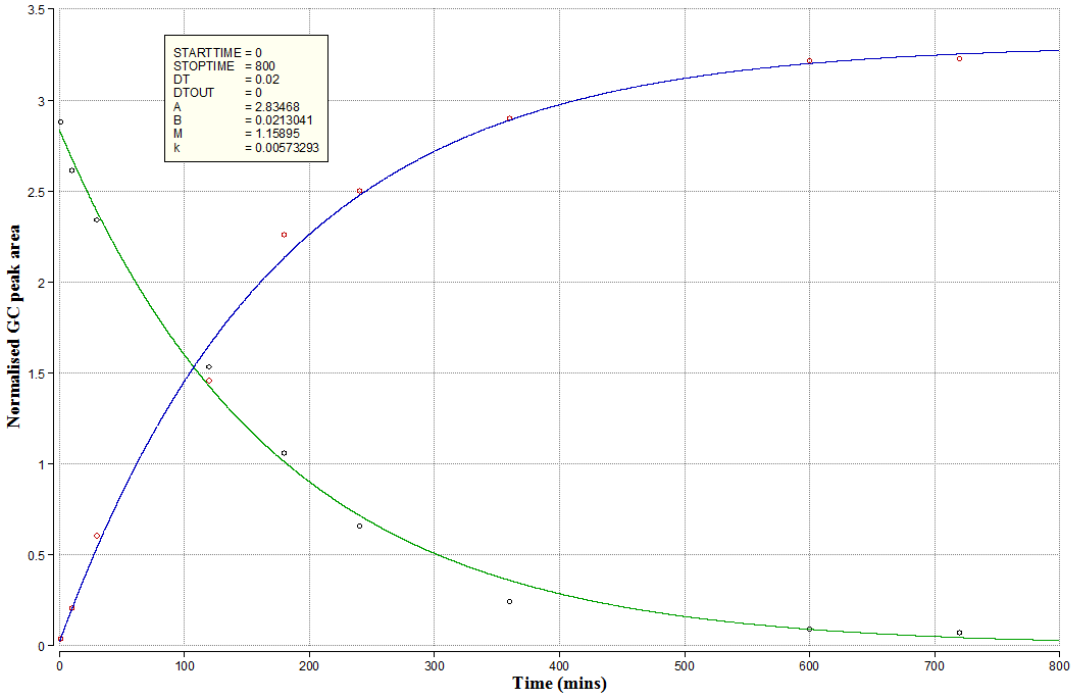

Figure 2.4.3 Berkley Madonna data fit to ester and amide for the ammonolysis reaction of propargyl phenylacetate in liquid ammonia.

From the model, a pseudo-first-order rate constant is generated; k_{obs} = 0.00573 min^{-1} (9.55x10^{-5} s^{-1}).

2.4.2 Conductivity

2.4.2.1 Glassware and conductance cell set-up for liquid ammonia

The Metrohm 5-ring cell has a pressure rating of 5 bar, which equates to the vapour pressure of liquid ammonia at around 5 °C. For safety reasons, however, it was deemed necessary to operate at around 50 % of the quoted pressure rating and so all conductivity measurements were carried out at -15 °C (~ 2.36 bar). Both conductivity probes have a shaft diameter of 12 mm and when fitted with two EPDM (ethylene propylene diene monomer) O-rings and the G19 cap screwed on to the vessel it gave a tight fit with no ammonia leaking (Figure 2.4.4). The top of the probe was clamped tightly to prevent ejection from the top of the vessel when pressurised.

Figure 2.4.4 Conductivity set-up in liquid ammonia with Metrohm 5-ring cell at -15°C

2.4.2.2 Conductivity vs. concentration (surfactants)

Conductance was used as a method for the detection of micelles and aggregates in liquid ammonia. The conductivity cell was clamped in place with the cap on and the chilled vessel was filled accurately with the appropriate amount of liquid ammonia from the burette. Manual readings were taken using either the Jenway platinum or Metrohm 5-ring conductivity cell. Initially, the method of increasing the concentration of electrolyte in the ammonia was by injecting high concentrations of the electrolyte (in ether or THF) into the vessel via the high-pressure syringe. An immediate concern here, however, was that the conductivity was not entirely that of the electrolyte/ammonia solution but the added solvents, and with the some of the ether solvents being notoriously hygroscopic, there was always a risk of higher than acceptable water content in the liquid ammonia solution. In addition to this, high concentrations of many of the electrolyte solutions for injection couldn't be prepared due to poor solubility even in the organic solvents and so the injection method was rejected. Ideally, the conductivity measurements would just be taken in ammonia solutions of the desired electrolyte only, with no additional impurities. A dilution method was therefore developed in which the starting concentration of analyte was

high and was then gradually diluted with fresh liquid ammonia, taking a conductivity reading at each step. This was done by utilising the dip tubing (sample tube) to remove a known amount of liquid ammonia solution and adding an accurate, fresh portion of ammonia from the burette. The volume of liquid ammonia below the dip tube was found prior to the experiment using water and accurate pipetting. Having taken a conductivity reading at the high concentration, the liquid ammonia was then expelled from the vessel until the dip tube is reached. Hence, there is now a known volume of a particular concentration of electrolyte solution which can be further diluted by accurate addition of liquid ammonia from the burette. This process can be repeated as many times as required to get the conductivity vs. concentration plot.

The conductivity of electrolytes in liquid ammonia is much different to that in water due to the lower dielectric constant of ammonia which promotes the association of free ions into non conducting ion-pair species. A model was developed using a quadratic solver to account for the ion-pairing phenomenon and derivation of the model can be found in the conductance chapter and appendix where it was used to profile the conductance of ionic surfactants for aggregation studies.

2.4.3 NMR procedure

Liquid ammonia solutions of the analyte were prepared in a reaction vessel in the same manner as described for a general ammonolysis reaction. Solutions for NMR studies were also pre charged with a small amount of a deuterated standard (<1 %) such as DMSO-d_6 to provide a deuterium lock. When studying chemical shift changes was the focus of the experiment, a standard compound was also added in small quantity (<1 %). For example, ammonium trifluoroacetate was used as standard when looking at the chemical shift changes for fluorinated surfactants by Fluorine-19 (^{19}F) NMR. All ^{19}F chemical shifts were adjusted relative to the -CF_3 singlet peak of ammonium trifluoroacetate (δ = -75.5100 ppm). The NMR tube was cooled in ice-water bath and the liquid ammonia was transferred carefully from the reaction vessel (at room temperature) to the cooled tube. The NMR tube was allowed to warm to room temperature before careful transfer to the NMR instrument. Spectra were recorded at a regulated temperature of 25 °C.

2.4.4 UV procedure

Liquid ammonia solutions of dye were prepared in the reaction vessel as described for the general solvolysis reactions. The high pressure UV cell was cooled in ice bath slurry and the liquid ammonia solution was transferred from the reaction vessel. To minimise ‘air bubbles’ in the UV cell which would give ambiguous readings, the vent valve was opened to expel excess ammonia and further cool the cell. This method for filling the high pressure UV cell led to concerns that the concentration in the UV cell when filled would not be consistent with that prepared in the vessel. This became apparent during experiments as repeat runs of the same dye solution in liquid ammonia yielded slightly different absorbance results on the UV spec. Thus it was concluded that the current set-up of our high pressure UV cell would only really allow for simple measurements such as wavelength confirmation rather than measurements where accurate absorbance is required such as solubilisation studies and reaction kinetics.

Chapter 3 - Ammonolysis of esters in liquid ammonia

3.1 Background

3.2 Results and Discussion

Publication:

J. Griffin, J. Atherton and M. Page, J. Phys. Org. Chem. 2013, **26,** 1032-1037

3.1 Background

Analogous to ester hydrolysis in water, esters can react in liquid ammonia to give amide and alcohol products and is generally thought to occur by an addition-elimination type mechanism (Scheme 3.1.1).

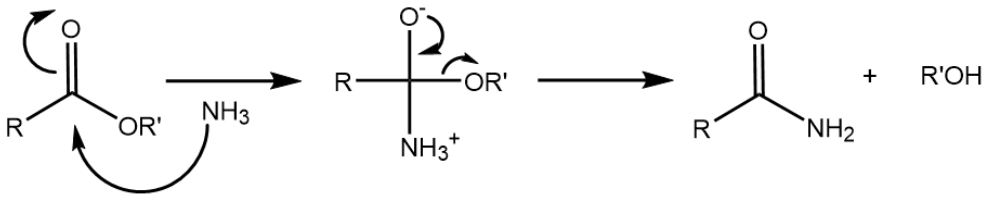

Scheme 3.1.1

Although the intrinsic mechanisms of esters ammonolysis have not been studied to any real extent, there are some general trends for the ammonolysis of esters in liquid ammonia:[89]

i. Introducing electron-withdrawing α-substituents accelerates the rate of ammonolysis. This presumably increases the electrophilicity of the ester carbonyl centre.
ii. The presence of the an α,β- double bond decreases the electrophilicity of the carbonyl centre resulting in a decrease in the rate of reaction.
iii. P. Ji found that phenol esters are particularly reactive.[90]
iv. Alkyl esters are more reactive than the corresponding aryl ester with the same pK_a of the leaving group alcohol (vide infra).
v. Ammonolysis rates can be increased with the addition of a metal amide.

Most early studies on kinetics of ester ammonolysis in liquid ammonia explore the reactivity of aliphatic esters at -33 °C. Simple, aliphatic esters were found to be very resistant to ammonolysis, even at higher temperatures, although it was found that the addition of ammonium salts could greatly accelerate the reaction (Table 3.1.1).

Table 3.1.1 Some early data for catalysed and uncatalysed ammonolysis of simple esters in liquid ammonia.[91, 92]

Ester substrate	conditions	yield
ethyl acetate	130 °C, 24 hr	No reaction
ethyl acetate	130 °C, 24 hr, NH_4Cl	43 %
diethyl malonate	0 °C, 24 hr	9 %
diethyl malonate	0 °C, 24 hr, NH_4Cl	79 %

3.2 Results and Discussion

3.2.1 Uncatalysed ammonolysis of esters in liquid ammonia

The solvolysis of a series of alkyl benzoates and alkyl phenylacetates and aryl benzoates in liquid ammonia gives the corresponding amide and alcohol/phenol products (Scheme 3.2.1).

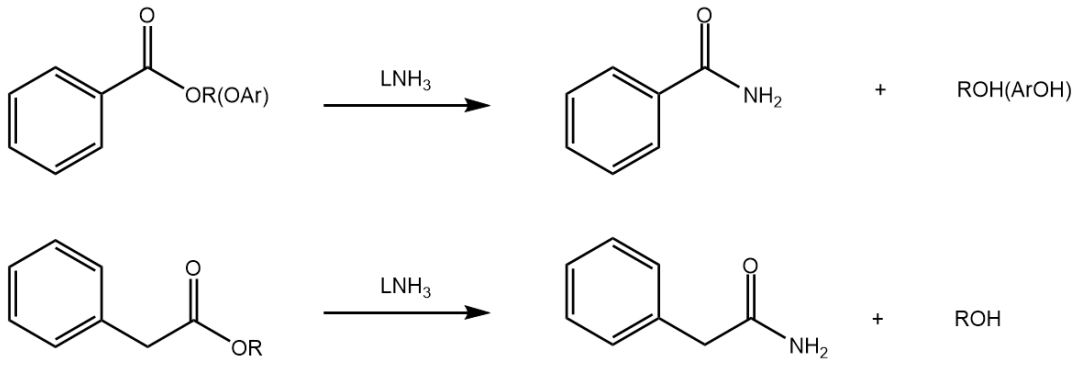

Scheme 3.2.1

The corresponding pseudo-first-order rate constants vary significantly with the substituent (Table 3.2.1) with the esters of more acidic alcohols being more reactive. Phenylacetate esters are roughly five-fold more reactive than the corresponding benzoate esters and alkyl esters appear to be more reactive than the corresponding aryl ester with same (pK_a) alkoxide leaving group.

Table 3.2.1 Observed pseudo-first-order rate constants for the solvolysis of various esters in liquid ammonia at 25 °C.

Ester type	**Alcohol leaving group**	**pK_a (aq) of alcohol**[a]	**k_{obs} s^{-1}**
Benzoates	ethyl	15.93	$3.36x10^{-8}$
	methyl	15.50	$1.07x10^{-7}$
	2-methoxyethyl	14.80	$3.31x10^{-7}$
	propargyl	13.55	$1.78x10^{-5}$
	vinyl	11.10[b]	$1.47x10^{-2}$
	4-methoxyphenyl	10.21	$1.24x10^{-3}$
	phenyl	10.00	$7.45x10^{-3}$
	4-chlorophenyl	9.40	n/a [c]
Phenylacetates	ethyl	15.93	$1.81x10^{-7}$
	2-methoxyethyl	14.80	$3.47x10^{-6}$
	propargyl	13.55	$9.59x10^{-5}$
	2,2,2-trifluoroethyl	12.37	$1.38x10^{-2}$

[a] reference [93]
[b] reference [94]
[c] reaction too fast to accurately measure

For alkyl esters of analogous carboxylate substituent, there is a linear relationship between the aqueous pK_a of the leaving group alcohol and logarithm (log_{10}) of the pseudo-first-order rate constant, showing a Brønsted correlation (Figure 3.2.1).

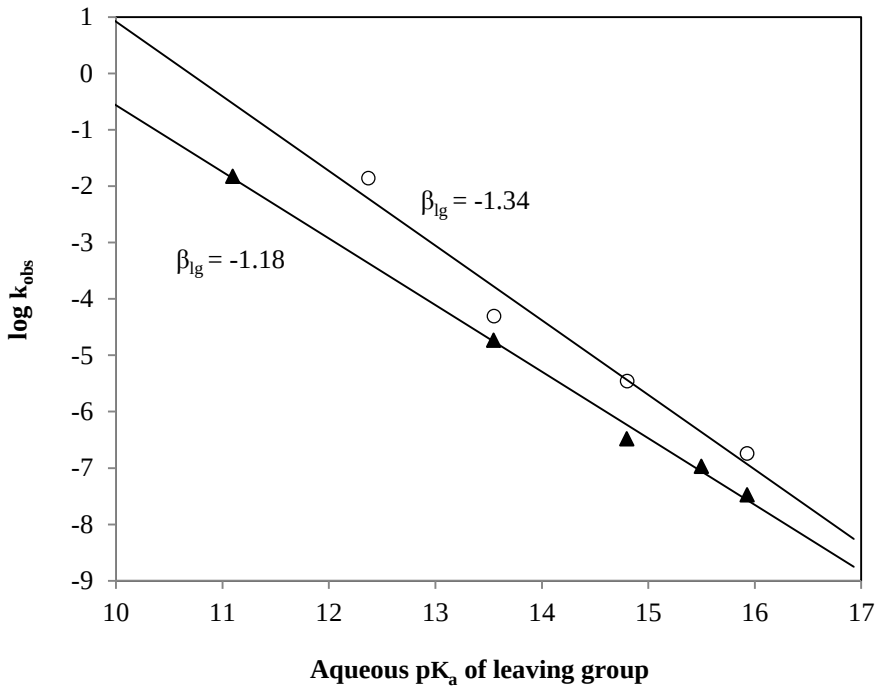

Figure 3.2.1 Brønsted plot for the pseudo-first-order rate constants for the solvolysis of alkyl esters of phenylacetic (○) and benzoic (▲) acid in liquid ammonia at 25 °C against the aqueous pK_a of the leaving group alcohol.

The relatively large β_{lg} values of -1.34 and -1.18 for the solvolysis of alkyl phenylacetate and benzoate esters in liquid ammonia respectively, appear to indicate a significant development of negative charge on the leaving group alcohol oxygen relative to that in the starting ester. At first sight it is tempting to think this is indicative of rate-limiting breakdown of the tetrahedral intermediate expelling the alkoxide anion. The effective charge on the oxygen in the ester is $\approx 0.7^{+}$, and the β_{lg} indicates the change in effective charge on oxygen in the transition state. [95, 96] However, these reactions are carried out in liquid ammonia and not water, and so using the aqueous pK_a values to try interpret structure-activity relationships of these solvolysis reactions in liquid ammonia is unwise, and certainly inconclusive. For that reason, knowledge of how the ionisation constant of the leaving group alcohol varies with substituents in liquid ammonia is required. Previous studies in liquid ammonia have demonstrated that phenols with aqueous $pK_a < 7.0$, but not those with $pK_a > 8.5$, are fully ionised at room temperature, [97] and there is a linear relationship between the apparent pK_a values in liquid ammonia and the corresponding aqueous ones with a slope of 1.67 (Figure 3.2.2).

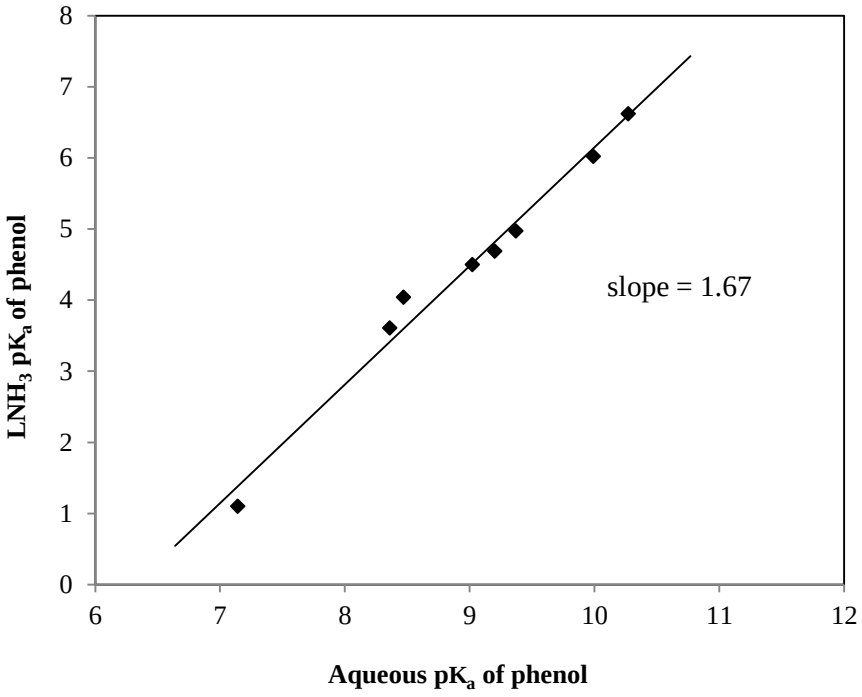

Figure 3.2.2 pK_a of phenols in liquid ammonia against the corresponding aqueous pK_a

The greater dependence of the acidity of phenols on substituents in liquid ammonia compared with water results from the poorer solvation of the phenoxide anions in the non-aqueous solvent and as a result their stability is more dependent on the negative charge delocalisation through the substituent. It is a reasonable assumption that a plot of pK_a of the leaving group alcohols in liquid ammonia against their corresponding aqueous pK_a values would give a slope of at least 1.7, given the value of 1.67 observed for phenols and the negative charge on alkoxide ions is likely to be more localised than that in phenols.

As a result, the Brønsted β_{lg} values obtained from a reconstituted plot of the log observed rate constant against the pK_a of the leaving group alcohol in liquid ammonia would thus be significantly reduced to around -0.7. This would amend the previous assumption of rate-limiting breakdown of the tetrahedral intermediate and suggest a reaction mechanism whereby the rate limiting step involves some kind of reaction of the tetrahedral intermediate with little C-OR bond fission in the transition state (Scheme 3.2.2).

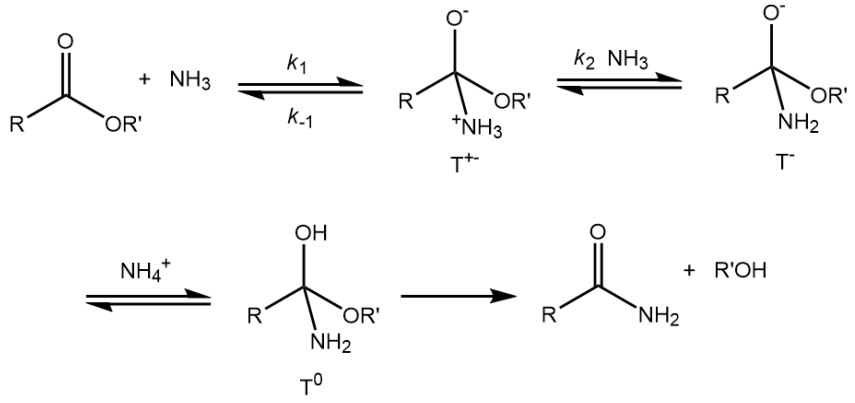

Scheme 3.2.2

Anions are poorly solvated in liquid ammonia compared with water and other polar solvents and so although expected to be better nucleophiles in the poorly solvating, aprotic system, it is expected that anions will generally be poorer leaving groups in liquid ammonia compared with polar solvents. It is therefore anticipated that the ammonolysis of esters in liquid ammonia will proceed by the nucleophilic attack of ammonia on the ester carbonyl group to form a zwitterionic tetrahedral intermediate T^{+-}, reversibly, because expulsion of ammonia (k_{-1}) will be faster than that of the alkoxide anion (Scheme 3.2.2). Furthermore, aminium ions are fully deprotonated in liquid ammonia, and so exist as their free bases.[97,98] As a consequence, deprotonation of the zwitterionic tetrahedral intermediate by solvent ammonia is thermodynamically favourable and very rapid (k_2) to give the anionic T^-. However, if the above suppositions are true about the 'corrected' Brønsted β_{lg} values of ~ -0.7, then breakdown of the anionic T^- cannot be the rate-limiting step as this would be incompatible with the rate law for the uncatalysed solvolysis. Given the relative instability of anions in liquid ammonia, the most stable form of the tetrahedral intermediate is the neutral T^0, which in the absence of an external catalyst could be formed by a 'proton switch' through the ammonium ion formed within the ion pair by a proton transfer to a solvent molecule.[99]

Alternatively, it has been proposed that T^- may be formed directly by a termolecular reaction involving two molecules of solvent, with one acting as a general base, similar to that proposed for some 'spontaneous' pH-independent hydrolysis reactions (Scheme 3.2.3)

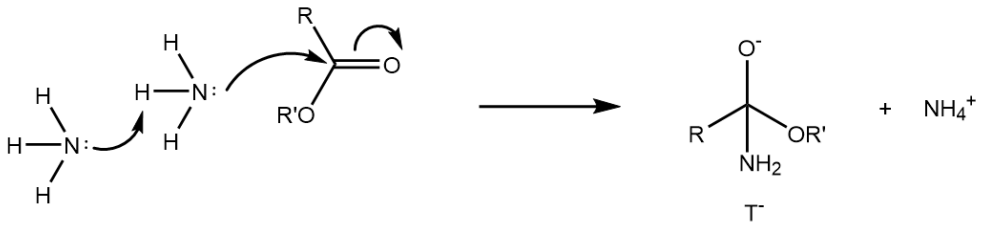

Scheme 3.2.3 Formation of T^- through a termolecular reaction involving two molecules of solvent ammonia with one acting as a general base

However, with an autoprotolysis constant giving a pK_a of 27.6 (25 °C), compared to with 14.0 for water (25 °C), ammonia is much less acidic than water.[35, 100] This reduced acidity renders the proton removal from the attacking ammonia energetically unfavourable until after significant N-C bond formation generating substantial positive charge on the N (rapid deprotonation of aminium ions). For this reason this concerted mechanism is probably less likely than the stepwise formation of the T^0. The reasons for postulating rate-limiting stepwise formation of T^0 is further supported when the effect of an ammonium catalyst on the solvolysis of esters in liquid ammonia is explored.

3.2.2 Ammonium catalysed ammonolysis of esters

As reported previously, early work on ester solvolysis in liquid ammonia demonstrated that the reaction can be catalysed by ammonium ions (Table 3.1.1). Likewise, the observed pseudo-first-order rate constants for the solvolysis of propargyl benzoate in liquid ammonia significantly increases with ammonium chloride concentration at constant ionic strength (Figure 3.2.3).

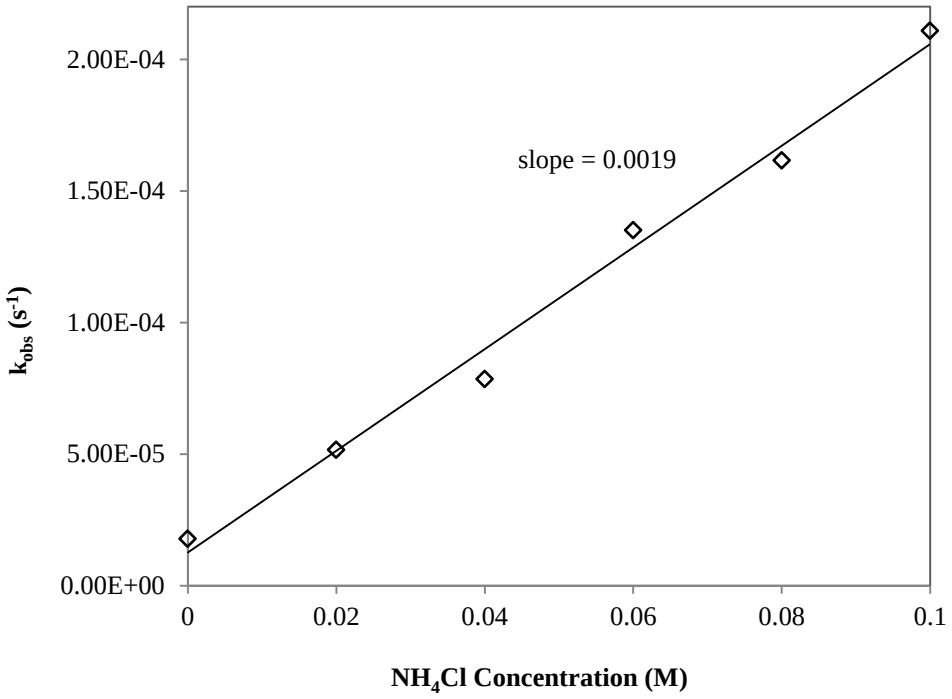

Figure 3.2.3 The dependence of the observed pseudo-first-order rate constants for the ammonolysis of propargyl benzoate on the ammonium chloride concentration in liquid ammonia at 25 °C. (I = 0.1M $KClO_4$)

Ionic strength itself has little effect upon the rate of ester solvolysis, with the background $k_0 = 1.78 \times 10^{-5}\ s^{-1}$, compared with $1.97 \times 10^{-5}\ s^{-1}$ with the addition of 0.1M $KClO_4$. Contrary to this, the observed rate, k_{obs}, increases nearly 10-fold with 0.1M ammonium chloride. The corresponding second-order-rate constant, $k_{NH4+} = 1.90 \times 10^{-3} M^{-1} s^{-1}$, and the reaction is thus overall a third-order rate equation:

$$\text{Observed rate} = k[\text{ester}][NH_3][NH_4^+]$$

On initial inspection, there are a couple of theories as to how the ammonium cation may be catalysing the ammonolysis of esters in liquid ammonia;

Firstly, the ammonium ion could be assisting in formation of a cationic tetrahedral intermediate, T^+, acting as an acid catalyst, concluding a rate limiting nucleophilic attack and proton transfer (Scheme 3.2.4).

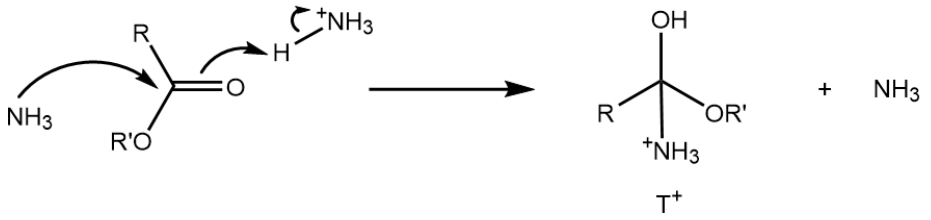

Scheme 3.2.4 Catalysis by the ammonium cation via the acid-catalysed formation of a cationic tetrahedral intermediate, T^+

However the rate limiting formation of T^+ does not appear to overcome the difficulty of expelling alkoxide ion compared with ammonia.

Alternatively, the catalytic effect of ammonium on the ammonolysis of esters could be due to general acid-catalysed breakdown of the zwitterionic T^{+-} or neutral T^0 tetrahedral intermediate by acting as a proton donor to the leaving group alkoxide (Scheme 3.2.5).

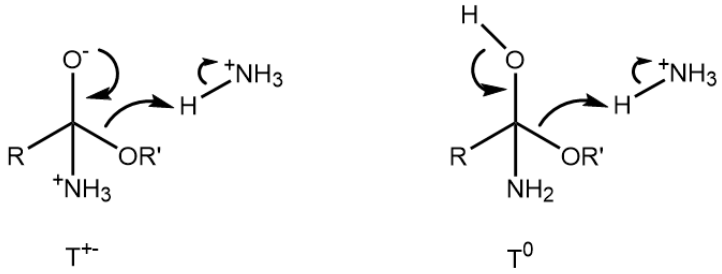

Scheme 3.2.5 General acid-catalysed breakdown of the zwitterionic T^{+-} (left) or neutral T^0 (right) by the ammonium cation.

However, Brønsted data generated for the ammonium catalysed reactions advocates that the general acid-catalysed breakdown of the T^{+-} or T^0 by the ammonium is not possible. The second-order rate constant for the ammonium chloride catalysed solvolysis of methoxyethyl benzoate, $k_{NH4+} = 2.79x10^{-5}$ $M^{-1}s^{-1}$. Using this data point in conjunction with the second-order rate constant for the ammonium catalysed solvolysis of propargyl benzoate, a two point Brønsted plot can be made generating a β_{lg} of -1.46. The same two data points for the uncatalysed solvolysis reactions generate a roughly comparable Brønsted β_{lg} of -1.38. Again, using liquid ammonia

pK_a values, the β_{lg} would be reduced to roughly -0.8 for the uncatalysed and ammonium catalysed reactions.

This surprising observation would indicate that the effective charge on the alcohol oxygen in the transition state is similar in both reactions. This would, therefore, imply that the ammonium cation does not interact directly with the leaving group, alcoholic oxygen.

It is concluded that the rate-limiting step for the ammonium-ion-catalysed solvolysis of alkyl esters in liquid ammonia is the diffusion-controlled protonation of the zwitterionic tetrahedral intermediate T^{+-} to give T^{+}, which is rapidly deprotonated to give T^{0}. This is compatible with the suggestion that the rate-limiting step for the uncatalysed reactions is the formation of the neutral T^{0} by a 'proton switch'.

Chapter 4 - Aggregation Studies

4.1 Background

4.2 Aggregation studies on ionic surfactants in water and liquid ammonia - Results and Discussion

4.3 Aggregation studies on perfluorinated amides in liquid ammonia - Results and Discussion

4.1 Background

4.1.1 The Cell - the unit of life

The basic unit of all life is the cell which allows a diverse range of chemical reactions to take place within a confined environment. It is in water that chemical structures are able to aggregate into spheres, trapping water inside, ultimately allowing life to survive and develop. These chemical structures form biological membranes that are impermeable to charged species and large molecules and thus allow the concentration of biomolecules within the cell to be much greater than the surrounding medium.[101] Additionally, the biological membrane allows for the controlled transport of solutes and the majority of cell functions such as osmosis, translocation, fusion, intracellular interactions, endocytosis and exocytosis are all mediated by the membrane. This protective environment and regulation is the basic protective unit of life and without the aggregation of these chemical structures into cellular membranes life may not have come into being. Hence, one may regard compartmentalisation, the aggregation of molecules into well-ordered structures, as one of the fundamental processes of life. More complex organisms contain intracellular membranes that perform more specialized functions. The cell nucleus and mitochondria, for example, both comprise of their own unique cell membranes, providing a distinct intracellular compartment enabling them to independently function at their full potential.[102]

The biological membranes of animal and plant cells are typically made up of 40-50 % lipids and around 50-60 % proteins. As proposed by Singer and Nicholson, these lipids and proteins arrange themselves into a cellular membrane best described as a fluid-mosaic model (Figure 4.1.1). According to the model, the membrane consists of a lipid bilayer composed of glycolipids and phospholipids which incorporates the proteins. [103] These proteins can be found on the interior or surface of the membrane bilayer and along with the lipid molecules are free to diffuse laterally in the plane of the membrane, hence the name ‘fluid-mosaic'.

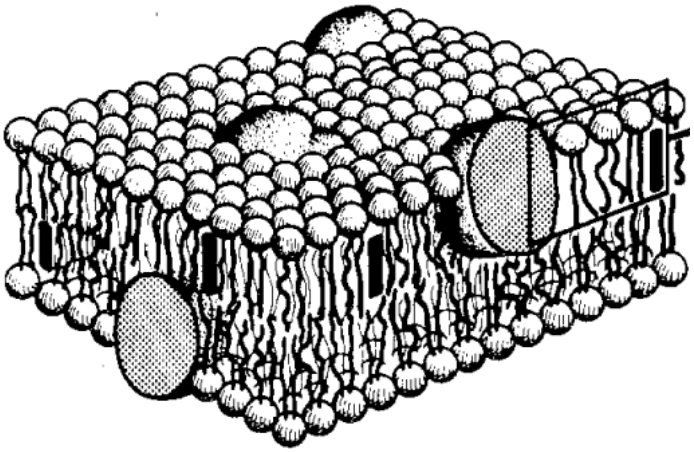

Figure 4.1.1 Fluid-mosaic model of the biological cell membrane.[104]

The driving force for the formation of the biological membrane arises from the chemical structure of the lipid. An example of a phospholipid is shown in Figure 4.1.2.

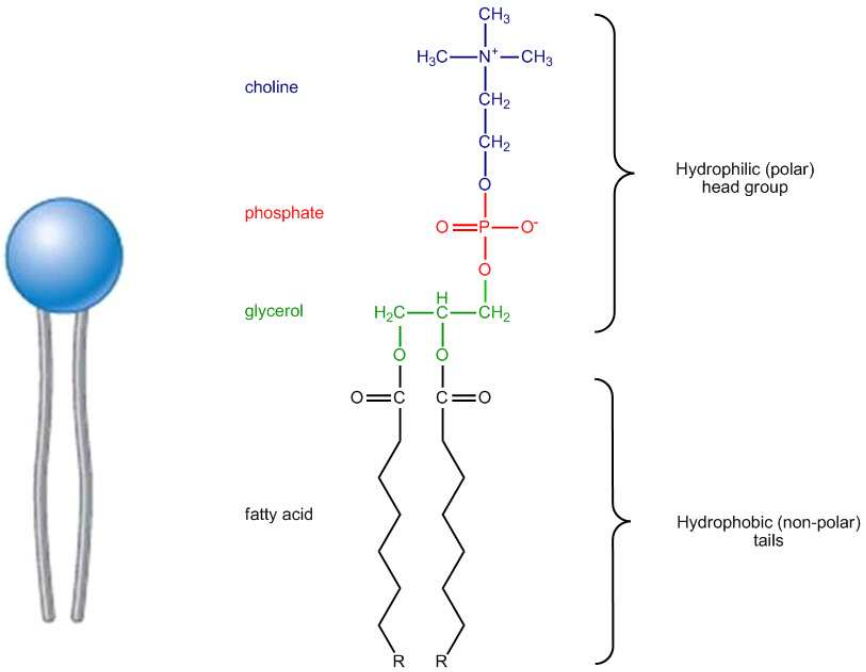

Figure 4.1.2 Schematic model of a phospholipid (left) and the general structure of a phosphatidylcholine (right).[105]

Phospholipids, which make up the biological membrane of the cell, are commonly regarded as amphiphilic molecules, which mean they consist of a polar, hydrophilic head group and a non-polar, hydrophobic tail. The polar, 'water loving' head group is generally a phosphate group such as a phosphatidyl choline, ethanolamine, serine or

phosphatidic acid, and the non-polar, 'water hating' tails are typically derived from a diglyceride portion, often with a palmitate or oleate chain.

The complex nature of the biological membrane has necessitated the use of simplified 'models' from which a more detailed and better understanding of the membrane can be obtained. The prospect of modelling these exquisitely optimized membranes in the laboratory is challenging and indeed Fendler has stated that *"Mother nature need not be slavishly reproduced"*.[106] Simple monolayers, micelles, bilayers, vesicles, host-guest systems are used as practical models to gain an insight into the workings and structure of the biological membrane and are generally referred to collectively as 'membrane mimetic agents'. Additionally, the mimicking of the membrane function in these simple model systems can often lead to novel applications such as drug encapsulation, molecular recognition and transport and even has potential use in photochemical solar energy conversion and storage.[107]

It is proposed that as a preliminary study to the possible formation of the more complex cell structures in liquid ammonia, a simple, membrane mimetic model should first be explored. If the simple membrane model can be applied to a liquid ammonia solvent system, then the notion that cell like structures can form in this harsh environment can be realised. One of the simplest membrane mimetic models that is widely studied in all kinds of media is the formation of a monolayered cell-like structure known as the micelle, which is comprised of a number of surfactant molecules in an aggregated system.

4.1.2 Surfactants - pseudo-phospholipids

4.1.2.1 Structure and properties of surfactants

Chemicals that have the ability to form aggregates in solutions have been recognized for their soap-like properties and cleaning ability for thousands of years. One of earliest recorded evidence of the utilization of soaps and detergent materials dates back to ancient Babylon around 2800 BC.[108] Likewise, eminent historical papers, such as the Egyptian Papyrus Ebers, tell of how the ancient Egyptians used animal fats and vegetable oils combined with an alkaline, soda ash type substance which they called Trona, for the preparation of soaps used for washing.[109] Countless more texts highlight the utilization of natural fats and oils in ancient societies up to the present,

more commercialised, products. There was not much insight into how or why these particular compounds behave as they do when in (normally aqueous) solution. In modern times, however, these compounds have been studied extensively and there is now a great understanding of the structures and properties of these compounds, which are commonly known as surfactants - surface active agents.

Surfactants, sometimes called detergents, have some structural similarities to phospholipids and are likewise classed as amphiphilic molecules with distinct hydrophobic and hydrophilic regions. The non-polar moiety of the surfactant molecule is generally a long chain hydrocarbon tail of varying length and may contain an unsaturated bond(s) and even consist of two or more chains. Depending on the chemical structure, the polar region of the surfactant molecule can be neutral, cationic, anionic or even zwitterionic like the phosphatidylcholine molecule. The classification of the surfactant molecule is usually attributed to the nature of this polar, hydrophilic head group:

- Non-ionic: Contains a surface active head group that carries no charge. Examples include hydroxyl groups, ethers, acetylene alcohols, glucoside alkyl ethers and amides
- Cationic: Contains a surface active head group with a positive charge. Examples include pH-dependent amines (1^0, 2^0 or 3^0) or the permanently charged quaternary ammonium salts.
- Anionic: Contains a surface active head group with a negative charge. Examples include sulfates, sulfonates, carboxylates and phosphates.
- Zwitterionic (amphoteric): Contains a more complex surface active head group with both a cationic and anionic head group. The cationic part is most commonly an amine (1^0, 2^0, 3^0 or quaternary salt) whereas the anionic part can be more variable as above. These head groups tend to be similar in structure to the head group found in phospholipids.[110]

Some examples of these four types of surfactants along with their potential applications can be found in Scheme 4.1.1.

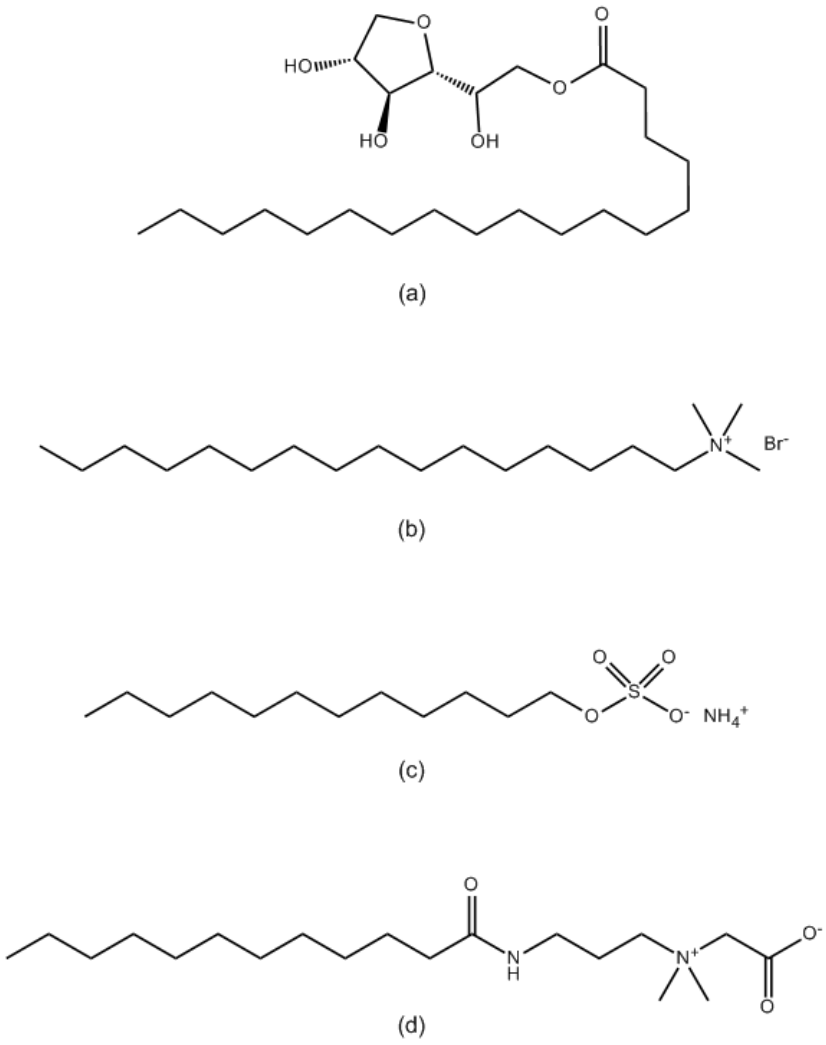

Scheme 4.1.1 Some examples of the various types of surfactants: (a) Non-ionic sorbitol monostearate, used in the manufacture of foods and healthcare products,[111] (b) Cationic cetrimonium bromide, used in buffer solutions for DNA extractions and synthesis of gold nano-particles,[112] (c) Anionic ammonium lauryl sulfate, used in shampoos and cleaning products,[113] (d) Zwitterionic cocamidopropyl betaine, used in cosmetics and hand soaps.[114]

Although the tail group of commercial surfactants can be silicon or fluorocarbon based, for almost 99 % of surfactants used in industry the hydrophobic, water insoluble tail is made up of hydrocarbon chains, the majority of which are linear due to biodegradability concerns.[110] In many cases, the hydrocarbon tail is derived from natural sources such as oils and animal fats although some synthetic sources such as petroleum based derivatives are available.

In a 2-phase water/organic system, it is the amphiphilic structure that gives the surfactant molecule the ability to adsorb at the liquid/liquid interphase, or if in a single phase polar system, at the liquid/air interface. Additionally, adsorption of these amphiphilic molecules can take place at a liquid /solid interface (Figure 4.1.3).

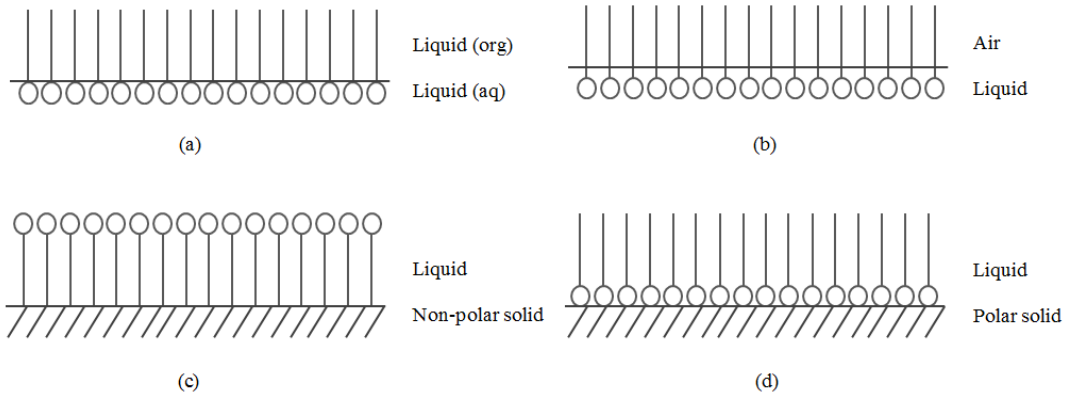

Figure 4.1.3 Adsorption of surfactant molecules at: (a) aqueous/organic interface, (b) liquid/air interface, (c) liquid/non-polar solid interface and (d), liquid/polar solid interface.[115,116]

The adsorption of the surfactant molecule is a consequence of its amphiphilic structure, whereby the polar, hydrophilic head group is readily solubilised in the aqueous phase and the non-polar hydrophobic carbon chain which has a poor affinity for water and so is either solubilized in the organic phase or content to orient towards the air, away from the surrounding water. The driving force for the surfactant molecule to adsorb at an interface is to reduce the free energy of that specific phase boundary.[117] Similarly, it is this driving force and the need to reduce the free energy that ultimately promotes the formation of aggregates from surfactants.

4.1.3 Micelles and aggregates

4.1.3.1 Aggregation of surfactants

When a surfactant is added to an aqueous environment the hydrophilic head group interacts strongly with the water molecules by dipole-dipole and ion-dipole forces whereas the hydrophobic tail interacts weakly or repulsively with the water. At low concentrations the surfactants are forced towards the interface of the system whereby the hydrophobic tails are oriented in a way to minimize contact with the water.[118, 119] This reduces the surface tension of the water, and hence the name surfactant - surface

active agent. However, there are limits to how much they can reduce the interfacial tension. Once all interfaces and surfaces have been occupied by the free surfactant monomers, they start to aggregate into monolayered cellular like structures known as micelles (from Latin mica; crumb, grain). The driving force for the aggregation is, again, the reduction of the free energy of the system. Thus in an aqueous environment, micelles have a core of favourably interacting hydrophobic tail groups no longer exposed to water and an outer layer of polar head groups still exposed to water. Conversely, if the surfactant is dissolved in a non-polar organic solvent quite the opposite occurs.[120] The hydrophobic tail is now at the surface of the micelle, exposed to the solvent, whereas the polar head groups reside deep within the micelle, oriented away from the apolar bulk environment. These types of aggregates are commonly known as reverse micelles or inverse micelles and have many applications. For example, a C_{16} chain ammonium surfactant, hexadecyltrimethylammonium bromide (CTAB), forms reverse micelles in the non-polar cyclohexane and these have been used as a microenvironment for enzyme catalysed reactions.[121] When used in this manner, reverse micelles usually comprise of three major components; a standard amphiphilic surfactant molecule, a non-polar solvent as the chief medium, and a small concentration of water. The water sphere within the reverse micelle mimics the microenvironment of the interior of a normal cell system in which the enzyme would usually function. This allows certain enzymatic reactions to occur in a largely organic system where they would normally not function at all without the aid of this aqueous microenvironment.[122] Figure 4.1.4 shows examples of the types of aggregates that can form surfactant molecules such as simple micelle structures to more complex vesicles.

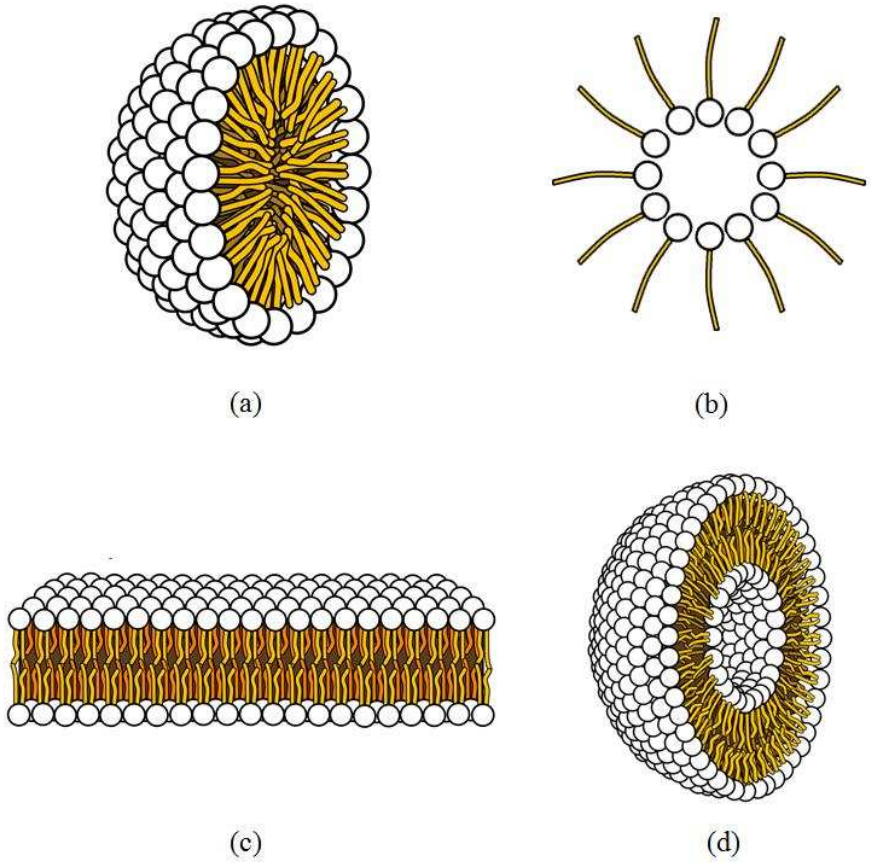

Figure 4.1.4 Cross sections of surfactant aggregates: (a) normal micelle, (b) reverse micelle (in an organic solvent), (c) bilayer and (d) a vesicle.[123]

In each case, the driving force for the aggregation process is essentially the desire for each part of the surfactant molecule (head group or tail) to be in their most favourable environment.

4.1.3.2 Early micelle studies and physical properties of micelles solutions

In the early twentieth century surfactant solutions began to be studied from a scientific standpoint. One of the leading pioneers in the chemical interpretation and understanding of these widely-used but somewhat 'mysterious' soapy, detergent compounds was James. W. McBain. As early as 1914 he observed that surfactant molecules acted as normal electrolytes below a clearly defined concentration, whereas above this concentration some of the physical properties of the surfactant solution, such as conductivity or osmotic activity, changed dramatically.[124] He postulated that this behaviour could be explained by molecule aggregation into a well-ordered, cell-type structure above a certain concentration which he defined as a critical micelle

concentration (cmc). At first this notion was regarded as preposterous: a leading physical chemist chairing a Royal Society London meeting responded to McBain's aggregation proposal with just two words- *"Nonsense, McBain"*.[125] Yet today, it is universally accepted that, in water at least, 30-150 surfactant molecules can assemble into micelles in order to position the non-polar, hydrophobic chains away from the solvent. His early work on surfactant molecules was thought to support a lamellar or plate-like micelle consisting of, in his own words, a *"double leaflet of soap molecules placed end to end and side to side"* however by the mid 1930's this model was abandoned in favour of the now more orthodox, roughly spherical model (Figure 4.1.5).[126, 127, 128]

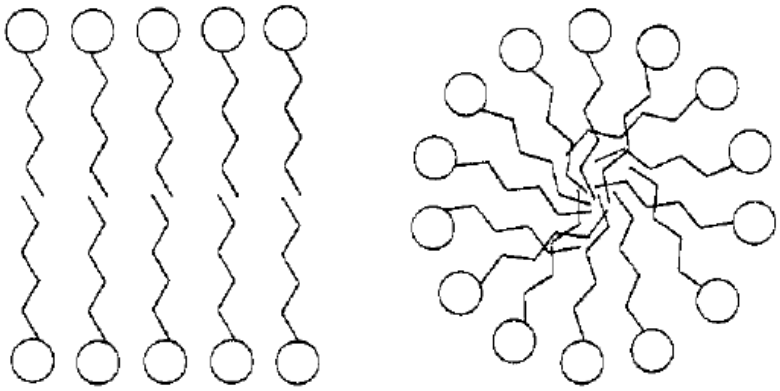

Figure 4.1.5 Cross section of a McBain 'double leaflet' lamellar micelle (left) and the Hartley spherical micelle (right).[125]

Without belittling the breakthrough work of McBain, the Hartley spherical micelle model became more accepted as it supported successive work on micelles relatively seamlessly: (i) If the lamella model was correct, there would be great sensitivity to the hydrophilic head groups which lie close in a flat bed of charge, yet cmc values on the whole are intrinsically more dependent on the carbon chain length rather than the nature of the ionic hydrophilic head group. [129] (ii) Micelles formed from a particular surfactant have been proven to have a relatively constant aggregation numbers under set conditions but the double leaflet model would probably not adopt a distinct size as they seem intuitively capable of accepting more and more molecules in succession. (iii) The hydrocarbon chains that flank the lamellar model appear to be grossly exposed to surrounding water which would be thermodynamically unfavourable in an aggregated system which by its very nature should be more stable such that it

promotes the orientation of all hydrocarbon chains away from the surrounding polar environment.

Below the cmc, the concentration of micelles is insignificant and so essentially all the surfactant is regarded as in monomeric form. Above the cmc, additional surfactant molecules added to the system form micelles, and the concentration of the free monomer remains virtually constant (Figure 4.1.6).

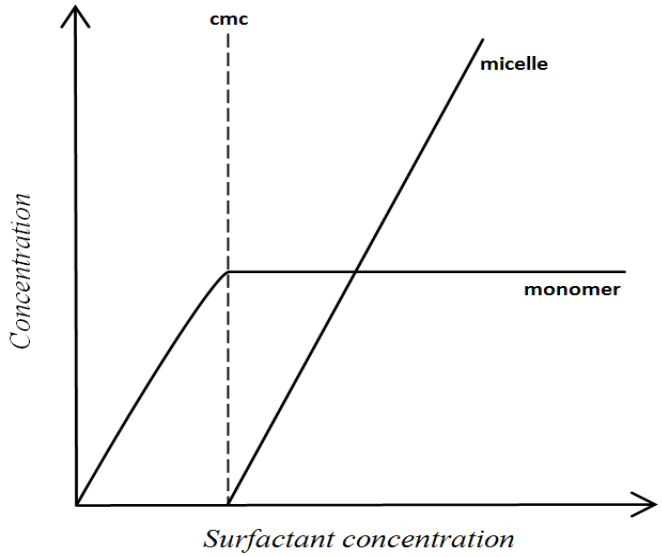

Figure 4.1.6 Concentration of individual monomer and micelle species in a typical surfactant solution over a range of surfactant concentration. [130]

The cmc is dependent on a variety of factors including the chemical structure of the surfactant and the nature of the solvent medium. In crude terms, the cmc value is indicative of the surfactant's 'desire' to aggregate, i.e. a lower cmc value means it is less favourable for the surfactant molecules to exist as monomers and so promote the formation of aggregates at a lower concentration to reduce the free energy. The cmc can therefore be reduced in a number of ways. One way is to increase the hydrophobicity of the hydrophobic moiety of the surfactant chain, thus increasing its desire to aggregate at a lower concentration. This can be achieved by increasing the chain length - most commonly used surfactants have chain length varying from C_{10} to C_{18}. Additionally, the hydrophobicity of the tail can be increased by introducing a more hydrophobic chain such as a fluorocarbon chain as opposed to the traditional hydrocarbon alkane chain. Equally, the nature of the head group will affect the cmc value. For ionic surfactants, the cmc can be lowered by adding electrolytes (simple

ionic salts) to the surfactant solution. Electrolytes lower the cmc as they reduce the electrostatic repulsion between ionic head groups.[131] These head groups of identical charge would naturally wish to repel one another and hence the reduction in this repulsion will promote the formation of a stable outer layer of the micelle. Additionally, one could argue that the presence of electrolytes will promote aggregation (i.e lower the cmc) as they would also increase the hydrophobicity of the alkyl chain due to increasing the polarity of the bulk solvent. It thus follows that on the whole non-ionic surfactants tend to have lower cmc values than their analogous ionics due to the reduction in these head groups repulsions; hence promotion of an aggregate is easier. [132]

Surfactant molecules behave differently depending on if they are present in solution as singular, free monomers or in an aggregated structure. Micelles, for example, are not surface active at all hence it is only the surfactant monomer that is responsible for decreasing the interfacial and surface tension.[133] Similarly, many other physical properties of the solution change in going from monomer to micelle. By observing these physical changes it becomes possible to detect the formation of a micelle. Figure 4.1.7 shows just some of the changes in general physical properties of the solution of monomer to micelle. The concentration at which these abrupt changes occur is generally assigned to the critical micelle concentration.

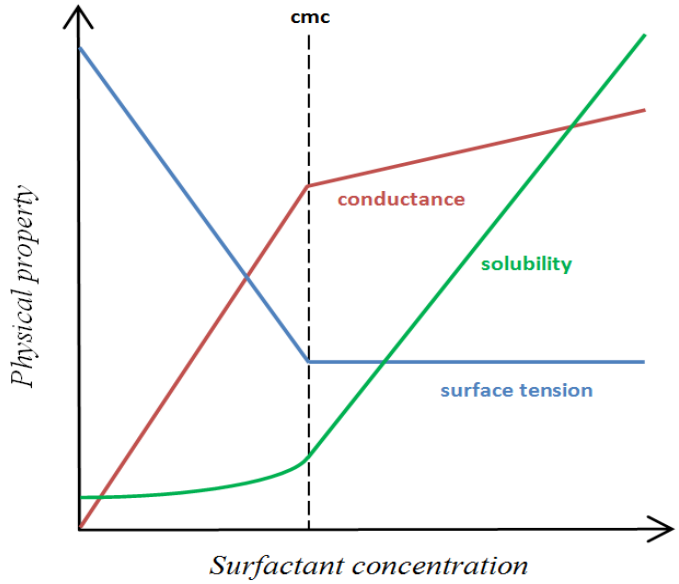

Figure 4.1.7 Changes in some physical properties of a typical surfactant solution below and above the critical micelle concentration. [134, 135]

For example, below the cmc, as the surfactant concentration is increased, the surface tension at the water-air interface is reduced as expected for these surface active agents. However, at the point of significant aggregation into the micelle, the cmc, the surface tension at the interface levels off and is no longer reduced. This is because the micelle itself has no surface active properties and so an increase in micelle concentration has negligible influence on the surface tension. The fact that the surface tension remains the same supports the notion that above the cmc the concentration of free monomer surfactant remains constant as in Figure 4.1.6. Surface tension is thus a principle method in the detection of micelles in aqueous systems.[136] Similarly, the conductance profile can be attributed to the formation of the micelle from ionic (charged) surfactants. Below the cmc, the conductivity increases linearly with concentration as more ionic surfactant is added. As the cmc is reached, the formation of micelles causes an abrupt change in the conductance isotherm. The linear increase in conductance is abruptly retarded due to the formation of the micelle, reasons for which will be discussed further in the conductance section of this chapter.[134] Similarly, the solubilising capacity of the surfactant system changes abruptly upon micellization. Surfactant monomers do not significantly affect the solubility of organic solutes and so below the cmc the solubility of non-polar organics is poor. However, the organic solute can partition into the non-polar, highly organic, micelle core in a phenomenon known as solubilisation. Thus, as aggregation ensues, the aqueous solubility of the organic solute increases significantly and, again, the sharp change in this particular physical property of the surfactant solution can be attributed to the cmc.[120] One of the most interesting things about these cell-type structures, however, is that they are not limited to just an aqueous medium.

4.1.3.3 Aggregation of surfactants in non-aqueous media

As previously described, the formation of aggregates in non-aqueous media is well studied as in the case with the formation of reverse micelles from common surfactants in non-polar, organic solvents. Likewise, the formation of regular micelles in non-aqueous solvents is also well studied. For a specific surfactant molecule it is, in general, the polarity of the solvent that dictates the micelle type and structure, whereby the formation of standard micelle occurs in polar solvents and in non-polar solvents the formation of reverse micelles takes precedence.

Singh et al studied the formation of micelles from a range of common surfactants in a variety of polar non-aqueous solvents (Table 4.1.1). [137]

Table 4.1.1 Critical micelle concentrations of sodium dodecyl sulfate (SDS) and cetyl trimethylammonium bromide (CTAB) in various polar solvents at 35 °C[137]

Solvent	ε_r	cmc SDS (mM)	cmc CTAB (mM)
N-methylformamide (NMF)	182	0.05	-
N-methylacetamide (NMA)	179	0.09	0.08
Formamide (FA)	109	1.05	0.94
Water (H_2O)	80	8.90	0.97
Dimethyl sulfoxide (DMSO)	49	42.6	35.4
Dimethylformamide (DMF)	37	16.7	10.9

ε_r = dielectric constant (25 °C)

It is apparent that the cmc values for both sets of surfactants is greatly influenced by the nature of solvent, in particular its polarity, or dielectric constant. Generally speaking, the magnitude of the cmc value increases with decreasing solvent polarity (lower dielectric constant). As discussed, the magnitude of the cmc value describes the 'desire' for a surfactant molecule to aggregate into a micelle, to reduce the overall free energy of the system. The lower the cmc value, the greater the driving force to form a thermodynamically stable micelle to reduce the free energy. As previously explained, for a given solvent system this can be influenced by the surfactant structure such that increasing the chain length of the surfactant or introducing fluorine groups, for example, will increase its hydrophobicity. This will reduce the solubility of the hydrophobic moiety and so promote micellization and so a lower cmc value is likely. In a solvent of lower polarity, the hydrophobic alkyl chain would not be as 'phobic' to the surrounding environment as it would be in a highly polar solvent. The need for aggregation would be greatly reduced and so it would be expected that the surfactant in the less polar solvent would aggregate at much higher concentration, giving a higher cmc value. This appears to be the case for these polar solvents. One would expect the cmc to increase further as the solvent polarity was reduced until the interaction between solvent and surfactant tail become so favourable, and interaction between head group and solvent so unfavourable, that reverse micellization is promoted. This is evident from the formation of reverse micelles of CTAB in cyclohexane as previously described ($\varepsilon_{r\ cyclohexane} \approx 2.0$)[138]. It would be expected that

lowest cmc values of normal micelles and reversed micelles would be at the extreme ends of polar and non-polar solvent scale, respectively.

4.1.3.4 The potential for liquid ammonia to support micelles

Liquid ammonia has a number of properties similar to water such as the ability to dissolve a diverse range of compounds and speculation has risen about the possibility of forming these cell-like structures in this dipolar aprotic solvent. Just like water, liquid ammonia is excellent at solubilising polar molecules, and shows reasonably poor solubility towards long chained, non-polar hydrocarbons, thus surfactant molecules may behave in an analogous manner to how they do in water. Due to its polar nature, it is predicted that surfactants in liquid ammonia would form regular micelle type structures rather than reverse micelles. As the surfactant molecules are added to the ammonia solvent, they would adsorb at the liquid-air interface. Eventually, as the concentration is further increased, a thermodynamically stable aggregate may form. These micelles would comprise of a number of surfactant molecules arranging themselves so that the hydrophilic ('ammoniaphilic') head group would be exposed to the ammonia solvent whilst the hydrophobic ('ammoniaphobic') tails would orientate themselves away from the bulk ammonia environment. A crude hypothesis is that if aggregation occurs in liquid ammonia, the cmc values would be higher than those in water and many of the solvents in Table 4.1.1. Owing to its relatively lower dielectric constant ($\varepsilon_{r\ \text{liquid ammonia}} \approx 16$) the hydrophobic effect would be vastly reduced and as previously explained, a higher concentration of surfactant required to promote the formation of aggregates.

The detection of micelles in surfactant solutions is not necessarily achieved by looking at a micelle macromolecule directly, but more so by observing the changes in physical and chemical properties of a system when going from a solution of free monomer surfactant molecules to the well-ordered, aggregated micelles. As previously described (Figure 4.1.7), these changes in physical properties of the micelle solution compared to the monomeric present an opportunity to detect this aggregation process. There are numerous methods for the detection of these self-assembling structures such that the method of choice is usually dependent on the micellar system in question. This can include the differences in surfactant structure, such as whether the polar head group is charged or neutral, or the nature of the

hydrophobic tail, which could be hydrogenated or fluorinated, for example. Likewise, the nature of the solvent may govern which method is used. Owing to its high vapour pressure (~ 9 bar) at room temperature it is anticipated that surfactant studies in liquid ammonia will give rise to some difficult experimental issues. For example, the traditional micelle detection method of surface tension studies would be difficult in liquid ammonia under such pressure.

4.2. Aggregation studies on ionic surfactants in water and liquid ammonia – Results and Discussion

Along with surface tension studies, conductivity is generally regarded as one of the most reliable and practical structure sensitive methods for investigating micellar systems in all kinds of media. The approach is entirely based on fact that the overall observed conductivity of a solution is summative of the individual conducting species present. This implies, therefore, that in a micelle/surfactant type system, the contributors to the overall conductivity are from free monomer surfactant ions and their counter-ions, as well as the large aggregate micelles as macroions which can also conduct.[139] Association of the charged micelle with the counter ions will also affect the conductivity.

Generally speaking, the formation of micelles from singular, monomeric, surfactant units is thought to affect the conductance of the solvent system in a number of ways: [140]

1) The total viscous drag on the aggregate is probably reduced upon aggregation. It can be visualised that a micelle with n surfactant molecules can carry a charge more efficiently that n individual molecules because the drag on the former is much lower than that of n individual surfactant molecules. Consequently, there is an increase in conductance of the micellar solution compared to the monomeric.

2) Due to the micelles high surface charge counter ions can become associated with the micelle which has two retarding effects on the conductivity of the solution. Firstly, the counter ion association with the micelle reduces the overall net charge of the bulky aggregate and so decreases its conductance. Secondly, it would follow that there is a reduction in the number of free counter ions available in solution to carry the current.

3) The high charge that the micelle carries would greatly increase the interionic attractions between the unattached counter ions and the macromolecule. Interionic attractions arise from when an ion is surrounded by an ionic atmosphere which has a net charge opposite to its own.[141] This creates a ‘drag’ effect. Thus in a micelle system, the increased ionic atmosphere around the free counter ions would reduce their mobility and hence the overall conductivity of the solution.

Each factor may be difficult to individually model and so the above systems may appear quite difficult to assimilate. Nevertheless, utilising the conductance method for the detection of micelles and aggregates, which is anticipated in liquid ammonia, is relatively straight forward and does not require much data manipulation. Factors 2 and 3, both of which cause a decrease in the molar conductivity with concentration above the cmc, tend to outweigh the effects of the first factor. The net result is that for the majority of ionic micelle systems the conductance profiles are quite definitive, as will be evident in the aqueous studies to be described. Both molar conductivity and specific conductivity plotted as a function of surfactant concentration can be used for cmc value determination.

The most useful application of conductivity to micelle solutions is the determination of the critical micelle concentration at the observed point at which retardation in conductance is observed. It is possible to determine some other micellar properties by the conductance method such as the degree of counter-ion binding (β) or aggregation number.[142,143] Nevertheless, given that nobody has reported micellization in liquid ammonia as of yet, investigation of cmc is a sensible starting point. A disadvantage of using the conductance method is that it is limited to ionic or charged surfactants where as other methods such as surface tension can allow for aggregation studies on neutral, non-ionic surfactant/micelle systems.

4.2.1 Conductivity studies on ionic surfactants in water

Prior to work in liquid ammonia, the methodology for micelle detection by conductance was tested in an aqueous environment, where it could be compared with literature as well as obtaining some new data. This would give an idea of the type of results one may expect in liquid ammonia with the hope of replicating some of the water data in the non-aqueous solvent.

An example of how conductance can be used to detect micelles in aqueous solution can be observed in Figure 4.2.1 with the anionic carboxylate surfactant, perfluorooctanoic acid (Scheme 4.2.1).

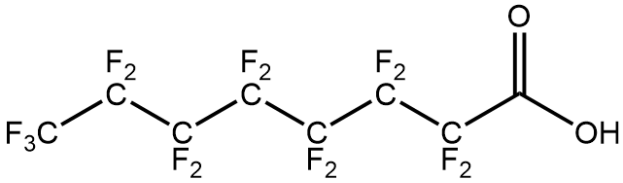

Scheme 4.2.1 Perfluorooctanoic acid (PFOA)

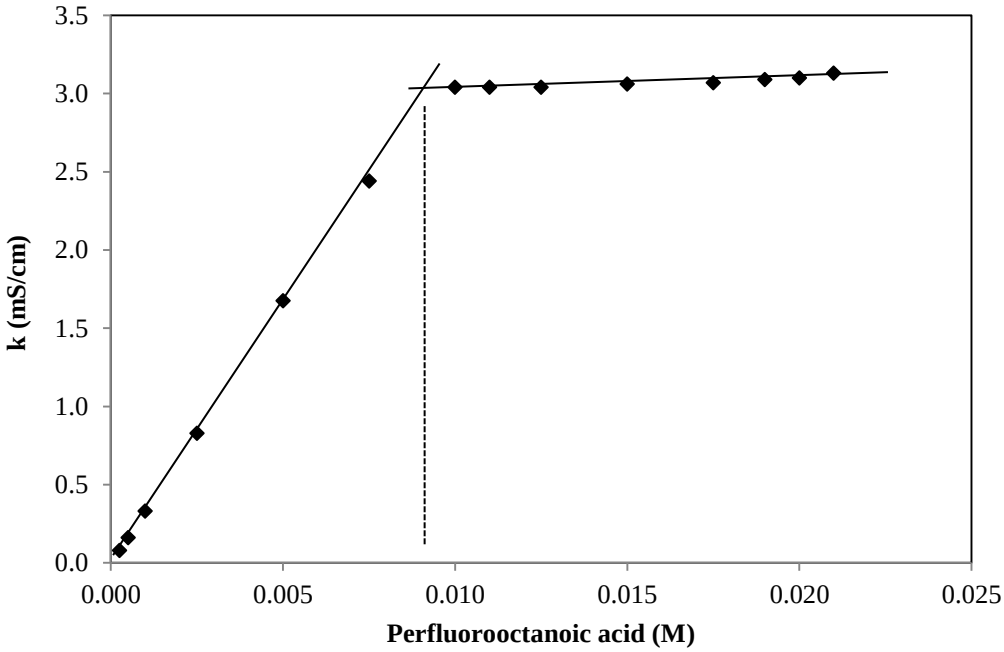

Figure 4.2.1 Specific conductivity of perfluorooctanoic acid as a function of concentration in water at 25 °C.

As the concentration of perfluorooctanoic is increased from zero, there is a good linear relationship between concentration and specific conductivity. Perfluorooctanoic acid is a strong acid with a pK_a of ~ 0 such that a 5 mM solution in water generates a pH of about 2.4. Hence it is fully ionised in water and so behaves as a strong electrolyte, just like general salts, KCl, NaBr etc. One could regard the fully dissociated acid as a 'hydronium salt' and so the observed conductivity is therefore from the additive conductivity of the monomer surfactant ion (carboxylate anion) and free counter-ion (hydronium). However, as the concentration of the perfluorooctanoic acid surfactant is further increased, an inflection in the conductivity isotherm is observed. This inflection occurs at the point of micellization when the thermodynamically stable aggregates form and this point can be assigned as the cmc of the surfactant in solution. At the cmc the conductivity increases less abruptly

because the newly formed micelle macro-ions have an overall retarding effect on the conductivity of the solution. The newly formed micelle likely impedes the conductance due to counter ion binding and an increase in the ionic atmospheres, as previously described. The cmc of perfluorooctanoic acid determined in Figure 4.2.1 of around 9.3 mM is consistent with literature value of 9.7 mM obtained from other detection methods such as surface tension.[144] Similarly, a plot of molar conductivity as function of surfactant concentration allows for determination of the cmc and as expected, above the cmc, the molar conductivity decreases with further increasing the surfactant concentration (Figure 4.2.2).

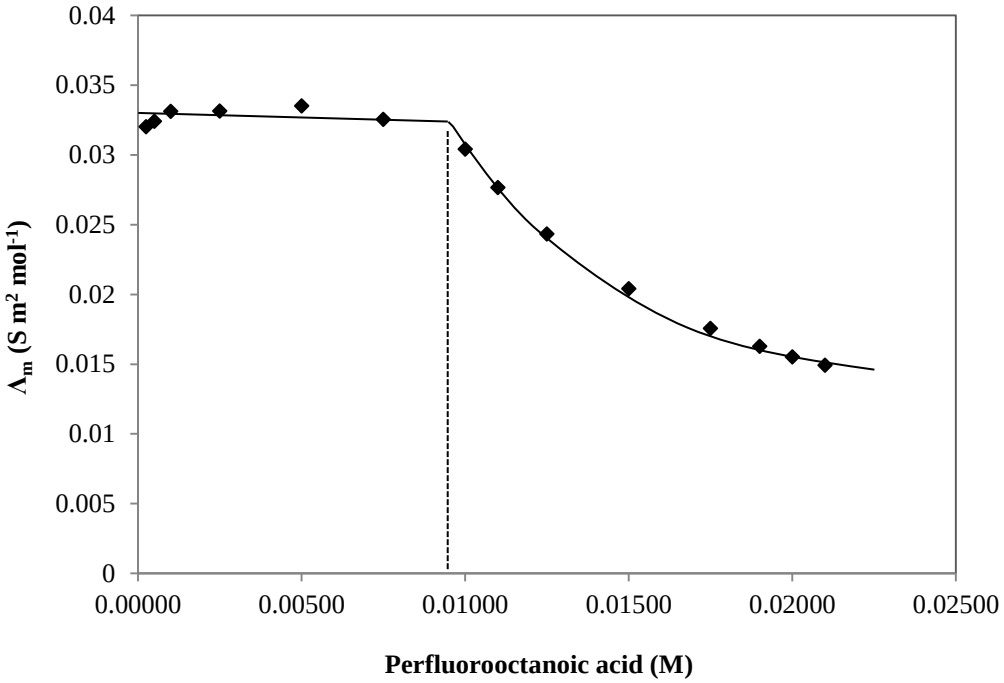

Figure 4.2.2 Molar conductivity of perfluorooctanoic acid as a function of concentration in water at 25 °C.

Molar conductivity is defined as the conductivity per unit concentration: [145]

$$\Lambda_m = \frac{\kappa}{c}$$

Where:

Λ_m = Molar conductivity (S m^2 mol^{-1})

κ = Specific conductivty (S m^{-1})

$c = \text{Concentration (mol m}^{-3})$

Likewise, the cmc can be determined at roughly 9 mM demonstrating that the both molar and specific conductivity can be used for micelle detection. Molar conductivity is often used as a means of measuring the 'efficiency' with which a particular electrolyte conducts current in a solution whereas specific conductance or conductivity can give a visual picture of the actual conductance of the solution as the concentration changes. They can be interconverted easily and in the literature both methods are widely used such that the use of one over the other appears to be individual preferences rather than necessity.

Figures 4.2.3 to 4.2.5 show more examples of how cmc values of other ionic surfactants (Schemes 4.2.2 to 4.2.4) in water can be determined using the conductometric method.

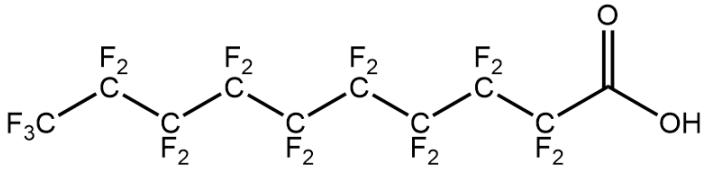

Scheme 4.2.2 Perfluorodecanoic acid (PFDA)

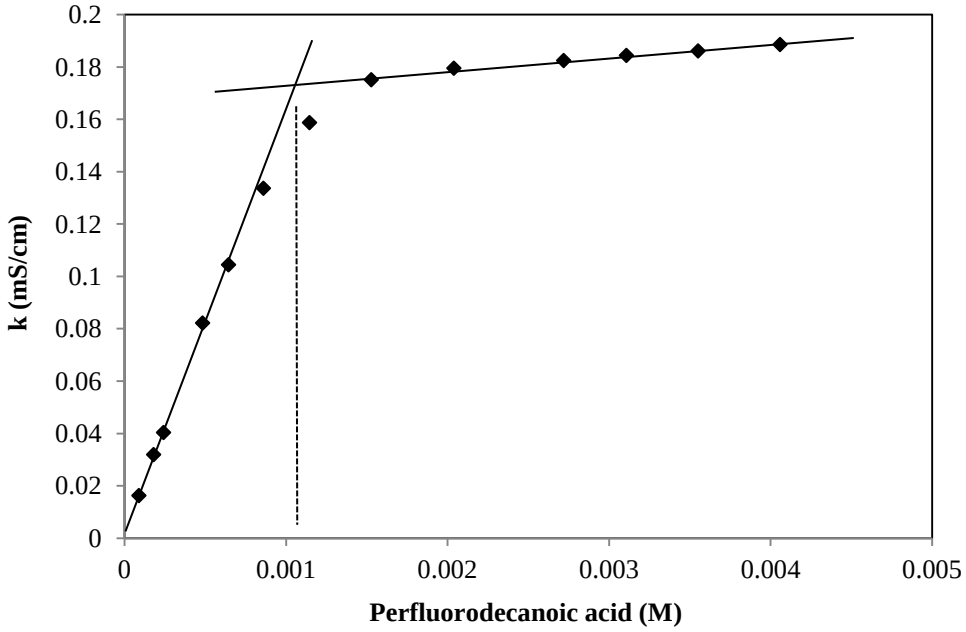

Figure 4.2.3 Specific conductivity of perfluorodecanoic acid as a function of concentration in water at 25 °C.

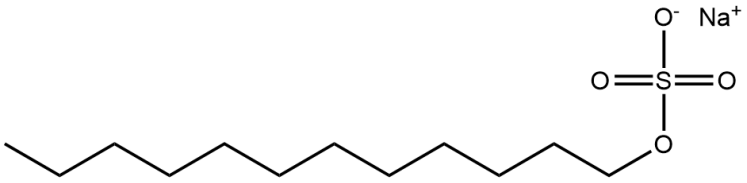

Scheme 4.2.3 Sodium dodecyl sulfate (SDS)

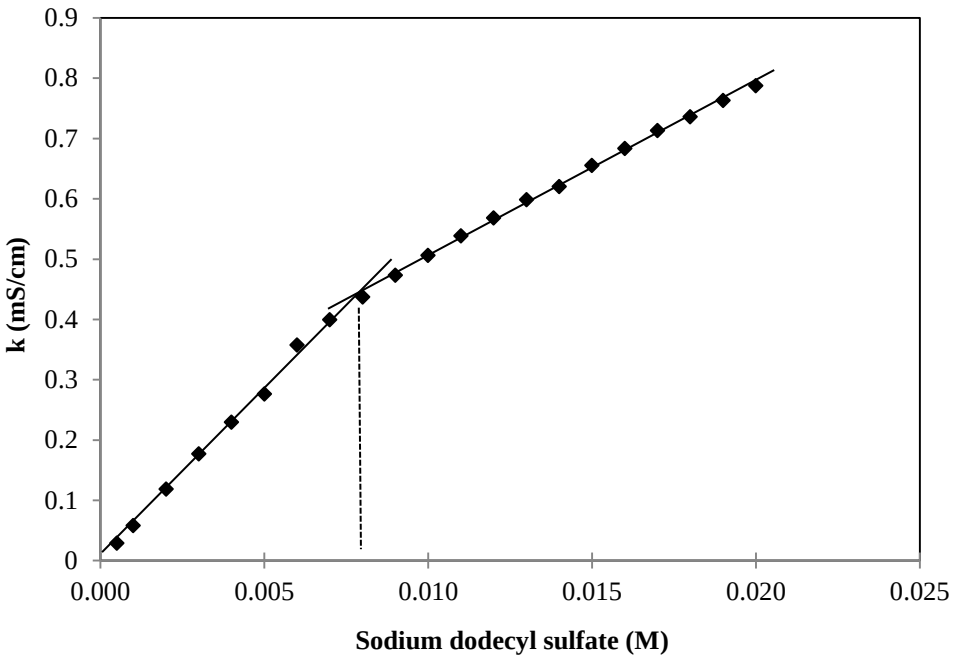

Figure 4.2.4 Specific conductivity of sodium dodecyl sulfate as a function of concentration in water at 25 °C.

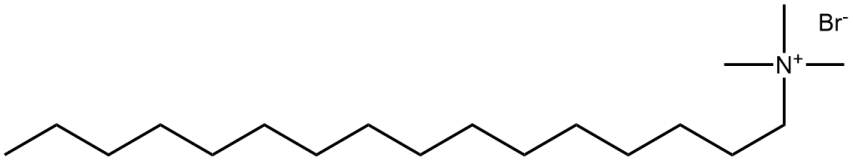

Scheme 4.2.4 Cetrimonium bromide (CTAB)

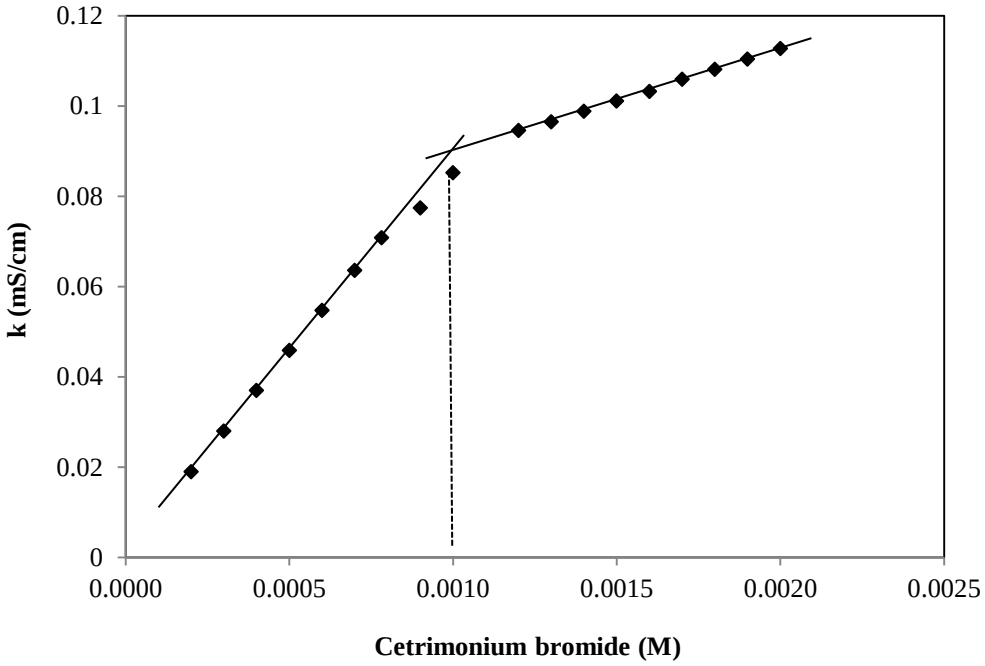

Figure 4.2.5 Specific conductivity of cetrimonium bromide as a function of concentration in water at 25 °C.

Some cmc values of ionic surfactants determined in water from both this work and the literature are shown in Table 4.2.1.

Table 4.2.1 Critical micelle concentrations of ionic surfactants in water at 25 °C.

Surfactant		cmc (mM)	Reference, detection method
Perfluoroheptanoic acid	$CF_3(CF_2)_5COO^-H^+$	25	85, NMR
Sodium perfluoroheptanoate	$CF_3(CF_2)_5COO^-Na^+$	83	85, surface tension
Perfluorooctanoic acid	$CF_3(CF_2)_6COO^-H^+$	9.7	144, unknown method
		9.3	this work, conductivity
Sodium perfluorooctanoate	$CF_3(CF_2)_6COO^-Na^+$	35	85, NMR
Perfluorononanoic acid	$CF_3(CF_2)_7COO^-H^+$	3.1	146, surface tension
		3.4	this work, conductivity
Sodium perfluorononanoate	$CF_3(CF_2)_7COO^-Na^+$	11.8	this work, conductivity
Perfluorodecanoic acid	$CF_3(CF_2)_8COO^-H^+$	1.1	this work, conductivity
Sodium perfluorodecanoate	$CF_3(CF_2)_8COO^-Na^+$	3.1	this work, conductivity
Perfluoroundecanoic acid	$CF_3(CF_2)_9COO^-H^+$	0.23	this work, conductivity
Sodium perfluoroundecanoate	$CF_3(CF_2)_9COO^-Na^+$	0.55	this work, conductivity
Perfluorododecanoic acid	$CF_3(CF_2)_{10}COO^-H^+$	0.11	this work, conductivity
Sodium perfluorododecanoate	$CF_3(CF_2)_{10}COO^-Na^+$	0.2	this work, conductivity
Perfluorooctane sulfonate (Et_4N^+)	$CF_3(CF_2)_7SO_3^-Et_4N^+$	4.1	this work, conductivity
Sodium dodecyl sulfate (SDS)	$CH_3(CH_2)_{11}OSO_3^-Na^+$	8.3	147, fluorescence
		8.2	148, conductivity
		8.1	this work, conductivity
Cetrimonium bromide (CTAB)	$CH_3(CH_2)_{15}N^+(Me)_3Br^-$	0.9	149, fluorescence
		1.0	this work, conductivity
Dioctyl sodium sulfosuccinate (Aersol OT)	$CH_3(CH_2)_3CH(CH_2CH_3)CH_2OOCCH(SO_3^-Na^+)CH_2COOCH_2CH(CH_2CH_3)CH_2(CH_2)_2CH_3$	2.7	150, unknown method

In a given solvent system the critical micelle concentration is dependent on a large number of parameters and is an indication of the surface activity of the amphiphilic monomer. The more surface active the molecule is, the greater its tendency for micellization, and hence aggregation occurs at a lower concentration giving a lower cmc value.[151] Increasing the chain length is one of the simplest ways to increase the surface active properties of the molecule. Consequently, the longer the hydrophobic tail of the surfactant, the lower the cmc value. This can be seen from the cmc values obtained for the long chained fluorinated carboxylic acids in Table 4.2.1, where by the

relationship between cmc value and number of carbon atoms in the hydrophobic tail is apparent (Figure 4.2.6).

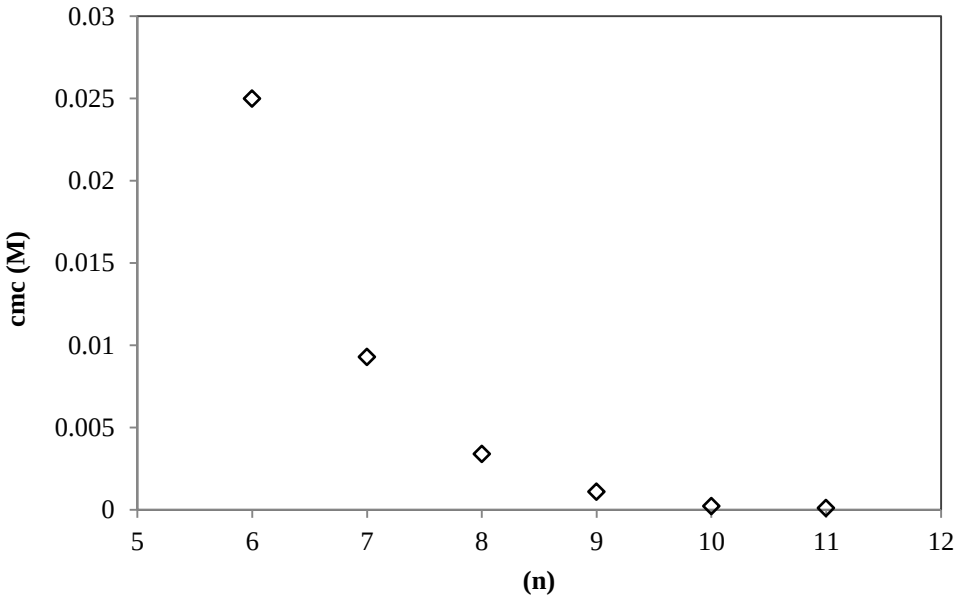

Figure 4.2.6 Critical micelle concentration (cmc) of perfluorinated carboxylates as a function of the number of carbons in the hydrophobic tail (n) in water at 25°C.

The cmc as a function of number of carbons in the surfactants hydrophobic, non-polar tail is non-linear, and in fact, for a homologous series of amphiphiles, cmc values are expected to follow the empirical Klevens rule, according to a logarithmic equation:[152]

$$log\ cmc = A - Bn$$

where cmc is critical micelle concentration of the surfactant, n is the number of carbon atoms in the hydrophobic chain, A and B are constants for a homologous series of surfactants in a given solvent system.

The constant A reflects the specific nature of the hydrophilic head group and its interactions with the solvent, whereas B displays the effect of each additional methylene unit, or as in this case, -CF_2- unit, on the cmc. The A value is generally independent of the B value suggesting that they are indicative of the nature of the head group and tail group, respectively. [153] A plot of log cmc as function of number of carbons for the fluorinated carboxylates shows the values are in good agreement with Klevens rule (Figure 4.2.7).

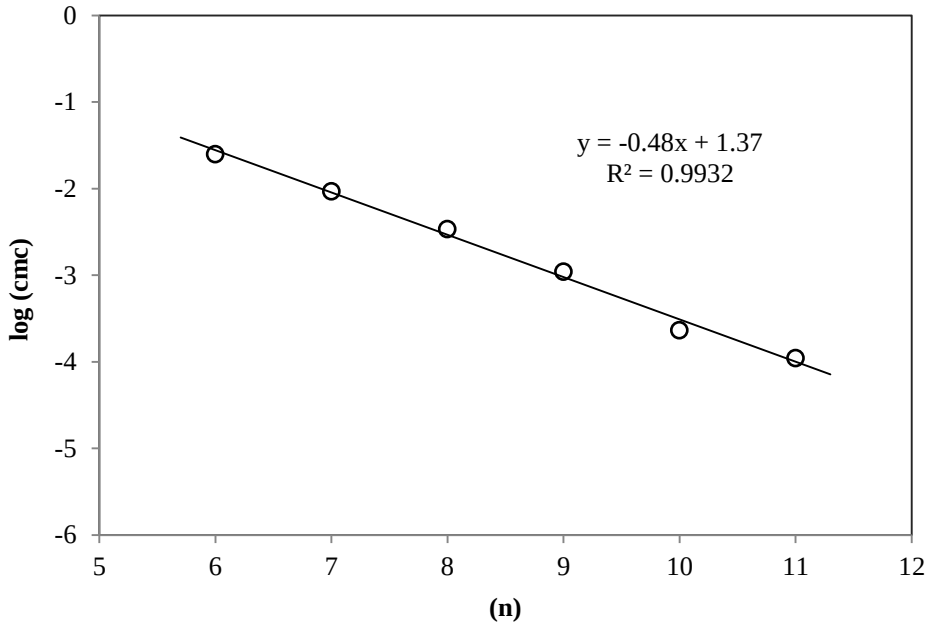

Figure 4.2.7 Logarithm of cmc (M) as a function of the number of carbon atoms in the hydrophobic tail (n) for a series of perfluorinated carboxylates in water at 25 °C.

The obtained values of A and B are 1.37 and 0.48, respectively. The value of 1.37 for A, the constant for the specific nature of the hydrophilic head group, is slightly less than that obtained for the fluorinated sodium salt carboxylates from this work (Table 4.2.2). These values of A and B can be compared with literature for normal alkyl carboxylates.

Table 4.2.2 Klevens constants for carboxylates in water at 25°C

Surfactant head group	Chain type	A	B	Reference
Na^+ carboxylate	hydrogenated	1.80	0.30	153
K^+ carboxylate	hydrogenated	1.90	0.29	153
H^+ carboxylate	fluorinated	1.37	0.48	this work
Na^+ carboxylate	fluorinated	1.60	0.44	this work

For non-fluorinated carboxylates, the B value of ~ 0.3 (approx. log2) indicates that the cmc is roughly halved for each additional methylene unit added. This is consistent with the majority of fully hydrogenated surfactants, even for surfactants with a wide variety of polar head groups: the cmc values of various length N-alkyl-N-methylpyrrolidinium bromides, for example, give a B value of 0.30, and n-alkyl-1-

sulfonates give a B value of 0.29.[152] However, the effect of introducing an extra -CF_2- group into the fluorinated surfactant chain has a greater effect on cmc, suggested by the higher B value of ~ 0.46, indicating that the cmc is lowered 3-fold per additional -CF_2-. From this, it can be deduced that one -CF_2- group is approximately equivalent to 1.4 -CH_2- units. For example, a fluorosurfactant with 8 carbons would, with regards to cmc, behave like a hydrocarbon surfactant with 11 or 12 carbons. This is no surprise because, as described previous, the cmc is indicative of the surface activity of the surfactant and so increasing the hydrophobicity of the tail will promote aggregation at a lower concentration. Introducing fluorinated groups into the chain will certainly increase its hydrophobicity and tendency to aggregate.

The Klevens relationship value will be discussed in further detail with regards to the aggregation of fluorinated amides in liquid ammonia and how it compares to the general surfactants in water (section 4.3).

4.2.2 Conductivity studies on ionic surfactants in liquid ammonia

4.2.2.1 Initial attempts to replicate the aqueous studies in liquid ammonia

By repeating the aqueous surfactant conductivity experiments in liquid ammonia, and hopefully seeing similar changes in the conductivity isotherm at a particular concentration (cmc), the potential formation of aggregates in liquid ammonia may be realised. Furthermore, if a variety of cmc values could be obtained for a series of homologous surfactants of varied chain length, the Klevens constants in liquid ammonia could be determined and compared to those in water.

Conductivity measurements in liquid ammonia were performed at -15°C due to the pressure limit on the conductivity cell. Interestingly, the observed conductivity of sodium dodecyl sulfate (SDS) in liquid ammonia shows a non-linear dependence on the concentration of the surfactant (Figure 4.2.8).

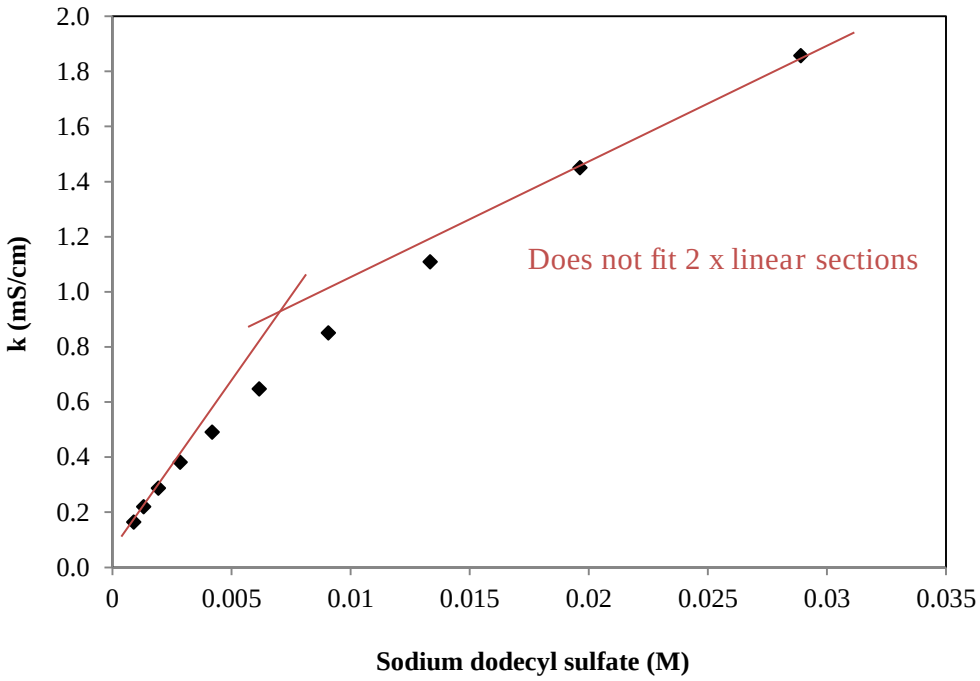

Figure 4.2.8 Specific conductivity of sodium dodecyl sulfate as a function of concentration in liquid ammonia at -15 °C.

However, the profile does not show a clear 'break' with two linear portions as observed with the aqueous surfactant solutions. This non-linear conductivity profile is observed with other ionic surfactants in liquid ammonia, including perfluorinated carboxylates and sulfonates (Figures 4.2.9 and 4.2.10 are just 2 examples).

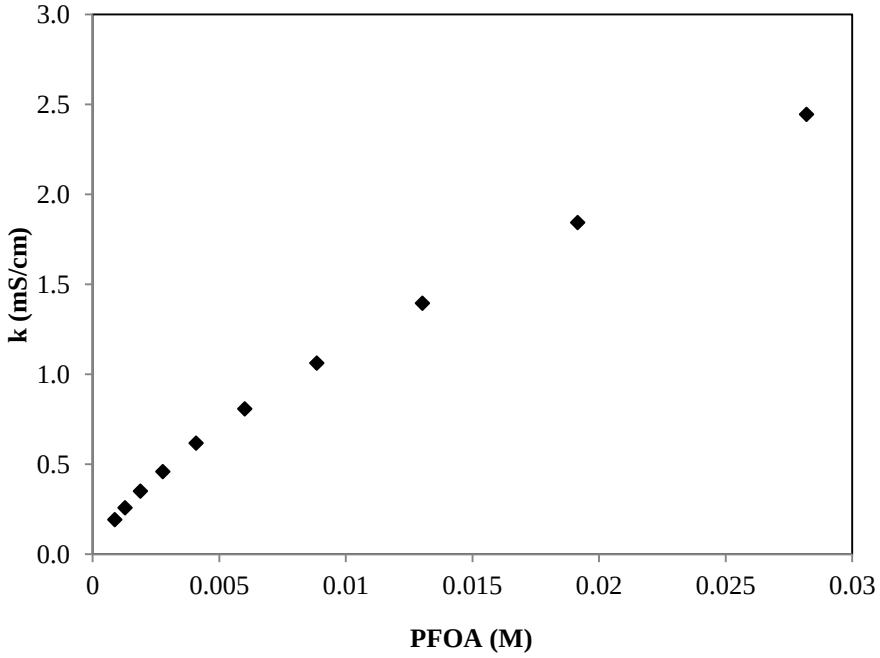

Figure 4.2.9 Specific conductivity of perfluorooctanoic acid as a function concentration in liquid ammonia at -15 °C.

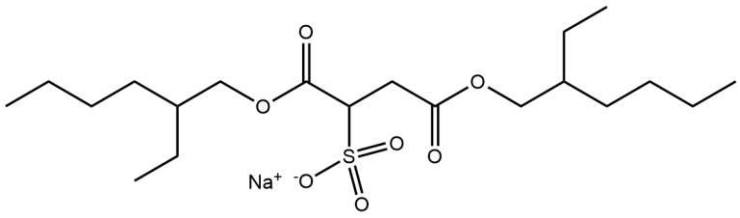

Scheme 4.2.5 Dioctyl sodium sulfosuccinate (Aerosol OT)

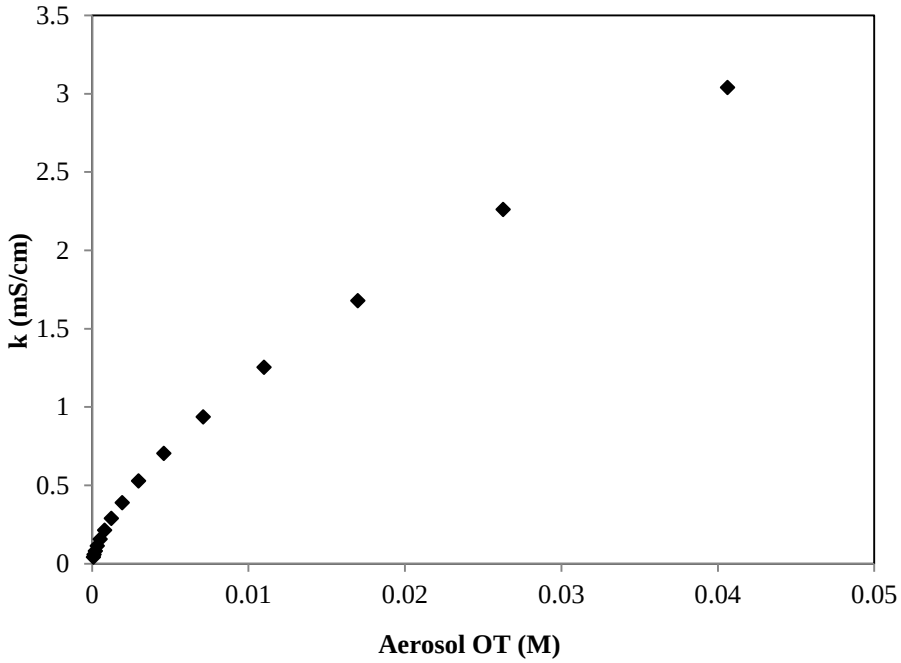

Figure 4.2.10 Specific conductivity of Aerosol OT (Dioctyl sodium sulfosuccinate) as a function of concentration in liquid ammonia at -15 °C.

These behaviours of the surfactant conductivity isotherms in liquid ammonia may be indicative of some kind of aggregation phenomena but probably not micelle formation. Further investigation into the conductance of these species in liquid ammonia was required.

4.2.2.2 Modelling conductivity in liquid ammonia

On initial inspection, the conductance of these surfactants in liquid ammonia is comparable to that of a weak electrolyte in water, such as that of acetic acid (Figure 4.2.11). Curvature here is due to a relative decrease in dissociation with increasing concentration.

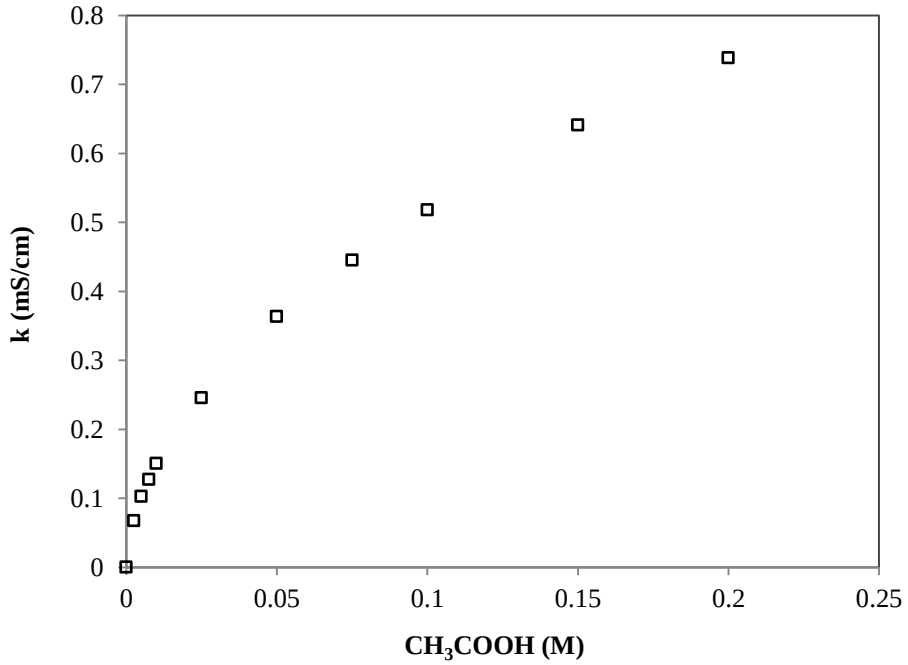

Figure 4.2.11 Specific conductivity of acetic acid (CH_3COOH) in ultra-pure water as a function of concentration at 25 °C.

As evident, the observed conductance profile for acetic acid in water is not too dissimilar to those of the surfactants in liquid ammonia, and so initially attempts were made to fit the liquid ammonia data to Ostwald's dilution law:

$$\frac{1}{\Lambda_m} = \frac{1}{\Lambda_m^\circ} + \frac{\Lambda_m c}{K_a(\Lambda_m^\circ)^2}$$

Where:

Λ_m = Molar conductivity (Sm^2mol^{-1})

Λ_m° = Molar conductivity at infinite dilution (Sm^2mol^{-1})

K_a = Acid dissociation constant

c = Concentration of electrolyte (M)

However, the conductivity and concentration relationship observed for the surfactants in liquid ammonia does not appear to correlate with Ostwald's dilution law. Ostwald's

dilution law governs the conductivity of weak electrolytes and is derived from the equilibrium of the acid dissociation (Scheme 4.2.6).[154]

$$HA + H_2O \overset{K_a}{\rightleftharpoons} H_3O^+ + A^-$$

Scheme 4.2.6

Acetic acid, ($pK_a \approx 4.7$) is not fully ionized in water and thus behaves as a weak electrolyte, as opposed to strong electrolytes, such as ionic compounds, which are fully ionized. Hence Oswald's law of dilution is observed for acetic acid in water. The surfactants in liquid ammonia, however, should all behave as strong electrolytes as they are all essentially ionic salts; even the fluorinated acids, all with pK_a values close to zero would be fully deprotonated and exist in liquid ammonia as the ammonium carboxylate salt. Therefore, it was not surprising that the conductance in liquid ammonia did not correlate with Ostwald's dilution law.

Under the assumption that the ionic species in liquid ammonia should behave as strong electrolytes, attention turned to the relationship that unifies the conductance of such species, according to Kohlrausch's law:

$$\Lambda_m = \Lambda_m^\circ - \mathcal{K} c^{1/2}$$

Where:

Λ_m = Molar conductivity (Sm^2mol^{-1})

Λ_m° = Molar conductivity at infinite dilution (Sm^2mol^{-1})

$\mathcal{K}$ = An empirical constant specific to the salt's stoichiometry

c = Concentration of electrolyte (M)

Again, the liquid ammonia data did not correlate with Kohlrausch's law equation as any common ionic salt such as sodium chloride or ammonium bromide would in water.[154] It would appear therefore that surfactant species in liquid ammonia do not follow the typical conductance profile of weak electrolytes, like a weak acid/base in water, or that of a strong electrolyte, like a fully ionized salt in water. This infers that

there is some property of liquid ammonia that governs the conductance of species in a different manner to that in a conventional aqueous medium.

Although generally considered a polar solvent, with the ability to solubilise a range of ionic species as well as organics, liquid ammonia is in fact only moderately polar compared with water. The dielectric constant of ammonia is roughly 5 times smaller than water and hence there is a noticeable difference not only on the ionisation, but also the dissociation of compounds in these two solvents. Take for example, a simple diatomic salt, A^-B^+, that is soluble in both water and liquid ammonia (Scheme 4.2.7). The attractive force between oppositely charged ions is inversely proportional to the dielectric constant of the medium.

$$A^- + B^+ \underset{K_{diss}}{\overset{K_{ip}}{\rightleftharpoons}} [\,A^-B^+\,]_{\text{ion-pair}}$$

Scheme 4.2.7

The high dielectric constant of water favours the full dissociation of ion-pairs, thus the equilibrium is significantly shifted to the left, and so a typical salt ionised in water would be vastly dissociated into free ions with zero or negligible ion-pairing. Conversely, however, liquid ammonia, with its comparatively non-polar nature and lower dielectric constant, greatly facilitates the ion-pairing of ionised compounds. Thus, a salt, even though still fully soluble in liquid ammonia, would show a reduction in the dissociation of the salt into its free ions with increasing concentration.[155]

The conductivity of a simple salt, ammonium chloride, for example, which is very soluble in both water and liquid ammonia, can be used to demonstrate the ammonia ion-pairing effect in the non-aqueous solvent compared to full dissociation in water. In water, the conductivity increases linearly with concentration as expected (Figure 4.2.12). Water facilitates the full dissociation of ammonium chloride into the free anion (Cl^-) and cation (NH_4^+), which are both conducting species, with zero of the non-conducting ion-pairs present, and so the concentration/conductivity isotherm is linear.

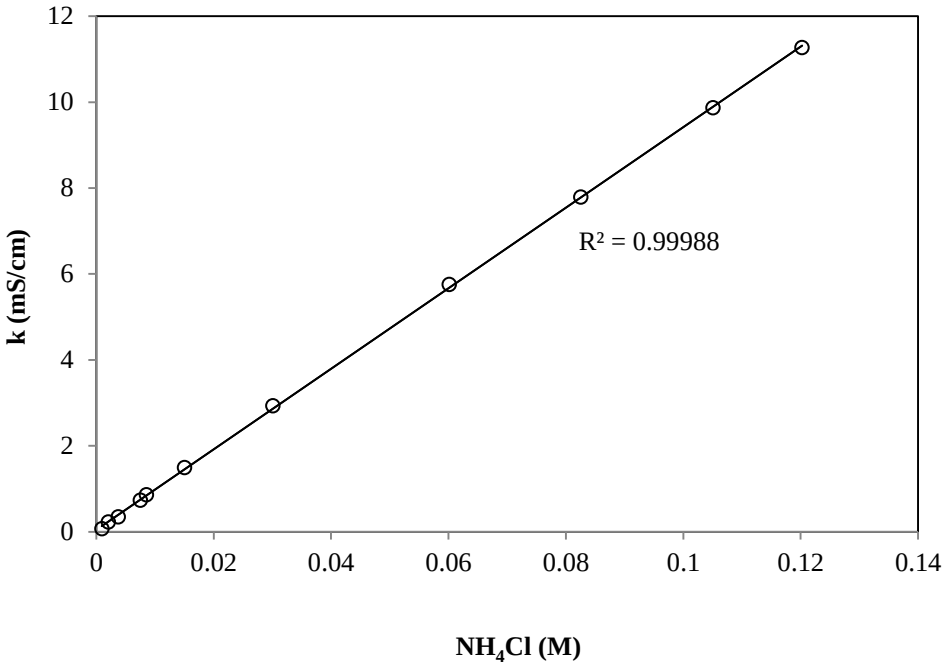

Figure 4.2.12 Ammonium chloride specific conductivity as function of concentration in water at 25 °C is linear.

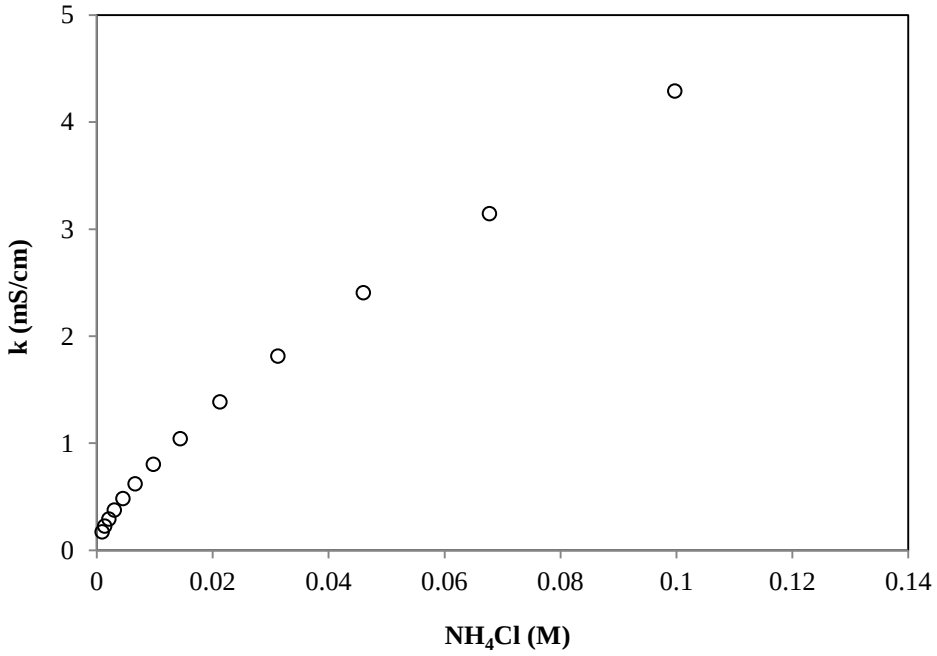

Figure 4.2.13 Ammonium chloride specific conductivity as a function of concentration in liquid ammonia at -15 °C is non-linear.

A plot of the conductivity against concentration for ammonium chloride in liquid ammonia is non-linear, showing the same type of curvature as was observed

previously with the ionic surfactants (Figure 4.2.13). It was also found that the liquid ammonia data for these simple salts, which are strong electrolytes in water, does not correlate to Kohlrausch's law for strong electrolyte conductance. This would suggest that there is some non-conducting species present which is concentration dependant, supporting the theory that the relatively reduced polarity of liquid ammonia facilitates the association of these species into neutral, non-conducting, ion-pairs. A model could be developed to describe and correlate the observed conductivity profile with this ion-pair phenomenon.

Using the mass balance equilibrium from Scheme 4.2.7, the dissociation constant for the ion-pair can be described from the concentration of the ion pair and freely dissociated species:

$$K_{diss} = \frac{[B^+][A^-]}{[B^+ A^-]_{ip}}$$

The total amount of salt present can be calculated from:

$$[A^-]_{tot} = [A^-] + [B^+A^-]_{ip}$$

Using a quadratic solver allows for modelling the conductance of ionic species in liquid ammonia (see appendix 7.2 for full derivation).

Where:

$$\Lambda = \lambda + \varepsilon[A^-]$$

and

$$[A^-] = \frac{-K_{diss} + \sqrt{{K_{diss}}^2 - (4 \times K_{diss} \times [A^-]_{tot})}}{2}$$

Where:

$\Lambda =$ Observed conductivity of solution ($S\ m^{-1}$)

$\lambda =$ Background NH3 conductivity ($S\ m^{-1}$)

$\varepsilon =$ Specific conductivity of A^- ions ($S\ m^{-1}\ M^{-1}$)

$[A^-]$ = conducting species (M)

$[A^-]_{tot}$ = total amount conducting species present (M)

K_{diss} = conducting species (M)

The quadratic solver model was compiled in the function fitting software Origin 8 and allows for a plot of conductance as a function of the total ionic species concentration.

Using this model it was hoped to distinguish between ion-pairing and higher aggregation in liquid ammonia. The fluorinated acids could be viewed slightly different to the 'salt like' surfactants such as SDS in that they firstly undergo ionisation in liquid ammonia (Scheme 4.2.8).

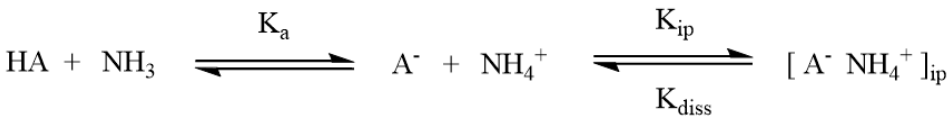

Scheme 4.2.8

However, as these fluoroacids are fully ionized in liquid ammonia, the left hand side of the scheme can be ignored and the system can be thought of as a general strong electrolyte 'salt' in solution. In DMF, with dielectric constant of around 38, pyrdinium hydrochloride ($[PyH^+]$ + $[Cl^-]$) has been shown to associate into a non-conducting ion pair ($[PyH^+Cl]_{ip}$) as well as exist as the dissociated conducting ion species, but additionally can exist as the deprotonated free base ([Py] + $[H^+]$ + $[Cl^-]$) in this moderately polar aprotic solvent.[156] This would require a more complex modelling method taking into account the equilibrium on the left hand side of Scheme 4.2.8.

The conductivity ion-pairing model was first applied to the simple salts in liquid ammonia such as ammonium chloride (Figure 4.2.14).

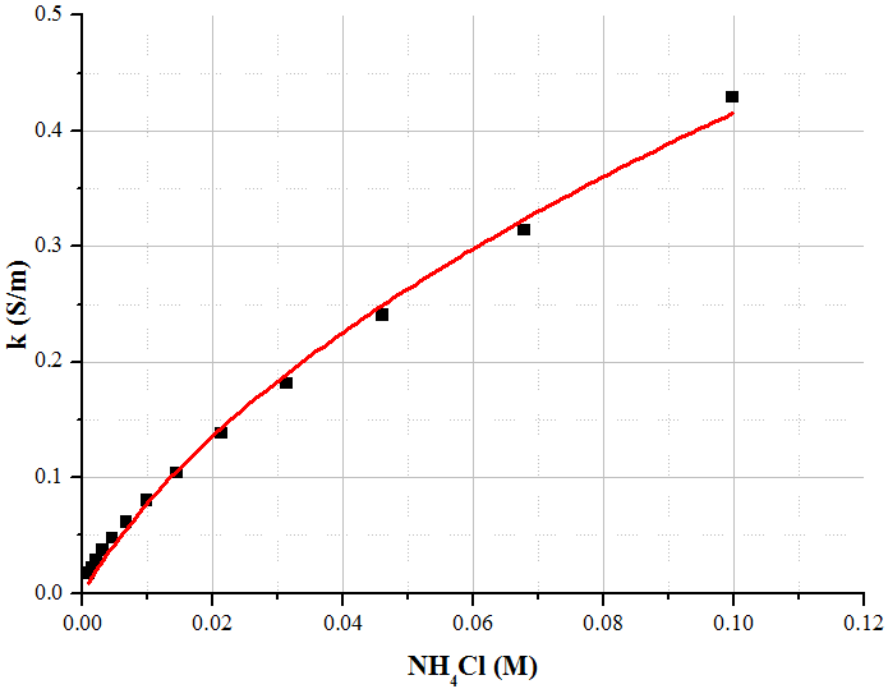

Figure 4.2.14 Specific conductivity of ammonium chloride as a function of concentration in liquid ammonia fit to the Origin ion-pairing model.

From the ammonium chloride ion-pairing model, a K_{diss} value of 0.0311 can be obtained, yielding an ion pairing constant of K_{ip} = 32. Another simple salt, tetrabutylammonium bromide (TBAB) also showed the non-linear conductance profile in liquid ammonia for which the dissociation constant and ion-pairing constant are 0.0158 and 63, respectively. Comparison of the two ammonium salts suggests that there is a higher degree of dissociation (less ion-pairing) with the smaller NH_4Cl compared to the bulky TBAB. It is likely that steric hindrance of the larger tetrabutylammonium cation is reducing the solvation by the ammonia molecule and thus promoting the formation of the neutral ion-pair. Contrary to this, the smaller ammonium cation with negligible steric hindrance can be solvated much better by the ammonia molecule and so a higher degree of dissociation would be anticipated, as evidently appears to be the case. Additionally, the smaller charge density in the $(Bu)_4N^+$ (more delocalised) may reduce the solvation by ammonia solvent, thus promoting ion-pairing.

It has therefore been established for simple salts in liquid ammonia, that the non-linear relationship between conductivity and concentration can be attributed to the formation of the non-conducting ion-pair species. The ion-pairing model was then

applied to the long chained surfactants in liquid ammonia to confirm that the observed conductance profile was also indicative of the ion-pairing phenomenon, as opposed to aggregation into micelles.

For a range of surfactants tested, the conductivity profiles did indeed follow the ion-pairing model. Figures 4.2.15 and 4.2.16 shows just two examples of ion-pair model fits for sodium dodecyl sulfate (SDS) and perfluorooctanoic acid (PFOA) in liquid ammonia. K_{diss} and K_{ip} values can be found in Table 4.2.3

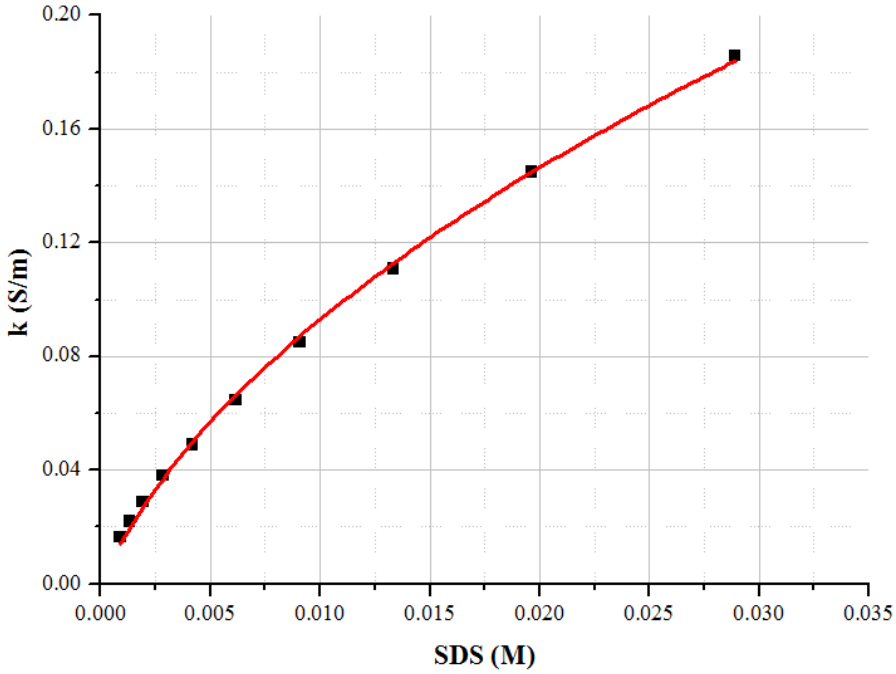

Figure 4.2.15 Specific conductivity of sodium dodecyl sulfate (SDS) as a function of concentration in liquid ammonia (-15 °C) fit to the Origin ion-pair model.

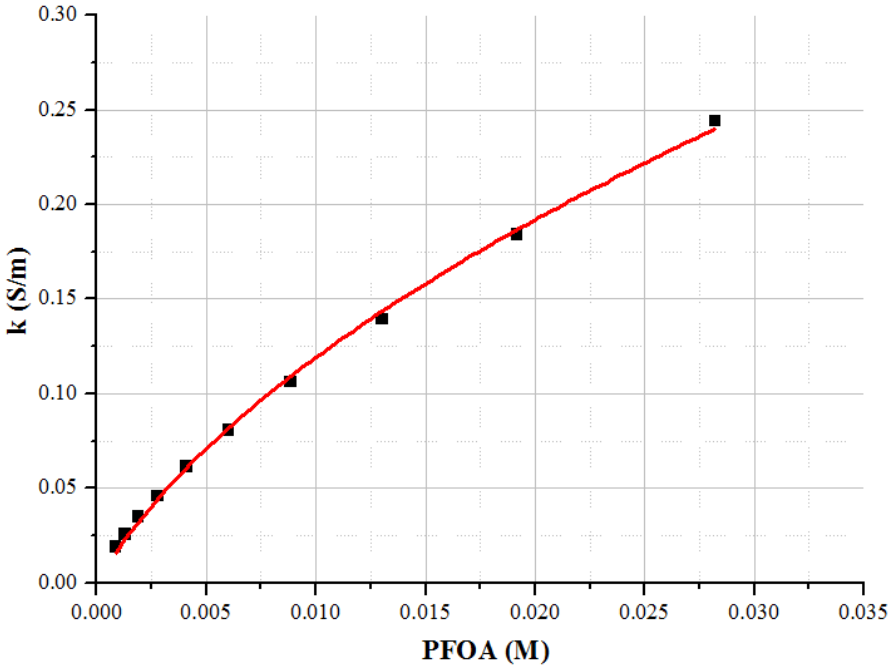

Figure 4.2.16 Specific conductivity of perfluorooctanoic acid (PFOA) as a function of concentration in liquid ammonia (-15 °C) fit to the Origin ion-pair model.

Table 4.2.3 K_{diss}, K_{ip} and ε values obtained from ion-pairing model of a range of surfactants and salts in liquid ammonia at -15 °C.

Salt/surfactant	**K_{diss} (M)**	**K_{ip} (M^{-1})**	**ε ($Sm^{-1}M^{-1}$)**
NH_4Cl	0.03109	32.2	9.8
TBAB	0.01580	63.3	17.3
Dioctyl sodium sulfosuccinate	0.00606	165.0	22.9
Sodium dodecyl sulfate	0.00590	169.5	17.6
Trifluoroacetic acid (C2)	0.01290	77.5	28.1
Perfluorooctanoic acid (C8)	0.00918	108.9	19.8
Perfluorononanoic acid (C9)	0.00689	145.1	21.5
Perfluorodecanoic acid (C10)	0.00418	239.2	23.2
Perfluoroundecanoic acid (C11)	0.00236	423.7	24.0
Perfluorododecanoic acid (C12)	0.00026	3913.8	50.9
Perfluorooctadecanoic acid (C18)	- - - - - - - Insoluble in LNH_3 at 2 mM - - - - - - -		
Pefluorooctane sulfonate (Et_4N^+)	0.00143	699.3	35.3
Decyltrimethyl ammonium iodide	0.00149	671.1	49.3

In an effort to compare the K_{diss} and K_{ip} constants for the various ionic surfactants in liquid ammonia, there appears to be some kind of trend with the fluorinated carboxylate surfactants. It appears that as the chain length is increased, the K_{diss} value is decreased, and hence an increase in ion-pairing is observed. The apparent trend raises questions as to why the ion-pairing is dependent on the chain length of the fluoro surfactant. For the longer chained fluoroacids, the influence of chain length is not expected to have much influence on the interactions between head group and counter ion. It is expected that the nature of the charged head groups influences ion pairing with the counter ion and solvent and thus for all long chained fluorinated carboxylic acids a reasonably constant ion pairing value would be anticipated. This appears to be the case with the sulfonate and sulfate head groups. Sodium dodecyl sulfate and dioctyl sodium sulfosuccinate (Aerosol OT), for example, both with Na^+ counter ion, yield similar K_{diss} and K_{ip} values, possibly owing to the similar structure of the sulfate and sulfonate anionic head group (Scheme 4.2.9).

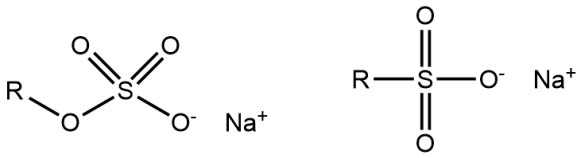

Scheme 4.2.9 Similarities between the sulfate (left) and sulfonate (right) head groups.

In fact, it is observed in water that straight chained alkane sulfonate and sulfate surfactants have remarkably similar cmc values as well as Klevens A and B values. For example, the cmc values of sodium tetradecyl sulfonate and sodium tetradecyl sulfate in water are 2.5 and 2.2 mM, respectively.[157] As they have the same hydrocarbon tail this suggests that the slightly different ionic head groups have similar interactions with the water solvent and sodium counter-ion or the cmc values would not be alike. This is also evident in their roughly comparable liquid ammonia ion pair values, indicating that specific nature of the head group of the surfactant should control the ion-pairing and not the chain length.

Therefore, one has to question why there is an apparent increase in the ion-pairing as chain length is increased for fluorinated carboxylates in liquid ammonia. One potential reason is that these longer chained fluoro surfactants, although not necessarily forming typical larger micelle-type structures, may be forming some kind

of higher aggregates such as dimers or trimers, for example. The formation of these higher aggregates could arise from favourable interactions between the adjacent fluorinated chains by van der Waals forces, as opposed to the unfavourable interactions with the ammonia solvent (Scheme 4.2.10).

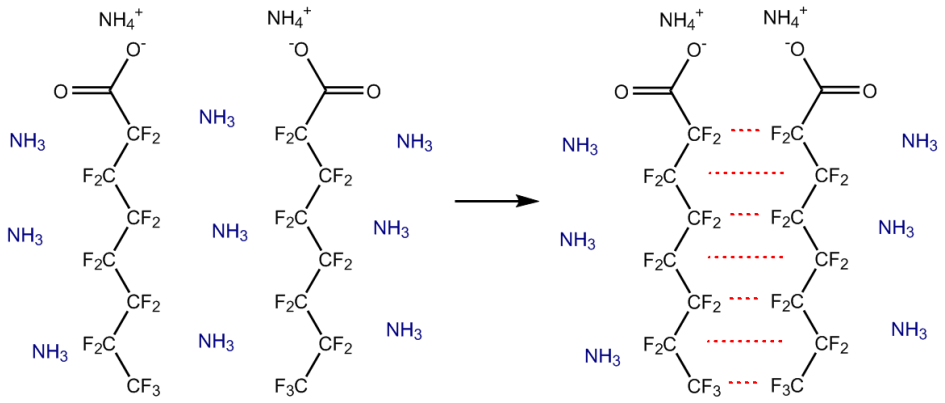

Scheme 4.2.10. As opposed to monomer surrounded by ammonia (left), the formation of a dimer with van der Waals interactions may be favoured (right).

With this in mind, attempts were made to fit the conductivity data to a model including the formation of the dimer type aggregate, but the data did not correlate with the model. This could be because that when including the possible formation of dimers and trimers and integrating them into the model, the number of variables and unknowns becomes too unpredictable. Say, for example, a dimer is formed from the 2 monomer surfactant molecules, as in scheme 4.2.10. This dimer could itself exist as an associated ion-pair with the two counter ions or as a freely dissociated dimer species. This would give rise to more ion-pairing constants and equilibrium constants for the dimerisation process and dimer ion-pairing equilibrium. Furthermore, if one postulates the notion that trimers or even higher aggregates may be forming, then the model becomes too complex (Scheme 4.2.11).

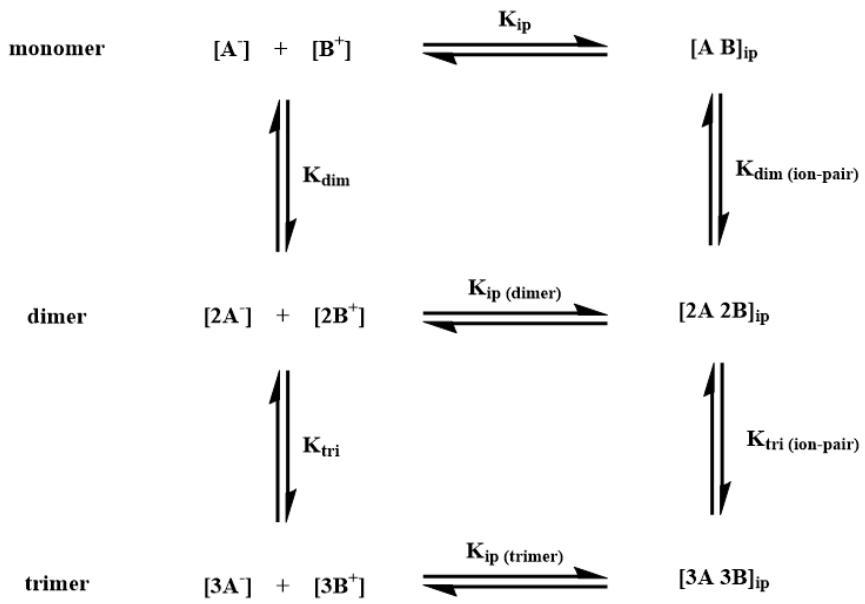

Scheme 4.2.11

If these fluorinated surfactants have the potential to form these higher aggregates, why does the simple, single ion-pairing model fit the conductance data and also give an increase in ion-pairing constant as chain length is increased? A simplistic overview of the conductivity ion-pairing model basically says that the curvature or reduced conductance observed as concentration is increased is because of the formation of some non-conducting species, which has initially being identified as a neutral ion-pair from the monomer species. But, equally, the formation of a dimer ion-pair or trimer ion-pair would also reduce the conductivity as they would also have zero conductance, such that a similar conductance isotherm would be expected. Additionally, one could argue that the formation of dimers and trimers that are dissociated from their counter-ions would also reduce the overall conductance. The formation of these large higher aggregates may, just like the macroion micelle in water, retard the conductance of the solution. Similarly to the aqueous micelle system, this could be due to an increase in ionic atmosphere of the solution with the higher aggregates causing a 'drag effect' on the free counter ions thus reducing their ability to conduct. It is postulated that the formation of dimers and trimers and higher aggregates, even if not tightly ion-paired and hence still conducting, would have a lower conductance than the monomer species, and thus hinder the overall conductance of the solution. Thus the curvature in the conductance-concentration profile would be observed.

For the long chained surfactants it is therefore proposed that the degree of reduced conductance, the K_{ip} value obtained, is representative of the formation of any poorly or non-conducting species in general, these being the monomer ion-pair, larger aggregate species such as dimers and trimers as well as their ion-pairs.

This notion can now be applied to the fluorinated carboxylates in liquid ammonia in trying to explain why there is an observed rise in K_{ip} value as the chain length is increased. Increasing the chain length by the additional $-CF_2-$ groups would increase the hydrophobicity or "ammonophobicity" of the molecule which would be expected to promote the formation of these higher aggregates. As the chain length is increased, the van der Waals forces between the surfactant tails would also increase and hence a higher degree of aggregation into a dimer etc. would be evident. Van der Waals forces play a key role in the intermolecular bonding of alkanes and it is actually these forces that give rise to the boiling point trend of hydrogenated alkanes where by the longer the chain length, the higher the boiling point.[158]

It is possible that some of the ionic surfactants in liquid ammonia do form these 'higher aggregates' due to van der Waals interactions between the fluorinated chains. It appears that there is no definitive evidence of full aggregation into a micelle structure. Under this assumption, one has to explore the reasons why these anionic surfactants do not form micelles in liquid ammonia as they do so very easily in an aqueous environment. The most plausible explanation is that the anionic polar head group does not have favourable interactions with the ammonia solvent that would allow the formation of a thermodynamically stable aggregate, as will now be explained.

4.2.2.3 Interpretation of the apparent lack of aggregation of ionic surfactants in liquid ammonia

The general assumption is that the main driving force for micellization is the hydrophobic effect provided by the non-polar tail, but the polar head group plays an equally important role in the formation of the aggregate macromolecule. Just as important to aggregation as the unfavourable solvent-tail interactions are the favourable solvent-head group interactions within the stern layer of the micelle. For the spherical micelle model, the polar head groups and associated counter-ions of an ionic micelle are found within the compact Stern layer. The free, dissociated, counter-

ions are located in the Gouy-Chapman electrical layer where they are free to exchange and bond with molecules distributed in the bulk of aqueous phase.[159] For a simple anionic carboxylate head group, for example, it is easy to see how the water solvent molecules would be able to well solvate the outer layers of the micelle and counter ions (Scheme 4.2.12).

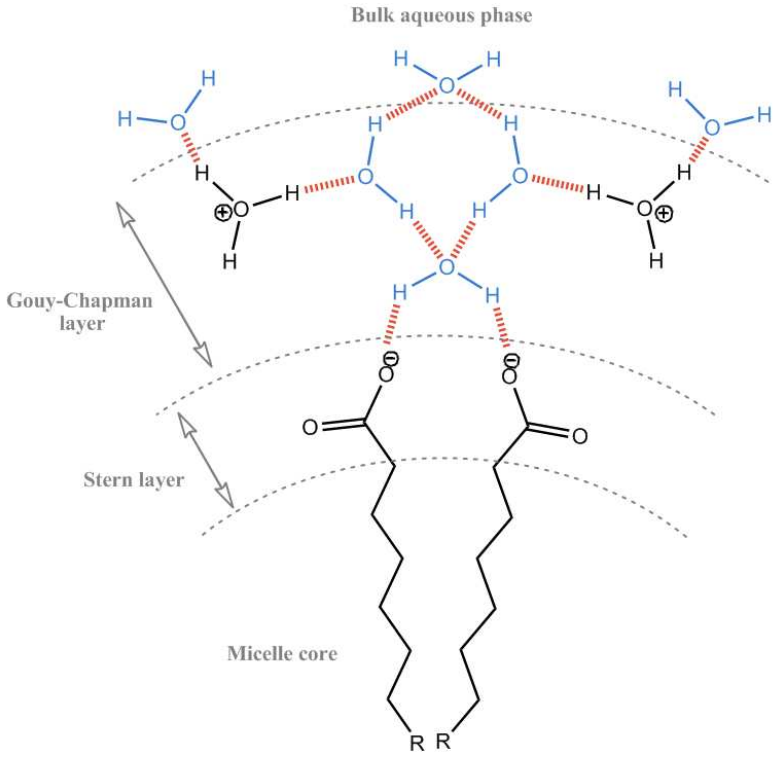

Scheme 4.2.12 Simplified two-dimensional representation of two adjacent carboxylate surfactant molecules in a spherical micelle in water.

Scheme 4.2.12 shows some of the types of hydrogen bonding that could occur at the surface of the micelle with good interactions of the solvent molecule with both the head group and counter ion. In reality, the model would likely be a very fluid system, with ions constantly exchanging and interacting in and around the Gouy-Chapman and bulk phase layers. Additionally, the ionic head groups of equal charge would naturally want to repel each other which should in theory hinder the formation of an outer micelle layer with head groups packed together. The hydrogen bonding provided by the polar water solvent reduces this repulsion and thus overcomes this issue of head group repulsion allowing for aggregation.

In contrast to this aqueous model, however, a hypothetical model for an anionic micelle in liquid ammonia seems less likely (Scheme 4.2.13).

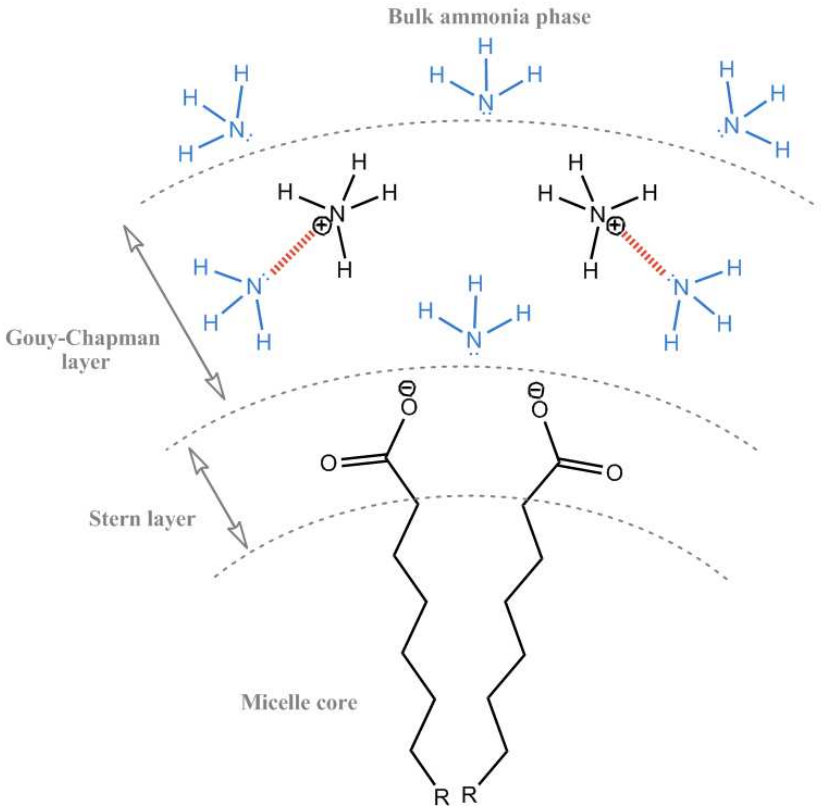

Scheme 4.2.13 Simplified two-dimensional representation of two adjacent carboxylate surfactant molecules in a spherical hypothetical micelle in liquid ammonia. (CF_2/CF_3 groups omitted for simplicity).

Certainly, as with the water micelle model, one would expect the positively charged counter ion, in this case ammonium ion, to be well solvated by the ammonia solvent in a Gouy-Chapman layer because of the solvent's ability to donate its electron pair and solvate cations. However, because of ammonia's relatively poor ability to donate hydrogen bonds, solvation of the anionic head group would be poor. Thus the formation of a thermodynamically stable micelle with good solvent interactions with head groups in a Stern-layer appears evidently unlikely. Equally, due to its relatively lower polarity, liquid ammonia may not be able to reduce the electrostatic repulsions between adjacent head groups of equal charge as water does so well and thus hinder the formation of the micelle. This may be the main factor in the lack of micelles from anionic surfactants in liquid ammonia as head group repulsion does appear to have a significant effect on the formation of micelles and, as a general trend, critical micelle values of non-ionic surfactants tend to have lower cmc values compared to analogous ionic counterparts.[160] Adjacent non-ionic head groups do not show any electrostatic

repulsion of one another such that the formation of a stable micelle interface is promoted, hence the lower cmc.

Thus for the fluorinated carboxylates in liquid ammonia, micelle formation is likely hindered by the poor solvent interactions with the head group which additionally leads to increased repulsion between these groups. Similarly, these explanations can be applied to the apparent lack of micelle formation from other anionic surfactants (sulfates, sulfonates) in liquid ammonia.

If anionic surfactants cannot form a stable outer layer due to the absence of a fluid bonding network with the ammonia solvent in and around the head group, attention turned to the possible use of some cationic surfactants, as the ammonia solvent could solvate the positively charged head group strongly by donating its electron lone pair. Interestingly, the cationic surfactants such as cetyl trimethylammonium bromide (CTAB) and benzalkonium chloride were both insoluble in liquid ammonia at concentrations as low as 5 mM. A general trend for salts in liquid ammonia is that the solubility decreases as lattice energy of their crystal increases. So for NaI, NaBr, NaCl and NaF, for example, solubility decreases in liquid ammonia as the lattice energy increases such that NaI is much more soluble than NaF.[25] With this in mind, the use of cationic surfactants with an iodide counter ion was explored, where this bulky anion with lower lattice energy would hopefully promote the solubility of the cationic surfactant. In comparison to the other cationic surfactants, it was observed that decyl trimethylammonium iodide (DTAI) was soluble in liquid ammonia at concentrations as high as 40mM supporting the theory that reducing the salt lattice energy by using a bulkier anion would increase solubility (Scheme 4.2.14). Thus, aggregation of DTAI in liquid ammonia initially looked promising.

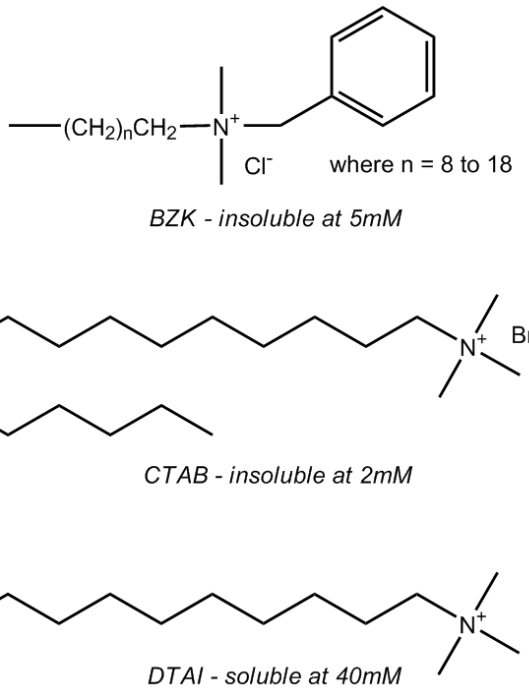

Scheme 4.2.14. Cationic surfactants with varying counter anion with observed solubility

However, the conductance of DTAI in liquid ammonia also generated a curved profile and the data fitted the ion-pairing model, with a K_{ip} value of 671 obtained (K_{diss} = 0.00149). At higher concentrations, the surfactant was insoluble and thus again, there was no obvious evidence of micellization with the cationic surfactant as anticipated but instead just the ion-pairing phenomenon.

In pursuit of an explanation as to why the cationic surfactants cannot form micelles in liquid ammonia, as was previously done with the anionics, a schematic of a theoretical DTAI micelle can be explored and scrutinized (Scheme 4.2.15).

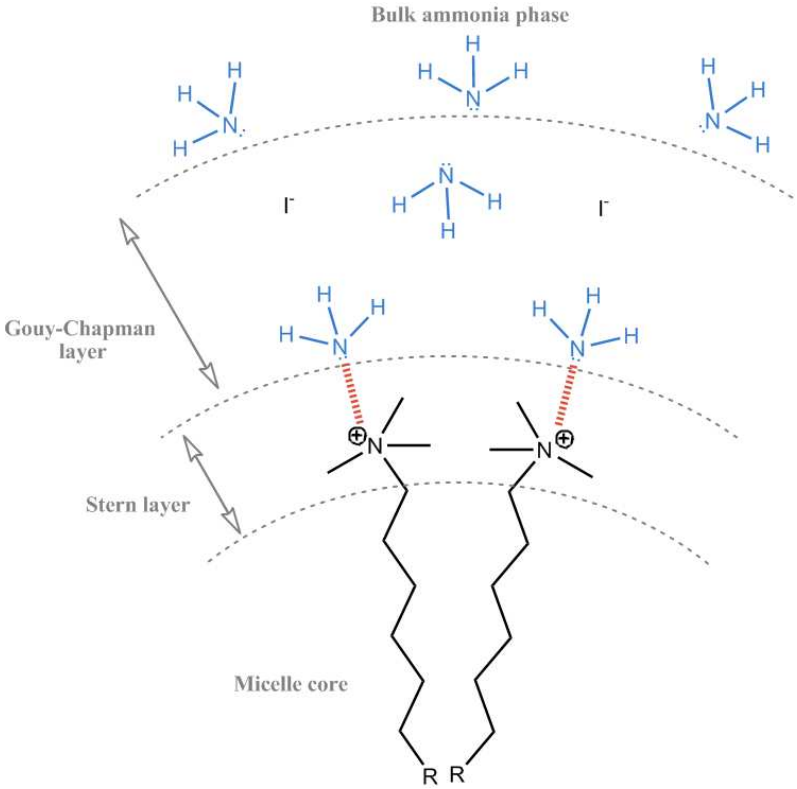

Scheme 4.2.15 Simplified two-dimensional representation of two DTAI surfactant molecules in a spherical hypothetical micelle in liquid ammonia.

In contrast to the anionic surfactant model in ammonia, this time there would likely be good interactions between the solvent ammonia and positively charged head group. This would in turn stabilize the positive charge on the head group and hence reduce the repulsion of adjacent surfactant head groups. Initially then, the possible formation of a cationic micelle appeared promising because, so far, the Stern layer of the micelle looks realistic, which of course wasn't the case with the anionics, contributing to their lack of micellization. The problem may arise from the poor solvation of the anionic counter ion in a Gouy-Chapman layer. There must be some degree of solvation of the iodide anion, owing to the higher solubilisation of DTAI compared to the bromide and chloride surfactants, and similarly the higher solubility of simple the iodide salts in general in comparison to salts with the less bulky anions. In fact any solubilised salt in liquid ammonia must have some degree of solvation of both cation and anion. It may just be that the solvation of the anion is just not good enough to create a stable Gouy-Chapman layer. This lack of solvation is probably evident in the reasonably high K_{ip} value obtained for DTAI. A high degree of ion-pairing is quite apparent (K_{ip} = 671) which is much higher than the anionic hydrogenated surfactants (K_{ip} SDS = 169, K_{ip}

Aerosol OT =165). As previously outlined, the K_{ip} may also be representative of some formation of the higher aggregates, such as dimers or trimers, but this is probably not the case with DTAI. The K_{ip} for DTAI is much higher than the analogous C_{10} chain length fluorinated carboxylate and even higher than the perfluorododecanoic acid (Table 4.2.3), which has been assumed to form these higher aggregates due to their increased hydrophobicity. The hydrogenated chain is not as 'ammoniaphobic' as the fluorinated chain so the DTAI would not be expected to form aggregates as readily. Hence the suggestion that the K_{ip} for DTAI is indicative of some degree of aggregation that is actually greater than that of the C_{10} and even C_{11} fluoro chain is unlikely. The possibility therefore is that the DTAI shows a high degree of ion pairing due to the poor solvation of the iodide anion.

Omitted from the above simplified micelle schematics for both ionic head groups in liquid ammonia is the possible ion pairing between the ionic head group and counter ion. This would occur at the Stern layer - Gouy-Chapman interface often described as the range of shear surface, and it could be argued that the ion pairing into a more 'neutral' head group would promote the formation of micelles, as the repulsion between head groups would be reduced.

However, on the whole, the lack of micellization is still evident from the conductance profile where it can be predicted that if aggregation was occurring the conductance profile would not be too dissimilar from the water profile. Similarly, the formation of the bulky macroion, the micelle, would show a noticeable change in the conductance isotherm at the cmc. A theoretical plot of what would be expected for the conductivity of a surfactant-micelle system in liquid ammonia is shown in Figure 4.2.17 with comparison to the general water model.

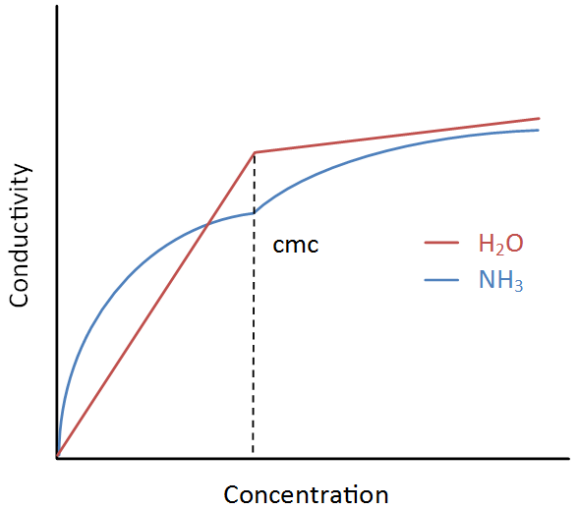

Figure 4.2.17 Conductivity as a function of concentration for a general ionic surfactant in water and a theoretical ionic surfactant in liquid ammonia that can form a micelle.

Prior to micellization, in water conductance is linear with concentration whereas in ammonia it is curved due to ion-pairing and maybe even dimerisation. Then, the formation of the bulky micelle with its overall reduced conductance effect would cause a dramatic 'break' in the conductance. Just like in water, a dramatic retardation in the conductance above the critical micelle concentration would be evident. It is anticipated that any charged micelle formed in liquid ammonia would also experience the same ion-pairing due to the reduced polarity of the solvent and thus a curved conductance would be expected for the micelle above the cmc. Again, this is just a hypothetical conductance model for an 'ideal ionic micelle' in liquid ammonia, but just demonstrates that none of the conductance profiles for the surfactants looked like this. Only the initial curved profile is observed indicating monomeric conductance with ion-pairing and possibly some degree of dimer/trimer aggregation for the more hydrophobic (fluorinated) surfactants but clearly not full aggregation into a micelle.

4.2.3 Summary of conductometric studies in liquid ammonia

In summary of the conductometric studies, the ionic surfactants demonstrated the ion-pairing phenomenon which is typical of simple salts in this solvent. It is the reduced polarity/dielectric constant of liquid ammonia (compared with water) that promotes the association of non-conducting, neutral, ion-pair species and thus a non-linear relationship between conductivity and concentration is observed. The formation of

higher aggregates such as dimers and trimers may also occur, as is evident with the fluorinated carboxylates, and these will in turn contribute to the non-linear conductance profiles. It was concluded that the anionic surfactants do not form micelles as the head group was not solvated well enough by the ammonia solvent in a Stern layer. This is in contrast to the cationic surfactants where by the lack of aggregation was likely due to poor solvation of the counter ion in the Gouy-Chapman layer of any potential micelle. Additionally, it may be that no ionic surfactant can ever form micelles because the relatively non-polar ammonia solvent cannot reduce the electrostatic repulsions between adjacent head groups as polar water does so effortlessly through hydrogen bonding.

Thus, it is anticipated that non-ionic surfactants in liquid ammonia may have the ability to form aggregate species as they would show zero head group repulsion. Additionally, having observed that the head group interactions with the solvent must play such a vital role in the stabilisation of this micellar outer layer, the principal approach for the non-ionic studies was to find a neutral functional group that would be best solvated by the ammonia. The amide group could potentially be the ideal candidate.

4.3. Aggregation studies on perfluorinated amides in liquid ammonia – Results and Discussion

4.3.1 Potential of fluoroamides to aggregate in liquid ammonia

The potential for long-chained, fully fluorinated amides to form aggregates in liquid ammonia is quite apparent just by looking at the likely interactions these types of molecules may have with the ammonia solvent (Scheme 4.3.1). Furthermore, during the synthesis of these amides it was observed that they showed a large degree of 'frothing and foaming' in liquid ammonia. This is typical of a surface active system in water which, admittedly not scientifically conclusive, does suggest that they have highly surface active properties in ammonia and thus their potential to aggregate into micelles was promising.

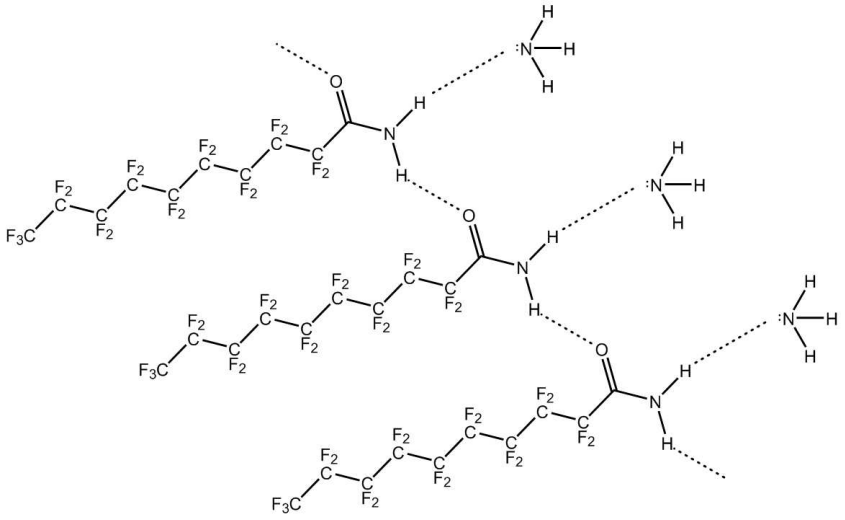

Scheme 4.3.1 The potential interactions of the long-chained fluorinated amides and liquid ammonia solvent are quite apparent.

As previously summarised, the reason that conductometric studies on carboxylate, sulphate and other surfactants showed little evidence of micellization in ammonia could be due to a lack of solvent and polar head group interactions that are needed for aggregation. Water, with its polar, amphoteric nature, can solvate cationic and anionic (as well as non-ionic) head groups so that the aggregation of both cationic molecules, such as CTAB, and anionic molecules, such as SDS, is not surprising. Contrary to this, liquid ammonia shows poor anion solvation and consequently a thermodynamically stable aggregate consisting of an outer layer with stable ammonia-

anion interactions is less plausible. On the other hand, the amide group is well solvated by the ammonia, owing to its electron lone pair with relatively high normalised donor number (DN^N) which is 1.52, greater than that of HMPTA (DN^N =1) and thus at least as a starting point, long chained amides (fluorinated or not) are expected to be more soluble in liquid ammonia than their carboxylate counterparts. The amide head group does possess the ability to form a stable outer layer of the micelle. The formation of micelles, which requires some degree of surfactant solubility in the first place, looks promising with the long chained fluorinated amides. As a rough comparison, perfluorododecanoic acid is insoluble in liquid ammonia at concentrations as low as 5 mM, whereas the amide analogue, perfluorododecanamide, appears fully soluble up to around 40 mM. This simple observation is consistent with poor anion solvation in liquid ammonia, as this acid, with $pK_a \sim 0$, is fully deprotonated in ammonia and thus exists as the carboxylate, $RCOO^-$, and the ammonium ion, NH_4^+. Ammonia is a poor hydrogen bond donor to the carboxylate anion and hence the poor solubility of the overall species is explained. As expected, the fluorinated amides show little or no solubility in water and even the medium chain length perfluorooctanamide is insoluble at concentrations as low as 2 mM, with the corresponding fluorinated acid soluble at 30 mM. These trends show that it is not only the polarity of the solvent that effects its ability to solubilise these amphiphilic compounds, but also the solvent capacity to solvate and hence bond with the polar head group of the surfactant.

Solvation of the polar amide group in ammonia would be well favoured, and, similarly to water, the non-polar, lipophilic, fully fluorinated chain would be poorly solvated by the ammonia, thus perfluorinated amides are ideal candidates to demonstrate aggregate phenomena in liquid ammonia. Conductometric studies on these perfluorinated amides showed that, as expected, they exist in liquid ammonia as uncharged, non-conducting species. Therefore the traditional method of detecting micelles by conductivity, looking for a ‘break’ in the conductance isotherm, would not be applicable with these neutral species. Accordingly, another micellar detection method was required for the fluorinated amides in liquid ammonia.

4.3.2 Initial attempts to detect aggregation

4.3.2.1 Solubilisation in micelles as a detection method

With the need for a different detection method to observe the aggregation of these neutral surfactant species, attention immediately turned to the unique property of the micelle that gives it such wide application; its ability to solubilise compounds into an environment in which they would otherwise be insoluble. The solubilisation of water-insoluble compounds into an aggregate surfactant phase in aqueous solutions is vital to many industrial applications such as drug delivery, textile dying, detergency and emulsion polymerization.[161, 162]

The ability for the micelle to therefore solubilise a particular compound can then be used as a method for the confirmation of surfactant aggregation. One of the principal ways of achieving this is by investigating the solubilisation of dyes in aqueous solutions of micelles.

4.3.2.1.1 Solubilisation of dyes into the micelle

Singh et al showed that the solubilisation of organic, water-insoluble, dyes such as Sudan I and Quinizarin into aqueous solutions of surfactant micelles can be used to find cmc values which are consistent with literature from the more traditional methods such as conductance and surface tension.[163] Using a UV-spectroscopic method, the cmc value was determined at the concentration of surfactant at which solubilised dye was detected by the instrument (Figure 4.3.1).

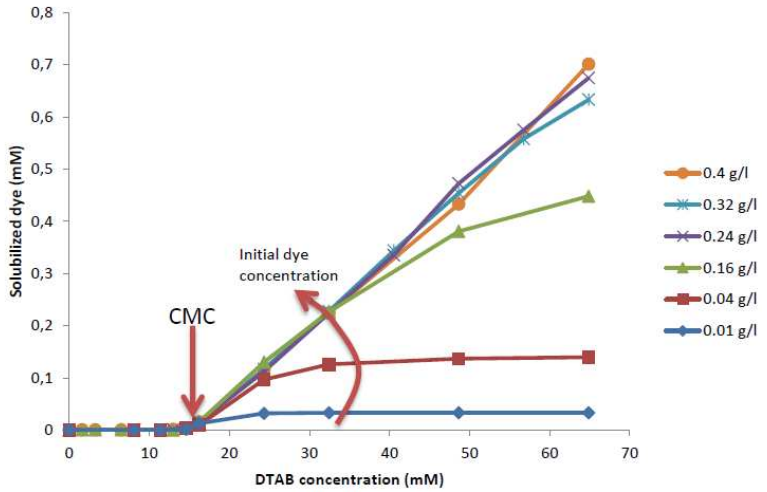

Figure 4.3.1 Solubilized dye (Sudan I) as a function of DTAB (dodecyltrimethyl ammonium bromide) concentration with varying amounts of initial dye concentration in water.[163]

Although the UV method was used to accurately identify the initial solubilisation of the organic dyes into the aggregated phase, their work highlighted that at the cmc, as solubilisation of the organic dye into the micelle ensued, the colour could be observed discernibly with the naked eye. This is no surprise, as the extinction coefficient of organic dyes is generally in the region of $1x10^4$ $M^{-1}cm^{-1}$.

Accordingly, the plan was to see if the aggregation of the fluorinated amides in liquid ammonia could be observed by the solubilisation of dyes into the non-polar hydrophobic core. This could be primarily achieved by simple visual detection to see if the theory is correct with a view to using the high pressure UV cell to get some accurate measurements of dye solubilisation as a function of surfactant concentration as was observed in the literature. This would perhaps allow some cmc values for the fluorinated amides in liquid ammonia to be obtained.

The detection of micelles by this method relies on using a dye that is initially insoluble in the solvent medium, such that a series of dyes were investigated in liquid ammonia to see their suitability for the method. The first candidate was beta-carotene, a highly non-polar, strongly coloured red pigment that is found widely in nature, particularly abundant in plants and fruits. It is this water-insoluble compound that contributes to the bright orange colour of carrots and other orange root vegetables.[164] In liquid ammonia, it was observed that this dye has some solubility giving a bright

yellow coloured solution (Figure 4.3.2). The solubility was not massive, as evident by the 2 phase system but the initial speculation that the dye would hopefully be totally insoluble in the ammonia was incorrect.

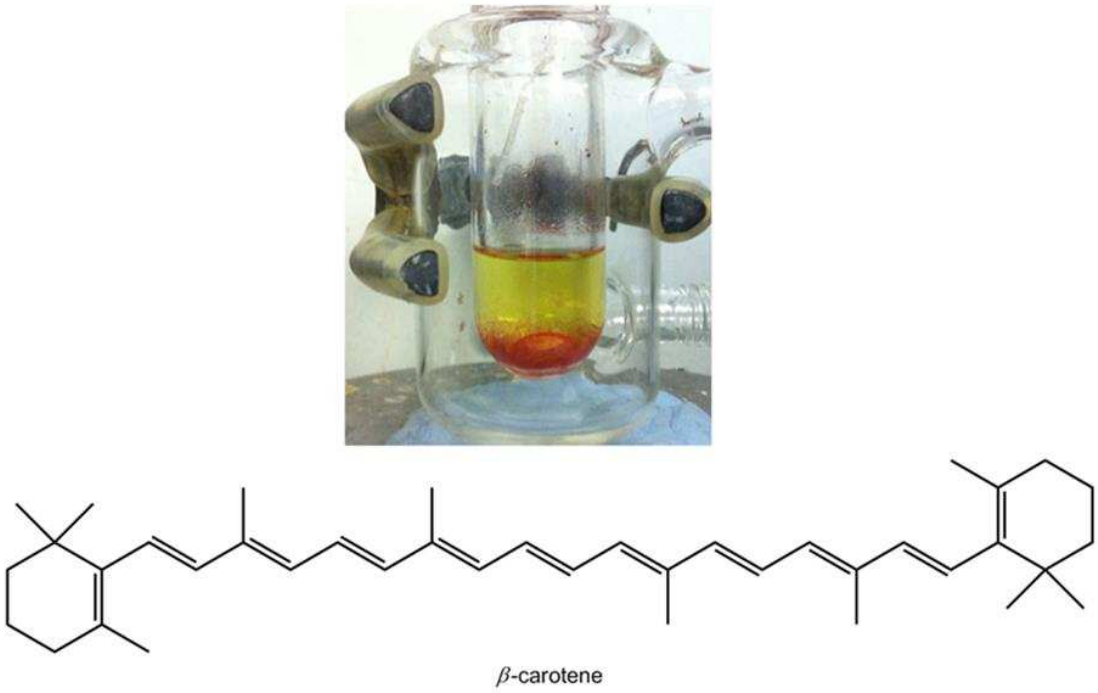

Figure 4.3.2 *β*-carotene was visibly soluble in liquid ammonia. Approximately 5 mg in 5ml (~ 2 mM).

The justification for this observed phenomenon was that this highly non-polar dye is soluble in liquid ammonia because ammonia has a much lower polarity than water, and thus has the ability to solubilise this species in similar fashion to organic solvents such as acetone and hexane. This would maybe imply that liquid ammonia can solubilize most organic soluble dyes but maybe not dyes on the opposite side of the polarity scale. Consequently, attention turned to the water-soluble azo-dyes such as Edicol Red and Tartrazine (Scheme 4.3.2).

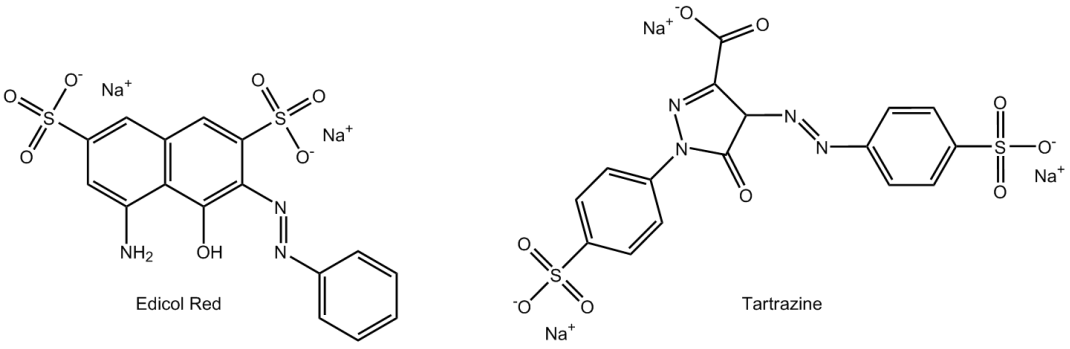

Scheme 4.3.2 Structures of water soluble dyes Edicol Red (l) and Tartrazine (r).

These types of dyes find use within the food industry, in the colouring of soft drinks, confectionary and cereals, for example. Unfortunately however, in similar fashion to the non-polar organic *β*-carotene, these highly polar dyes were very soluble in liquid ammonia. In fact over a wide range of dye types, it was observed that they were all soluble in liquid ammonia. Using the high pressure UV cell, the spectra of these dyes in liquid ammonia were obtained and some maximum absorbance values (λ_{max}) determined. In comparison, the solubility and subsequent absorbance of the dyes was investigated in other solvents including water and hexane (Table 4.3.1). The colour change for the brilliant yellow is likely due to the ionisation of the phenolic groups.

Table 4.3.1 λ_{max} values obtained by UV spectroscopy for a range of dyes in water, liquid ammonia and hexane at 25 °C.

Dye	**Water (ε_r = 80)**		**LNH_3 (ε_r = 16)**		**Hexane (ε_r = 1.8)**	
	colour	λ_{max} (nm)	colour	λ_{max} (nm)	colour	λ_{max} (nm)
Edicol Red	purple	521	purple	509	- - - insoluble - - -	
Tartrazine	yellow	426	yellow	431	- - - insoluble - - -	
Brilliant Yellow	orange	400	purple	542	- - - insoluble - - -	
β-carotene	- - - insoluble - - -		yellow	447	yellow	450
Sudan II	- - - insoluble - - -		orange	484	orange	468
Solvent Green 3	- - - insoluble - - -		pale blue	634	blue	636

Liquid ammonia evidently has the ability to solubilise the full spectrum of dyes ranging from the non-polar hydrocarbon type dyes, which are soluble in the organic

solvents such as hexane, to the water soluble azo-dyes which are essentially salts with a conjugated system. The results are somewhat surprising as they indicate that liquid ammonia solvent, typically classified as a polar, aprotic solvent, has properties which allow it to also mimic a non-polar type solvent. Initial speculation was that the ammonia solvent, with its dielectric constant of about 16 is really 'in the middle' of the polarity scale of solvents and thus has the ability to solubilise the range of dyes from non-polar to polar. Yet it is well observed that short to medium chain alkanes such as hexane are insoluble in liquid ammonia so one would not expect the even larger hydrocarbons such as β-carotene to be soluble.[33] Liquid ammonia, however, has an interesting property as a solvent in that ammonia molecules exert large van der Waals forces, and for this reason, the highly conjugated system of the hydrocarbon dyes, even though non-polar, are well solvated by ammonia.[165] The attractive field of ammonia as a solvent is divided almost equally between an orientation of polar forces (from the lone pair) and van der Waals effect, in contrast to water solvent in which there is much smaller contribution of the van der Waals forces in comparison to the polar attractive field. It is thought that these van der Waals forces in liquid ammonia contribute to the solvents ability to solubilise alkenes (even mono-unsaturated) better than alkanes such that it is not surprising that a whole range of dyes, which are always highly conjugated systems by their very nature, are well solubilised in liquid ammonia.

Due to the apparent limited solubility of β-carotene in liquid ammonia as evident in Figure 4.3.2, it was speculated that maybe the solubilisation of dyes could still yield some interesting results. The solubilisation with added surfactant could have been measured against a small background solubilisation, but, as discussed in the experimental section, our current high pressure UV set-up is not quantitatively accurate.

4.3.2.1.2 Solubilisation of a lipophilic compound into the micelle

Having highlighted that the dye method for detection of micelles in liquid ammonia was unfeasible due to the solubility of a wide range of dyes, attention turned to the possible use of non-dye, highly lipophilic compounds that are definitely not soluble in the ammonia but may be in an aggregate hydrophobic core. Comparable to the dye method, this technique works on the principle that the analyte is insoluble in the

ammonia solvent but then solubilised by the micelle core of the fluorinated amide aggregate (Figure 4.3.3).

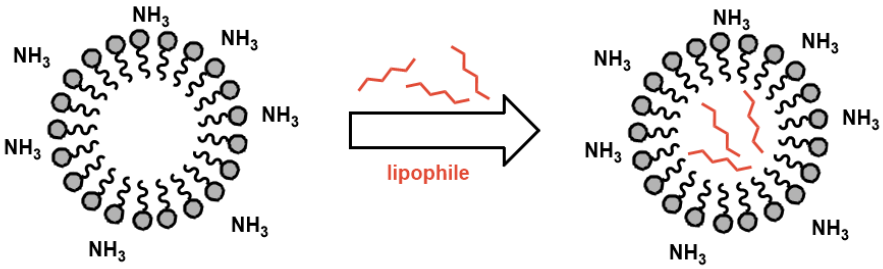

Figure 4.3.3 Schematic of micelle solubilisation of a fatty substance into the interior core of the micelle.

Long chain alkanes are insoluble in liquid ammonia, so a primary candidate for these trials was a fully fluorinated alkane such as perfluorohexane (pfh). It was anticipated that the pfh would have limited or zero solubility in liquid ammonia and so any solubility increase with the presence of surfactants could be attributed to micelle solubilisation. A method was required to monitor this process. The chosen route was to use the Omnifit dip-tubing as a means of taking out samples from the liquid ammonia to test for pfh by GC-MS. A set amount of pfh would be injected into the ammonia solvent with vigorous stirring. After a time period, the stirrer would be switched off and the insoluble lipophile left to sink to the bottom of the vessel ($\rho_{pfh} \approx 1.7$ g ml^{-1}). A sample would then be taken from the dip-tubing situated near the top of the solution for analysis. It was possible to detect the presence of any pfh by GC-MS using a non-polar HP-5 column with standard run parameters (pfh boiling point ≈ 56 °C). Figure 4.3.4 shows a theoretical overview of the process.

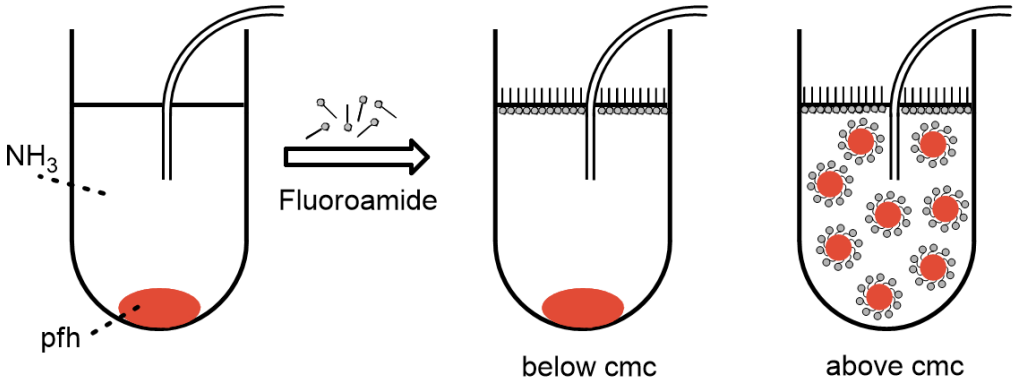

Figure 4.3.4 Overview of method for solubilisation of pfh in fluorinated amide micelles in liquid ammonia; without fluoroamide (left), with fluoroamide prior to aggregation (centre) and with an aggregated fluoroamide surfactant (right).

It was anticipated that without the micelles, the sample obtained would contain zero pfh, whereas in the samples with the fluorinated surfactants, if pfh was present then this may indicate solubilisation into the micelle. Ideally, this would only be the case above a certain fluoroamide surfactant concentration, indicative of the cmc value at which aggregates form.

The baseline test in liquid ammonia only showed that the proposed method may be workable; pfh (~50 mM) in liquid ammonia with stirring for 2 hours and then left to settle for 30 minutes prior to sampling into hexane did not show up by GC-MS analysis. This process was then repeated with varying concentrations of the fluorinated amides of different chain length: perfluoroheptanamide (25 and 170 mM), perfluorooctanamide (15, 50 and 90 mM), perfluorononanamide (15 and 60 mM), and perfluorodecanamide (10, 20 and 40 mM). The results, however, were disappointingly inconclusive. For all the experiments, no pfh was observed when sampling from the solution possibly suggesting zero solubilisation into any aggregate. This doesn't necessarily dismiss the notion that these fluoroamide surfactants are forming micelles, but maybe that this simplified method in liquid ammonia is not working. Exploring the literature around this subject supports this notion. For example, Seedher et al investigated the micellar solubilisation of some generally poorly soluble anti-diabetic drugs.[166] Their experimental procedure showed that the solubilisation of these sulfonylurea-type compounds into aqueous solutions of CTAB, SDS and Tween-80 required a *"vigorous centrifuging"* process followed by filtration. Similarly, other

techniques that report the solubilisation of drugs into micelles entail the robust mechanical shaking of the mixtures for periods of up to a day.[167] In fact, some reports even suggest that in order to solubilise their drugs into micellar solutions, a stirring period of up to 5 days at elevated temperatures was necessary.[168] Although, different techniques may be used for different compounds and micelle systems, the underlying principle appears to be that the method for solubilising compounds into micelles often requires a highly vigorous and hands-on practical approach. The use of techniques such as centrifuging or mechanical shaking whilst working at 10 bar pressure in small scale glassware is not practical. Thus it was concluded that the possible observation of micelles by the simplistic solubilisation technique outlined in Figure 4.3.4 was not going to work. It may have been that with longer periods of vigorous stirring by magnetic flea (days, weeks?) the technique may have had some merit but this was not pursued.

As a consequence, another technique was required to observe the micelles with the aim of using an analytical tool that is well known in the field of aggregation studies and can be simpler, repeatable and give conclusive results. NMR studies had the potential to fulfil these requirements.

4.3.3 Aggregation studies on surfactants using NMR

4.3.3.1 In water

The use of NMR as a tool for the detection of micelles in water is widely reported within the literature.[85] It is based on the principle that NMR chemical shift is extremely sensitive to the environment. Since neighbouring solvent molecules contribute to the environment it thus follows that chemical shifts are sensitive to the nature of the solvent as well as its molecular chemical environment. NMR theory states that the heavier the atom is, with more electrons, the greater its shielding and hence chemical shift range. Heavier atoms also tend to show a stronger solvent effect. For these reasons, the observation of micellization is much easier by ^{19}F NMR (fluorinated surfactants) than ^{1}H NMR (hydrogenated surfactants). Similarly, the ^{13}C nuclei of alkyl surfactants can exhibit large solvent shifts but the applications are limited because of their low natural abundance (1.1%) and so are not used much in the detection of micelles.[169]

The observation of micelle formation by NMR is based on the fact that the chemical shift of an atom is sensitive to its chemical environment. For example, the terminal CF_3 group of trifluoroethanol shows a significant decrease in ^{19}F chemical shift in going from the highly polar water solvent (δ = 76.8 ppm) to the aliphatic non-polar hexane solvent (δ = 78.32 ppm) (Figure 4.3.5).

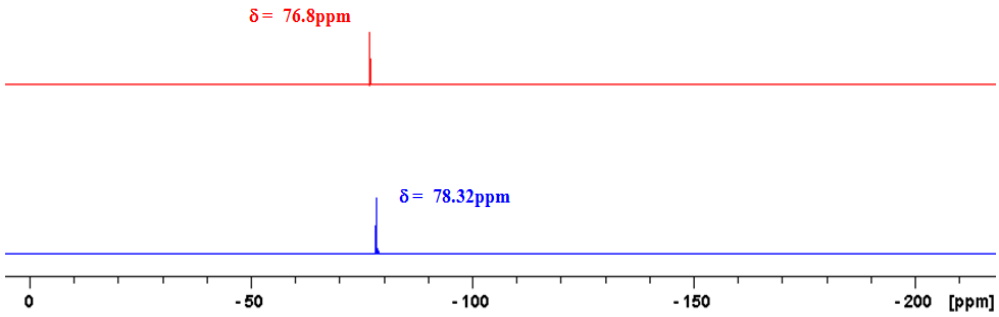

Figure 4.3.5 ^{19}F NMR chemical shift of CF_3 group of trifluoroethanol in water (red) and hexane (blue).

One of the most extensive studies on micelles by NMR was done by Guo et al.[85] They investigated the detection of aqueous micelles from the changes in chemical shift observed for a number of long chained fully fluorinated carboxylic acids and their salts. In particular, they were interested in the change in chemical shift of the terminal -CF_3 group in going from the free monomer in an aqueous environment to deep within a micelle aggregate which could be classed as a non-polar 'fluoroalkane' type environment. Beneficial to their work, as they used ionic surfactants, was that they could also use conductance and hence confirm that their cmc findings by the NMR method were consistent with the widely accepted traditional detection method. ^{19}F NMR spectra were obtained for the fluorinated acids over a wide concentration range and it was apparent that there was a distinct change in chemical shift of the terminal -CF_3 group as micellization occurred. Using the ^{19}F NMR method, a number of critical micelle concentration values were obtained by Guo et al for a variety of long chained fluorinated carboxylate surfactants consistent with other detection methods (See Table 4.2.1 from earlier section).

4.3.3.2 In Liquid Ammonia - Results and Discussion

4.3.3.2.1 Initial attempts at observing micelles from alkyl amides using ^{1}H NMR

It was initially speculated that it may be possible to observe micelle formation in liquid ammonia for typical surfactants as is observed in water. Disappointingly, the conductance chapter showed that ionic surfactants cannot form micelles most likely because of the electrostatic repulsion between neighbouring head groups that arise from their poor solvation from the borderline polar/nonpolar ammonia solvent. Therefore attention turned to the fluorinated amides as potential suitable candidates for micellization in liquid ammonia. Prior to testing the fluorinated amides in liquid ammonia their alkyl counterparts were also briefly explored. The notion that these could form micelles in liquid ammonia is of great interest because, as will be observed in the next chapter, they can be synthesised readily in liquid ammonia from triglycerides in processes that can also be catalysed by lipases. Although, as described above, the use of NMR for micelle detection is commonly used for fluorinated surfactants, as their shifts are easily observed, there is some literature indicating ^{1}H NMR may be also be utilised. Zhao and Fung showed that the -CH_3 terminal group of sodium dodecyl sulfate exhibits an observable change in ^{1}H NMR shift coinciding with the critical micelle concentration,[170] reasons for which will be explained with the fluorinated amides. A plot of 1/c vs. chemical shift allows determination of the cmc of SDS in water and is consistent with literature from conductance and surface tension methods.

Similarly, it was anticipated that this technique could be used to observe micelles of alkyl amides in liquid ammonia by observing changes in the chemical shift of the terminal -CH_3 group in going from monomer to micelle. Unfortunately, however, for alkyl amides in liquid ammonia, the ammonia solvent peak swamps the peak of interest (-CH_3) which is expected to have a shift of roughly 0.8 ppm, and therefore it would be difficult to observe any shift changes in this triplet peak (Figure 4.3.6).

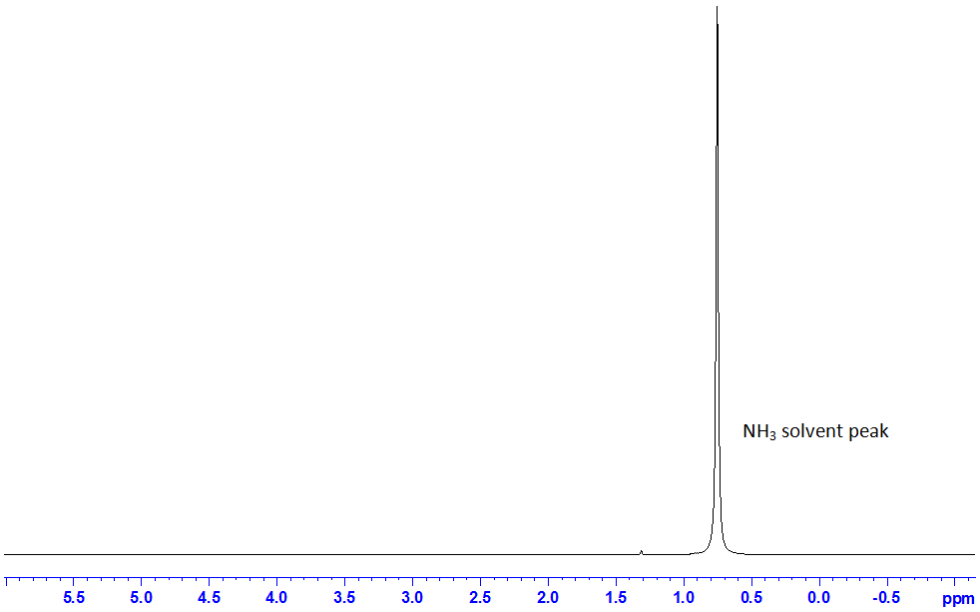

Figure 4.3.6 ^{1}H NMR of 40 mM dodecanamide in liquid ammonia was swamped with the ammonia solvent peak.

The slightly discernible peak at around 1.3 ppm is likely attributed to the 'middle-chain' -CH_2- groups of the C_{12} amide.

Obviously, with a lack of an ammonia peak and completely different shift range altogether, the fluorinated amide NMR's changes in chemical shift would be much easier to observe.

4.3.3.2.2 ^{19}F NMR of perfluorinated amides in liquid ammonia

For all fluorinated amide surfactants studied by ^{19}F NMR, depending on concentration and hence resolution, reasonably distinct peaks and couplings can be observed for 3 of the peaks. The peaks in question results from the terminal ω -CF_3 group, its adjacent -CF_2- group, and the α carbon -CF_2- group. The signal of the other -CF_2- groups in the middle of the chain were not resolved very well due to such high degree of long-range splitting, this becoming more prevalent with increasing the fluorocarbon chain length. Despite the complex splitting patterns for these 'middle' groups however, integration of all the peaks was consistent with the correct number of fluorine atoms in the molecule. Figure 4.3.7 shows a typical ^{19}F NMR spectrum of perfluorononamide in liquid ammonia.

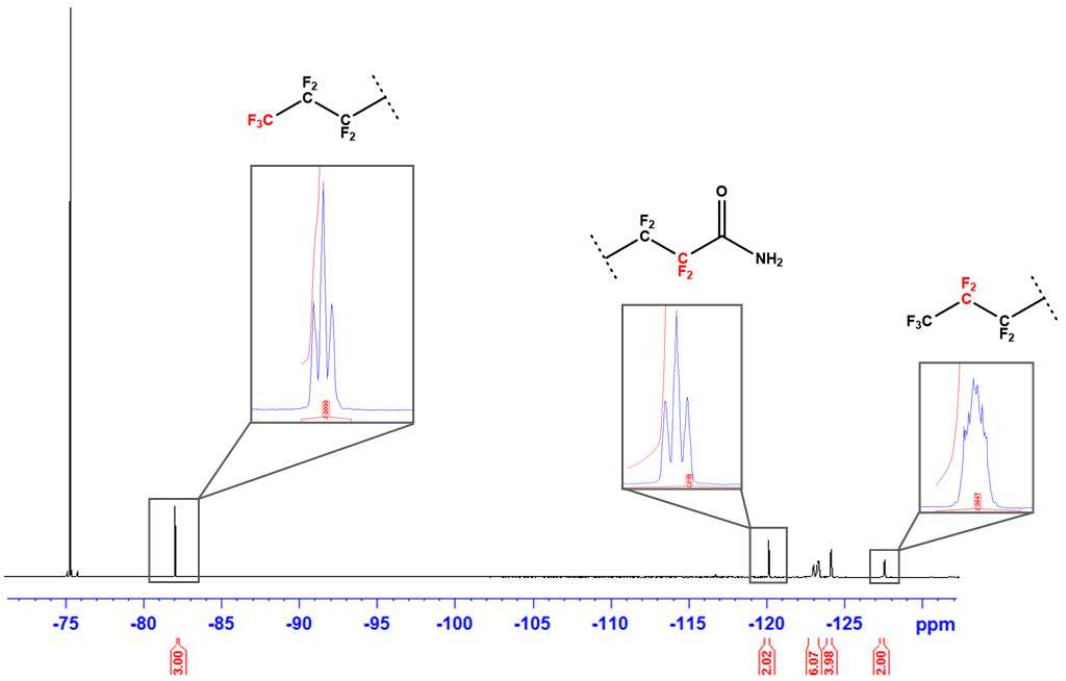

Figure 4.3.7 ^{19}F NMR spectra of 16.9 mM perfluorononanamide in liquid ammonia at 25 °C (relative to ammonium trifluoroacetate δ = -75.5100 ppm).

The chemical shift for any particular CF_2/CF_3 group is easily identified from the peak splitting/integration and the shift is reasonably consistent with those of the long chained fluorinated acids in water.[85] The -CF_3 terminal peak (ω) shows a discrete triplet observed at around -82.2 ppm, with a coupling constant of 10.6 Hz. Similarly, a triplet is observed for the α carbon -CF_2- peak at around -120.0 ppm and a coupling constant of 12.2 Hz. The -CF_2- group adjacent to the ω carbon is not as well resolved as the previous due to more long range splitting but has a chemical shift of around -127.4 ppm. To confirm the view that these peak shifts can be used to detect micellization of the amide surfactants, ^{19}F NMR spectra were recorded over a wide concentration range in liquid ammonia.

It was first observed that there was a clear decrease in chemical shift of the well resolved peaks, with the terminal CF_3 group showing the largest decrease at the concentration extremities (Figure 4.3.8).

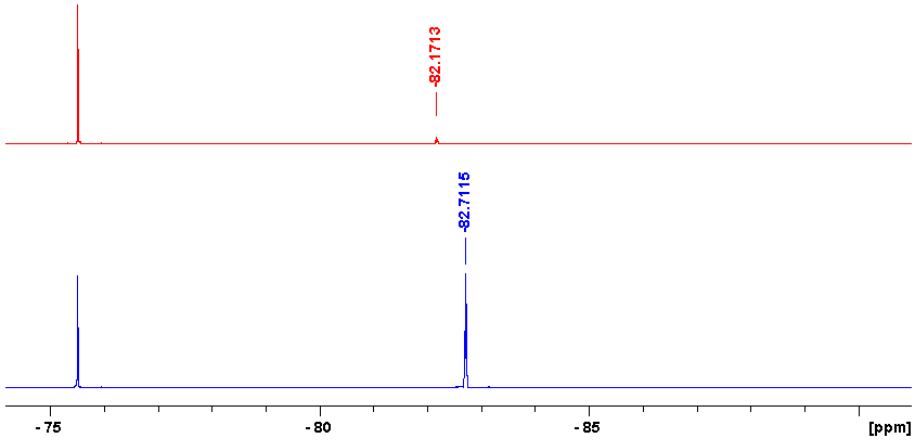

Figure 4.3.8 ^{19}F NMR spectra of terminal -CF_3 group of 9.1 mM (red) and 280 mM (blue) perfluorononanamide in liquid ammonia at 25 °C (relative to ammonium trifluoroacetate δ = -75.5100 ppm).

The initial hypothesis was that there would be a distinct chemical shift of the monomer -CF_3 group in the reasonably polar ammonia environment. Subsequently, if micellization into aggregates occurs, there would be a distinct chemical shift of the -CF_3 groups that are now deep within the extremely non-polar, fluorinated environment. The chemical shift over the full concentration range, however, showed that this was not the case. For example, for perfluorononanamide there appears to be a relatively constant chemical shift for the -CF_3 group of around -82.17 ppm for low concentrations (9 mM – 32 mM). However, above this concentration there is a decrease in chemical shift that appears to be roughly linear with further increasing concentration of the surfactant (Figure 4.3.9). This trend was also observed with C_7, C_8, and C_{10} fluorinated amide NMR chemical shifts over a wide concentration range.

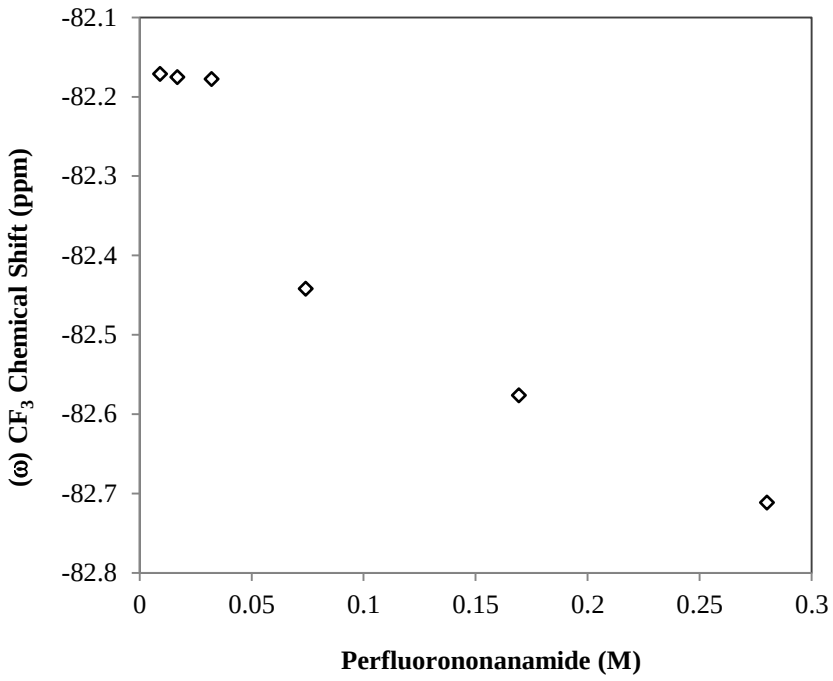

Figure 4.3.9 CF_3 chemical shift as a function of concentration for perfluorononamide in liquid ammonia at 25 °C.

The results are quite promising as they suggest that there is something happening at a certain concentration (~0.05 M) that is causing this sudden decrease in chemical shift. If aggregation was occurring and the -CF_3 group was now embedded deep within the micelle, in a fully fluorinated environment, one would expect an increase in shielding from neighbouring fluorine atoms and thus a decrease in chemical shift, as appears to be the case. This suggests that this phenomenon is actually indicative of micellization and so this is the first real indicator that aggregation is occurring in liquid ammonia. Under the assumption for now, therefore, that this is micellization one has to question why their appears to be a continuing decrease in chemical shift as the concentration is further increased, as the expectation was that there would be a specific chemical shift for the free monomer in the ammonia and a specific chemical shift for the aggregated species.

Studies by Guo et al on the fluorinated compounds in water also yielded comparable relationships to ours in liquid ammonia between the ^{19}F chemical shift and concentration. They observed that up to a certain concentration the chemical shift remained constant and then there was a gradual decrease in chemical shift.[85] By various means, they clarified that this was due to the rapid exchange of the

fluorocarbon molecules between the monomer species and micellar aggregate, and the observed peaks shifts are weighted averages of the two environments. It is reported that the mean lifetime of the aggregates from fluorinated acids (as well as other surfactants) in water is usually in the order of 10^{-6} s and the exchange between and monomer and micelle is thought to be diffusion controlled.[171] To confirm that the observed chemical shift was a weighted average of the two species (monomer & micelle), Guo et al studied their spectra at two different frequencies. At a higher spectrometer frequency, a broader peak was observed in comparison to the lower frequency and this peak broadening was interpreted as confirmation that the chemical shift line broadening effect is caused by chemical exchange between the two environments.

Having established, therefore, that the ^{19}F NMR chemical shifts above the cmc can be interpreted as exchange of molecules in different environments, one can now quantitatively analyse the data from the fluorinated amide shifts in liquid ammonia. A mass action model approximation can be applied to the chemical shift vs. concentration, where by the observed chemical shift δ_{obs} can be expressed as

$$\delta_{obs} = \delta_a + (cmc/c)(\delta_m - \delta_a)$$

where cmc is the molar concentration at which micelles or aggregates begin to form, c is the total surfactant molar concentration of the solution, δ_m is the chemical shift of the free surfactant monomer and δ_a is the chemical shift of the micellar or aggregated phase.[172]

Applying this mass action model approximation to all of the long chained fluorinated amides in liquid ammonia shows that the results are consistent with what was observed in water with the fluorinated acids. A plot of δ_{obs} as a function of 1/c consists of 2 linear segments that intersect at 1/c = 1/cmc. Figures 4.3.10 and 4.3.11 show plots of the chemical shift ($-CF_3$) as a function of the reciprocal of concentration for perfluorononanamide and perfluorodecanamide in liquid ammonia.

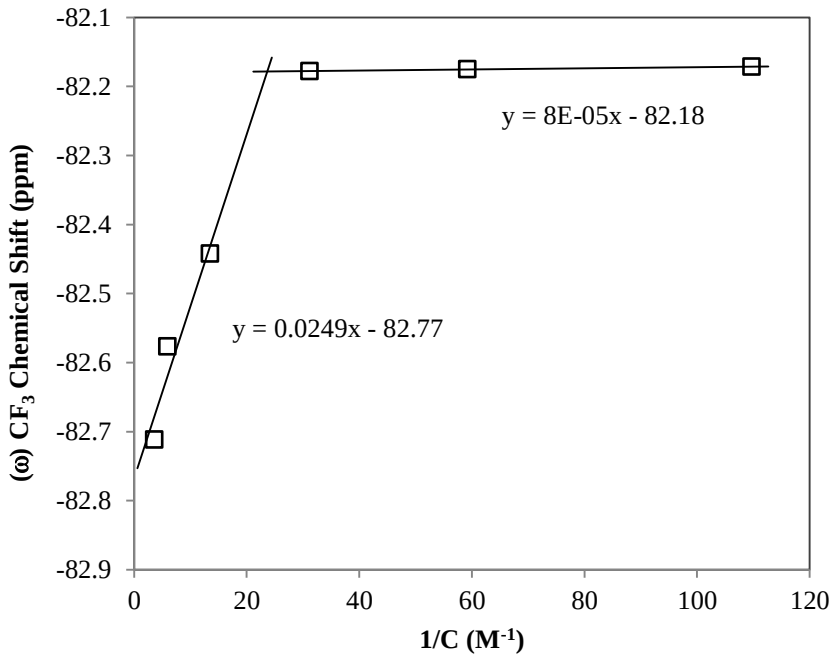

Figure 4.3.10 The chemical shift of the ω terminal -CF_3 group as a function of the reciprocal of concentration for perfluorononanamide in liquid ammonia at 25 °C.

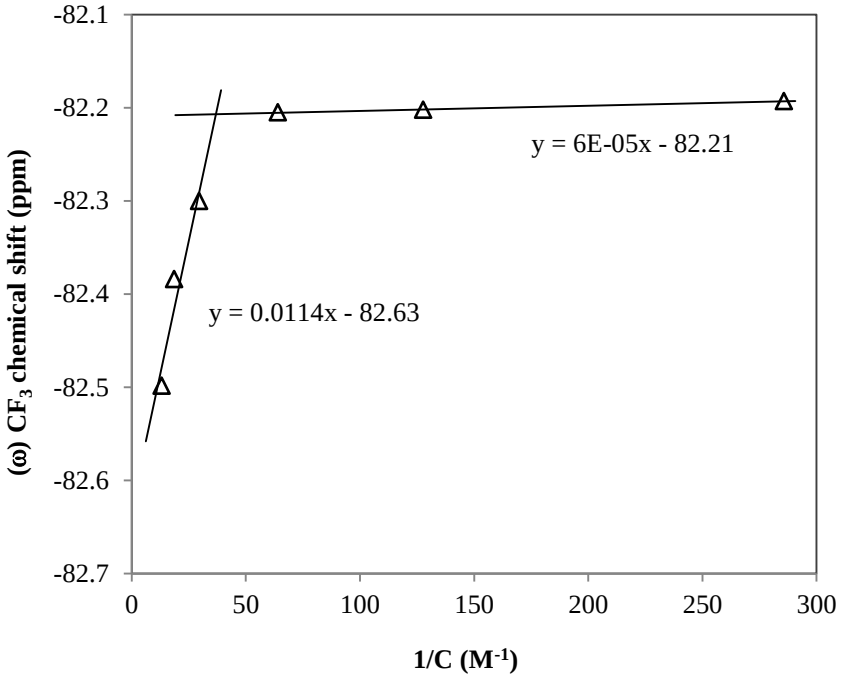

Figure 4.3.11 The chemical shift of the ω terminal -CF_3 group as a function of the reciprocal of concentration for perfluorodecanamide in liquid ammonia at 25 °C.

Likewise, perfluoroheptanamide and perfluorooctanamide give similar plots. Accordingly, the critical micelle concentration can be calculated by solving simultaneous equations for x for the 2 linear equations at the intersect. This was applied to the varying chained fluoroamides in liquid ammonia and cmc values obtained are shown in Table 4.3.2.

Table 4.3.2 cmc values of perfluoroamides in liquid ammonia.

Surfactant	**total carbons**	**1/C intersect (M^{-1})**	**cmc in liquid ammonia (M)**
perfluoroheptanamide	7	9.59	0.104
perfluorooctanamide	8	15.08	0.066
perfluorononanamide	9	23.65	0.042
perfluorodecanamide	10	37.03	0.027

It is appears clear from the plots in Figures 4.3.10 and 4.3.11, as would be expected, that at c < cmc, δ_{obs} is independent of the surfactant concentration and can thus be identified with δ_m, the observed chemical shift of the free monomer. Conversely, by extrapolation of the linear section c > cmc to 1/c = 0, the chemical shift of the aggregate, δ_a, can be found. In reality one could most likely never observe this chemical shift even at very high micellar concentrations due to the rapid exchange of micelle to monomer as previously explained but, theoretically, the individual chemical shifts of both monomer and micelle have been obtained and are distinctly different as was hypothesized.

4.3.3.2.3 Trends that confirm aggregation in liquid ammonia

As with micelles in water and other medium, one does not necessarily confirm micellization directly, by 'looking' at the aggregate itself. Instead, one looks for trends that support aggregation is occurring such as the following of trends and rules related to the chain length, for example.

4.3.3.2.3.1 Critical micelle concentration vs. chain length

Having therefore reported that a number of cmc values for varying chain length of fluorinated amides in liquid ammonia have been determined from the mass action approximation models, one can now confirm aggregation in liquid ammonia by seeing if these apparent cmc values are indicative of the chain length relationship. i.e. Klevens rule. As presented with the conductance data (chapter 4.2.1), with the fluorinated acids in water, Klevens rule is the empirical formula that unifies the relationship between surfactant chain length and cmc for a series of homologous surfactants in a given solvent system.[152,153] Interestingly, the cmc values obtained for the fluorinated amides in liquid ammonia do appear to follows Klevens rule, showing an excellent linear relationship between the number of carbons in the hydrophobic chain (n) and log cmc (Figure 4.3.12).

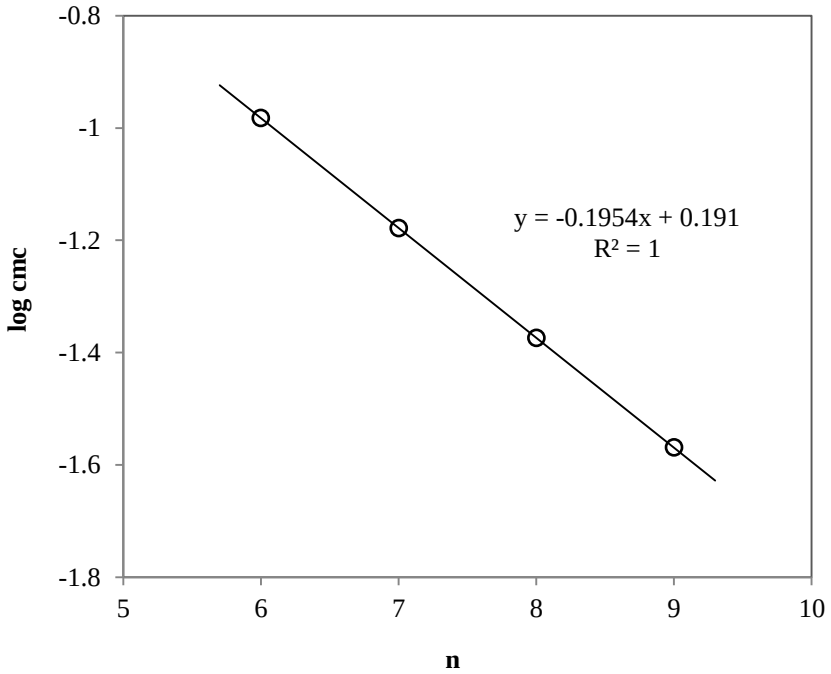

Figure 4.3.12 Logarithm of cmc (M) as a function of the number of carbon atoms for a series of perfluorinated amides in liquid ammonia at 25 °C.

Reminder:

$$\text{Klevens Rule: } \log \text{cmc} = \text{A} - \text{Bn}$$

Values obtained for these constants for the fluorinated amide surfactants in liquid ammonia, A and B, are 0.191 and 0.195 respectively. In comparison to earlier results,

for hydrogen and fluorinated chain, in water, the relatively low B value of 0.19 in liquid ammonia is not surprising (Table 4.3.3)

Table 4.3.3 Klevens B values for various surfactants in water and liquid ammonia.

Surfactant chain type/solvent	B value from Klevens plot
hydrocarbon/water	0.30
fluorinated/water	0.48
fluorinated/liquid ammonia	0.19

As discussed in aqueous medium, the B value for the fluorinated chain is higher than that for the hydrogenated because the effect of adding an extra $-CF_2-$ increases the hydrophobicity of the chain more than the addition of a methylene group. Thus aggregation is promoted by the addition of a $-CF_2-$ compared with a $-CH_2-$ at a lower concentration and a reduction in cmc is observed. The value of 0.19 obtained for the fluorinated chain in liquid ammonia is much lower than both the hydrogenated and fluorinated chains in water. This is expected as liquid ammonia is much less polar than water ($\varepsilon_{ammonia} = 16.0$, $\varepsilon_{water} = 80$) and thus the introduction of an extra $-CF_2-$ or $-CH_2-$ has less effect in ammonia than it does in water. This would also suggest that liquid ammonia has the ability to solubilise alkane chained $-CF_2-$ groups even better than water can solubilise $-CH_2-$ groups. Effectively, the B-values are an indication of the free-energy of transfer of the monomer in the solvent to the aggregate micelle. The transfer of a $-CF_2-$ group from liquid ammonia to its aggregate is less than half the corresponding transfer from water. This is due to the much greater changes in the Lennard Jones interactions between the fluorocarbon and water compared with those in liquid ammonia.[173,174]

Similarly to the B values obtained in water for the fluorinated/hydrogenated chains, in liquid ammonia one would expect that introducing a $-CF_2-$ group into the chain to have a greater effect than adding a $-CH_2-$. Although, unfortunately, as seen above, the alkyl amides were not investigated in liquid ammonia to any major extent due to the ammonia peak overlapping with $-CH_3$ group.

As a very crude prediction, using the ratio of two values obtained in water for hydrogenated (B = 0.30) and fluorinated (B = 0.48) surfactants, one could estimate that the B value for hydrogenated surfactants in liquid ammonia would be about 0.12. This is of course under the assumption that they would aggregate in liquid ammonia and some predicted cmc values can be obtained for fatty acid amides in liquid ammonia (Table 4.3.4).

Table 4.3.4 Experimental and predicted cmc values for fluorinated and hydrocarbon amides in liquid ammonia at 25°C.

Number of carbons in hydrophobic tail (n)	Fluoro amide cmc (M)	Alkyl amide cmc (M)*
6	0.104†	0.224
7	0.066†	0.169
8	0.042†	0.129
9	0.027†	0.098
11	0.011	0.056
13	0.004	0.032
15	0.002	0.019

†denotes experimental obtained cmc, others are determined from Klevens rule. *Using theoretical Klevens parameters A = 0.19 and B = 0.12 for alkyl amides in liquid ammonia

With regards to the Klevens A value obtained in liquid ammonia for the fluorinated amides (0.19) it is difficult to evaluate as it is specific of the head group-solvent interactions and having only investigated the amide head group in ammonia there is nothing to compare it with. Generally speaking, within the literature, there is not much information on the specifics of the A value obtained from this empirical formula as it is dependent on a number of factors. These include interactions of the polar head group with the solvent molecules, adjacent head group interactions within the Stern layer and counter ion interactions for ionic surfactants and other solvation effects. As it is determined at the y-intercept, where n = 0, it could be regarded as a 'theoretical' cmc value of the polar head group, which will obviously not form micelles. The lower value of A gives a lower 'cmc value' at n = 0, and hence the easier it is to form

micelles suggesting better the head group-solvent interactions and reduced head group-head group repulsion. In water, for example, a common A value for sodium carboxylates is around 1.8 , whereas it was observed that for a series of ionic liquid surfactants with aminium head groups, the A values were much higher in aqueous solution than the carboxylate surfactants (Scheme 4.3.3).[152]

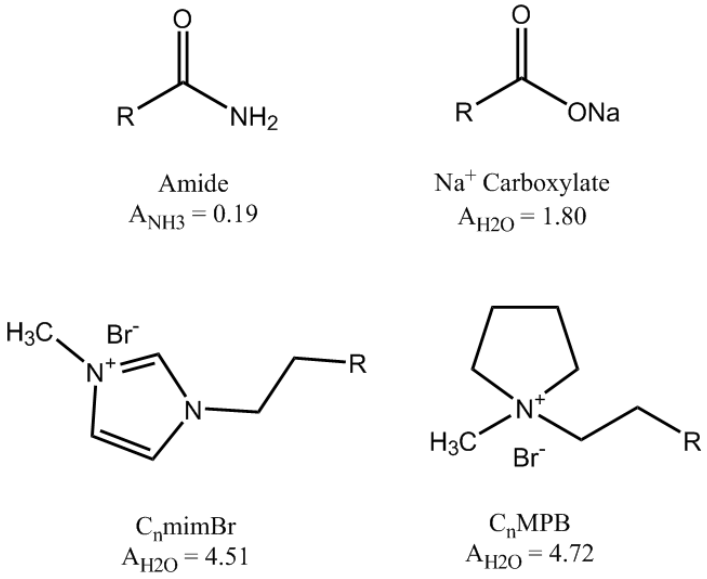

Scheme 4.3.3 Klevens A values of various head groups in water and the amide in liquid ammonia (where R = hydrophobic tail)

Comparing the A values obtained for $C_n$mimBr (1-alkyl-3-methyl-imidazolium bromides) and C_nMPB (N-alkyl-N-methylpyrrolidinium bromides) in water, the smaller value obtained for the former suggests that the ability to form micelles in aqueous solutions of $C_n$mimBr is superior to that of C_nMPB. Although much more complex with the additional methyl/alkyl groups attached, a crude comparison of the two head groups shows that the imidazole (dipole moment = 3.61 D) head group is more polar than the pyrrole (dipole moment = 1.58 D) such that the tendency of the former to aggregate in water is greater due to better interactions with the polar water solvent, which is then evident in the slightly lower A value ('cmc' at n = 0).

Similarly, the even lower value of the carboxylate suggests this polar head group has even better interactions with the water solvent through strong H-bonding and thus promotes the formation of a stable aggregate easier. Formamide has a dipole moment of 3.37 D and dielectric constant 109.5 so is not surprising that the extremely polar

amide head group, with good interactions with the ammonia solvent, has an even lower Klevens A value in ammonia than the carboxylate and amines in aqueous systems.

Non-ionic surfactants in general tend to have lower cmc values than ionics due to the lack of head group repulsion, allowing the formation of micelles at a lower concentration. There is currently a lack of data in the literature on Klevens values for non-ionics but it would be expected that, in water at least, the A value would be reasonably low just like that for the neutral amides in liquid ammonia. B values would be expected to be similar for both ionics and non-ionics, but still dependant on the nature of the tail, i.e. fluorinated or hydrogenated.

Thus, the cmc values obtained for the fluorinated amides in liquid ammonia have been shown to follow the trends that are observed with general surfactants in water, with regards to the Klevens rule linear plot of log(cmc) vs. chain length. Ideally, one would like to compare the Klevens A and B values for some other surfactants in liquid ammonia but unfortunately this has not been the case. The lower B value obtained does conform to the notion that the addition of hydrophobic groups into the chain has less of an effect in the moderately polar liquid ammonia than it does in the highly polar water solvent. Similarly, the low value of A does support the original speculation that the head group interactions of ammonia solvent and amide, as well as adjacent amide-amide head groups would be very strong, favouring the formation of a thermodynamically stable aggregate.

4.3.3.2.3.2 NMR chemical shift vs. position in micelle

The detection of micelles by the NMR method, in liquid ammonia in particular, is much more time consuming and generally less practical than the traditional conductivity method and yet the use of this technique does have its benefits that can surpass the conductance method. The application of Klevens rule relies on obtaining cmc values for a series of homologous surfactants of differing chain lengths, as was achieved. However, the NMR method actually allows one to confirm that each of the individual fluorinated amides are aggregating by looking at the specific changes in chemical shift in going from monomer to micelle.

The general method for obtaining the cmc values was done using the changes in chemical shifts of the terminal -CF_3 group of the fluoroamide as this group is expected to undergo the largest change in chemical environment. However, as observed previous, in Figure 4.3.7, the distinct peaks can be observed for the -CF_2- group adjacent to the terminal as well as the alpha carbon -CF_2-. In fact, applying the mass action model over the concentration range for both of these peak shift changes, allows for the cmc to be obtained for the fluoroamide, and is consistent with using the -CF_3 group. Figures 4.3.13 and 4.3.14 are examples of α and θ peak chemical shift for the perfluorodecanamide (Scheme 4.3.4).

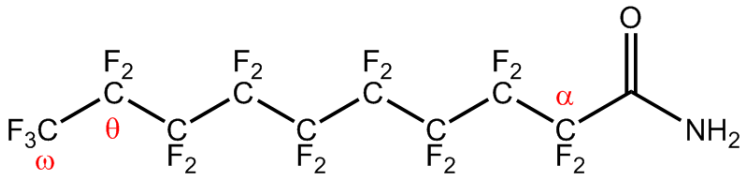

Scheme 4.3.4 Perfluorodecanamide with labelled carbon atoms.

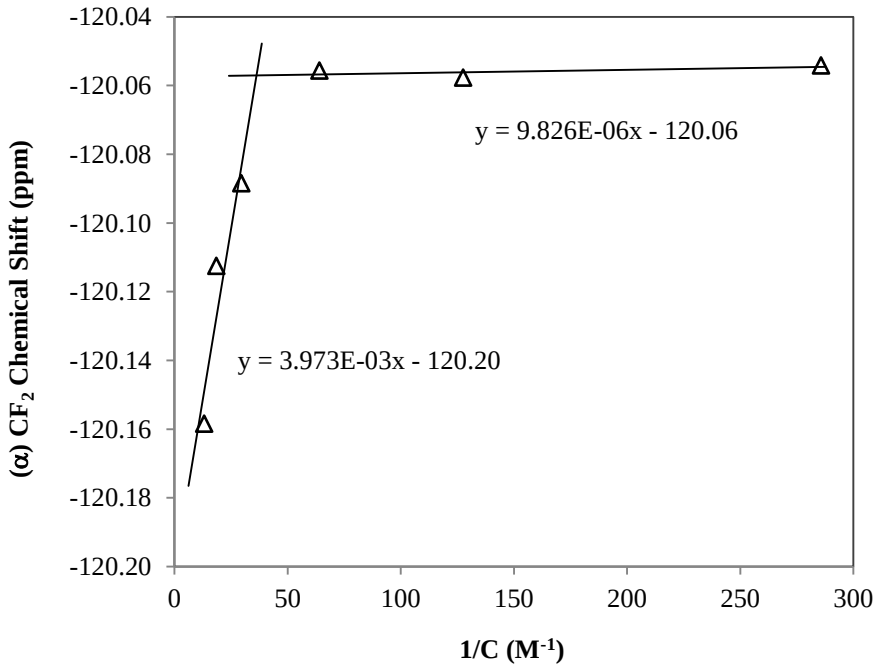

Figure 4.3.13 The chemical shift of the α carbon -CF_2- group as a function of the reciprocal of concentration for perfluorodecanamide in liquid ammonia at 25 °C.

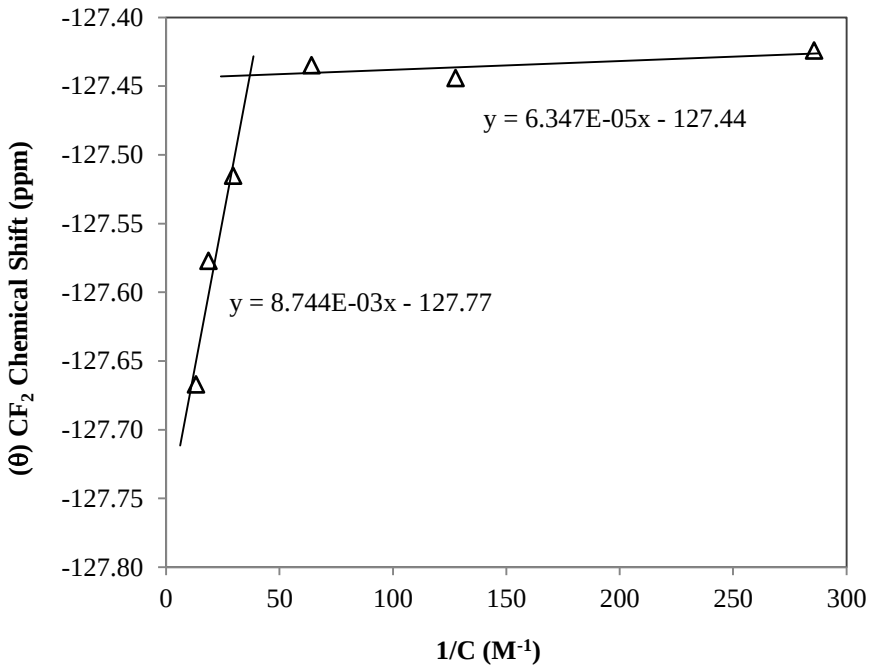

Figure 4.3.14 The chemical shift of the θ -CF_2- group (adjacent to the ω CF_3) as a function of the reciprocal of concentration for perfluorodecanamide in liquid ammonia at 25 °C.

By solving simultaneous equations for the two lines to find the intersect (c^{-1}), critical micelle concentration values obtained from the plots of the chemical shifts of the α peak and θ peak are 0.028 M and 0.027 M respectively, consistent with the value obtained from the ω -CF_3 plot (0.027 M). Comparable to the ω plot, the α and θ monomer (δ_m) can be extrapolated to the y-intercept at c < cmc and similarly, the aggregate shift (δ_a) can be extrapolated from the line equations at 1/c = 0 (the y-intercept at c > cmc).

For the three fluorinated carbons of interest, the magnitude of chemical shift change in going from monomer to aggregate can be calculated as δ_m-δ_a and values for perfluorodecanamide can be found in Table 4.3.5.

Table 4.3.5 ^{19}F chemical shifts of perfluorodecanamide monomer and aggregate peaks in liquid ammonia at 25 °C.

carbon	δ_m	δ_a	δ_m-δ_a
α	-120.06	-120.20	0.14
θ	-127.44	-127.77	0.33
ω	-82.21	-82.63	0.42

All values obtained for δ_m-δ_a are positive because there is a decrease in chemical shift in going from monomer to micelle. The -CF_2- and -CF_3 groups in the monomers are surrounded by a polar ammonia environment whereas in the aggregated micelle they are surrounded by neighbouring C-F groups from the adjacent hydrophobic chains, thus the shielding effect is observed.

However, more significant is the trend observed with regards to the magnitude of chemical shift change vs. carbon position. For the perfluorodecanamide, the magnitude of chemical shift change (δ_m-δ_a) increases further along the surfactant chain towards the end terminal group, with smaller change in chemical shift for the α group. This useful data is compatible with micellization occurring as it suggests that as one goes further along the chain, deeper into the micelle structure, the fluorinated environment dominates and thus a greater change in chemical shift observed. The α carbon, for example, would be going from a polar ammonia environment to a semi-fluorinated environment near the surface of the micelle, still exposed to some of the ammonia solvent, so only experiences 'mild' shielding effect and hence a small change in chemical shift expected. On the other hand, the ω -CF_3 group is going from one extreme to the other. As a monomer, it is likewise exposed to the polar ammonia solvent environment, yet when micellization occurs it now resides deep within the core of the micelle where the non-polar fluorinated environment predominates, with negligible exposure to the ammonia solvent on the outside. Thus a greater change in chemical shift would be expected and this does appear to the case. In standard aqueous micelle systems, water has the ability to penetrate deep into the micelle, and the same would be expected with the ammonia fluoroamide micelles.[175] Hence, for

the -CF_2 group adjacent to the ω -CF_3, the magnitude of shift is not as great as the -CF_3 probably due to ammonia penetrating deep into the micelle.

For all the fluorinated amides in liquid ammonia, δ_m-δ_a values were calculated for the α, ω, and -CF_2- adjacent to terminal, by the same means as previous, and are compiled in Table 4.3.6.

Table 4.3.6 ^{19}F chemical shifts of all fluorinated amide surfactant monomer and aggregate peaks in liquid ammonia at 25 °C.

	Fluorinated amide δ_m-δ_a			
Carbon number	**C_7**	**C_8**	**C_9**	**C_{10}**
2	0.06	0.10	0.19	0.14
6	0.17	-	-	-
7	0.29	0.20	-	-
8	-	0.38	0.39	-
9	-	-	0.58	0.33
10	-	-	-	0.42

*colour key: ω -CF_3 group, -CF_2- adjacent to the -CF_3, α -CF_2- group

Over the wide range of fluoroamides of varying chain length, the trend is apparent. In going from the α carbon towards the terminal groups, an increase in the magnitude of the chemical shift change is observed, which concurs with the above hypothesis.

There are also apparent trends between the surfactants of varying chain length. With regards to the ω -CF_3 group's δ_m-δ_a for example, as the surfactant chain length is increase from C_7 to C_8 to C_9 there is an increase in the change in chemical shift of monomer to micelle. This is expected as one could easily visualise that the terminal -CF_3 group of a C_9 chain would reside deeper into a micelle core than the terminal -CF_3 of the C_7 chain, for example. Consequently, the former would exhibit a greater change in environmental shift as it is further away from the polar ammonia and hence shows a greater change in chemical shift. There is, however, an apparent anomaly in the results. For the C_{10} fluorinated amide, the overall trend, of magnitude of shift

increasing further along the chain is still observed. But, a lower than expected value for δ_m-δ_a for the -CF_3 is observed, with a value somewhere in between that of the C_8 and C_9 chain length. A similar trend is observed for the α and θ -CF_2- groups which also give a lower than expected value for the perfluorodecanamide. It is difficult to explain this apparent anomaly but one sensible theory may be that the C_{10} surfactant molecules aren't as tightly packed together, allowing for further penetration of ammonia deeper into the micelle.

4.3.3.2.3.3 ^{19}F NMR of a 'non-aggregating' fluoroamide

It had been established that the changes in NMR chemical shifts for the various fluorinated amides can be attributed to their aggregation in liquid ammonia. Although having previously surmised that the chemical shift is reliant on the solvent environment in general, one may argue that the observed concentration-shift profile may be indicative of a general molecule over a large concentration range, because in theory as the concentration of analyte is increased, the solvent system is essentially changing. To totally dismiss this notion, the chemical shift profile of a fluoroamide that would be unlikely to aggregate was investigated. The micellization of very short chained molecules does not occur and thus it is anticipated that the shortest chained fluorinated amide, trifluoroacetamide, would not aggregate (Scheme 4.3.5) Over a reasonably large concentration range, the chemical shift of the (ω/α) -CF_3 group for this C_2 fluoroamide was reasonably constant, with slight scatter most likely within experimental/instrument error margins. The chemical shift as a function of both concentration and reciprocal of concentration can be seen in Figures 4.3.15 and 4.3.16, respectively.

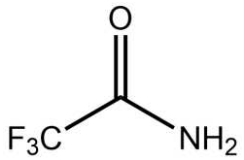

Scheme 4.3.5 Trifluoroacetamide

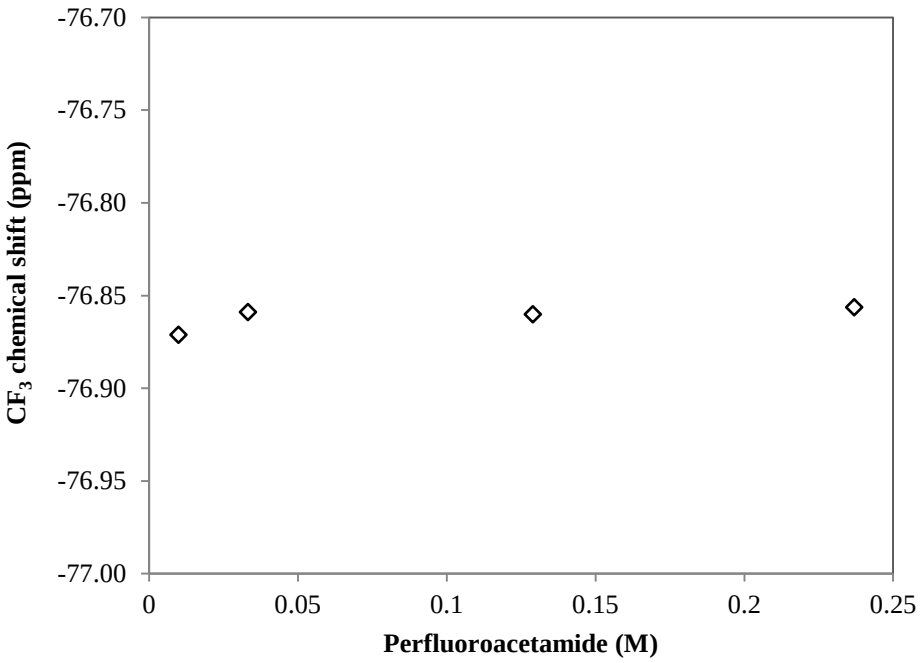

Figure 4.3.15 CF_3 chemical shift as a function of concentration for perfluoroacetamide in liquid ammonia at 25 °C.

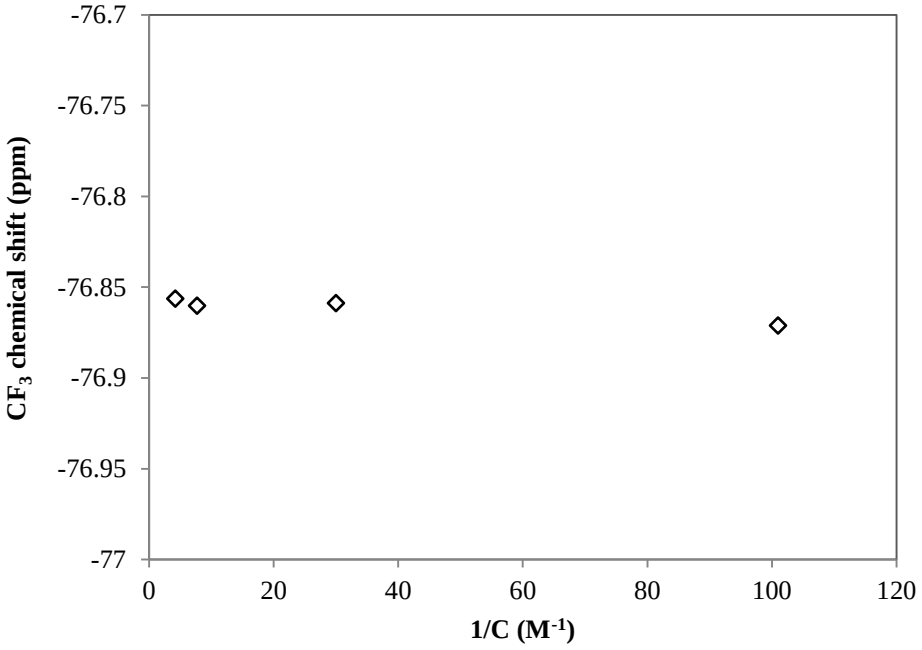

Figure 4.3.16 CF_3 chemical shift as a function of the reciprocal of concentration for perfluoroacetamide in liquid ammonia at 25 °C.

From the plots, it is apparent that over a quite a large concentration range, there is no noticeable change in the chemical shift. If anything, there is an apparent decrease in

chemical shift at the lowest concentration of trifluoroacetamide, as opposed to at the higher concentrations which the longer chained amides showed as a sign of aggregation, but this is most likely due to experimental variation as discussed. Similarly, in water, a rough test showed that the simple fluorinated acid, perfluorobutyric acid showed these kinds of trends over a wide concentration range. There was a medium scatter of chemical shift in the range of around 0.05ppm but, again, nothing as noticeable as with the long chained fluorinated acids and salts that showed a distinct decrease in the chemical shift to conclude the formation of an aggregate species.

4.3.3.2.4 Catalysis in micelles

Changes in organic reactivity in aqueous solutions of micelles have been used to explore the structure of micelles[176,177,106] themselves and utilise micelles as models for simple cells.[178, 125] The interior of the micelles in water and the head-group/solvent interface act as pseudophases distinct from the bulk solvent, and can accelerate or inhibit reactions, depending on the mechanism involved with the reactions as well as the rate constants and reactant concentrations in the two distinct regions.[179] It is therefore of wide interest to explore organic reactivity in liquid ammonia in the presence of these aggregate/micelles.

The observed pseudo-first-order rate constant for the ammonolysis of propargyl benzoate was found to increase approximately 6-fold in the presence of 90 mM perfluorononanamide. More remarkably, over a range of perfluorononanamide concentrations, the rate increase appears to roughly coincide with concentrations around the cmc obtained from the above NMR studies, approximately 42 mM (Figure 4.3.17).

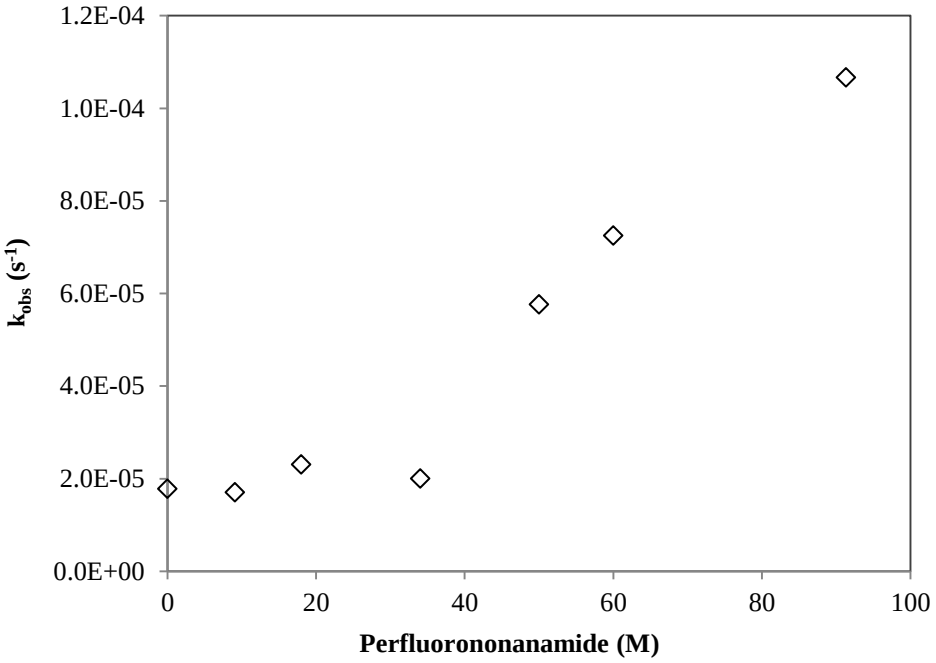

Figure 4.3.17 Observed rate for ammonolysis of propargyl benzoate as a function of perfluorononanamide concentration in liquid ammonia at 25 °C.

The moderate rate enhancement seen in the presence of surfactant is typical of the magnitude seen in aqueous micelle catalysed reactions and thus further evidence of aggregation of the perfluoroalkyl amides in liquid ammonia. Having deduced that the rate limiting step for the uncatalysed solvolysis reaction involves late formation of the zwitterionic tetrahedral intermediate or a neutral tetrahedral intermediate with little C-OR bond fission in the transition state, one can speculate how the presence of micelles may enhance the rate. Presumably, the transition state is stabilised at the micelle-ammonia interface either because of increased polarity of the region or due to direct H-bond interaction between the amide and tetrahedral intermediate (Scheme 4.3.6).

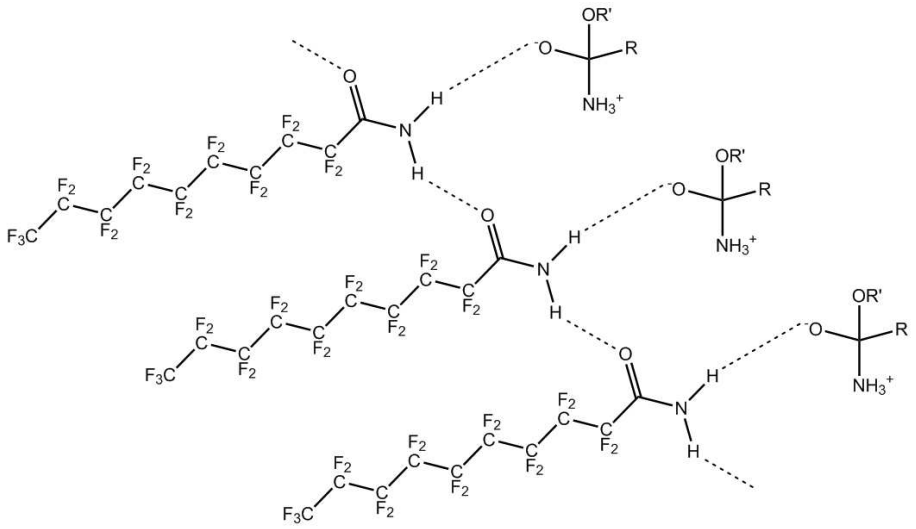

Scheme 4.3.6

Similarly, over the range of fluoroamide surfactants, a moderate rate enhancement was observed for a variety of the simple esters and appeared to roughly coincide with the cmc values determined from the NMR studies.

4.3.4 Summary of fluorinated amide studies

In summary of the aggregation studies on fluorinated amides in liquid ammonia, it was apparent during their synthesis in liquid ammonia that they were particular highly surface active, showing a good degree of frothing and foaming. However, unlike the ionic surfactants, due to their neutral charge another detection method was required in order to confirm aggregation. Initial attempts using a solubilisation method were unsuccessful. Due to the mid polarity of liquid ammonia, the full range of dyes tested had some solubility in liquid ammonia and so this detection method was not examined further. Likewise, solubilisation of pfh into a liquid ammonia micelle was unsuccessful, but may have some merit if a safer method for more vigorous agitation of the mixture could be developed. ^{19}F NMR showed significant changes in chemical shift over a concentration range, in particular for the terminal -CF_3 group, which is indicative of aggregation of a monomeric species into a micelle. From these changes in shifts, cmc values could be calculated which appeared to follow the Klevens relationship between cmc and hydrophobic chain length. Furthermore, the magnitude of the chemical shift change increases further along the chain towards the terminal group. This is consistent with the notion that the terminal group undergoes the

extreme change in environment in going from monomer to deep within the micelle core. In comparison, the α -CF_2- group in the micelle is likely still surrounded by solvent ammonia that can penetrate the outer layer of the micelle, thus only a moderate change in chemical shift is observed. Additionally, micelles of fluorinated amides in liquid ammonia appear to have some catalytic function, on the ammonolysis of esters at least. The modest rate enhancement in the presence of the micelle could be due to stabilisation of a tetrahedral intermediate or an increased region of polarity. With further investigation, there may be some industrial application for the micelles in liquid ammonia. The studies do however suggest that aggregation of molecules in liquid ammonia is possible just like aggregation in water allows for compartmentalisation of cells. Thus liquid ammonia may have some capacity to support a 'living' cell-type aggregate. Admittedly, only the fluorinated amides were shown to aggregate (alkyl amides could not be monitored by NMR), but the general principle that molecules may aggregate in liquid ammonia stands true and one of 'life's processes', compartmentalisation of lipids, is certainly conceivable in this non-aqueous solvent.

Chapter 5 - Enzyme Studies

5.1 Background

5.2 Enzyme studies in liquid ammonia - Results and Discussion

5.1 Background

5.1.1 Enzymes as nature's catalysts

Within the protective aqueous microenvironment that is the interior of the cell there are multiple reactions and chemical interconversions that help to maintain life. The vast majority of these reactions are non-spontaneous, slow and would not be able to meet the demand to sustain life if unaided. It is enzymes, nature's catalysts, which are responsible for the many thousands of reactions within the cell that help to preserve and develop life and so enzyme activity can be regarded as one of the fundamental processes of life along with cell aggregation.[180] Enzymes are generally highly selective catalysts and so not only greatly accelerate the rate of reactions in nature but also dictate the specific metabolic pathways within the cell. Additionally, some enzymes play a key role in catalysing extracellular reactions like the breakdown of macromolecules in all living species and, in particular, these types of enzymes are an integral part of the digestive function of the fungi kingdom.[181] Both intracellular and extracellular enzymes are synthesized within the cell, and are globular proteins but sometimes require the presence of co-enzymes and metal-ions for full activity.[182]

5.1.2 Enzymes as industrial catalysts

In addition to their role as biological catalysts, enzymes play a key role in the field of catalysis within the chemicals manufacturing industry. In the current climate, where the desire for 'green chemistry' is becoming more prevalent, there is a drive towards the reduction, or preferably eradication, of waste produced by classical synthesis methods, and many industries are turning to enzymes to achieve this.[183, 184] Enzymes offer the potential to manufacture high yields of pure products with a reduction in energy consumption and waste as they usually operate at mild temperatures, under moderate conditions and are highly selective towards the substrate. For example, the traditional method of disaccharide hydrolysis within the confectionary industry used to be accomplished using inorganic acids so that further purification would be required to remove by-products. The process can be made much more efficient, with little waste, using a hydrolase such as invertase to cleave the glycosidic bond (Scheme 5.1.1).

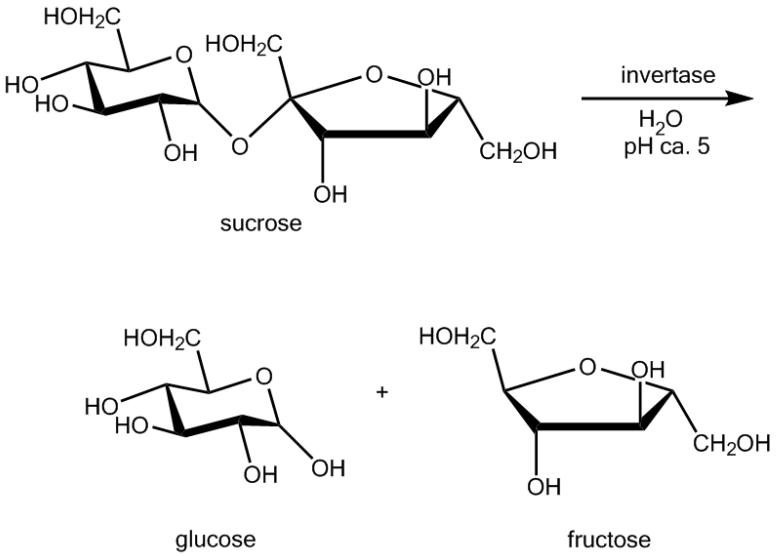

Scheme 5.1.1 The action of invertase on sucrose to liberate glucose and fructose.[185]

In more complex synthetic procedures, the enzyme's highly selective nature eliminates the need for protecting groups thus reducing the chemical derivatives that would be needed for further de-protecting, which overall reduces both the number of reactants and waste.[186] A major test as to the extent at which enzymatic catalysis will replace conventional stoichiometric conversions within the manufacturing industry is sometimes determined by the enzymes ability to function out of its natural 'comfort zone' of aqueous dominated media and its capacity to replace its natural reactants with the non-conventional as substrates. The potential for enzymes to catalyse reactions under anhydrous conditions has been well documented, particularly in organic solvents.[187]

5.1.3 Enzyme activity in non-aqueous environments

In the aqueous based environment in which life flourishes it is tempting to assume that enzymes only work in moderate, aqueous conditions. This can be reflected in that in the majority of enzymatic studies, water has been the orthodox reaction solvent as it is fundamentally the enzyme's natural habitat. However, many enzymes only work in a weakly aqueous environment, for example those which are membrane bound and catalyse reactions within a lipid phase.

Many people have brewed beer and wine and made cheeses and yoghurts via enzymatic procedures for many centuries, but one of the first successful, scientific

industrial applications of enzymes was achieved by the Upjohn Company in 1951. They applied microbiological catalysis fermentation to a progesterone nucleus to introduce an 11-hydroxyl group which could then be transformed into cortisone, a steroid hormone.[188]

More recent industrial applications of enzymes are highlighted in the synthesis of 7-butyroyl-castanospermine, a highly effective inhibitor of HIV. This process utilises two enzymes in three separate steps (Scheme 5.1.2).

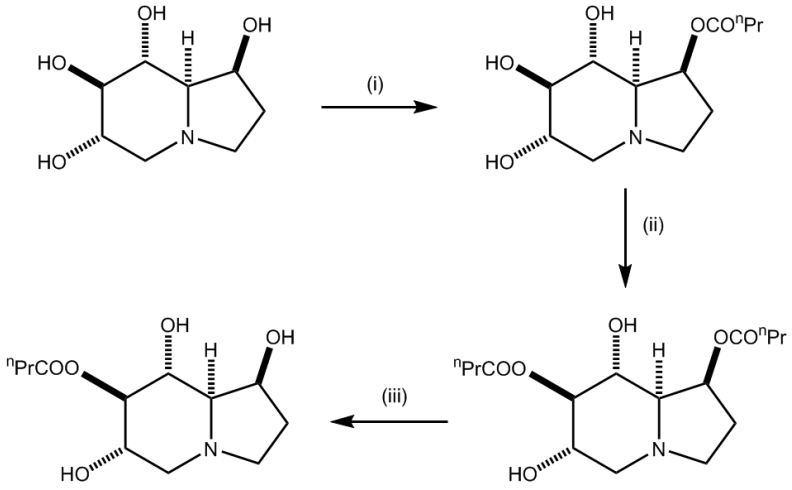

Scheme 5.1.2 Reagents: (i) subtilisin, n-PrCOOCH$_2$CCl$_3$, pyridine, 92 hr, 84 %; (ii) Lipase CV, n-PrCOOCH$_2$CCl$_3$, THF, 72 %; (iii) Subtilisin, phosphate buffer, pH 6.0, 64 %.

Firstly, in non-aqueous conditions (pyridine), castanospermine is transformed into its 1-butyroyl ester via a subtilisin catalysed transesterification. The monoester is then converted to the 1,7-dibutyroyl ester with lipase catalysis in tetrahydrofuran and finally subtilisin is used to cleave the 1-butyroyl ester.[189, 190]

The above cases demonstrate how these biological catalysts can be utilised outside what one would normally regard their optimum aqueous environment that is the protective interior of the compartmentalised biological cell.

5.1.4 Choosing an enzyme and substrate for liquid ammonia studies

5.1.4.1 A wide choice of enzymes, substrates and conditions

Some enzymes are thus capable of showing catalytic activity out of their natural aqueous environment and so with a view to observing enzyme activity in liquid ammonia, there is a vast array of enzymes commercially available that could be examined. Additionally, with the many preparations of these enzymes available (lyophilized, immobilized, solubilised in co-solvent etc.) and the huge array of substrates for these biotransformations, a clearly defined plan must be set out as to the choice of enzyme, substrate and reaction conditions for the enzymatic studies in liquid ammonia. In, general, bio-catalysts are used in the laboratory and industrially in either a whole-cell system, such as yeast cells, or as isolated enzymes, which may be used free or immobilised, such as lipases. Although often cheaper, using whole cell systems in liquid ammonia does not appear to be a viable project.

5.1.4.2 Enzyme catalysis in an ammoniacal environment

Enzyme activity in a pure, anhydrous, liquid ammonia medium has not been previously reported. Although enzyme activity in a wide range of non-aqueous media is well studied, the use of nature's catalysts in an ammonia dominated environment has only briefly been explored. An example is Sheldon's pioneering work on the lipase catalysed ammonolysis of triglycerides in ammonia saturated organic solvents (Scheme 5.1.3). He demonstrated that in ammonia saturated tert-butanol, a number of triglycerides could be smoothly converted to the fatty acid amide by Candida antarctica Lipase B (CALB). In the absence of enzyme, no reaction was observed.[191]

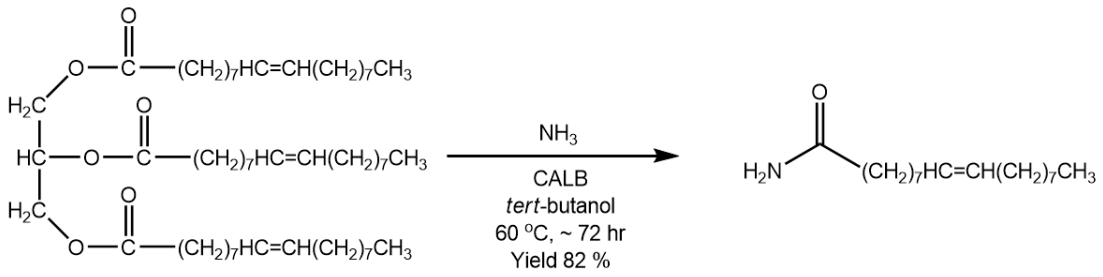

Scheme 5.1.3 Lipase catalysed ammonolysis of triolein in ammonia saturated tert-butanol

A sensible approach to the liquid ammonia enzyme studies would be to mimic some of the reactions that Sheldon explored in ammonia saturated tert-butanol. If the formation of fatty acid amides from triglycerides could be catalysed by lipases in liquid ammonia then this could support an ammonia-based life system as well as offer some prospective industrial applications. The cell aggregation studies reported earlier were preliminary studies of very basic cell-type structures in ammonia. They demonstrated that, having observed micelles with simple surfactants, it may be possible to form more complex, biological-type cells from phospholipids. Any enzyme catalysis observed in liquid ammonia, even if not as efficient as in its 'normal environment' would at least demonstrate the principle that ammonia has the potential to support a biological catalyst.

Additionally, the potential products, fatty acid amides, are analogous to the fluorinated amide surfactants that were shown to aggregate into cell-like structures in liquid ammonia. Admittedly, the aggregation of alkyl amides in liquid ammonia was not explored but if the enzymes can catalyse the synthesis of alkyl amides in liquid ammonia then it may be possible to piece together two individual processes of life - synthesis of lipids and formation of cells from these lipids. As referenced to in the introduction, the definition of 'life' is not necessarily by observing an individual reaction or process, but more likely by combining a collection of these life-type processes.

From an industrial perspective, the enzymatic synthesis of long chained fatty acid amides in liquid ammonia could be very interesting, as fatty acid amides are widely used commodities with applications in industry, the commercial market and medicinal research.

5.1.4.3 Fatty acid amides

5.1.4.3.1 Structure and applications

Fatty acid amides (FAA's) are carboxylic acid amides comprising of an aliphatic chain and amide group (Scheme 5.1.4)

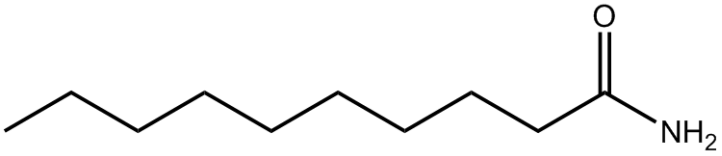

Scheme 5.1.4 General structure of a fatty acid amide, decanamide.

Due to the amide head group they can form intermolecular hydrogen bonds and thus show higher melting points than their corresponding acids and esters.[192] Conversely, they tend to show lower solubility in organic solvents than the analogous fatty acid esters.[193]

One of ways of classifying fatty acid amides is by their carbon chain length:[194]

- Short-chain fatty acid amides - aliphatic chains with fewer than 6 carbons such as butyramide.
- Medium-chain fatty acid amides - aliphatic chains with between 6-12 carbons such as octanamide.
- Long-chain fatty acid amides - aliphatic chains with between 13 to 22 carbons such as oleamide.
- Very long-chain fatty acid amides - aliphatic chains with greater than 22 carbons.

Additionally, fatty acid amides can be characterised by the nature of their aliphatic tail, whereby fatty acid amides with one or more carbon-carbon double bonds are known as unsaturated whilst fatty acid amides without double bonds are classed as saturated.

Medium and long chain fatty acid amides are very similar in structure to the surfactants studied in the aggregation chapter, comprising of a polar and non-polar moiety, and likewise can adsorb at a surface interface. It is the amphiphilic nature of fatty acid amides that make them useful commodities in various industries. They are primarily used as lubricating agents within the plastics industry and, because they have low toxicity, some FAA's (usually as diethanolamides) are replacing traditional surfactants in everyday consumer products such as hair shampoos, washing liquid, foam stabilizers and other detergents.[195]

In addition to their industrial and commercial applications, some fatty acid amides have recently been identified for their use in medicinal research. For example, oleamide (cis-9-octadecenamide) (Scheme 5.1.5) induces sleep in animals and accumulates in the cerebrospinal fluid during sleep deprivation.[196] It is being studied as a potential treatment for sleep and mood disorders although the intrinsic mechanisms of action of this cannabinoid analogue are still under investigation.[197]

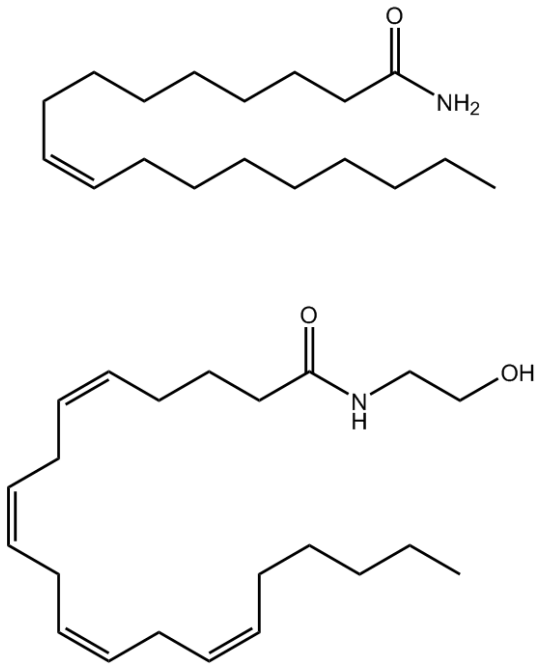

Scheme 5.1.5 Oleamide (top) is structurally related to the endogenous cannabinoid, anandamide (bottom), and has the ability to bind to the Cannabinoid receptor type 1 (CB_1) receptor as a full agonist.

The current global scale of fatty acid amide synthesis is in the region of 300,000 tons per year with market values estimated to be worth around £500 M.[198] Hence, for both industrial and medicinal applications, there is a wide interest in the synthesis methods of fatty acid amides.

5.1.4.3.2 Synthesis of fatty acid amides - current methods and liquid ammonia potential

Fatty acid amides are most commonly prepared by reacting the fatty acid with anhydrous ammonia at high temperatures (> 200 °C) and pressures for extended

periods of time. Dehydration of the ammonium salt of the fatty acid produces the primary amide (Scheme 5.1.6).[199]

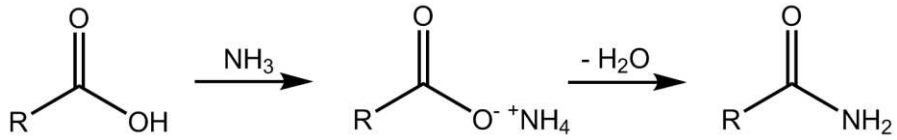

Scheme 5.1.6 Fatty acid amide synthesis from the fatty acid

Alternatively, there are some catalytic procedures available that allow for relatively shorter reactions time, but often still require elevated temperatures. One report uses a catalyst compound from metals of Groups 3 and 4 of the periodic table and claims yields of > 95 % fatty acid amides after 8 hours reaction in ammonia and an alcohol co-solvent at 180 °C.[200] Another method uses a silica based surface catalyst and gaseous ammonia with high yields of > 99 % after 48 hr reaction at 160 °C.[201]

Reaction times can be vastly reduced to less than 30 minutes using a microwave oven and a Lewis acid catalyst and urea as source of ammonia (yields > 90 %).[202] However, microwave reactions are difficult to scale up and so this method is not effective for an industrial scale continuous processes. The fatty acids used for the above synthesis methods are routinely prepared by the hydrolysis of triglycerides (fatty acid esters) into the acid.

Alternatively, the direct amidation of the triglyceride to prepare fatty acid amides is of great interest to the chemicals industry (Scheme 5.1.7).

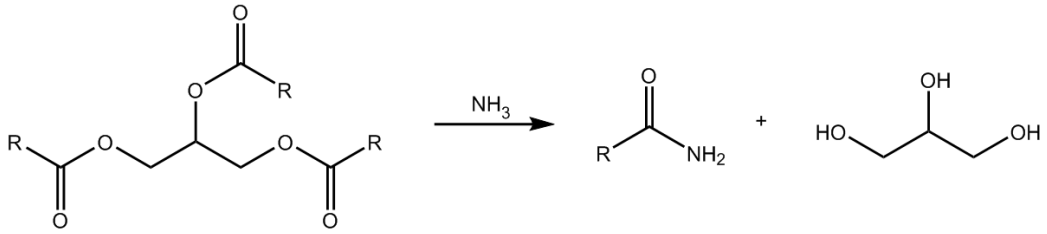

Scheme 5.1.7 Fatty acid amide synthesis direct from a triglyceride

Unfortunately, the literature surrounding synthesis of fatty acid amides via this pathway is quite ambiguous and inconsistent. Balaty and others found relatively low yields of amide conversion (< 50 %) after reaction of various triglycerides in liquid ammonia at 25 °C for 92 hr.[203] Contradicting this, one patent reports full conversion

of coconut oil (mainly C_{10}-C_{14} fatty acid content) to the corresponding fatty acid amide upon standing in liquid ammonia at room temperature for only 12 hr.[204] As with the amidation of fatty acids, the more efficient uncatalysed triglyceride amidation requires elevated temperature and pressure. For example, Roe and others report the ammonolysis of various oils with anhydrous ammonia at 170 bar and 170 °C for 6 hr.[205]

In summary, current industrial methods for fatty acid amide synthesis, either from fatty acids or triglycerides, requires a catalytic procedure and/or reaction at high temperature and pressure, all of which can be costly and yield unwanted by-products. Catalyst free procedures under moderate conditions require long reaction times. Furthermore, some fatty acid amides are reported to be very heat sensitive and so most industrial scale synthesis methods would require additional purification steps in order to meet specifications. This poses a significant problem particularly in the manufacture of the fatty acid amides for medicinal research, as described above, where extremely high purity of the FAA is critical. This can possibly be reflected in the high price of oleamide where, from commercial biochemical suppliers, it can be priced as high as £2500 per gram (pharmaceutical grade), with the corresponding carboxylic acid from which it is prepared, oleic acid, available at costs as low as £7 per gram.[206, 207] This suggests that the purification of oleamide from the standard synthesis methods is costly and time consuming and therefore any low-temperature synthesis methods of fatty acid amides that can bypass additional purification steps would be very attractive. The highly selective nature of an enzyme catalysed reaction could possibly meet this demand.

In addition to Sheldon's work in ammonia saturated tert-butanol there are only a few other methods for the bio-catalytic amidation of triglycerides and fatty acids. One author reports the direct amidation of oleic acid to oleamide using lipase from Candida antarctica and a stoichiometric equivalent of ammonium carbamate as a source of ammonia. The yield is reported as 95 % (4 days reaction, 35 °C) using methyl isobutyl ketone (MIBK) as a solvent.[208] Other reports suggest that some long chained fatty acid amides can be synthesised directly from oils by fermentation with microorganisms (B. subtilis 50), although yield were as low as 22 % after 5 days reaction.[209]

It appears that the lipases have the ability to function sufficiently outside their aqueous environment and given that fatty acid amides are potentially very high value commodities, it seems worthwhile to search for enzyme catalysis in liquid ammonia with this class of enzyme.

5.1.4.4 Lipases

5.1.4.4.1 Mechanisms of action

Lipases (EC 3.1.1.3) are the lipid-splitting catalysts that excel in natural catalytic biotransformations involving the carboxylate group.[210] More specifically, they play a key role in catalysing the hydrolysis of fatty esters. The mechanism operates fundamentally the same as serine proteases, utilising the catalytic triad in which the active site consists of serine, histidine and aspartate residues (Scheme 5.1.8). Deprotonation of the serine –OH group by histidine coordinates the attack of the serine residue on the carbon centre of the ester substrate forming a tetrahedral intermediate. The excess negative charge on the carbonyl oxygen is stabilised by the 'oxyanion hole'. The tetrahedral intermediate collapses to form the serine ester with the expulsion of the leaving product alcohol by accepting a proton from the histidine imidazole conjugate acid. The nucleophile (water) is then deprotonated by the histidine nitrogen lone pair facilitating the nucleophilic attack on the serine ester carbonyl carbon. This generates a second tetrahedral intermediate which subsequently collapses via the expulsion of the serine residue by protonation from the imidazolium ion, releasing the carboxylic acid product and the enzyme to its original state.

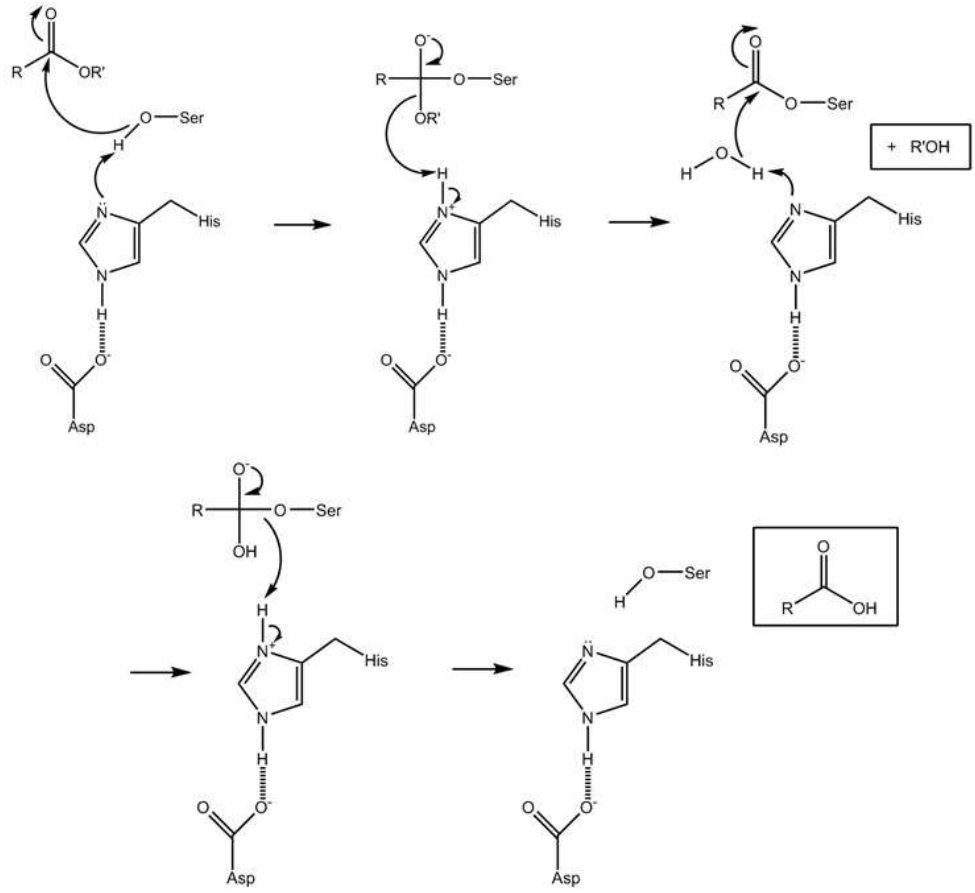

Scheme 5.1.8 Mechanism of lipase catalysed hydrolysis of an ester

The simplicity of the lipase mechanism means that there is potential to utilise this enzyme outside its natural environment and replace its orthodox reactants with the non-conventional. Hence, these biological catalysts have been used extensively in a range of carboxylate based biotransformations including transesterification, aminolysis and esterification where the natural water nucleophile can be substituted for amines or alcohols. In principle, the above lipase mechanism could support many nucleophiles capable of reacting with the acyl-enzyme intermediate (serine ester).

It is proposed that if the water nucleophile can be replaced by an amine or alcohol, for aminolysis or transesterification reactions, respectively, then there may be potential for an ammonia nucleophile and the ammonolysis reaction in pure liquid ammonia, provided that the enzyme can maintain a degree of catalytic activity in this solvent.

5.1.4.4.2 Considerations for lipase studies in liquid ammonia

Lipases are abundant in nature, and common enzymes for their use in laboratory biotransformations include the porcine pancreatic lipase (PPL), those from microbial

sources (Arthrobacter sp.) and extracts from yeasts and fungi such as Candida antarctica, Aspergillus niger and Candida rugosa.[211] Additionally, many different forms of lipases are available (powdered, immobilised, solubilised in co-solvent), and the choice of them can greatly affect the efficiency of the biotransformation. For Sheldon's work in ammonia saturated alcohol the enzyme of choice was Candida antarctica Lipase B (CALB). This specific lipase has proven to be an extremely robust and versatile natural catalyst for numerous biotransformations in both aqueous and non-aqueous media.[212] In their natural form, the enzyme is solubilized in an aqueous solution and so can be obtained commercially as a lyophilized powder. However, the use of lipases in non-aqueous media often necessitates a different enzyme 'form' and many of these lipases in their free, powdered form often show little activity in non-aqueous solvents.

In their orthodox aqueous environment lipases adsorb at the water-lipid interface and can be described as "interfacially activated".[210] A helical 'lid' or 'flap' on the lipase is responsible for the characteristics of this interfacial activation by blocking the enzymes active site (Figure 5.1.1).[213]

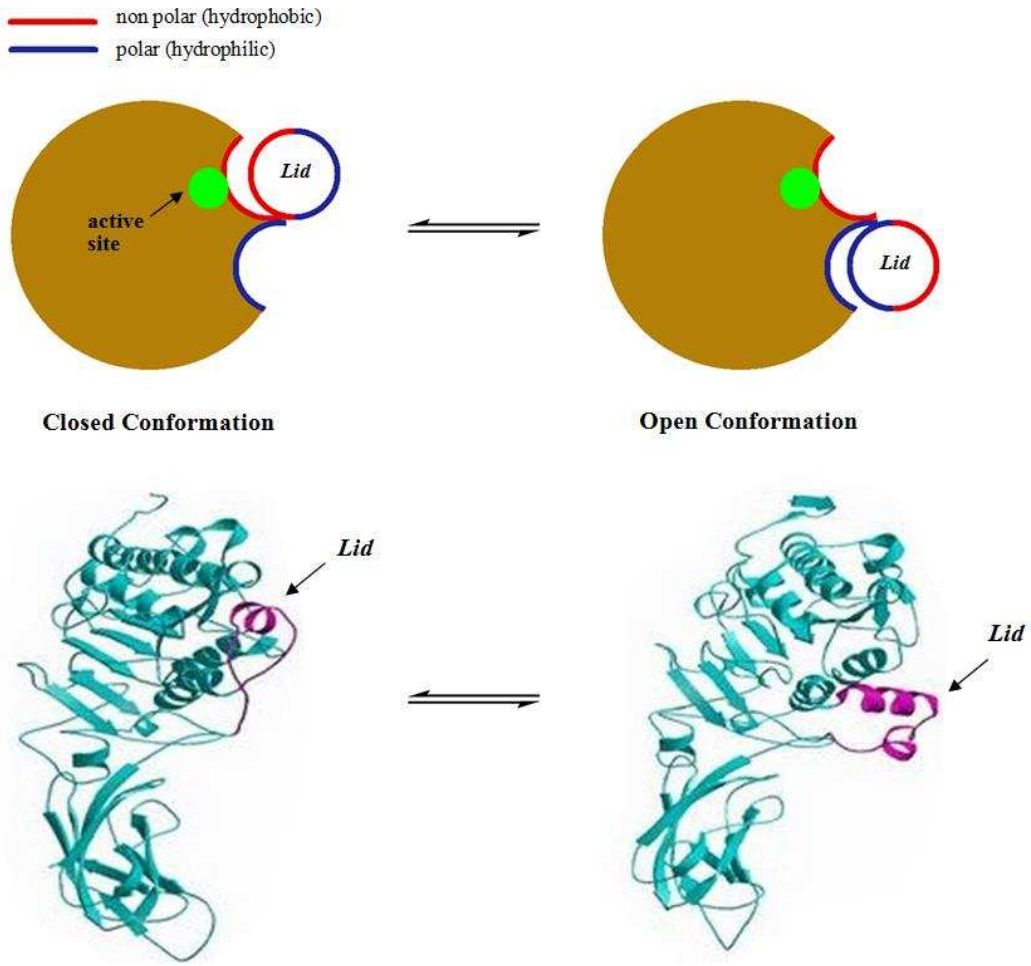

Figure 5.1.1 Schematic (top) and ribbon diagram (bottom) of lipase 'lid' conformations to cover (left) or expose (right) active site.[214]

A freely dissolved lipase in highly polar water, in the absence of the nonpolar-polar (lipid-aqueous) interface, remains inactive with the lid covering the active site. It is proposed that there is an equilibrium between open and closed forms.[215] In a standard aqueous medium the lipase requires both the presence of a polar phase, provided by water, and a nonpolar lipid phase, provided by the substrate, to become activated for catalysis.

Consequently, in non-aqueous solvent biotransformations, where presumably the solvent of choice may be less polar than water (organic solvents), this interfacial adsorption is lacking due to the absence of a polar phase. It could be argued that the lack of polar phase should not necessarily inactivate the enzyme as Figure 5.1.1 would suggest that in a non-aqueous (nonpolar) environment the lipase exists entirely in an open conformation and so should be catalytically active towards any lipophilic

substrates. However, without the polar phase, solubility of the free enzyme in the non-aqueous solvent may be limited in the first place and so the protein folding (or lack of) needs to be considered. The activity of enzymes is fundamentally determined by their three-dimensional structure, arising from the unique folding of the protein. In water, this folding is driven by interaction of the long chains of amino acids with the polar solvent ultimately resulting in an 'ideal' structure with the active site available for substrate binding, subsequent reactions and release of products and enzyme.

Thus, a lipase in a non-polar solvent may not necessarily be inactive due to absence of interfacial activation, but is more likely denatured in the first place from a lack of the unique protein folding usually provided by the polar, aqueous medium.

For many lipases, it appears that immobilisation of the enzyme onto a polar solid support can enhance enzyme activity, stability and selectivity in non-aqueous environments.[216] This can be reflected in some of the current methods described for non-aqueous aminolysis/ammonolysis biotransformations, where the majority of methods use lipases adsorbed on a macroporous resin. This immobilisation method is used to overcome the problem of using non aqueous solvents, where there is a lack of polar phase and likely protein unfolding and denaturing of the enzyme. The polar solid support in principle mimics the natural polar aqueous phase that can adsorb the enzyme, with the substrate again providing the nonpolar phase and so lipase interfacial activation can be achieved.

CALB is a widely used lipase immobilized onto acrylic resin beads and commercially available as Novozyme 435. In addition to providing the polar phase for enzyme adsorption and subsequent activation, the immobilisation of the lipase onto the macroporous beads allows for a larger surface coverage of the enzyme. The acrylic beads, of diameter 0.3-0.9 mm, have an average surface area of 130 m^2 g^{-1}.[217] The spread of lipase over this large surface area can allow for a greater proportion of available active sites for catalytic function and furthermore can likely facilitate the mass transfer of substrates and products with the bulk phase.[187]

Due to liquid ammonia's reduced polarity, in comparison to water, it is anticipated that this solvent alone would not provide the interface required for the lipase to work if a 'free' preparation of enzyme is used. It is therefore expected that, analogous to the biotransformations in organic media as described previously, liquid ammonia lipase

catalysis may require the solid supported enzymes to provide a highly polar phase to allow for the essential folding of the protein to render it catalytically active.

5.2. Enzyme studies in Liquid Ammonia - Results and Discussion

5.2.1 General structure and reactions of triglycerides

Comparable to simple mono esters, containing carboxylate and alcohol residues, triglycerides are larger molecules derived from glycerol (a polyol) and three fatty acid residues (Scheme 5.2.1).

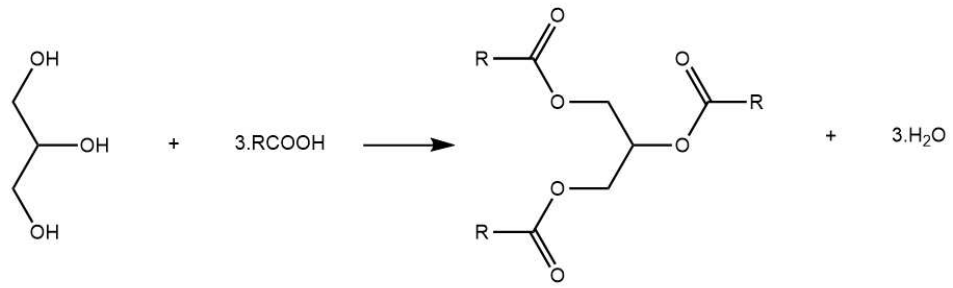

Scheme 5.2.1

Triglycerides, also called triesters, may undergo attack from a nucleophile at the carbonyl carbon centre which could be a solvolysis reaction, if using a nucleophilic solvent. These reactions may be spontaneous or require a catalyst depending on the reactivity of the nucleophile or triester substrate, and the products formed are often of wide interest.

Analogous to the surfactants studied for aggregation in the previous chapter, the more commercially used soaps are similarly comprised of a polar head group and hydrophobic tail, which tends to be hydrocarbon rather than fluorinated.[218] They are often prepared by the base catalysed hydrolysis of the triglyceride and this 'soap making' technique, also known as saponification, has been used for thousands of years to prepare these simple, but useful molecules.[109] Triglycerides are abundant in nature and sources include animal and vegetable fats. Indeed, the word "soap" comes from the Germanic word "saipa" which takes its origins from the Latin word "sebum", meaning fat or tallow.[219] Tallow, a rendered form of beef or mutton fat consists of triglycerides whose main constituents are derived from stearic and oleic acids, and so a simple lye saponification (base hydrolysis) of these fats will produce the soaps sodium stearate and sodium oleate, and sodium stearate is one of the most common soaps used today.[220]

Furthermore, the attacking nucleophile can be an alcohol group, for a transesterification reaction, or an amine, for aminolysis (Scheme 5.2.2).[221, 222] Indeed, the molecules in biodiesel are predominantly FAMEs (fatty acid methyl esters) which are routinely prepared by the transesterification of oils and fats with methanol, usually requiring a sodium hydroxide catalyst.[223]

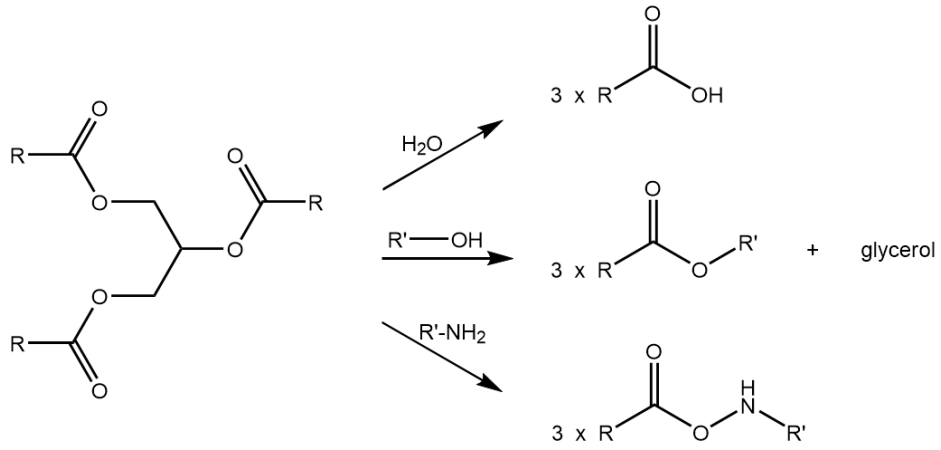

Scheme 5.2.2

As discussed previously, the production of long chained amides (fatty acid amides) from an enzymatic process would be of wide interest as these surfactant molecules have uses in the manufacturing industry as lubricants as well as potential medicinal uses. Additionally, lipase catalysis in liquid ammonia would satisfy another of life's processes, suggesting that ammonia may be a suitable candidate to replace water as life's medium. With this in mind, attention will initially focus on the ammonolysis of some simple, short chained triglycerides to see if any lipase catalysis is possible. Although, their products, short chained fatty acid amides are not necessarily high value commodity products, this will establish at least an initial, baseline knowledge of the potential for these enzymes in liquid ammonia, which can then be applied to longer chain fats and oils.

5.2.2 Solvolysis of short chained triglycerides in liquid ammonia only

A simple view of triester solvolysis in liquid ammonia would be the stepwise conversion of triester to diester and amide product which one would expect to be pseudo-first-order due to the vast excess of ammonia, as was evident with the basic mono esters (Chapter 3). One of the simplest triglycerides, triacetin for example,

would react with ammonia to form diacetin and acetamide (Scheme 5.2.3). This simple scheme assumes that the diacetin is much less reactive than triacetin and the reaction effectively stops after this first ammonolysis. As will be shown later this is an oversimplification but can be used as a rough comparison for lipase-catalysed and uncatalysed ammonolysis.

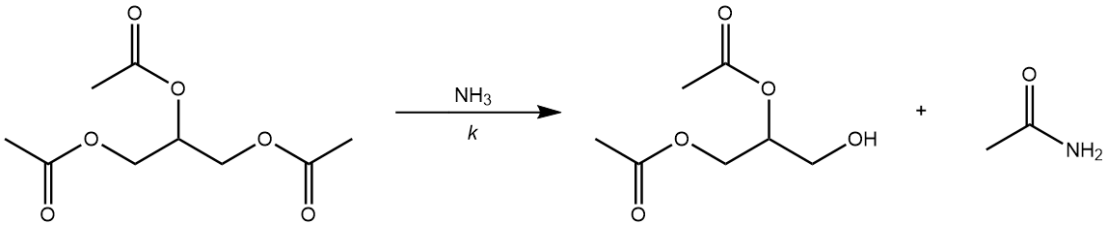

Scheme 5.2.3

The rate profile for the solvolysis of the triglyceride can be monitored easily by GC and so a baseline rate of conversion of triacetin to diacetin can be established. Again, as with simple esters, the observed rate can be generated from either the natural log method or differential equation using data fitting Berkeley Madonna (Figure 5.2.1).

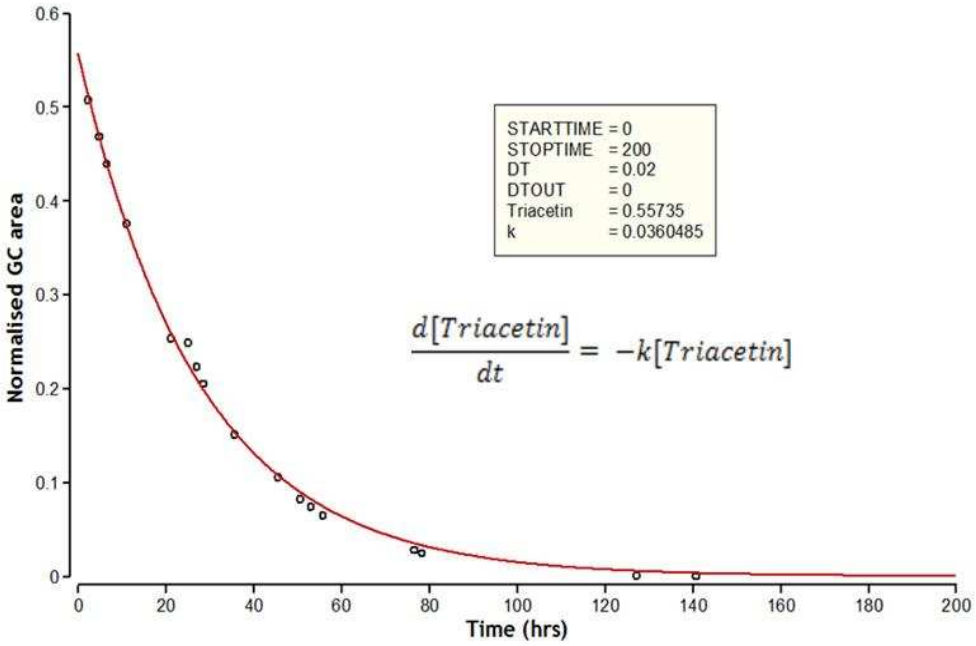

Figure 5.2.1 Berkeley Madonna pseudo-first-order fit for the baseline solvolysis of triacetin to diacetin in liquid ammonia at 25 °C.

This generates pseudo-first order rate constant, k_{obs}, of 0.0360 hr^{-1} ($1.00x10^{-5}$ s^{-1}) with half-life of 19¼ hr. The pseudo-first-order rate constant obtained using the natural log method (ln GC area vs. time) is 0.0358 hr^{-1} ($0.99x10^{-5}$ s^{-1}), in good agreement with the Madonna differential method.

However, to get an overall view of if and how lipases may be catalytically active towards these triglycerides in liquid ammonia, one has to appreciate the complexity of the triester ammonolysis process. As its name suggests, the triester or triglyceride is composed of three ester functional groups attached to its glycerol 'backbone' and so the basic view of triester to diester outlined above is only the first step in what is a rather complex process. The diester produced from the triester ammonolysis can itself undergo solvolysis by ammonia solvent, producing a monoester as well as an additional amide product (acetamide in this case). This process is repeated further with the newly formed monoester undergoing ammonolysis, finally liberating the glycerol and a third amide molecule. Each of tri, di, and mono ester thus react independently with the ammonia solvent under pseudo-first-order conditions as outlined above and generate their own individual rate constants for each ammonolysis step (Scheme 5.2.4).

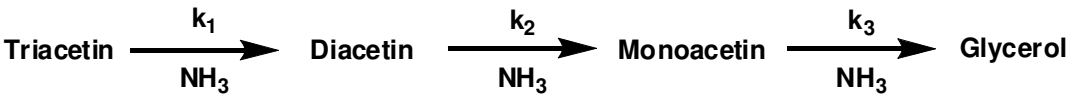

Scheme 5.2.4 An overview of triacetin ammonolysis process

The modelling of this process, to find these individual rate constants, is not as simple as just saying that there are three separate esters each with a basic pseudo-first-order profile as seen above with the triacetin (Figure 5.2.1). The process is more complex as it proceeds via both the consecutive and simultaneous ammonolysis of each ester, such that as soon as diacetin is produced, it is further reacting to form the monoacetin, and subsequently as soon as the monoacetin is produced, it reacts to form the glycerol, all the while the triacetin substrate is still undergoing ammonolysis.

5.2.2.1 GC-MS analysis of triacetin ammonolysis and data modelling

In order to fully understand the reaction profile, with the individual rate constants, it was necessary to fully process the raw GC-MS or GC-FID data, to identify the

individual peaks in the chromatogram as each of the reactants, products and internal standard (Figure 5.2.2).

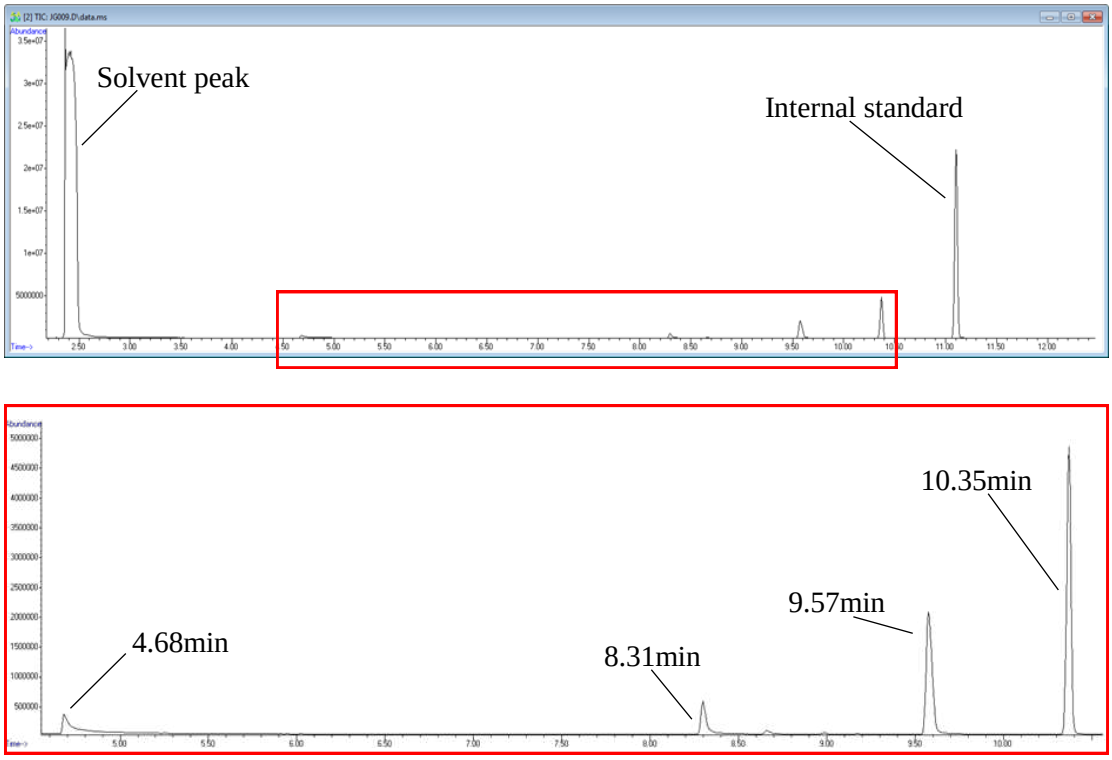

Figure 5.2.2 Total ion-chromatogram (TIC) of 28½ hr sample for reaction of triacetin in liquid ammonia at 25 °C.

For a typical sample taken from the triacetin reaction in liquid ammonia, each peak has its own mass spectrum and by using its ion fragmentation pattern, MS software Mass Hunter combined with NIST library is able to accurately identify each peak (Figures 5.2.3 to 5.2.6).

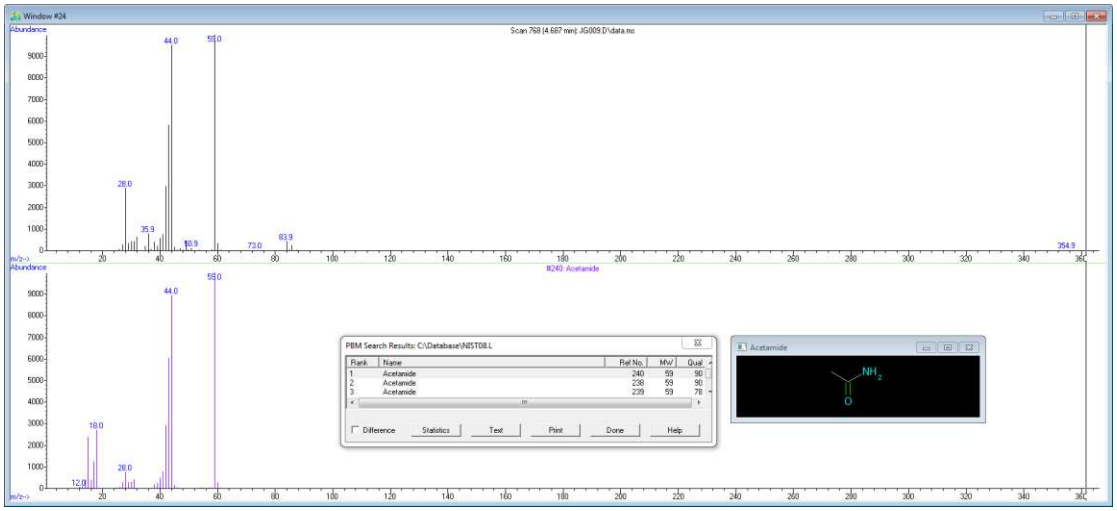

Figure 5.2.3 Mass spectrum of peak at 4.68 min matched with acetamide.

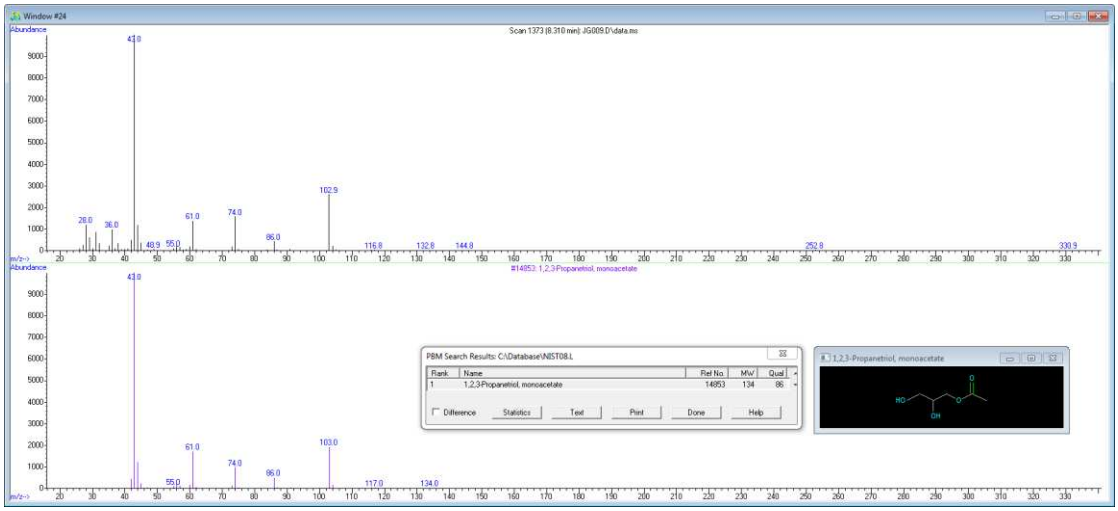

Figure 5.2.4 Mass spectrum of peak at 8.31 min matched with monoacetin.

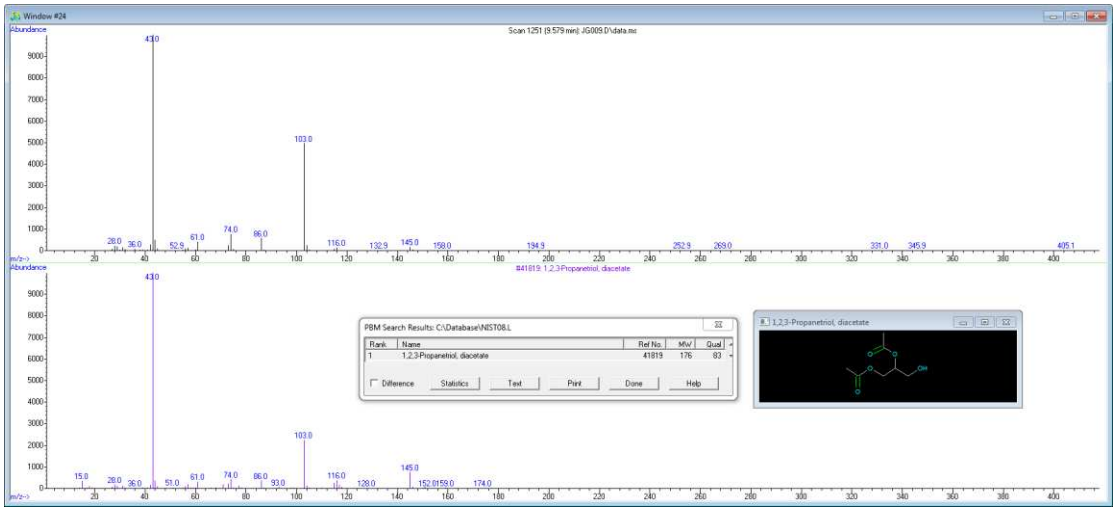

Figure 5.2.5 Mass spectrum of peak 9.57 min matched with diacetin.

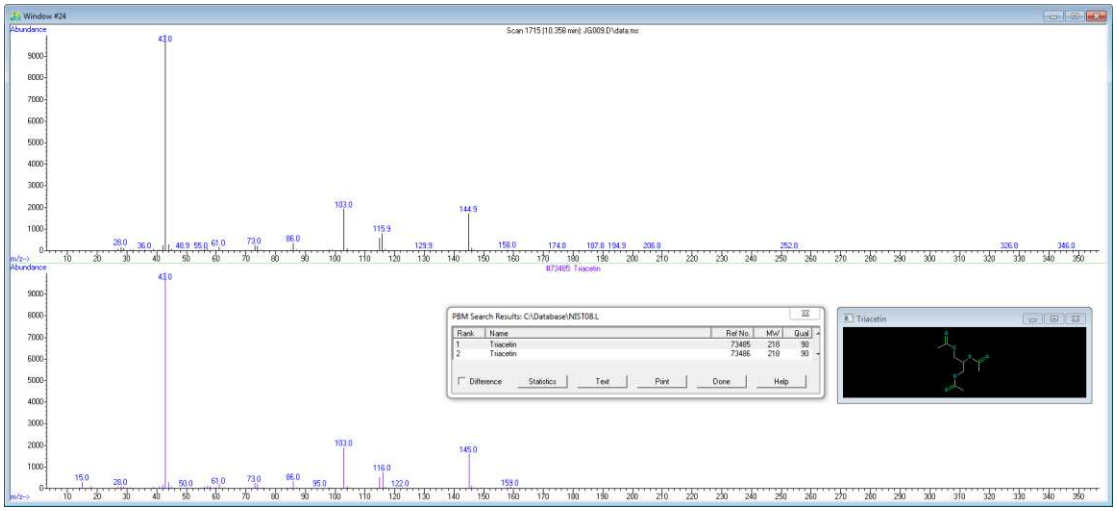

Figure 5.2.6 Mass spectrum of peak at 10.35 min matched with triacetin.

Retention times are consistent with GC theory that, as a rough guide, for molecules of comparable structure (triacetin, diacetin, monoacetin), the compounds of lower molecular weight tend to be more volatile and so elute from the column first (Table 5.2.1).[224]

Table 5.2.1 GC-MS peak retention times for reactants, products, internal standard and solvent.

Compound	**GC-MS RT† (min)**	**M.W (g/mol)**
DCM (solvent peak)	2.36	84.93
Acetamide	4.68	59.07
Monoacetin	8.31	134.13
Diacetin	9.57	176.17
Triacetin	10.35	218.20
Diethylene glycol dibutyl ether (IS)	11.07	218.33

†RT = retention time

As the chromatogram and peak analysis suggest, there is an absence of glycerol in the samples analysed. In comparison to the main analytes of interest (esters, internal standard), glycerol is quite a polar molecule. Samples were prepared for GC-MS using dichloromethane, in which glycerol is insoluble. Furthermore, for GC analysis,

a moderately nonpolar HP-5 column is used in order to achieve optimised peak shape and resolution for the tri, di, mono esters and internal standard. In order to follow glycerol carefully, the samples could be re-run using a polar column and water as solvent, but then there would be internal standard solubility concerns. Thus, accurate glycerol formation was not resolved.

The kinetics of the overall ammonolysis of triacetin in liquid ammonia was followed by measuring the changes in these peaks with time. The integrated peak areas of the identified compounds were normalised against the internal standard and tabulated, and a plot of normalised peak area against time shows the complexity of the full reaction profile for triacetin ammonolysis (Figure 5.2.7).

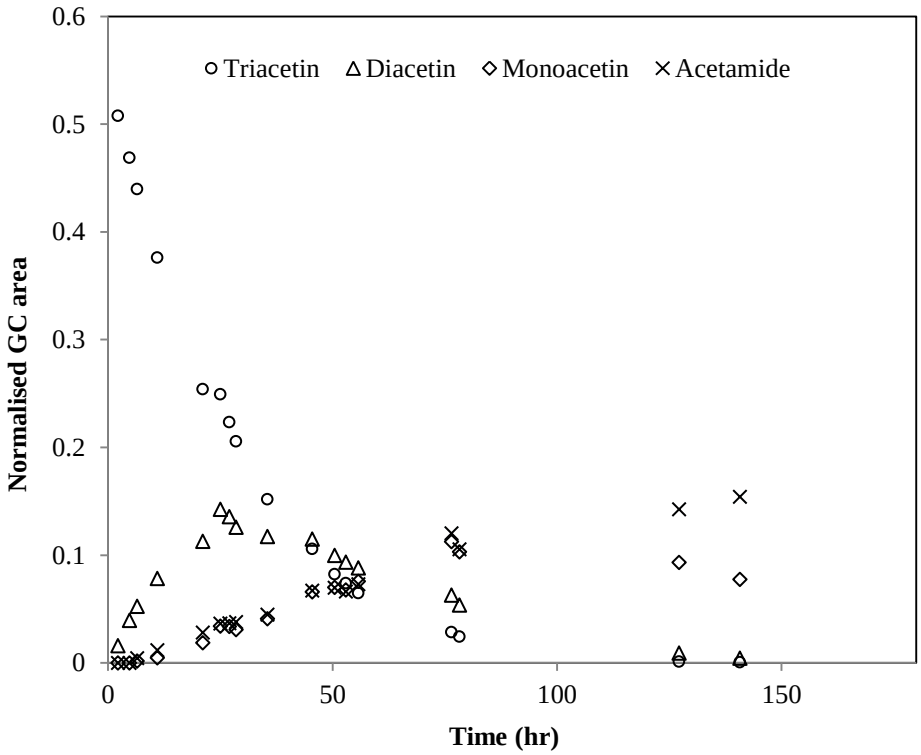

Figure 5.2.7 Normalised GC area as a function of time for triacetin ammonolysis in liquid ammonia at 25 °C.

The fact that diacetin formation is observed and reaches a maximum concentration before eventually decreasing shows that rate constants k_1 and k_2 are of similar magnitude. If $k_1 > k_2$ then almost one molar equivalent of diacetin would be formed and the maximum would be reached when all the triacetin had disappeared. Conversely, if $k_2 > k_1$ then little diacetin would be observed. Differential solver

Berkeley Madonna, however, does possess the ability to data fit multiple and more complex differential equations simultaneously, and therefore modelling via this method was an option. The full complexity of the triester ammonolysis is outlined in Scheme 5.2.5.

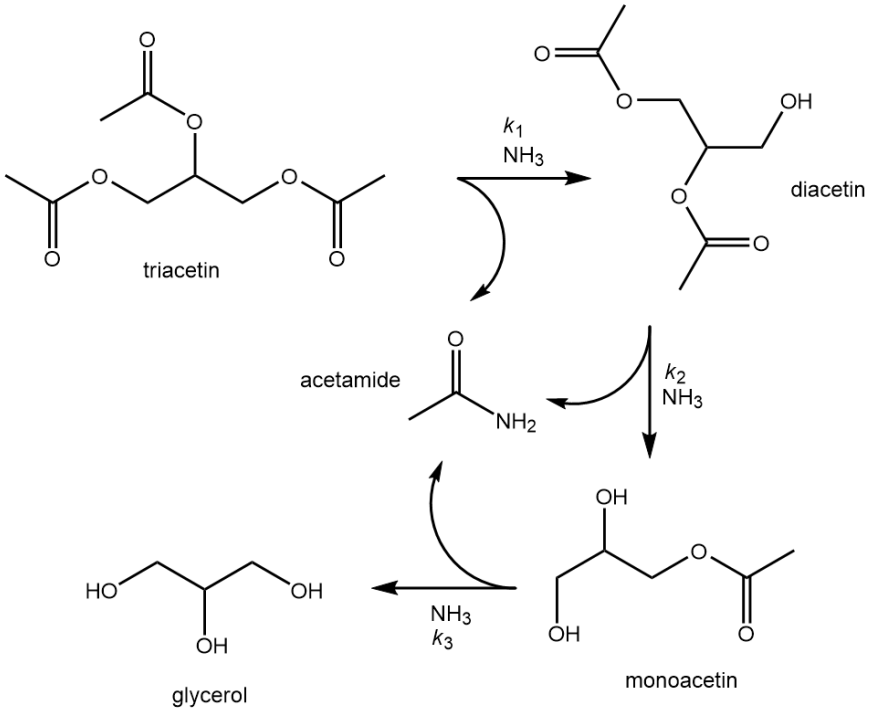

Scheme 5.2.5

From the reaction profile in Scheme 5.2.5, differential equations can be formed for each of the steps observed rate constants, k_1, k_2 and k_3:

$$\frac{d(Tri)}{dt} = -k_1\,[Tri]$$

$$\frac{d(Di)}{dt} = k_1\,[Tri] - k_2\,[Di]$$

$$\frac{d(Mono)}{dt} = k_2\,[Di] - k_3\,[Mono]$$

$$\frac{d(Amide)}{dt} = k_1\,[Tri] + k_2\,[Di] + k_3\,[Mono]$$

The differential equations generated above can be fitted along with the data into Berkley Madonna with the following model:

METHOD RK4

```
STARTTIME = 0
STOPTIME= 200                          {hours}
DT = 0.5

T' = -k1*T                             {differential eqn. for Triester}
D' = (k1*T - k2*D)*M1                  {differential eqn. for Diester}
M' = (k2*D - k3*M)*M2                  {differential eqn. for Monoester}
A' = (k1*T + k2*D + k3*M)*M3           {differential eqn. for Amide}

k1 = 0.1                               {initial guess for k1}
k2 = 0.1                               {initial guess for k2}
k3 = 0.1                               {initial guess for k3}

init T = 0.55                          {guess initial Triester normalised peak area at time = 0}
init D = 0                             {initial Diester normalised peak area}
init M = 0                             {initial Monoester normalised peak area}
init A = 0                             {initial Amide normalised peak area}

M1 = 0.5                               {initial guess for Diester GC response modifier}
M2 = 0.5                               {initial guess for Monoester GC response modifier}
M3 = 0.5                               {initial guess for Amide GC response modifier}
```

The modifiers (M values) were put into the model to take into account the differing response factors of the different compounds by GC-MS which is evident in the raw data of the normalised peak areas. Stoichiometrically, 3 moles of acetamide are produced per mole of triacetin and therefore a true plot of the concentration against time for this would (at the end) show 3 times as much acetamide as initial triacetin concentration. Each individual peak is normalised against an internal standard and thus the modifier is there to ‘clarify’ to Madonna that the response factor of each reactant/product is quantitatively different.

Normalised GC-MS peak areas were simultaneously fitted in the model (Figure 5.2.8) and the individual rate constants obtained for the ammonolysis of triacetin in liquid ammonia (Table 5.2.2).

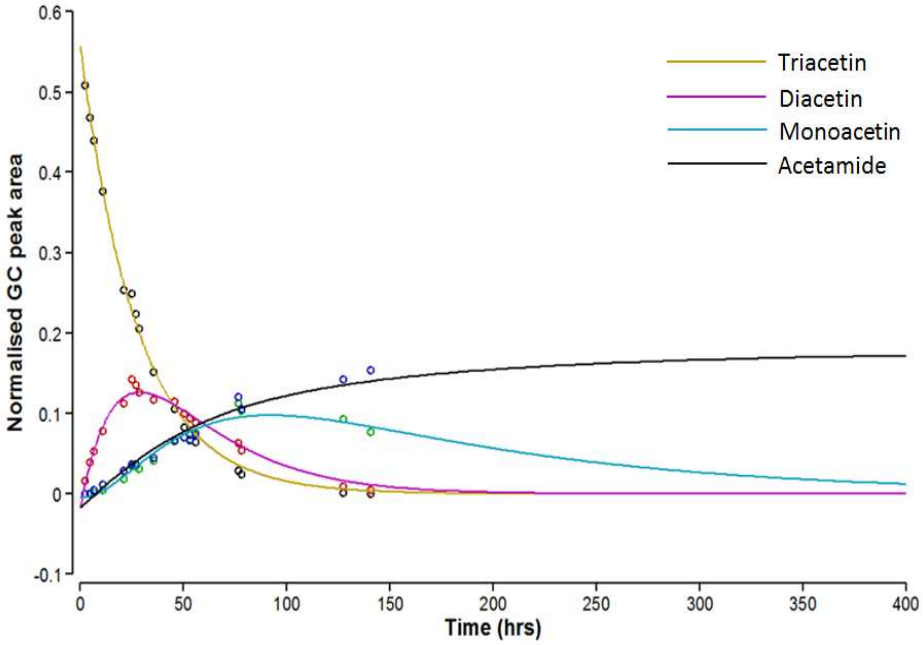

Figure 5.2.8 Berkeley Madonna fit of normalised GC area as a function of time for ammonolysis of triacetin in liquid ammonia at 25 °C. Initial triacetin concentration is 6.6 mM.

Table 5.2.2 Optimised rate constants provided by Berkeley Madonna for the ammonolysis of triacetin in liquid ammonia at 25 °C.

pseudo-first-order rate constant	**s^{-1}**
k_1	1.00×10^{-5}
k_2	1.56×10^{-5}
k_3	6.75×10^{-6}

5.2.3 Initial experiments with 'free' lipase

Liquid ammonia is a mid-polarity solvent that exhibits properties of both nonpolar/organic and polar/aqueous illustrated in its ability solubilize organic and inorganic species to varying degrees. Lipases, like most enzymes, are highly soluble in water, their natural habitat, and with liquid ammonia's medium polarity, lipase solubility and function in liquid ammonia was genuinely speculation. If solubilised,

then the protein folding may be analogous to that in water, and so the enzyme may be catalytically active.

Lyophilized preparations of lipase B from Candida antarctica (CALB) and lipase from Candida Rugosa (CR) were selected for the initial triglyceride ammonolysis studies. The molecular weights of CALB and CR are approximately 33.5 kDa and 60 kDa, respectively.[225, 226] At concentration as low as 5 μM in liquid ammonia both lipases appeared to be insoluble by visual inspection but were still tested for their catalytic activity. Triacetin reactions were performed under similar conditions to those described previously with added lipases and reactions monitored to obtain the rate constants k_1, k_2 and k_3. Both lipase reactions showed virtually no rate enhancement with all three steps observed rates roughly comparable to the background rates:

CALB (7.46 μM)†: $k_1 = 1.06 \times 10^{-5}\ s^{-1}$, $k_2 = 1.47 \times 10^{-5}\ s^{-1}$ and $k_3 = 6.69 \times 10^{-6}\ s^{-1}$.

CR (8.3 μM)†: $k_1 = 0.92 \times 10^{-5}\ s^{-1}$, $k_2 = 1.67 \times 10^{-5}\ s^{-1}$ and $k_3 = 6.35 \times 10^{-6}\ s^{-1}$.

†Lipase concentrations are denoted as if fully soluble in liquid ammonia.

These preliminary results were inconclusive as the lack of rate enhancement could be for a variety of reasons:

- Firstly, the enzyme may have very low solubility in liquid ammonia, even though they appeared insoluble to the eye, but be unreactive and so it could be argued that the lack of catalytic activity means that these particular lipases cannot function in a purely anhydrous, ammonical environment. The protein may even be folded correctly but the catalytic mechanisms just not compatible with the solvent.
- Secondly, if the enzyme was unequivocally insoluble in liquid ammonia then the lack of catalytic activity is due to the type of enzyme preparation (as a free lyophilized powder) rather than its incapacity to function in liquid ammonia. This supports the initial hypothesis that an immobilised preparation of the lipase may be required in order to provide an environment that allows the 'ideal' folding of the protein to make it catalytically active and also allow for interfacial activation of the lipase. This is the case with many of the reactions catalysed by lipases in organic media where the free enzyme is insoluble and

showed zero catalytic activity but biotransformations were vastly improved with the immobilised lipase.

It was speculated that maybe a polar co-solvent could be used to solubilize the lipase into the liquid ammonia medium but with the vast array of solvents to choose from this method was not investigated to any real extent. Moreover, some of these solvents may render the enzyme inactive or act as a nucleophile themselves (water, methanol) and so further obscure the results. Ideally, to test the notion that enzymes can function in an ammoniacal environment, pure anhydrous liquid ammonia was the preferred solvent.

Accordingly, attention turned to the immobilised form of the Candida antarctica lipase B on acrylic resin beads (Novozyme 435) and so from hereon, all liquid ammonia studies used this immobilised lipase.

5.2.4 Candida antarctica lipase B (CALB) catalysed ammonolysis of short and medium chain triglycerides in liquid ammonia at 25 °C

5.2.4.1 Triacetin

Triacetin ammonolysis was repeated with the addition of the CALB beads and an initial look at the normalised GC data was encouraging. Compared with the background reaction, with 25 mg of CALB beads there was an observable reduction in the time taken for the triester to disappear (Figure 5.2.9). This is the first suggestion that the lipase may be active in liquid ammonia.

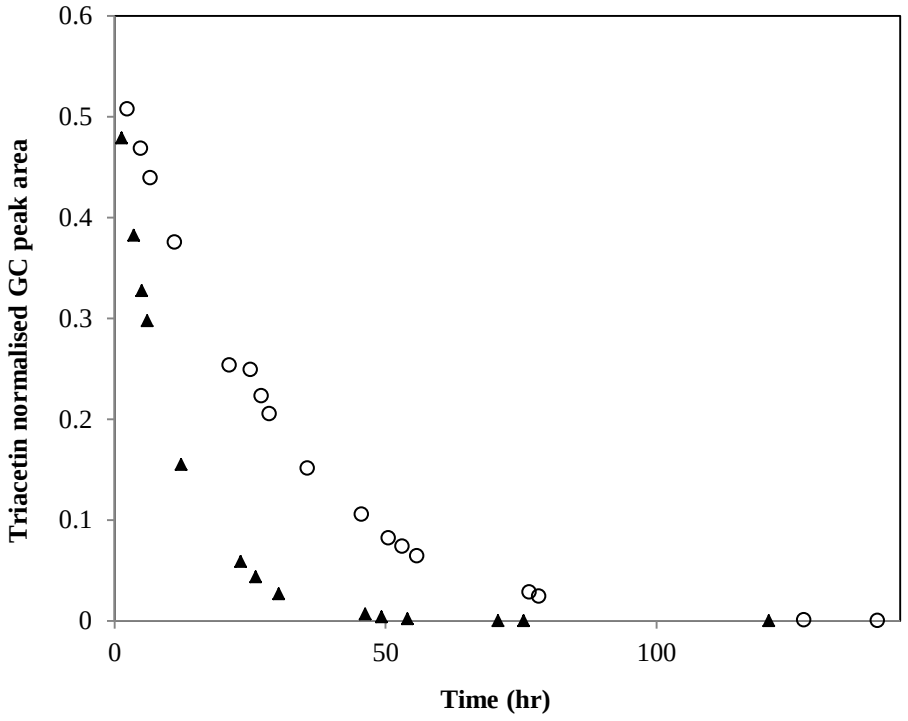

Figure 5.2.9 Normalised GC peak area of triacetin for baseline reaction (○) and reaction with 25 mg CALB beads (▲) in liquid ammonia at 25 °C.

As with the baseline reaction, the individual rate constants for each ammonolysis step were obtained by fitting the data to the Berkeley Madonna model (Figure 5.2.10). For the ammonolysis reaction with added 25 mg CALB beads the model gives optimised values of $k_1 = 2.75 \times 10^{-5}\ s^{-1}$, $k_2 = 1.53 \times 10^{-5}\ s^{-1}$ and $k_3 = 6.75 \times 10^{-6}\ s^{-1}$.

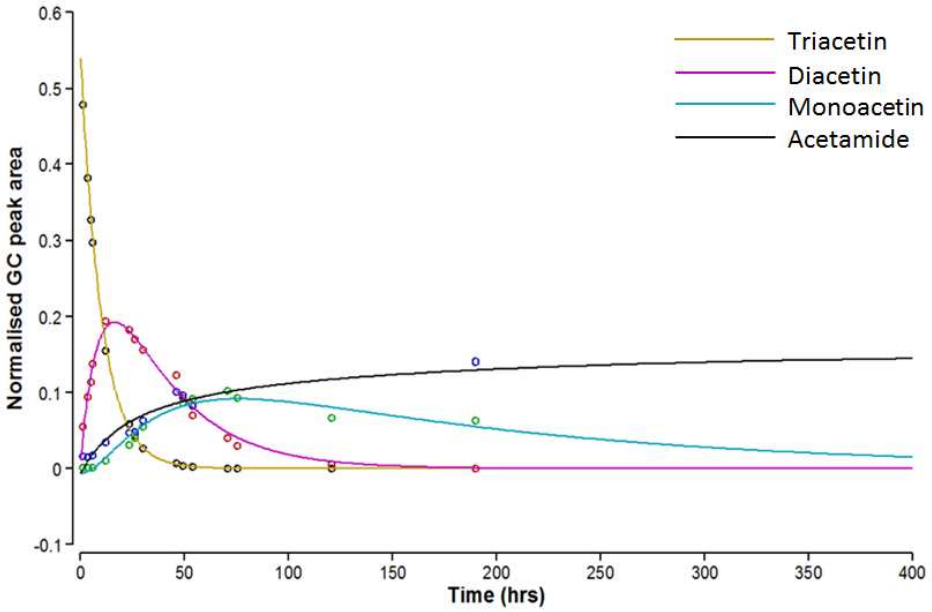

Figure 5.2.10 Berkeley Madonna fit of normalised GC area vs. time for ammonolysis of triacetin in liquid ammonia at 25 °C with the addition of 25 mg CALB beads.

Interestingly, compared with the background rates, the value for k_1 increases nearly 3-fold with the added 25 mg CALB and yet no increase is observed for the other rate constants, k_2 and k_3, for the ammonolysis of diacetin and monoacetin, respectively. This trend is observed with increasing masses of CALB beads (Table 5.2.3).

Table 5.2.3 Berkeley Madonna pseudo-first-order rate constants as a function CALB beads concentration for the ammonolysis of triacetin in liquid ammonia at 25 °C

CALB beads (mg)	k_1 (s^{-1})	k_2 (s^{-1})	k_3 (s^{-1})
0	1.00×10^{-5}	1.56×10^{-5}	6.75×10^{-6}
25	2.75×10^{-5}	1.53×10^{-5}	6.75×10^{-6}
50	4.67×10^{-5}	1.58×10^{-5}	6.56×10^{-6}

CALB immobilised on acrylic resin beads in liquid ammonia do, therefore, show apparent catalytic activity with triacetin as the substrate, increasing the ammonolysis rate for conversion of triacetin to diacetin, with a ~ 5-fold increase with the addition of 50 mg CALB beads. The observation that the k_1 step is affected by CALB but not those of k_2 or k_3 is indicative of selectivity, compatible with enzyme catalysis.

There is an apparent linear dependence of k_1 on CALB (Figure 5.2.11) suggesting a first-order dependence on CALB.

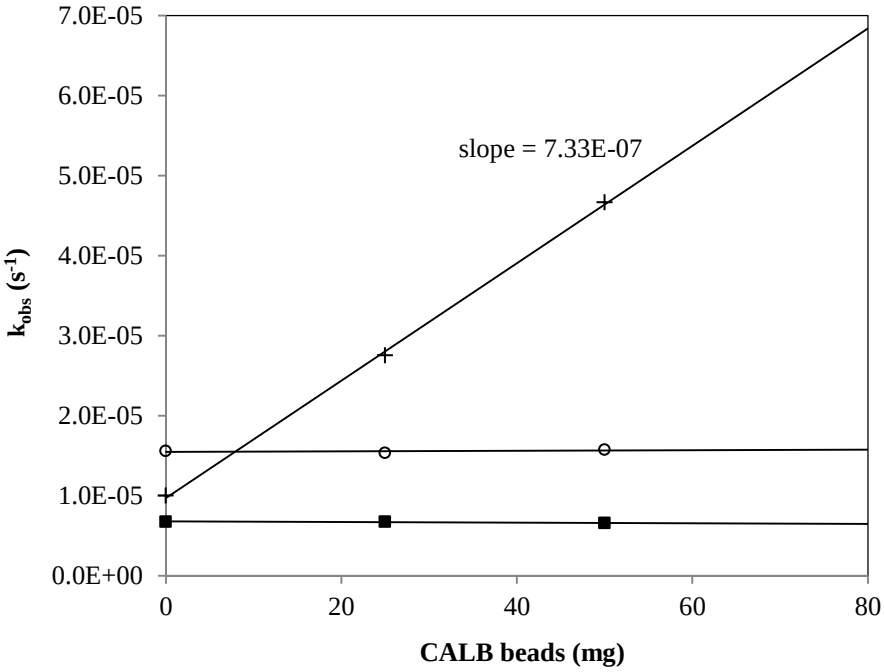

Figure 5.2.11 Observed rates k_1 (+), k_2 (○) and k_3 (■) vs. CALB beads added for reaction of triacetin in liquid ammonia at 25 °C.

The apparent second order rate constant for the first ammonolysis step, k_1, can be expressed as 7.33×10^{-7} $s^{-1}mg^{-1}$.

For these reactions, the total volume of liquid ammonia used was 20 ml and initial triacetin concentration was 0.0066 M (6.6 mM). Figure 5.2.12 shows a plot of k_{obs} as a function of the mass of CALB beads per unit volume.

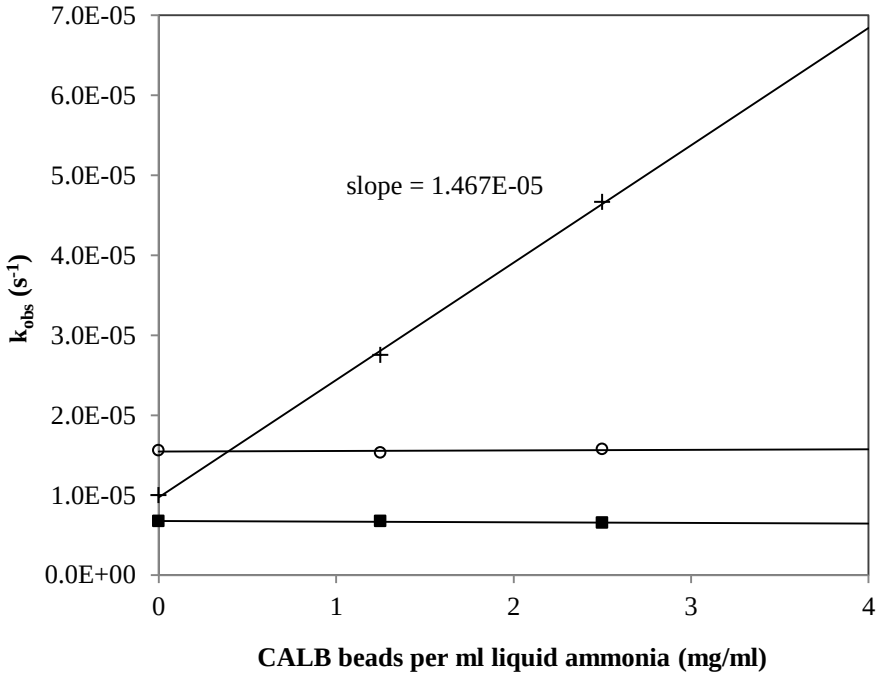

Figure 5.2.12 Observed rates k_1 (+), k_2 (○) and k_3 (■) as a function of CALB beads/ml for the reaction of triacetin in liquid ammonia at 25 °C.

This gives an apparent second-order rate constant for k_1 expressed as a function of CALB beads per ml of liquid ammonia as 1.47×10^{-5} $s^{-1}mg^{-1}ml^{-1}$.

Initially, there were some doubts that the apparent catalytic activity of the CALB beads in liquid ammonia may be due to some kind of heterogeneous bead catalysis effect, whereby possibly a functional group of the acrylic bead surface may be catalysing the triacetin to diacetin ammonolysis process, but not the other ammonolysis steps. To rule out this possibility, blank beads, prior to any enzyme immobilisation, were obtained from supplier (Lanxess, Germany). The triacetin reaction was performed under the same conditions with the addition of 50mg 'blank' beads and the modelled data yielded observed rates consistent with the baseline liquid ammonia reaction; $k_1 = 9.69 \times 10^{-6}$ s^{-1}, $k_2 = 1.63 \times 10^{-5}$ s^{-1} and $k_3 = 7.02 \times 10^{-6}$ s^{-1}. This data confirms that the increase observed in the triacetin to diacetin rate, k_1, is a result of some kind of enzymatic process, due to the lipase.

The enzyme appears to be catalysing only the reaction of the triester and not the ammonolysis of the diester or monoester which would suggest that the CALB lipase

is selective towards the triester. The selectivity of enzymes towards only specific structures and functional groups is, not surprisingly, very common.

5.2.4.2 Tributyrin

To investigate the effect of increasing the alkyl chain length in the carboxyl residue, a short-medium chain triglyceride, tributyrin (Scheme 5.2.6) was reacted in ammonia with the addition of CALB lipase. Firstly, the baseline liquid ammonia rates were established and compared with those obtained with the addition of CALB beads (Table 5.2.4).

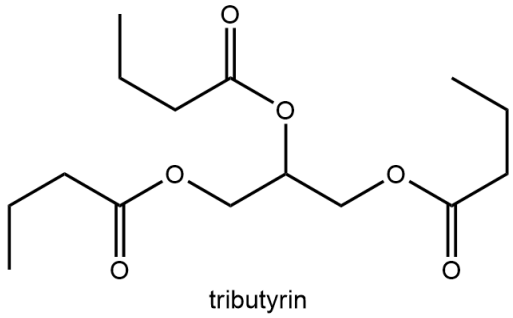

Scheme 5.2.6

Table 5.2.4 Berkeley Madonna observed rate constants as a function of CALB beads added for ammonolysis of tributyrin in liquid ammonia at 25 °C.

CALB beads (mg)	k_1 (s^{-1})	k_2 (s^{-1})	k_3 (s^{-1})
0	3.66×10^{-6}	3.72×10^{-6}	1.05×10^{-6}
35	2.32×10^{-5}	6.64×10^{-6}	4.17×10^{-6}

The rates of background ammonolysis are lower than those for the triacetin background reaction. Interestingly, and in contrast to the triacetin catalysed ammonolysis, the rates for all three ammonolysis steps for tributyrin appear to be enhanced by the lipase (Figure 5.2.13).

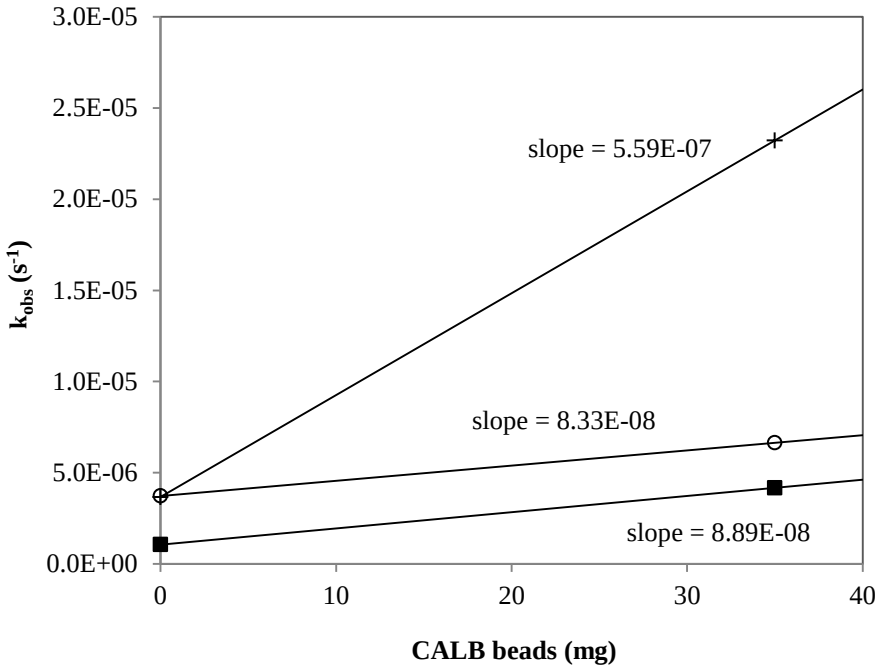

Figure 5.2.13 Observed rates k_1 (+), k_2 (○) and k_3 (■) as a function of CALB beads added for reaction of tributyrin in liquid ammonia at 25 °C.

The apparent second order rate constants can be expressed as:

$k_1 = 5.59 \times 10^{-7}\ s^{-1}mg^{-1}$

$k_2 = 8.33 \times 10^{-8}\ s^{-1}mg^{-1}$

$k_3 = 8.89 \times 10^{-8}\ s^{-1}mg^{-1}$

The second order rate constant for the first ammonolysis step, k_1, is slightly lower but of comparable magnitude to that obtained for the triacetin lipase reactions (7.33×10^{-7} $s^{-1}mg^{-1}$). Furthermore, k_2 and k_3 are not massive but do suggest that CALB beads can catalyse the ammonolysis of dibutyrin to monobutyrin and monobutyrin through to glycerol. This is in contrast to the triacetin ammonolysis reactions where there was no rate enhancement of k_2 and k_3 with any added mass of CALB.

Figure 5.2.14 shows a plot of k_{obs} as a function of the mass of CALB beads per unit volume.

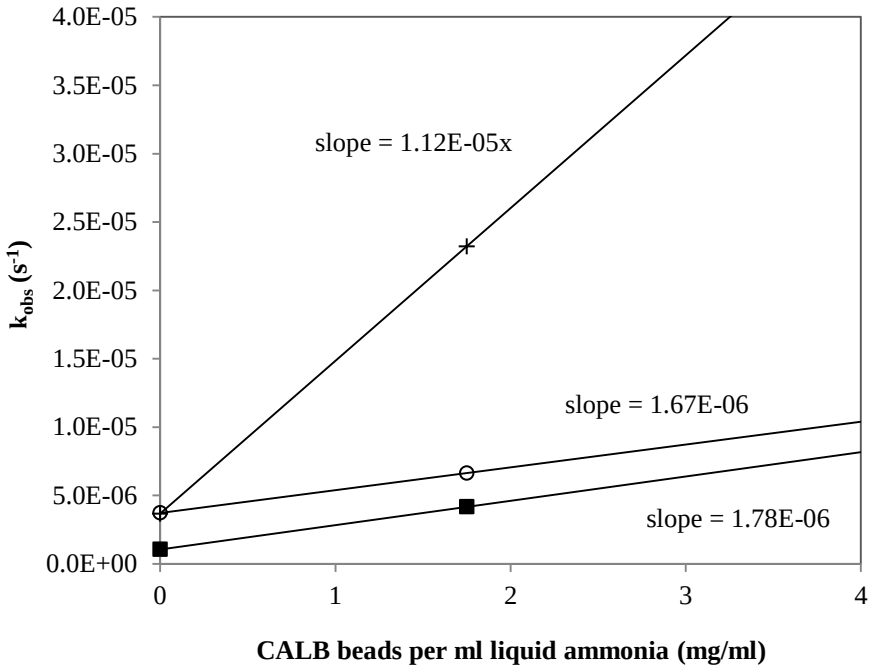

Figure 5.2.14 Observed rates k_1 (+), k_2 (○) and k_3 (■) as a function of CALB beads/ml added for the reaction of tributyrin in liquid ammonia at 25 °C.

$k_1 = 1.12x10^{-5}\ s^{-1}mg^{-1}ml^{-1}$

$k_2 = 1.67x10^{-6}\ s^{-1}mg^{-1}ml^{-1}$

$k_3 = 1.78x10^{-6}\ s^{-1}mg^{-1}ml^{-1}$

A summary for the second order rate constants for triacetin and tributyrin CALB ammonolysis in liquid ammonia can be found in Table 5.2.5.

Table 5.2.5 Second order rate constants expressed as k_{obs} per mass of CALB triglycerides in liquid ammonia at 25 °C.

Triglyceride	**Second order rate constants ($s^{-1}mg^{-1}$)**		
	k_1	**k_2**	**k_3**
Triacetin	$7.33x10^{-7}$	nd	nd
Tributyrin	$5.59x10^{-7}$	$8.33x10^{-8}$	$8.89x10^{-8}$

nd = not detected

Likewise, comparisons can be made between the second order rate constants expressed as functions of mass of beads per volume of liquid ammonia (Table 5.2.6).

Table 5.2.6 Second order rate constants expressed as k_{obs} per mass of CALB per volume of liquid ammonia triglycerides in liquid ammonia at 25 °C.

Triglyceride	Second order rate constants ($s^{-1}mg^{-1}ml^{-1}$)		
	k_1	k_2	k_3
Triacetin	$1.47x10^{-5}$	nd	nd
Tributyrin	$1.12x10^{-5}$	$1.67x10^{-6}$	$1.78x10^{-6}$

nd = not detected

The results would suggest that for these reactions in liquid ammonia, CALB lipase may have some selectivity towards larger molecules.

5.2.5 *Candida antarctica* lipase B (CALB) catalysed ammonolysis of longer chain triglycerides in liquid ammonia at 25 °C

In contrast to amides produced from short and medium chained triglycerides, longer chained fatty acid amides have many applications. Industrially, the market for fatty acid amides is mainly dominated by the unsaturated amides such oleamide (cis-9-octadecenamide) and erucamide (cis-13-docosenamide) which are used as lubricants in the plastic industry, with some also having potential medicinal uses as cannabinoid neurotransmitter analogues. Additionally, the substrates required for the production of these fatty acid amides, triglycerides, are abundant in nature and can be extracted at very low cost.[227] Triolein (a symmetrical triglyceride derived from the unsaturated fatty acid oleic acid containing a C_{17} alkyl chain and a cis double bond at C_9) is a major component of many plant and vegetable oils including sunflower seeds and olive oil.[228] The lipase catalysed ammonolysis of triolein to the useful commodity, oleamide, could be of wide interest. Naturally sourced triglycerides however tend to be unsymmetrical and comprise of mixtures of fatty acids and so this work will initially focus on triolein obtained from commercial scientific suppliers with high purity.[229]

5.2.5.1 Initial tests on triolein reactions in liquid ammonia and identification of oleamide

The short and medium chained triglycerides both appeared soluble in liquid ammonia and reacted with ammonia in the absence of the lipase catalyst. Triolein, with its three monounsaturated C_{17} chains, appeared to be insoluble in liquid ammonia so it was proposed that any background ammonolysis may only occur at a phase boundary. After 100 hr of stirring triolein in liquid ammonia, the insoluble substrate remained at the bottom of the vessel ($\rho_{triolein}$ = 0.95 g/ml)[230], suggesting negligible reaction with ammonia. In contrast, however, a repeat of the triolein reaction with the addition of 100mg CALB beads yielded an interesting observation. After just 24 hr at room temperature, there was a noticeable change in the ammonia solution, which now appeared to have a white, 'milky' complexion. One supposition was that this appearance was from leaching of the lipase into solution, which has been reported elsewhere.[231] With these immobilised CALB beads (Novozyme 435), the lipase is not covalently linked onto the acrylic resin carrier but only adsorbed.[232] However, for all the above work in liquid ammonia (triacetin, tributyrin) this phenomenon has not been observed with any mass of CALB beads, suggesting that the appearance of the solution is indicative of a reaction, and that the poorly soluble precipitate is likely to be oleamide.

After removal of ammonia, a white solid was obtained and was separated from the beads by dissolving in chloroform and subsequent recrystallization. Using mass spectroscopy, the compound gave $[M+H]^+$ ion at 282.2790 m/z with mass of neutral compound determined as 281.2718 m/z compared with the theoretical mass of oleamide as 281.2719 m/z. This gives a mass difference of 0.26 ppm (>99.99% match) confirming oleamide is produced.

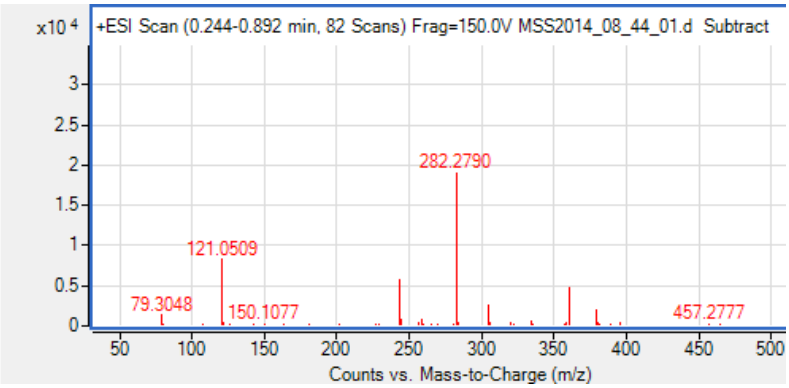

Figure 5.2.15 Mass spec of product shows oleamide was observed.

The melting point was found to be 74 °C and ^{1}H NMR (400 MHz, DMSO-d_6) showed two olefin protons at 5.32 ppm as a multiple and two NH protons at 7.2 and 6.7 ppm, consistent with the literature.[233]

5.2.5.2 Monitoring the lipase catalysed ammonolysis of triolein

Therefore, in addition to their catalytic activity towards medium and short chained triglycerides, it appears that lipases, in their immobilised form at least, can function on long chained triglycerides in liquid ammonia. For the shorter chained lipids, the reaction was easy to monitor by GC due to the relatively low boiling points of the various tri, di and mono esters, and amide products. In comparison, triolein has a much higher boiling point, outside the maximum working temperature of standard GC (Table 5.2.7).

Table 5.2.7 Boiling points of the three triglycerides used for ammonolysis in liquid ammonia

Triglyceride	Boiling point (°C)
triacetin	259[a]
tributyrin	305-309[b]
triolein	606[c]

[a] reference 234
[b] reference 235
[c] predicted value - triolein reportedly decomposes below boiling point [236]

Equally, it is expected that the products of triolein ammonolysis, diolein and monoolein, would have similarly high boiling points and thus incompatible with GC analysis.

As a result, it was concluded that the triolein reaction would not be easily monitored by GC, whereby by the individual rate constants, k_1, k_2, k_3 could be obtained. Instead, a more industrial perspective was taken, focusing on yields of product as a function of time and total reaction times with varying amounts of enzyme etc. The formation of oleamide or other fatty acid amides via these biotransformations in liquid ammonia could have industrial potential and so the efficiency of the process should be established.

A method was still required for monitoring the reaction progress by following the formation of the 2 major products of the reactions, glycerol or oleamide.

5.2.5.2.1 Monitoring glycerol product formation

Glycerol is an excellent indicator of reaction progression as it is only observed once the final ester product, monoolein, has undergone ammonolysis to liberate the third mole of oleamide (Scheme 5.2.7).

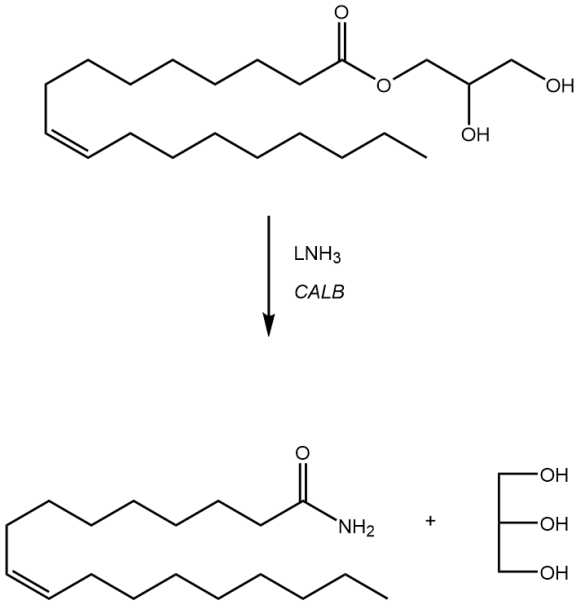

Scheme 5.2.7

A GC method was developed to quantify the formation of polar glycerol (ε_r = 40.1)[237] using a highly polar DB-WAX column. Glycerol was calibrated against an internal standard (ethylene glycol) so that the concentration in the vessel at the time of sampling could be quantified. In the absence CALB beads zero glycerol was observed after 70 hr indicating no background ammonolysis reaction. However, after just 20 hr, glycerol was present in the samples from CALB reactions (Figure 5.2.16). In this figure, the glycerol formed is calculated as % yield from the initial moles of triester used (1 mole triolein liberates 1 mole glycerol) as a function of the amount of CALB used.

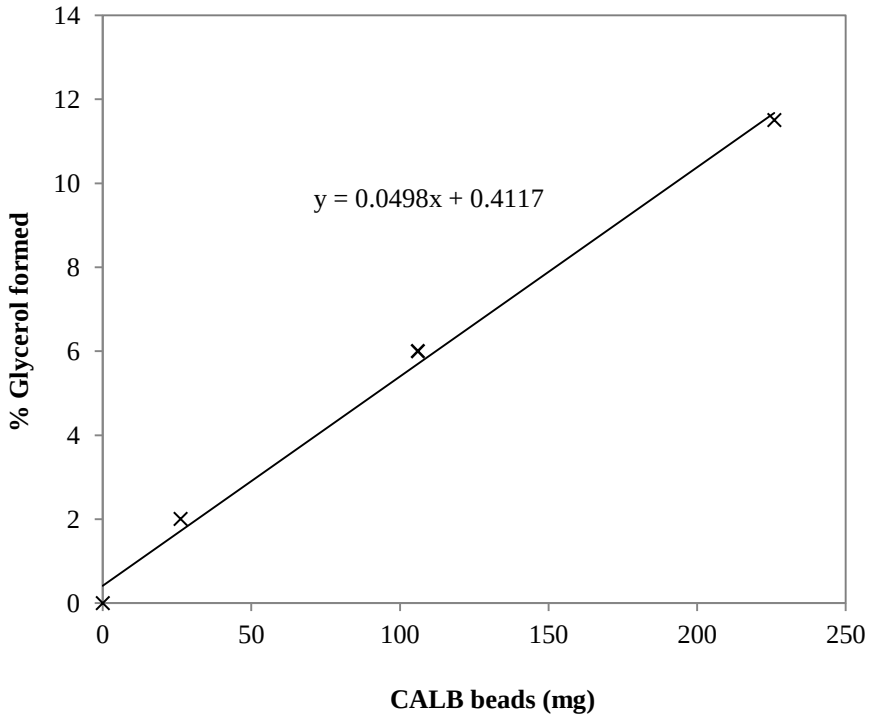

Figure 5.2.16 Glycerol formed after 20 hr calculated as a % of initial triolein concentration with varying amounts of CALB beads for ammonolysis of 45 mM triolein in liquid ammonia at 25 °C.

Although the percentage yield of glycerol is low, it is produced at a greater rate with increasing the mass of lipase confirming catalytic activity toward the long chained triglyceride. There were, however, concerns about the accuracy of following the reaction by monitoring glycerol. The beads used for lipase immobilisation are of moderately polar character and there are some reports suggesting that the polar Lewatit VP OC 1600 supporting beads may be susceptible to the adsorption of

glycerol.[238] Severac et al showed that residual glycerol concentrations decreased over a period of 24 hours in tert-butanol with varying masses of beads.[239]

Presumably, the adsorption of glycerol onto the polar beads is solvent dependent such that the use of a low polarity medium promotes the adsorption process. Small scale reactions were set up with the incubation of glycerol and CALB beads in water and in liquid ammonia but both showed no reduction in glycerol concentration over a period of 24 hr. tert-butanol, with dielectric constant of 12.4 is a much less polar solvent than water ($\varepsilon_r = 80$), and slightly less polar than liquid ammonia ($\varepsilon_r = 16$), and so seemingly promotes the adsorption of the polar glycerol onto the polar beads.[240] During the triolein ammonolysis reactions, fatty acid di/mono esters and amides are produced and may, to some extent, be solubilised into the ammonia solvent. This would have a net effect of reducing the polarity of the medium and consequently may promote adsorption of any glycerol produced.[241] The polarity of the solvent would then be a function of the reaction progress and so profiling glycerol for each reaction may be complicated. This may be evident from the glycerol formed as a function of time for the reaction of triolein with 105 mg CALB beads (Figure 5.2.17).

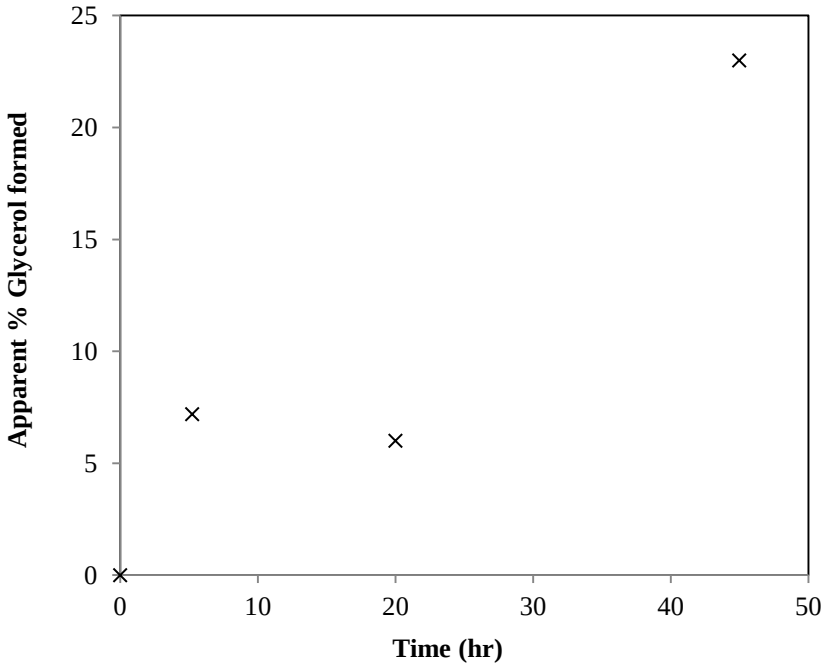

Figure 5.2.17 Apparent glycerol % as a function of time for the ammonolysis of triolein in liquid ammonia with 105 mg CALB lipase at 25 °C.

The apparent scatter at low concentration of glycerol formed may be explained by the fact that it is adsorbed onto the beads until the beads are saturated with glycerol. Above this point, as more glycerol is produced it remains in solution and an increase in concentration is observed.

It would appear that accurately following the reaction by monitoring glycerol formation may be subject error due to the complexity of the processes involved and possible glycerol adsorption.

In addition to these points that could affect the accurate monitoring of glycerol, glycerol adsorption onto the beads may affect the catalytic activity of the immobilised lipase and there are some conflicting reports on the subject. Lee et al incubated Novozyme 435 with varying amounts glycerol prior to activity assay and observed no effect on enzyme activity for the production of biodiesel from canola oil.[242] In contrast, some reports suggest enzyme activity may be affected by the formation of glycerol.[243, 244] Glycerol may form a polar, hydrophilic coating on the surface of the immobilised lipase bead, which obstructs the active site of the enzyme from the nonpolar triglyceride substrate and so have an adverse effect on lipase activity.[245]

5.2.5.2.2 Monitoring and quantifying oleamide product formation

Oleamide had already been characterised as the main product of the reaction by NMR, mass spectroscopy and melting point analysis but a method was required for quantifying it. Although the initial attempts at GC and GC-MS analysis of triolein were unsuccessful, high temperature GC methods have been reported for analysis of compounds similar in structure to oleamide. Zhao's analysis of the Chinese brandy Changyu XO identified long chained monounsaturated fats including oleic acid and Yasar et al actually reported the presence of (z)-octa-9-decenamide (oleamide) in their GC analysis of flowers, stems and root extracts of the sunflower Tripleurospermum callosum. [246, 247] Both methods used a high temperature oven profile with a non-polar HP-5 column. A method was developed to analyse oleamide by GC that could be used to quantify the triolein reaction (see Experimental section for GC parameters). For any reaction, GC-MS could be used to confirm that the product was oleamide by matching the spectra to the NIST library search.

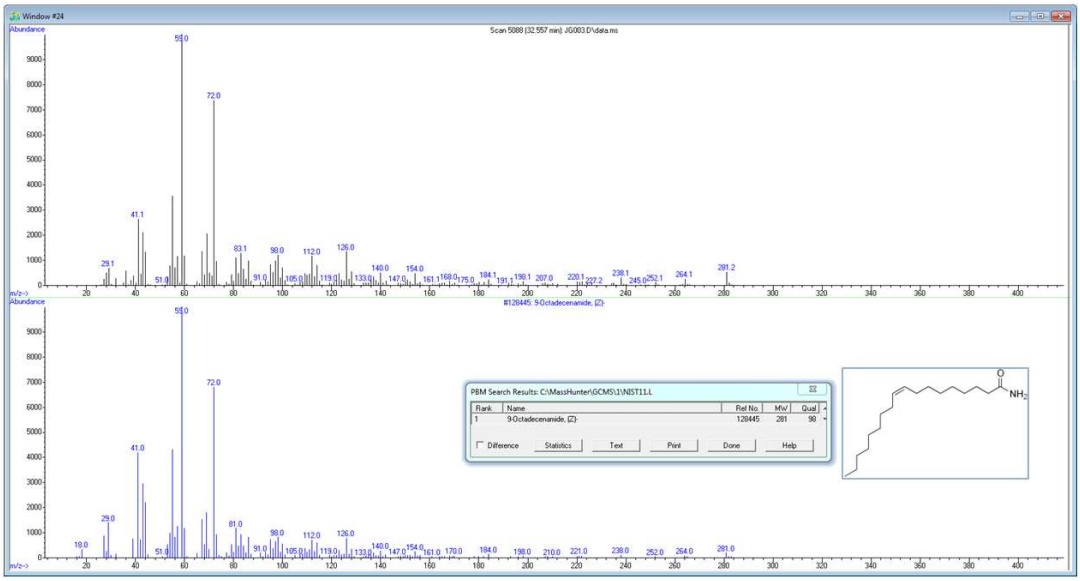

Figure 5.2.18 GC-MS confirmation of oleamide with retention time 32.5 min.

Using GC-FID, oleamide was calibrated along with the internal standard for the reaction, biphenyl. A typical GC-FID chromatogram can be seen in figure 5.2.19.

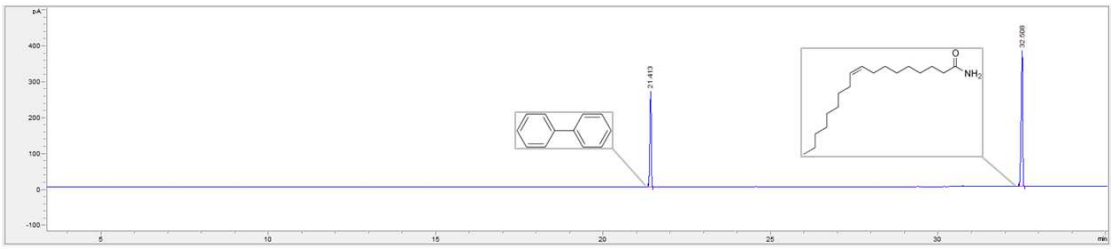

Figure 5.2.19 GC-FID chromatogram of oleamide (RT = 32.5 min) and biphenyl (RT = 21.4 min).

5.2.5.3 CALB catalysed ammonolysis of triolein in liquid ammonia

Initially, reactions were performed in a similar fashion to those described earlier for the general ammonolysis reactions with sampling over time. However, oleamide is not very soluble in liquid ammonia and so sampling from a liquid with precipitated amide could lead to inconsistencies. Alternatively, the method adopted was to leave the contents of the reaction for a set time, vent off the ammonia, and analyse the full contents of the vessel by solubilising in DCM or chloroform for GC analysis.

As with previous reactions, the extent of background ammonolysis was to be explored. The glycerol tests, admittedly with their potential inaccuracies, showed that no glycerol had formed after 70 hr but this does not necessarily indicate negligible

ammonolysis as glycerol is only liberated after the final ammonolysis stage. A baseline experiment with triolein (≈ 46 mM) in liquid ammonia at 25 °C indicated a 0.7 % conversion to oleamide after 68 hr. This yield percentage is calculated from the maximum potential oleamide yield which is three times the molar charge of the triester (i.e. 1 mole of triester can form 3 moles of amide). Although appearing insoluble in liquid ammonia, triolein charge is expressed as a concentration to assist with calculations of oleamide yields.

The ammonolysis of triolein in liquid ammonia was repeated with varying amounts of CALB beads and stopped after 68 hr. The yield of oleamide is dependent on the mass of CALB beads, suggesting an enzymatic process (Figure 5.2.20).

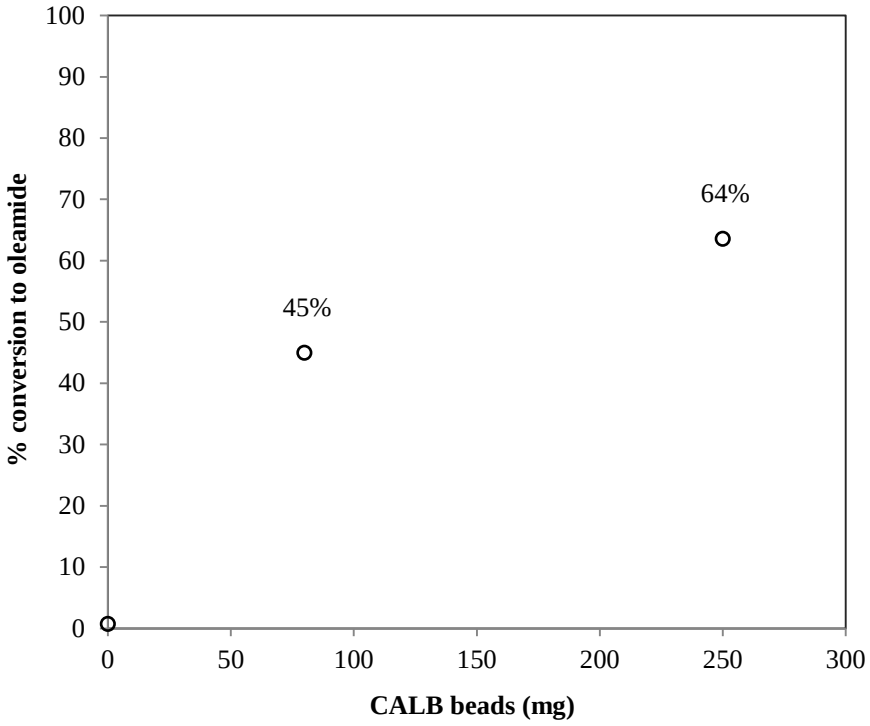

Figure 5.2.20 % conversion of triolein (≈ 46 mM) to oleamide in liquid ammonia after 68 hr with varying mass of lipase beads at 25 °C.

If only one of the ester groups reacted then the maximum yield of oleamide would be 33 % and, if two reacted, 66 % yield. To investigate if all ester groups reacted, corresponding to 100 % yield of oleamide, for the reaction with 250 mg CALB, the oleamide produced was monitored over time (Figure 5.2.21). A reasonably smooth curve is obtained suggesting a total reaction time of about 180 hr, and would correspond to around 0.4 g of oleamide produced.

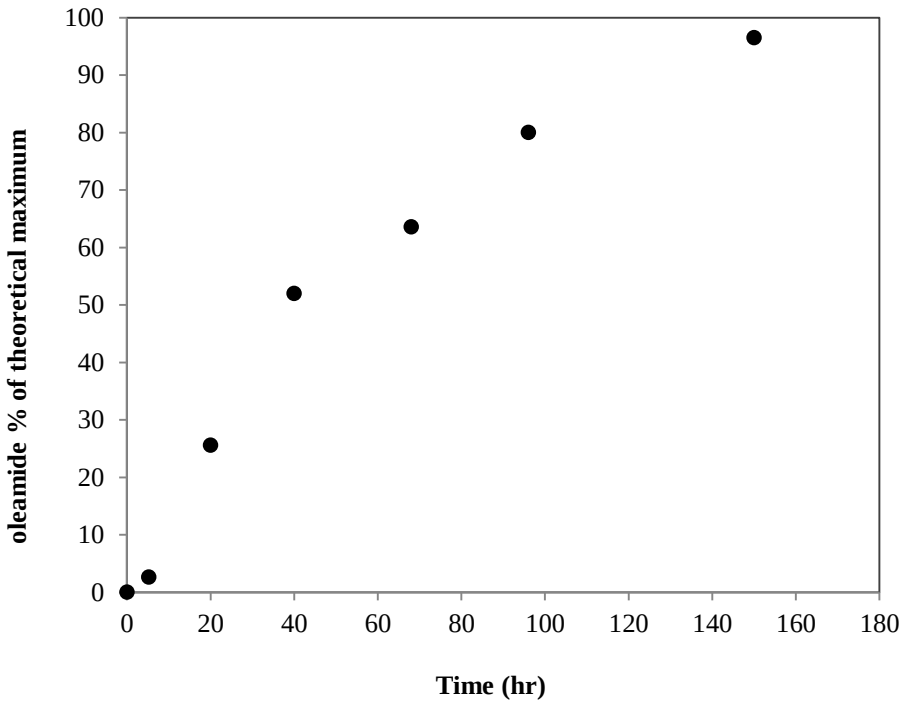

Figure 5.2.21 % conversion of triolein (≈ 46 mM) to oleamide in liquid ammonia with 250 mg CALB beads at 25 °C.

The conversion of triolein to oleamide via the liquid ammonia biotransformation is quite impressive compared with the negligible background conversion in the absence of enzyme. Once more it was speculated that the observed catalysis may be due to the beads acting as some kind of surface catalyst, which seems more plausible this time given that the triolein ammonolysis reaction is a multi-phase process; triolein, liquid ammonia, CALB beads, oleamide. A test with 250 mg 'blank' beads showed just 0.6 % conversion to oleamide after 68 hr, analogous to the background ammonolysis with no added CALB beads (~ 0.7 %).

Given that a near 100 % conversion of triolein to oleamide was observed in Figure 5.2.21, it can be assumed that CALB catalyses all three ammonolysis steps (Scheme 5.2.8).

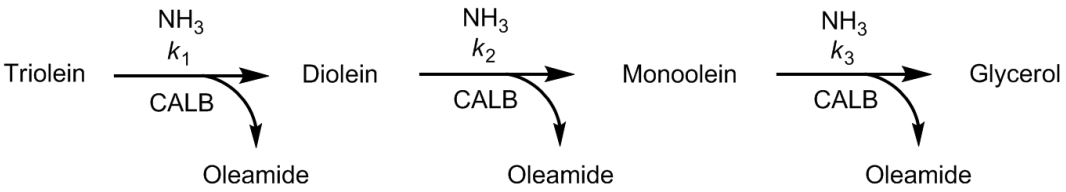

Scheme 5.2.8

Having not directly followed triolein, diolein and monoolein through the reaction, the extent at which CALB catalyses each ammonolysis step is unknown. The first ammonolysis step, k_1, is evidently enhanced by the enzyme, as the conversion of triolein to diolein without CALB is negligible. It may be that, as with triacetin and tributyrin, only the first step is catalysed to any major extent by the enzyme. The reaction may then just progress through to completion, uncatalysed, if diolein and monoolein are highly reactive in liquid ammonia. However, given the poor reactivity of triolein, which may also be a phase boundary issue, it is unlikely that diolein and monoolein are highly reactive in ammonia unaided. This would infer that for the uncatalysed reaction, k_2 and $k_3 >> k_1$, which seems improbable having observed that for tributyrin and triacetin background ammonolysis, all three rate constants are of comparable magnitude. Thus the observation that adding the CALB beads makes the reaction go through to completion suggests the lipase is catalysing all three ammonolysis steps; k_1, k_2 and k_3.

The potential industrial application of lipase catalysed ammonolysis in liquid ammonia can be explored by comparing the results with other enzymatic ammonolysis methods. Currently, the only major reported ammonolysis of triolein via a biotransformation is the work of Sheldon et al in ammonia saturated tert-butanol.

Table 5.2.8 Comparison of two methods for CALB catalysed ammonolysis of triolein; in liquid ammonia and ammonia saturated tert-butanol.

Solvent	CALB (mg/ml)	temp (°C)	conversion (time)
liquid ammonia	0	25	0.7 % (68 hr)[d]
liquid ammonia	8[a]	25	44.9 % (68 hr)[d]
liquid ammonia	25[b]	25	63.6 % (68 hr)[d]
[†]NH_3 sat tert-butanol	5[c]	60	82.0 % (72 hr)[e]

[†] Reference 191

[a] 80 mg CALB beads in 10.4 ml; [b] 250 mg CALB beads in 10.4 ml; [c] 250 mg CALB beads in 50 ml; [d] Initial triolein = 0.407 g, 0.46 mmol, 46 mM ; [e] Initial triolein = 5 g, 5.6 mmol, 113 mM.

Comparing the CALB catalysed ammonolysis of triolein in liquid ammonia with Sheldon's work is not easy. Sheldon's reactions are at 60 °C in comparison to the moderate conditions in liquid ammonia (25 °C). Indeed, the CALB lipase in this immobilised form is well known for being quite a robust enzyme. For a variety of biotransformations, many authors report optimum temperature of the Novozyme 435 lipase as roughly 50-60 °C. [248, 249] Remarkably, Overmayer et al report enzyme function at temperatures as high as 160 °C in their studies in supercritical CO_2, but maximum activity at around 80 °C. [250] Certainly it would appear that the optimum temperature is a function of the specific biotransformation and solvent medium etc. but this does indicate that there is some potential for the liquid ammonia reaction which is currently limited to 25 °C due to pressure limits on the glassware available.

Additionally, Sheldon's reaction of triolein necessitated that the *"reaction mixture was shaken…."*[191] whereas the liquid ammonia reaction is mixed in a comparably milder manner, with agitation by magnetic flea. Again, for safety reasons, vigorous shaking of liquid ammonia reactions in their current set-up with glass vessels is not practical but this does highlight the issues associated with using heterogeneous systems, as simple things like the stirring rate of the flea would likely influence the reaction. The reaction in liquid ammonia is essentially a three or four-phase system; bulk solvent ammonia, insoluble triolein and solid support enzyme beads, plus the oleamide product that appears to have limited solubility. Presumably, it would follow

that maximising the contact between all three reactants as much as possible would likely promote the catalytic effect, evident by Sheldon's need for vigorous agitation.

For the liquid ammonia biotransformations, the effect of triolein charge on the mass of oleamide produced was investigated by charging various masses of triolein into liquid ammonia with constant mass of beads. The mass of oleamide produced was determined after 40 hr (Figure 5.2.22).

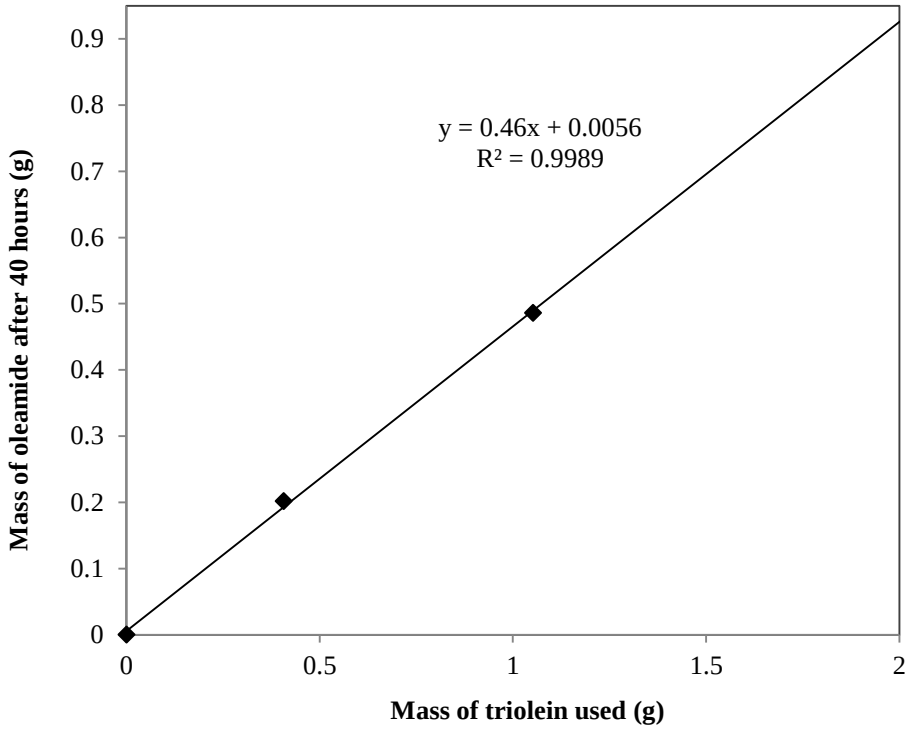

Figure 5.2.22 Mass of oleamide produced after 40 hr for the reaction of triolein in 10 ml liquid ammonia with 250 mg CALB beads (25 mg/ml liquid).

Interestingly, over this range of triolein charge, the % conversion of oleamide (calculated as a % of the theoretical maximum yield) versus time is roughly the same; with 0.407 g of triolein, the mass of oleamide produced after 40 hr is 0.201 g, corresponding to a 52 % conversion and likewise, with 1.05 g of triolein 0.48 g of oleamide is produced giving a yield conversion of 55 %.

5.2.6 Reaction rate vs. triglyceride chain length

Directly comparing the rates of lipase catalysed ammonolysis as a function of triglyceride chain length is not easy because, for the long chained triolein, the individual rate constants, k_1, k_2, and k_3, were not obtained. The progress of the

reaction can be roughly compared by using the total reaction time as a guide to the effect of lipases on various chain lengths with additional comparison to the background ammonolysis. Figure 5.2.21 illustrated that triolein in 10 ml liquid ammonia with 250 mg CALB beads has a total reaction time of around 180 hr. For the shorter chained triglycerides, where a lower mass of CALB was used, the apparent linear relationship between lipase mass per volume of LNH_3 and individual rate constant, can allow for approximate extrapolation to 250 mg CALB beads, or more specifically, 25 mg/ml. For example, triacetin with 25 mg/ml CALB beads would yield an approximate observed $k_1 = 3.77x10^{-4}\ s^{-1}$, with k_2 and k_3 as same as the background rates, as these were shown not to increase with lipase. Using these optimized values in the Berkley Madonna model allows for a theoretical profile with 250 mg (25 mg/ml) beads and total reaction time obtained and compared to the background ammonolysis (Table 5.2.9).

Table 5.2.9 Approximate total reaction time of triglycerides in liquid ammonia only and with 250 mg (25 mg/ml) CALB added.

Triglyceride	**Background, approx. reaction time**	**25 mg/ml CALB beads, approx. reaction time**
Triacetin	650 hr	250 hr
Tributyrin	1600 hr	70 hr
Triolein	10000 hr (estimate)	180 hr

With the extrapolated rates, for a theoretical reaction with 250 mg CALB beads in 10 ml liquid ammonia, the overall reaction time for triacetin is decreased by 2½-fold whereas with tributyrin it is decreased roughly 20-fold. Given that the background triolein reaction showed only 0.7 % conversion after 68 hr it is difficult to estimate a total reaction time. Even a generous estimate of 10000 hr would equate to over a 50-fold reduction in the total reaction time with 250 mg CALB. This observation

supports the earlier assumption that lipases would show greater catalytic activity with longer chained triglycerides.

5.2.7 Summary of lipase studies in liquid ammonia

In summary of the enzyme studies in liquid ammonia, the results on the whole were encouraging. Initially, free lipases showed no catalytic effect on the rates of triglyceride ammonolysis probably due to poor solubility or inactivity of the lipase. Immobilised forms of lipase B from Candida antarctica (Novozyme 435) showed moderate rate enhancement with the short and medium chain triglyceride ammonolysis. There appears to be some selectivity which is indicative of enzyme activity, whereby the ammonolysis of the short chain diacetin and monoacetin was not catalysed by the lipase but the triacetin ammonolysis was. For the slightly larger tributyrin, the triester ammonolysis was also catalysed by the lipase, with the di and mono ester showing very modest rate enhancement with the addition of the lipase beads. In comparison, the long chained triolein appears to be a very good substrate for these lipases in liquid ammonia. Although difficult to monitor the individual ammonolysis steps, the overall conversion of triolein to oleamide is increased greatly with the addition of CALB beads. This may have some industrial applications due to the high commodity value of fatty acid amides, in particular in the plastics industry and in the area of medical research. Due to limitations of the current set-up work was only carried out at ambient temperatures whereas CALB beads are well known for their robustness and high activity at elevated temperatures.

Chapter 6 - Conclusions and Future work

6.1 Conclusions

6.2 Future work

6.1 Conclusions

6.1.1 Ammonolysis of esters

Alkyl esters of benzoic and phenylacetic acid undergo ammonolysis in liquid ammonia to form the corresponding amide and alcohol products. The reaction rates of ammonolysis increase with acidity of the leaving group alcohol and a Brønsted correlation using liquid ammonia pK_a values generates a β_{lg} of ~ -0.7. This indicates little C-OR bond fission in the transition state and a rate-limiting step involving a reaction of the tetrahedral intermediate. The ammonolysis of esters is subject to significant catalysis by the ammonium ion, which, surprisingly, generates a similar Brønsted β_{lg} indicating little interaction between the ammonium ion and the leaving group. It is concluded that the rate-limiting step for the ammonium-ion-catalysed solvolysis of alkyl esters in liquid ammonia is the diffusion-controlled protonation of the zwitterionic tetrahedral intermediate T^{+-} to give T^{+}, which is rapidly deprotonated to give T^{0}. This is compatible with the rate-limiting step for the uncatalysed reaction being the formation of the neutral T^{0} by a 'proton switch'.

6.1.2 Aggregation Studies

Ionic surfactants in liquid ammonia do not show the typical conductance profile that is observed for the aggregation of surfactants in water. However, a curved conductance profile can be attributed to the association of neutral, non-conducting, ion-pair species. In water, salts behave as strong electrolytes because the polar solvent has the ability to fully separate the oppositely charged species whereas the lower polarity of liquid ammonia promotes ion-association. Ion-pairing data suggests that there may be some formation of higher aggregates such as dimers or trimers, in particular with the fluorinated carboxylates, but in general there is no distinct evidence of micellization for ionic surfactants. Ionic surfactants have charged head groups that repel one another which may hinder the formation of a micelle, evident by the fact that cmc values of non-ionics tend to be lower than ionics. The high polarity of water reduces these adjacent head group repulsions with the help of hydrogen bonding. In contrast, the reduced polarity of liquid ammonia may not possess the ability to sufficiently reduce adjacent head group repulsions, thus aggregation of ionic surfactants in liquid ammonia may not occur. Perfluorinated amides are neutral surfactants that do not

show head group repulsion and form micelles in liquid ammonia as determined by a ^{19}F NMR method. Chemical shifts changes of the terminal -CF_3 group over a range of concentrations suggested that fluorinated amides were aggregating, and cmc values were obtained for surfactants of varied chain length. The cmc values follow Klevens rule showing that as the surfactant tail length is increased, the concentration at which aggregation occurs is reduced. Moreover, the magnitude of the -CF_2-/-CF_3 chemical shift change increased from the alpha carbon towards the terminal group, consistent with formation of a micelle with a fluorine dominated core and amide head groups exposed to ammonia. The fluorinated micelles also appeared to catalyse the ester ammonolysis reaction, possibly by stabilizing the zwitterionic tetrahedral intermediate.

6.1.3 Enzyme Studies

Triglycerides undergo ammonolysis in liquid ammonia and the reaction is catalysed by CALB lipase. For short chain triglycerides, the rate enhancement with the addition of lipase is not massive and for the triacetin substrate only k_1, the rate constant for triacetin to diacetin ammonolysis, is enhanced. For tributyrin, the lipase shows moderate rate enhancement for each ammonolysis step, k_1, k_2 and k_3. Thus the enzyme may be selective towards long chain triglycerides which are, essentially, the natural substrates of lipases. Triolein was very unreactive in liquid ammonia which may be due to the reaction occurring at a phase boundary owing to the poor solubility of the long chain lipid. The ammonolysis of triolein to the useful commodity oleamide can be greatly enhanced with the addition of the CALB enzyme. Individual rate constants, k_1, k_2 and k_3, were not determined for the triolein reaction but a general comparison of reaction times for the catalysed and uncatalysed reaction of each triglyceride appears to confirm that the enzyme is particularly selective towards the long chain substrate.

6.2 Future work

Liquid ammonia has been shown to support both aggregation, a necessary prerequisite for forming a cell-type compartment, and a biological catalyst and thus the potential for this non-aqueous solvent to support life may have some merit. The fact that this project is one of the first to examine these life-type processes in liquid ammonia means that there are numerous paths that could be taken in order to further investigate the life-supporting potential of liquid ammonia, including looking at some replication

or phosphorylation processes. Further investigation into the aggregation of surfactants could include finding a viable detection method for alkyl amides. These neutral surfactants could not be investigated by conductance and the NMR method was not pursued to any major extent due to the ammonia peak swamping the peaks of interest. However, in an 'ammonia-life' system, fluorinated amides are unlikely to be naturally abundant whereas the normal alkyl amides might be readily available to form the basis of a cell container. Furthermore, alkyl amides can be synthesised in liquid ammonia in a process that can be significantly enhanced by a lipase catalyst, particularly for the longer chained triglycerides. Thus, investigation into aggregation of alkyl amides may be a primary concern because two of life's processes may be able to function together in liquid ammonia (Scheme 6.2.1).

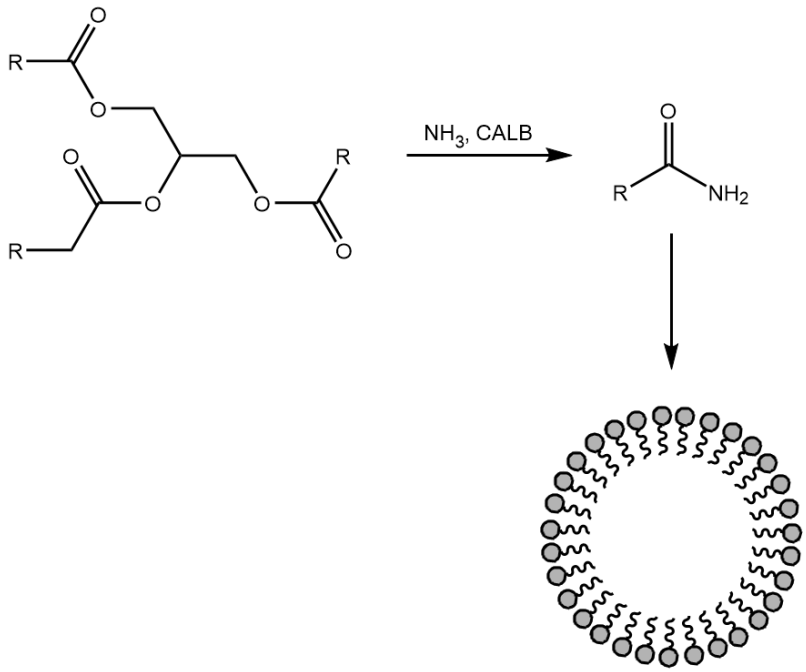

Scheme 6.2.1 Potential synthesis and subsequent aggregation of alkyl amides in liquid ammonia.

As there have not been any previous reported studies of biocatalytic processes in liquid ammonia, the initial focus of this project was to see if, and to what extent, any enzyme may function in this 'harsh' environment. Further work could focus on the lipase catalysed ammonolysis process from a more biological perspective, understanding how the enzyme functions in liquid ammonia and if the mechanism is equivalent to that in its natural aqueous habitat, utilising the 'catalytic triad' and an

oxyanion hole for stabilisation of the TI. Site-specific mutagenesis could be one way of achieving a better understanding of the mechanism in liquid ammonia.

From an industrial perspective, there is potential for some future work on the lipase catalysed ammonolysis of long chained triglycerides. Fatty acid amides have many industrial applications and are used in medical research. An optimised enzymatic method for their preparation in liquid ammonia could be economically viable and 'green' due to the recyclability of both liquid ammonia and enzymes. CALB on acrylic resin beads (Novozyme 435) is reportedly very robust and able to operate at high temperatures. Future work could look at the design of a stronger, steel-based vessel that could be used to safely operate liquid ammonia reactions at higher temperatures. Moreover, this may allow for vigorous agitation of the multiphase reaction mixture that could further enhance the enzymatic process.

Chapter 7 - Appendix

7.1 Safety, hazards and risk mitigations

7.2 Derivation of ion-pairing model for general salt in liquid ammonia

7.1 Safety, hazards and risk mitigations

To be read carefully prior to any laboratory work and handling of liquid ammonia.

7.1.1 COSHH (Control of Substances Hazardous to Health) assessment

A thorough COSHH assessment must be completed before any experiments are carried out. This complies with UK regulations and additionally gives general insight into the dangers associated with any chemicals that are to be used. All chemicals obtained from commercial supplies are provided with an MSDS (Material Safety Data Sheet) from which the relevant COSHH data can be found as well as important information such as what do in case of emergency/spillage/cleaning/disposing etc.

7.1.2 Major risks involved in liquid ammonia handling

The vapour pressure of liquid ammonia at 25 °C is approximately 10 bar and it is classified as a toxic compound. The 3 major risks when working with liquid ammonia are:

1) A catastrophic failure of the glass vessel resulting in ejection of glass and liquid/vapour into the immediate working area.

2) Unexpected pressure increase due to lack of venting in the vessels (from gas evolution). This can lead to the same outcome as described in risk 1).

3) Splashing with liquid ammonia during venting and sampling can lead to burns. Additionally, inhalation of liquid ammonia vapour at very high concentration can lead to unconsciousness.

7.1.3 Glassware design and pressure testing

Glassware is specially designed for the liquid ammonia work and the glassblower is made aware of the intended use and required operating pressures. Prior to use all glassware is pressure tested to at least twice the operating pressure. The procedure for pressure testing vessels is as follows:

The vessel is filled with water and then connected to a HPLC pump. Before switching the pump on, the vessel is submerged in a bucket of water with a Perspex sheet over the top. The vessel is sealed using an Omnifit stopper and water is pumped in at a very low flow rate (≈ 0.1 ml/min) and an increase in the pressure is observed from the HPLC read-out. The pump is set to automatically switch off as a pressure limit is

reached, which in this case would be set at around 20-25 bar (operating pressure is 10 bar). The vessel is kept at this high pressure for around 10 min and then the pressure is released and the glassware inspected for any failures. The procedure is repeated every 2-3 months and records kept.

7.1.4 Personal protective equipment (PPE)

For all laboratory work, correct PPE to be worn at all times. This includes lab coat, goggles and gloves (when required). Also available is a full face shield for use when judged appropriate.

7.1.5 Fume hood and laboratory precautions

Glassware under pressure is to be shielded at all times by a Perspex sheet of at least 8mm thickness. All persons in the lab are to be made aware of on-going liquid ammonia experiments and the hazards/risk procedures involved and there is to be no working alone in the laboratory when handling liquid ammonia.

7.2 Derivation of ion-pairing model for general salt in liquid ammonia

$$A^- + B^+ \underset{K_{diss}}{\overset{K_{ip}}{\rightleftharpoons}} [A^- B^+]_{\text{ion-pair}}$$

$$K_{diss} = \frac{[B^+][A^-]}{[B^+ A^-]_{ip}} \qquad \text{also} \qquad [B^+] = [A^-]$$

Hence:

$$K_{diss} = \frac{[A^-]^2}{[B^+ A^-]_{ip}}$$

The total amount of salt present can be calculated from:

$$[A^-]_{tot} = [A^-] + [B^+ A^-]_{ip}$$

Rearrangement and substitution into equilibrium equation:

$$[A^-]_{tot} - [A^-] = \frac{[A^-]^2}{K_{diss}}$$

This can be rearranged to a quadratic form:

$$K_{diss}\,[A^-]_{tot} - K_{diss}\,[A^-] = [A^-]^2$$

$$0 = [A^-]^2 + K_{diss}\,[A^-] - K_{diss}\,[A^-]_{tot}$$

$$0 = ax^2 + bx + c$$

Where:

$a = 1$

$b = K_{diss}$

$c = -K_{diss}\,[A^-]_{tot}$

$x = [A^-]$

Using the quadratic solver (positive):

$$x = \frac{-b + \sqrt{b^2 - 4ac}}{2a}$$

$$[A^-] = \frac{-K_{diss} + \sqrt{{K_{diss}}^2 - (4 \times K_{diss} \times [A^-]_{tot})}}{2}$$

The quadratic solver can be used in tandem with the conductivity equation of electrolytes in solution, which states that the overall observed conductivity is summative of the specific conductivity of charged species and their concentration, plus a background solvent conductance:

$$\Lambda = \lambda + \varepsilon[A^-]$$

Where:

$\Lambda = \text{Observed conductivity of solution (S m}^{-1}\text{)}$

$\lambda = \text{Background NH3 conductivity (S m}^{-1}\text{)}$

$\varepsilon = \text{Specific conductivity of A}^- \text{ ions (S m}^{-1}\text{ M}^{-1}\text{)}$

$[A^-] = \text{conducting species (M)}$

Substitution of the conducting species concentration, [A-], from the quadratic solver into the conductivity relationship:

$$\Lambda = \lambda + \varepsilon \frac{-K_{diss} + \sqrt{{K_{diss}}^2 - (4 \times K_{diss} \times [A^-]_{tot})}}{2}$$

The quadratic solver model was compiled in the function fitting software Origin 8.

Chapter 8 - References

[1] J. P. Amend, K. J. Edwards and T. W. Lyons, Sulfur Biogeochemistry: Past and Present, Issue 379, The Geological Society of America, Inc. Boulder, Colorado, 2004.

[2] E. J. Javaux and V. Dehant, Astron. Astrophys. Rev., 2010, **18,** 383-416.

[3] P. M. Zelisko, Bio-Inspired Silicon –Based Materials, Springer, London, 2014.

[4] Abundances of silicon and carbon in the earth's crust taken from website: http://www.periodictable.com/Properties/A/CrustAbundance.an.log.html data provided by *Mathematica's* Element Data function from Wolfram Research, Inc.

[5] The Basics of Silane Chemistry, A Guide to Silane Solutions, provided by Xiameter from Dow Corning.

[6] F. Franks, Water: A Matrix of Life, The Royal Society of Chemistry, Cambridge, 2000.

[7] NASA official website. Feature - Water: The Molecule of Life. http://www.nasa.gov/vision/universe/solarsystem/Water:_Molecule_of_Life_prt.htm

[8] J. A Baross, S. A Benner, G. D. Cody, S. D. Copley, N. R. Pace, J. H. Scott, R. Shapiro, M. L. Sogin, J. L. Stein, R. Summons and J. W. Szostak, The Limits of Organic Life in Planetary Systems, National Academies Press. Washington, 2007.

[9] A. Hanslmeier, Water in the Universe, Springer, New York, 2010.

[10] Drawing by R. Grossman, The New Yorker Magazine, Inc. New York (1962), taken from The Worlds of David Darling, ammonia-based life, website; http://www.daviddarling.info/encyclopedia/A/ammonialife.html

[11] J. B. S. Haldane, *'The Origin of Life',* Penguin, Harmondsworth, 1954.

[12] V. A. Firsoff, Life Beyond the Earth: A Study in Exobiology, Basic Books, New York, 1963.

[13] M. Conde, Thermo physical Properties of NH_3 + H_2O Mixtures for the industrial design of absorption refrigeration equipment, Engineering, Zurich, 2006.

[14] J. Kestin, M. Sololov and W. A. Wakeham, J. Phys. Chem. Ref. Data, 1978, **7 (3),** 941-948.

[15] A. D. Fortes, Icarus, 2000 **146 (2),** 444-452.

[16] J. M. Bragger, R. V. Dunn and R. M. Daniel, Biochim. Biophys. Acta, 2000, **1480 (1-2),** 278-282.

[17] V. Kolb, Int. J. Astrobiology, 2007, **6,** 51-57.

[18] I. C. Shaw and J, Chadwick, Principles of Environmental Technology, Taylor & Francis Ltd, London, 1998.

[19] F. A. Carey, Organic Chemistry 4th Edition, McGraw Hill College, Boston, 2000

[20] R. Breslow, Artificial Enzymes, John Wiley & Sons, Weinheim, 2006.

[21] Article published on news-medical.net titled Scientists develop 3-D artificial enzyme cascade that mimics biochemical pathway using DNA molecules, 2014.

[22] L. E. Limbird, Cell Surface Receptors: A Short Course on Theory and Methods, Springer, 2005.

[23] D. Summers, Senior Scientist in SETI project *"Lipids and the Origin and Evolution of Life"* web: http://www.seti.org/seti-institute/project/lipids-and-origin-and-evolution-life

[24] D. Schulze-Makuch and L. N. Irwin, Life in the Universe, Expectations and Constraints, Second Edition, Springer, Heidelberg, 2008.

[25] D. Nicholls, Inorganic Chemistry in Liquid Ammonia, Topic in Inorganic and General Chemisry, Monograph 17, Elsevier Scientific Publishing Company, Amsterdam (1979)

[26] A. F. Wells, Structural Inorganic Chemistry 5th edition, Clarendon Press, Oxford, 1984.

[27] J. D. Swalen, J. A. Ibers, J. Chem. Phys.,1962, **36,** 1914-1918.

[28] C. Kölmel, C. Ochsenfeld and R. Ahlrichs, Theor. Chim. Acta.,1991, **82,** 271-284.

[29] C. Reichardt, Solvents and Solvent Effects in Organic Chemistry, 3rd Edn, Wiley, Weinheim, 2003.

[30] W. Brown, B. Iverson, E. Anslyn and C. Foote, Organic Chemistry, Wadsworth Cengage Learning, Belmont, 2013.

[31] G. Billaud, A. Demortler, J. Phys. Chem., 1975, **79,** 3053–3055.

[32] D. H. Howard, F. Friedrich and A. W. Browne, J. Amer. Chem. Soc., 1934, **56,** 2332–2340.

[33] H. Smith, Organic Reactions in Liquid Ammonia, Chemistry in Nonaqueous Ionizing Solvents, Vol. Part2 (Eds. G. Jander, H. Spandau and C. C. Addsion), J. Wiley & Sons Inc., New York, London, 1963.

[34] Smallwood, I. M. Handbook of Organic Solvent Properties, John Wiley&Sons Inc., New York, 1996.

[35] J. Lagowski, J. Synth. React. Inorg., Met-Org., Nano-Met. Chem., 2007 **37,** 115-153.

[36] M. Herlem, A. I. Popov, J. Amer. Chem. Soc., 1972, **94,** 1431–1434.

[37] D. T. Sawyer, J. L Roberts, Experimental Electrochemistry for Chemistry, J. Wiley & Sons Inc, New York, 1995.

[38] V. Gutmann, Coord. Chem. Rev., 1976, **18,** 225-255.

[39] D. D. Nelson, Jr., G. T. Fraser and W. Klemperer, Science., 1987, **238,** 1670–1674.

[40] D. C. Luehurs, R. E. Brown and K. A. Godbole, J. Solution Chem., 1989, **18,** 463–469.

[41] W. C. Johnson, Chem. Rev., 1940, **62,** 1-2.

[42] C. A. Kraus and W. C. Bray, J. Am. Chem. Soc., 1913, **35,** 1315-1434.

[43] L. F. Audrieth and J. Kleinberg, Non-Aqueous Solvents, John Wiley & Sons Inc., New York, 1953, Chapter 3.

[44] G. W. Watt, W. B. Leslie and T. E. Moore, Chem. Rev., 1942, **31,** 525-536.

[45] C. A. Kraus, J. Am. Chem. Soc., 1907, **29,** 1557-1571.

[46] W. G. Dauben and R. E. Wolf, J. Org. Chem., 1970, **35,** 374-379.

[47] N. L. Bauld, J. Am. Chem. Soc., 1962, **84,** 4345-4347.

[48] K. N. Campbell and L. T. Eby, J, Am. Chem. Soc., 1941, **63,** 2683-2685.

[49] A. J. Birch, Quart. Rev., 1950, **4,** 69-93.

[50] A. J. Birch and H. Smith, Quart. Rev., 1958, **12,** 17-33.

[51] G. W. Watt, Chem. Rev., 1950, **46,** 317-379.

[52] P. H. Rieger, I. Bernal, W. H. Reinmuth and G. K. Fraenkel, J. Am. Chem. Soc., 1963, **85,** 683-693.

[53] A. R. Buick, T. J. Kemp, G. T. Neal and T. J. Stone, Chem. Commun., (London), 1968, 1331-1332.

[54] J. K. Brown, D. R. Burnham and N. A. Rogers, J. Chem. Soc. B, 1969, 1149-1154.

[55] L. Kuda and V. Boekelheide, Org. Syn., 1962, **43,** 22.

[56] J. W. Hoffman and J. T. Charles, Org. Syn., 1968, **90,** 23.

[57] E. M. Kaiser, C. G. Edmonds, S. D. Grubb, J. W. Smith, D. Tramp, J. Org. Chem., 1971, **36,** 330-335.

[58] A. Ricci, Amino Group Chemistry: From Synthesis to the Life. John Wiley & Sons, Weinheim, 2008.

[59] S. L. Buchwald, C. Mauger, G. Mignani and U. Scholz, Adv. Synth. Catal., 2006, **348,** 23-39.

[60] D. S. Surry and S. L. Buchwald, J. Am. Chem. Soc., 2007, **129 (34),** 10354-10355.

[61] J. McMurry, Organic Chemistry: A Biological Approach, Thomson Brooks/Cole, Belmont, 2008.

[62] U.S. patent 2,034,427, B. F. Goodrich Company, 1936.

[63] C. K. Ingold, Structure and Mechanism in Organic Chemistry, Cornell University Press, 1953.

[64] P. Ji, J. H. Atherton and M. I. Page, J, Org. Chem., 2011, **76,** 3286-3295.

[65] US patent 2,001,284, Dr. F. Rasehig G. m. b. H., Ludwigshafen-on-the-Rhine, 1935.

[66] P. Ji PhD thesis, The University of Huddersfield repository, pages 186-187.

[67] L. A. Pinck and G. E. Hilbert, J. Am. Chem. Soc., 1934, **56,** 490-491.

[68] H. R. Strain, J. Am. Chem. Soc., 1930, **52,** 820-823.

[69] P. Ji PhD thesis, The University of Huddersfield repository, page 126.

[70] US patent 7,683,214 B2, BASF SE, 2010.

[71] European Patent 1,426,047, Takahata, Kureha Chemical Industry Co. Ltd. 2004.

[72] C. S. J. Walpole, R. Wrigglesworth, S. Bevan, E. A. Campbell, A. Dray, I. F. James, K. J. Masdin, M. N. Perkins and J. Winter, J. Med. Chem, 1993, **36,** 2373-2380.

[73] S. D. Tuorinsky, Medical Aspects of Chemical Warfare, United States Department of the Army, Government Printing Office, Washington D.C., 2008.

[74] T. R. Roberts, D. H. Hutson, Metabolic Pathways of Agrochemicals: Herbicides and plant growth regulators, Royal Society of Chemistry, Cambridge, 1998.

[75] A. P. Rajput and R. P. Gore, Der Pharma Chemica, 2011, **3 (3),** 409-421.

[76] Historical dates for Carl Schotten, Eugen Baumann and the Schotten-Baumann process provided by http://www.uni.illinois.edu/~ewinter3/history.html.

[77] M. B. Smith, Organic Chemistry: An Acid-Base Approach, CRC press, Florida, 2010.

[78] G. E. Veitch, K. L. Bridgwood and S. V. Ley, Organic Letters, 2008, **10,** 3623-3625.

[79] Information taken from BOC anhydrous ammonia data page from the official BOC website;http://www.boconline.co.uk/en/products-and-supply/packaged-chemicals/gaseous-chemicals/ammonia/ammonia.html

[80] Sigma-Aldrich product page for phenyl benzoate, sigmaaldrich.com

[81] IR Spectroscopy Introduction tutorial, CHM427 IR scans, chemrat.com

[82] A. Sethi, Systematic Lab Experiments in Organic Chemistry, New Age International, New Delhi, 2003.

[83] Data page for 4-chlorophenyl benzoate from NIST web database, webbook.nist.gov

[84] MSDS for 4-chlorophenyl benzoate, sigmaaldrich.com

[85] W. Guo, T. Brown and B. Fung, J. Phys. Chem., 1991, **95,** 1829-1836.

[86] MSDS for perfluoroheptanamide, apolloscientific.co.uk

[87] MSDS for perfluorooctanamide, apolloscientific.co.uk

[88] MSDS for perfluorodecanamide, matrixscientific.com

[89] J. S. Hine, Physical Organic Chemistry, McGraw-Hill Book Co., New York, 1956.

[90] P. Ji PhD thesis, The University of Huddersfield repository, page 124.

[91] W. C. Fernelius and G. B. Bowman, Chem. Reviews., 1940, **26 (1),** 3-48.

[92] Summary of early ester ammonolysis work, H. Sun PhD thesis, The University of Huddersfield repository, page 43.

[93] W. P. Jencks, Handbook of Biochemistry, ed. H. A. Sober, pp. J150-J189, Chemical Rubber Co., Cleveland, 1968.

[94] J. P. Guthrie, Can. J. Chem., 1979, **57,** 1177-1185.

[95] M. I. Page and A. Williams, Organic and Bio-Organic Mechanisms, Longmans, Harlow, 1997.

[96] A. Williams, Adv. Phys. Org. Chem., 1992, **27,** 1-55.

[97] P. Ji, J. H. Atherton, M. I. Page, J. Org. Chem., 2011, **76,** 1425-1435.

[98] P. Ji, J. H. Atherton, M. I. Page, Org. Biomol. Chem., 2012, **10,** 5732-5739.

[99] J. P. Fox, M. I. Page, A. C. Satterthwaite, W. P. Jencks, J. Am. Chem. Soc., 1972, **94,** 4729-4731.

[100] L.V. Coulter, J. R. Sinclair, A. G. Cole, G. C. Rope, J. Am. Chem. Soc., 1959, **81,** 2986-2989.

[101] R. H. Horton, L. A Moran, R. S. Ochs, Principles of Biochemistry 3rd Edition, Prentice Hall, 2003.

[102] Q. A. Acton, Intracellular Membranes - Advances in Research and Application, Scholarly Edition, Atlanta, Georgia, 2013.

[103] S. J. Singer and G. L. Nicholson, Science, 1972, **175,** 720-731.

[104] J. H. Fendler, Acc. Chem. Res., 1980, **13,** 7-13.

[105] E. N. Harris, T. Exner, G. R. V. Hughes and R. A. Asherson, Phospholipid-Binding Antibodies, CRC Press, Florida, 1991.

[106] J. H. Fendler, Membrane Mimetic Chemistry, John Wiley & Sons, New York, 1982.

[107] J. Bharadwaj, A. Ameta, Journal of Natural Sciences, 2013, **1(2),** 12-17.

[108] M. Willcox, in H. Butler Poucher's Perfumes, Cosmetics and Soaps, 10th edition, Kluwer Academic Publisher, Dordrecht, p. 453-466, 2000.

[109] H. Verbeek, Surfactants in Consumer Products, Historical Review, Springer. Berlin Heidelberg, p. 1-2, 1987.

[110] M. R Porter, Handbook of Surfactants, Springer, Netherlands, 1994.

[111] G. L. Hassenhuettl and R. W. Hartel, Food Emulsifiers and Their Applications, Springer Science and Business Media, New York, 2008.

[112] R. Narayanan and J. M. Anderez, Interfacial Processes and Molecular Aggregation of Surfactants, Springer Science and Business Media, New York, 2008.

[113] S. Q. Field. *Why There's Antifreeze in Your Toothpaste: The Chemistry of* Household Ingredients, Chicago Review Press, Chicago, 2007.

[114] R. J. G. Rycroft, T. Menne, P. J. Frosch, J. P. Lepoittevin, Textbook of Contact Dermatitis, Springer Science and Business Media, Heidelberg, 2001.

[115] D. Attwood and A. T. Florence, Physical Pharmacy, Second Edition, Pharmaceutical Press, London, 2012.

[116] P. Ghosh, Colloid and Interface Science, PHI Learning Private Limited, New Delhi, 2009.

[117] K. Holmberg, B. Jönsson, B. Kronberg and B. Lindman, Surfactants and Polymers in Aqueous Solution, 2nd Ed., Wiley. Chichester, 2003.

[118] M. J. Rosen, Surfactants and Interfacial Phenomena, 3rd Ed., Wiley, New York, 2004.

[119] T. F. Tadros, Applied Surfactants: Principles and Applications, Wiley, New York, 2005.

[120] J. L. Attwood, J. W. Steed, Encyclopedia of Supramolecular Chemistry, Taylor & Francis, New York, 2004.

[121] F. Marhuenda-Egea, S. Piera-Velázquez, C. Cadenas, E. Cadenas, Archaea, 2002, **1 (2),** 105-111.

[122] D. Madamwar and A. Thakar, Applied Biochemistry and Biotechnology, 2004, **118 (1-3),** 361-369.

[123] Image from Wikipedia, Micelle information page, http://en.wikipedia.org/wiki/Micelle

[124] J. W. McBain and H. E. Martin, J. Chem. Soc., Trans., 1914, **105,** 957-977.

[125] F. M. Menger, Accounts of Chemical Research., 1978, **12 (4),** 111-117.

[126] J. W. McBain and O. A Hoffman, J. Phys. Colloid Chem., 1949, **53 (1),** 39-55.

[127] G. S. Hartley, Trans Faraday Soc., 1935, **31,** 31.

[128] G. S. Hartley, Q Rev., Chem. Soc., 1948, **2,** 152.

[129] F.Menger, Bioorganic Chemistry, Vol III, Macro and Multimolecular Systems, E.E. Van Tamelen, Ed., Academic Press, New York, 1977.

[130] Image from Kino; Professionals In Interface Chemistry. Determining the critical micelle concentration of a surfactant, http://www.surface-tension.org/news/58.html

[131] E. Kissa, Fluorinated Surfactants and Repellents, Second Edition, Marcel Dekker, Inc., New York, 2001.

[132] J. Lyklema, Fundamentals of Interface and Colloid Science: Soft Colloids, Academic Press, Amsterdam, 2005.

[133] D. J. McClements, Food Emulsions: Principles , Practice and Techniques, CRC Press, Florida, 1998.

[134] A. Berthod and C. Garcia-Alvarez-Coque, Micellar Liquid Chromatography (Chromatographic Science Series), CRC Press, New York, 2000.

[135] C. O. Rangel-Yagui, A. Pessoa-Jr and L. Costa Tavares, J. Pharm. Pharmaceut. Sci., 2005, **8(2),** 147-163.

[136] N. Funasaki and S. Hada, The Journal of Physical Chemistry. 1979, **83,** 2471-2475.

[137] H. N. Singh, S. M. Saleem, R. P. Singh, J. Phys. Chem. 1980, **84,** 2191-2194.

[138] M. S. Dhillon and H. S. Chugh, Journal of Chemical and Engineering Data, 1978, **23,** 263-265.

[139] G. Aleiner, O, Us'yarov, Colloid Journal., 2010, **72,** 588-594.

[140] Y. Mido and S. A. Iqbal, Colloidal and Surface Chemistry, Discovery Publishing House, Delhi, 1996.

[141] A. S. Negri and S. D Anand, A Textbook of Physical Chemistry, New Age International, Delhi, 2007.

[142] G. Sugihara, A. A. Nakamura, T. H. Nakashima, Y. I. Araki, T. Okano and M. Fujiwara, Colloid Polym. Sci., 1997, **275,** 790-796.

[143] D. G. Marangoni, A. P. Rodenhiser, J. M. Thomas and J. C. T. Kwak, Langmuir, 1993, **9,** 438-443.

[144] A. R. Ivanov, A. V. Lazarev, Sample Preparation in Biological Mass Spectrometry, Springer, Dordrecht, 2011.

[145] K. K. Arora, A Crash Course In Aieee Chemistry, Pearson Education in South Asia, Delhi, 2009.

[146] M. F. Torres, R. H. de Rossi and M. A. Fernandez, J. Surfact. Deterg., 2013, **16,** 903-912.

[147] Khan, S. S. Shah, J. Chem. Soc. Pak., 2008, **30,** 186-191.

[148] N. Dubey, Surface Sci. Technol., 2008, **24,** 139-148.

[149] W. Li, M. Zhang, J. Zhang and Y. Han, Frontiers of Chemistry in China., 2006, **4,** 438-442.

[150] Specialty Additives AERSOL® Surfactants, Cytec industries Inc. 2013.

[151] E. J. Fendler, J. H. Fendler, Catalysis in Micellar and Macromolecular Systems, Academic Press Inc, New York, 1975.

[152] M. Zhao, L. Zheng, Physical Chemistry Chemical Physics., 2011, **13,** 1332-1337.

[153] M. J. Rosen, J. T. Kunjappu, Surfactants and Interfacial Phenomena, 4th Edition, Wiley, 2004.

[154] C. E. Housecroft and E. C Constable, Chemistry 3rd Edition, Pearson Education Limited, Bilboa, Spain, 2006.

[155] G. Sciaini, E. Marceca, R. Fernandez-Prini, J. Chem. Phys. 2008, **112,** 11990-11995.

[156] N. T. Powles, PhD Thesis; A Physical Organic Approach to the Improvement of Oligonucleotide Synthesis, University of Huddersfield, 2005.

[157] P. D. T. Huibers, V. S. Lobanov, A. R. Katritzky, O. D Shah, M. Karelson, J. Colloid Interface., 1997, **187,** 113-120.

[158] A. Amit, Hydrocarbons (Alkanes, Alkenes And Alkynes), Discovery Publishing House, Delhi, 2006.

[159] H. Wennerström, B. Lindman, Physical Chemistry of Surfactant Association, Volume 51, Issue 1 of Physics Reports, North Holland Publ, 1979.

[160] J. C. Berg, An Introduction to Interfaces & Colloids: The Bridge to Nanoscience, World Scientific Publishing, Singapore, 2010.

[161] M. J. Rosen, Surfactants and Interfacial Phenomena, 3rd Ed., Wiley, New York, 2004.

[162] S. S. Shah, K. Naeem, S. W. H. Shah and G. M Laghari, Colloids and Surfaces A: Physiochem. En. Aspects., 2000, **168,** 77-85.

[163] R. Singh, MSc Thesis, Division of Applied Surface Chemistry, Chalmers University of Technology, Gothengurg, Sweden, 2012.

[164] M. S. Micozzi, E. D. Brown, B. K. Edwards, J. G. Bieri, P. R. Taylor, F. Khachik, G.R Beecher and J. C. Smith, Am. J. Clin. Nutr., 1992, **55 (6),** 1120-1125.

[165] F. London, Trans Farad. Soc., 1937, **33,** 8.

[166] N. Seedher and M. Kanojia, AAPS Pharm. Sci. Tech.,2008, **9 (2),** 431-436.

[167] S. Gokturk, E. Caliskan, R. Y. Talman and U Var, Scientific World Journal, Online journal**,** 2012.

[168] M. Crothersa, Z. Zhoua, N. Ricardo, Z. Yang, P. Taboada, C. Chaibundit, D. Attwood and C. Booth, International Journal of Pharmaceutics, 2005, **293,** 91-100.

[169] I. Furo, Journal of Molecular Liquids, 2005, **117,** 117-137.

[170] J. Zhao and B. M. Fung, Langmuir, 1993, **9 (5),** 1228-1231.

[171] E. A. Aniansson, S. N. Wall, M. Almgren, H. Hoffmann, I. Kielmann, W. Ulbricht, R. Zana, J, Lang and C. Trondre, J. Phys. Chem., 1976, **80,** 905.

[172] N. Muller and R. H. Birkhahn, J. Phys. Chem., 1967, **71 (4),** 957-962.

[173] M. Graupe, M. Takenaga, K. Thomas, R. Colorado Jr. and T. R. Lee, J. Am. Chem. Soc., 1999, **121,** 3222-3223.

[174] C. J. Van Oss, M. K. Chaudhury and R. J. Good, Chem. Rev., 1988, **88,** 927.

[175] P. Somasundaran, Encyclopedia of Surface and Colloid Science. Volume 2, CRC Press, New York, 2006.

[176] M. N. Khan, Micellar Catalysis, CRC Press, 2006.

[177] C. A. Bunton and G. Savelli, Adv. Phys. Org. Chem., 1986, **22,** 213.

[178] F. M. Menger and C. E. Portnoy, J. Amer. Chem. Soc.,1967, **89,** 4698.

[179] C. A. Bunton, ARKIVOC **vii,** 490, 2011.

[180] B. S Chauhan, Principles of Biochemistry and Biophysics, University Sciences Press, Boston, 2008.

[181] J. Dighton, J. F White Jr., J. White and P. Oudemans, The Fungal Community: Its Organization and Role in the Ecosystem, Third Edition, Taylor and Francis Group, Florida, 2005.

[182] T. Palmer and P. L. Bonne, Enzymes: Biochemistry, Biotechnology, Clinical Chemistry, Horwood Publishing Limited, Cambridge, 2001.

[183] R. A. Sheldon, Journal of Chemical Technology and Biochemistry, 1997, **68,** 381-388.

[184] K. R. Jegannathan and P. H. Nielsen, The Journal of Cleaner Production, 2013, **42,** 228-240.

[185] H. Uhlig, Industrial Enzymes and Their Applications, John Wiley and Sons, Canada, 1998.

[186] J. A. Tao and R. J. Kazlauskas, Biocatalysts for Green Chemistry and Chemical Process Development, John Wiley and Sons, New Jersey, 2011.

[187] A. M. P. Koskinen and A. M. Klibanov, Enzymatic Reactions in Organic Media, Blackie Academic and Professional, Glasgow, 1996.

[188] D. H. Paterson and H. C Murray, J. Amer. Chem. Soc,. 1952, **74,** 1871-1872.

[189] A. L. Margolin, D. L. Delinck, M. R. Whalon, J. Amer. Chem. Soc., 1990, **112,** 2849-2854.

[190] M. Therisod and A. M. Klibanov, J. Amer. Chem. Soc., 1987, **109,** 3977-3981.

[191] R. A. Sheldon, M. C. Zoete, A. C. Kock-van Dalen, F. van Rantwijk, Journal of Molecular Catalysis B. Enzymatic, 1996, **1,** 109-113.

[192] S. Stoker, General, Organic, and Biological Chemistry, Cengage Learning, 2012.

[193] Small scale tests by J.Griffin showed higher solubility of methyl esters than corresponding amides in hexane and DCM (very rough test, unpublished).

[194] C. Agostoni and M. G. Bruzzese, Pediatr. Med. Chir., 1992, **14(5),** 473-479.

[195] K. Holmberg, Novel Surfactants: Preparation, Applications and Biodegradability. Second Edition, Revised and Expanded. Marcel Dekker, New York, 2003.

[196] W. B. Mendelson and A. S. Basile, Neuropsychopharmacology, 2001, **25,** 36-39.

[197] R. Mechoulam, E. Fride, L. Hanu, T. Sheskin, T. Bisogno, V. Di Marzo, M. Bayewitch and Z. Vogel, Nature, 1997, **389,** 25-26.

[198] http://lipidlibrary.aocs.org/lipids/amides/index.htm

[199] J. Richmond, Cationic Surfactants: Organic Chemistry, CRC Press, New York, 1990.

[200] U.S patent number U.S. 3,801,610, Henkel & Cie, 1974.

[201] U.S patent number U.S. 2,013,108, I. G. Farbenindustrie Aktiengesellschaft, 1935.

[202] U.S patent number U.S. 7,098,351, Malaysian Palm Oil Board, 2006.

[203] V. F. Balaty, L. L. Fellinger and L. F Audrieth, Industrial and Engineering Chemistry, 1939, **31 (3),** 280-282.

[204] U.S patent number U.S. 2,070,991

[205] E. T. Roe, J. M Stutzman, J. T Scanlan and D. Swern, The Journal of American Oil *Chemists' Society*, 1952, **29,** 18-22.

[206] Based on price per gram for 50mg purchase of oleamide from Enzo Life Sciences, New York, enzolifesciences.com

[207] Based on price per gram for 25g batch purchase of oleic acid from Sigma, sigmaaldrich.com

[208] M. J. J. Litjens. A. J. J. Straathof, J. A Jongejan, J. J. Haijnen, Chem. Commun., 1999, **13,** 1255-1256.

[209] O. Lozada and A. Victor, Biocatalytic and synthetic routes for the preparation of valuable products, Pro Quest, University of Iowa, 2008.

[210] A. B. Salleh and M. Basri, New Lipases and Proteases, Nova Publishers, New York, 2006.

[211] PowerPoint from T. Sipos, A. Batta, S. Das, A. Halton and K. Kercsmar, Digestive Care Inc., Bethelehem, PA

[212] A. Bukhari, A. Idris, Biotechnology Advances, 2012, **30,** 550-563.

[213] S. Rehm, P. Trodler, J, Pleiss, Protein Sci., 2010, **19(11),** 2122-2130.

[214] J. M. Palomo, M. Fuentas, G. Fernandez-Lorente, C. Mateo, J. M. Guisan and R. Fernandez-Lafuente, Biomacromolecules, 2003, **4,** 1-6.

[215] Y. Pookari, S. J. Clarson, Biocatalysis and Agricultural Biotechnology, 2013, **2,** 7-11.

[216] P. Adlercreutz, Chem. Soc. Rev., 2013, **45(15),** 6406-6436.

[217] Product information sheet for Lewatit® VP OC 1600 macroporous beads provided by Lenntech.com

[218] J. Toedt, D. Koza and K. Van Cleef-Toedt, Chemical Composition of Everyday Products, Greenwood Publishing Group, Westport, 2005.

[219] Saponification –Soap Making and Other Things, website: http://www.brothers-handmade.com/saponification.html

[220] W. H. Simmons and H.A Appleton, The Handbook of Soap Manufacture, Twenty-Seven Illustrations, London, 1908.

[221] E. F Jordan Jr., B. Artymyshyn, C. R. Eddy and A, N. Wrigley, Journal of American Oil Chemists Society, 1966, **43 (2),** 75-8.

[222] D. E. Lopez, J. G Goodwin Jr., D. A Bruce and E. Lotero, Applied Catalysis A: General, 2005, **295 (2),** 97-105.

[223] D. A. Katz, The Synthesis of Biodiesel from Vegetable oil, lab procedure from Chymist; http://www.chymist.com/Synthesis%20of%20Biodiesel.pdf., 2012

[224] K. Goodner and R. Rouseff, Practical Analysis of Flavor and Fragrance Materials, Blackwell Publishing Ltd, Chichester, 2011.

[225] J. N. Trbojević, A. S. Dimitrijević, D. V. Veličković, M. Gavrović-Jankulović and N. B. Milosavić, Hem. Ind., 2013, **67 (5),** 703-706.

[226] J. Uppenberg, M. T Hansen, S. Patkar and T. A. Jones, Structure, 1994, **2,** 293-308.

[227] M. E. Ensminger and A. H, Ensminger, Foods & Nutrition Encyclopedia, Two Volume Set, CRC Press, Florida, 1993.

[228] C. Adams, Asthma Solved Naturally: The Surprising Underlying Causes and Hundreds of Natural Strategies to Beat Asthma, Logical Books, Delaware, 2013.

[229] F. Bettelheim, W. Brown, M. Campbell, S. Farrell and O. Torres, Introduction to General, Organic and Biochemistry, Brooks/Cole Cengage Learning, Belmont, 2012.

[230]Information on triolein density taken from http://www.worldofchemicals.com/chemicals/chemical-properties/triolein.html

[231] B. Chen, J. Hu, E. M. Miller, W. Xie, M. Cai and R. A. Gross, Biomacromolecules, 2008, **9,** 463-471.

[232] K. Loos, Biocatalysis in Polymer Chemistry, Wiley-VCH, Weinheim, 2011.

[233] J. H. Y. Park, E. J. Kim, H. Jin and J. Jun, Bull. Korean Chem. Soc., 2002, **23 (10),** 1373-1374.

[234] G. A. Burdock, Encylcopedia of Food and Color Additives, Volume 3, CRC Press, Florida, 1997.

[235] L. S. Weatherby, l. McIlvaine and D. Matlin, Journal of the American Chemical Society, 1925, **47 (8),** 2249-2252.

[236] Z. Tang, Z. Du, E. Min, L. Gao, T. Jiang and B. Han, Fluid Phase Equilibria, 2006, **239 (1)**, 8-11.

[237] E. Jungermann, N. O. V. Sonntag, Glycerine: A Key Cosmetic Ingredient. Marcel Dekker, New York, 1991.

[238] N. D. Ognjanović, S. V. Šaponjić, D.I. Bezbradica and Z. D. Knežević, Acta Periodica Technologica, 2008, **39,** 161-169.

[239] E. Severac, O. Galy, F. Turom, C. A. Pantel, J-S. Condoret, P. Monsan and A. Marty, Enzyme and Microbial Technology, 2011, **48,** 61-70.

[240] C. H. Bamford, R. G. Compton, C. F. H. Tipper, Electrophilic Substitution at a Saturated Carbon Atom, Elsevier, Amsterdam, 1972.

[241] D. B. Troy, P. Beringer, Remington: The Science and Practice of Pharmacy, Lippincott Williams & Wilkins, Baltimore, 2006.

[242] M. Lee, J. Lee, D. Lee, J. Cho, S. Kim, C. Park, Enzyme and Microbial Technology, 2011, **49 (4),** 402-406.

[243] Z. Duan, W. Du and D. Liu, Processes Biochemistry, 2010, **45 (12),** 1923-1927.

[244] M. R. Talukder, J. C. Wu, T. B. Van Nguyen, N. M. Fen and Y. L. S. Melissa, Journal of Molecular Catalysis B: Enzymatic, 2009, **60 (3-4),** 106-112.

[245] I. C. Véras, F. A. L. Silva, A. D. Ferrão-Gonzales and V. H. Moreau, Bioresource Technology, 2011, **102 (20),** 9653-9658.

[246] Y. Zhao, J. Li, Y. Xu, H. Duan, W. Fan and G Zhao, Chinese J. Chromatogr., 2008, **26 (2),** 212-222.

[247] A. Yasar, O. Üçüncü, C. Güleç, H. Inceer, S. Ayaz and N. Yayh, Pharm. Biol., 2005, **43 (2),** 108-112.

[248] H. Chen. H. Ju, T. Wu, Y. Liu, C. Lee C. Chang, Y. Chung and C Shieh, Journal of Biomedicine and Biotechnology,2011, **2011**, 1-6.

[249] P. Yao, G. Huang, W. Yan, X. Zhang, Q. Li and Y. Wei, Advances in Chemical Engineering and Science, 2012, **2,** 204-211.

[250] A. Overmayer, S. Schrader-Lippelt, V. Kasche and G. Brunner, Biotechnology Letters, 1999 **21,** 65-69.